Assessment of Anti-Merozoite Antibody Function in the Context of Blood-Stage Malaria Vaccine Development

Thesis submitted for the degree of Doctor of Philosophy

Trinity Term 2014

David C. C. Llewellyn

St John's College

Word Count: ~40,000

Assessment of Anti-Merozoite Antibody Function in the Context of Blood-Stage Malaria Vaccine Development

David C. C. Llewellyn, St John's College, University of Oxford

Thesis submitted for the degree of Doctor of Philosophy, Trinity Term 2014

ABSTRACT

In regions endemic for malaria, natural exposure results in an acquired immunity which protects individuals from severe disease. However, no vaccine against the blood-stage of malaria, against which naturally-acquired immunity is targeted, currently exists that is capable of emulating, or out-performing, natural protection. To rationally direct the next generation of blood-stage malaria vaccine development, a greater understanding of the immunological mechanisms involved in clinical protection is required.

To date, the assessment of naturally-acquired and vaccine-induced immunity to the blood-stage of malaria has suffered from a paucity of *in vitro* immunological assays that are both robust and reproducible, whilst allowing for assessment of anti-parasitic activity induced by antibodies, either alone, or in conjunction with immune cells. Thus this Thesis describes the development of the antibody-dependent respiratory burst (ADRB) assay, for assessment of blood-stage immunity against *Plasmodium falciparum*, as well as the Duffy antigen receptor for chemokines (DARC) – Duffy binding protein (DBP) binding inhibition assay, for assessing antibody mediated immunity to *P. vivax*. A reproducible and standardised assay of ADRB activity was developed here and applied to studies of immunity in both mice and humans. ADRB activity, which assesses antibodies' ability to activate oxidative burst in neutrophils via Fc receptor (FcR)-dependent pathways, was shown to associate with clinical protection in a cohort from Mali where FcR-independent immunological assays, such as the assay of growth inhibition activity, did not. This work thus elucidates the importance of FcR-dependent immunity to *P. falciparum* malaria and establishes the ADRB assay as a useful tool for future vaccine development. In addition, the DARC-DBP binding inhibition assay was established and utilised to assess inhibitory activity of antibodies induced in the first Phase I clinical trial of this antigen. Results identify the need for significant improvements in vaccine design, and show the utility of the assay as a tool for assessing future blood-stage vaccine development efforts against this neglected parasite.

ACKNOWLEDGEMENTS

Firstly, thank you to Simon Draper for your fantastic supervision, support, academic mentorship, enthusiasm and friendship. Having decided that a PhD with an aging professor was the safest option, I wasn't sure what a young guy "building an exciting new group" would entail. However, from the project proposal on 5th January 2010, to the 3rd October 2014 and the thesis herewith, I have been lucky to have been surrounded by an engaging and stimulating group of people. The academic output from, and sense of community within, the blood-stage malaria group, are testaments to your leadership, and I am immensely grateful to have been welcomed.

A special thanks to the incredible crowd of students from the Jenner for your help, support and all the good times. In particular, Rhea, Cait, Simone, Joe, Dasha, and Dan, you guys are awesome and have helped me immensely with this work as well as being great mates – the future of global health is safe in your hands.

Thank you to everyone at the Jenner for your support and advice. I'd especially like to thank Sumi Biswas, Andrew Williams, Julie Furze, Rebby Brown, Kathryn Hjerrild, Jing Jin, Drew Worth and everyone in the blood-stage and transmission-blocking teams. Also, my sincere thanks to Adrian Hill for the opportunity to study at the Jenner Institute.

I'd like to thank all the collaborators who have been involved in this work, especially Kazutoyo Miura, Michael Fay, and Carole Long from the NIH without whom much of this work would have been impossible.

I owe the great experiences, and unrivalled education, I have had here to the opportunity afforded to me by the Rhodes Trust. Particular thanks go to the former Warden, Don Markwell, for ongoing support and for facilitating the broader education which has been such an important part of my time in Oxford.

To friends, far and near, thanks for the endless support, chats, runs, kicks, travels, dinners, beers, debates, laughs and dreams.

Finally, I would not be here without a lucky combination of genes, engaging and enriching experiences, and unwavering support. Born into a pair of gumboots, it was impossible not to be consumed by the infectious passion for science and the natural world fostered within my family. Mum, Dad, Kim – without your support and encouragement, I would not have made it this far – for this, I can't thank you enough.

TABLE OF CONTENTS

TABLE OF FIGURES

TABLE OF TABLES

ABBREVIATIONS

A/I	Activatory to inhibitory ratio
ADCC	Antibody dependent cellular cytotoxicity
ADCI	Antibody-dependent cellular inhibition
AdHu5	Human adenovirus serotype 5
Ad-M	Adenovirus-prime MVA-boost immunisation regime
ADRB	Antibody-dependent respiratory burst
AMA1	Apical membrane antigen 1
AP	Adenovirus prime – protein boost vaccination regime
APC	Antigen presenting cell
API	Annual parasite incidence
AS	Heterozygous sickle cell trait genotype
AU	Antibody units
AUC	Area under the curve
BAP	Biotin acceptor peptide
BCR	B cell receptor
BSA	Bovine serum albumin
BTK	Bruton's tyrosine kinase
$CD32b^{-/-}$	FcγRIIb knockout
ChAd63	Chimpanzee adenovirus 63
CI	Confidence interval
C_L	Immunoglobulin light chain constant domain
CMV	Cytomegalovirus
CPEC	Circular polymerase extension cloning
CSP	Circumsporozoite protein
DARC	Duffy antigen receptor for chemokines
DBL	Duffy binding-like
DBP	Duffy binding protein
DC	Dendritic cell
dsDNA	Double stranded DNA
E64	Epoxysuccinyl-L-leucylamido(4-guanidino)butane
EBL	Erythrocyte binding-like
EDTA	Ethylenediaminetetraacetic acid
ELISA	Enzyme-linked immunosorbent assay
Fab	Fragment, antigen binding, region of immunoglobulin molecule
Fc	Fragment, crystallisable- non-antigen-binding region of immunoglobulin molecule
FcR	Fc receptor
Fy	Gene encoding Duffy antigen
G6PD	Glucose-6-phosphate dehydrogenase
$\gamma^{-/-}$	Fc common gamma chain knockout
GC	Germinal centre
GIA	Growth inhibition activity

GLURP	Glutamine rich protein
GPI	Glycosylphosphatidylinositol
GST	Glutathione S-transferase
Hb	Haemoglobin
HBsAg	Hepatitis B surface antigen
HBSS	Hank's balanced salt solution
His	Six histidine tag
HIV	Human immunodeficiency virus
i.m.	Intramuscularly
i.p.	Intraperitoneally
i.v.	Intravenous
IC	Immune complex
ICC	Interclass correlation coefficient
ICGEB	International centre for genetic engineering and biotechnology
IFN	Interferon
ifu	Infectious units
Ig	Immunoglobulin
IL	Interleukin
IMX313	Oligomerisation domain based on the chicken orthologue of human complement protein C4bp α-chain
iRBC	Infected red blood cell
iRLU	Indexed relative light units used in the mouse ADRB assay
ITAM	Immunoreceptor tyrosine-based activation motif
ITIM	Immunoreceptor tyrosine-based inhibition motif
IU	Isotype units
LL	LogLikelihood
mAb	Monoclonal antibody
MAC	Membrane attack complex
MHC	Major histocompatibility complex
MIIC	Major histocompatibility complex class II containing compartment
MPO	Myeloperoxidase
MSP	Merozoite surface protein
MVA	Modified vaccinia virus Ankara
Mz	Merozoite
NADPH	Reduced form of nicotinamide adenine dinucleotide phosphate
NAI	Naturally acquired immunity
NET	Neutrophil extracellular trap
NIAID	National institute of allergy and infectious diseases
NK	Natural killer
OD_{405}	Optical density measured at 405 nm
OR	Odds ratio
Ova	Ovalbumin
PAGE	Polyacrylamide gel electrophoresis
PBS	Phosphate buffered saline

PCR	Polymerase chain reaction
PEMS	Parasitophorous vacuolar membrane-enclosed merozoite structures
pfu	Plaque forming units
PI3K	Phosphoinositide 3-kinase
PK	14 amino acid epitope tag also known as V5
PLC	Phospholipase C
PMN	Polymorphonuclear cells
pNPP	p-nitrophenyl phosphate
PPP	Three dose protein-in-adjuvant immunisation regime
PR	Annual mean parasite rate
Py17XNL	Non-lethal strain of *P. yoelii*
RBC	Red blood cell
RESA	Ring-infected erythrocyte surface antigen
RH5	Reticulocyte-binding protein homologue 5
RLU	Relative light units
RLU_p	Relative light units indexed against a positive control used in the human ADRB assay
ROS	Reactive oxygen species
RT	Room temperature
s.c.	Subcutaneously
SEC	Size exclusion chromatography
SEM	Scanning electron microscopy
SERP	Serine repeat protein
SHIP	SRC-homology-2-domain-containing inositol-5-phosphatase
SOS	Son of sevenless homologue
SRA	Surface reactivity assay
SS	Homozygous sickle cell trait genotype
TAE	Tris-acetate-EDTA
TCR	T cell receptor
TCS	Thrombin cleavage sequence
T_{FH}	T follicular helper cell
TLR	Toll-like receptor
Tm	Melting temperature
TNF	Tumour necrosis factor
TO	Tuck ordinary
tPA	Human tissue plasminogen activator
Treg	Regulatory T cell
V_H	Variable domain of the immunoglobulin heavy chain
V_L	Variable domain of the immunoglobulin light chain
WHO	World health organisation
WT	Wild type

PUBLICATIONS FROM THESE STUDIES

Llewellyn, D., de Cassan, S.C., Williams, A.R., Douglas, A.D., Forbes, E.K., Adame-Gallegos, J.R., Shi, J., Pleass, R.J. & Draper, S.J. (2014) Antibody-dependent respiratory burst in mouse neutrophils and assessment of Fc-dependent pathways on *Plasmodium yoelii* challenge outcome. *Journal of Leukocyte Biology* **95**(2): 369-382.

Llewellyn, D., Miura, K., Fay, M.P., Williams, A.R., Murungi, L.M., Shi, J., Hodgson, S.H., Douglas, A.D., Fairhurst, R.M., Diakite, M., Pleass, R.J., Long, C.A. & Draper, S.J. (2015) Standardization of the antibody-dependent respiratory burst assay with human neutrophils and Plasmodium falciparum malaria. *Scientific Reports* **5**: 14081.

Goodman, A.L., Forbes, E.K., Williams, A.R., Douglas, A.D., de Cassan, S.C., Bauza, K., Biswas, S. Dicks, M.D.J., **Llewellyn, D.** Moore, A.C., Janse, C.J., Franke-Fayard, B.M., Gilbert, S.C., Hill, A.V.S., Pleass, R.J. & Draper, S.J. (2013) The utility of *Plasmodium berghei* as a rodent model for anti-merozoite malaria vaccine assessment. *Scientific Reports*. **3**:1706. **DOI**: 0.1038/srep01706

Forbes, E.K., de Cassan, S.C., **Llewellyn, D.**, Biswas, S., Goodman, A.L, Long, C.A., Brandt, W., Pleass, R.J., Hill, F., Hill, A.V.S. & Draper, S.J. (2012) T cell responses induced by adenoviral vectored vaccines can be adjuvanted by fusion of antigen to the oligomerization domain of C4b-binding protein. *PLoS ONE*. **7**(9): e44943.

CHAPTER 1

INTRODUCTION

1. INTRODUCTION

1.1. Malaria

Malaria is a disease caused by the infection of a vertebrate host with apicomplexan parasites of the genus *Plasmodium*. While there are over 250 species of *Plasmodium*, only five are known to infect and cause disease in humans: *P. falciparum*, *P. vivax*, *P. ovale*, *P. malariae*, and *P. knowlesi*. The first medical records of malaria-like illnesses come from more than 4,500 years ago (Nei Ching, *The Canon of Medicine*, 2700BC), and since then, reports consistent with malarial disease are present throughout the historical literature of many civilisations (1).

It wasn't until 1880 that malaria parasites were first observed and described in the blood by Alphonse Laveran followed 17 years later by Ronald Ross' proof of the role of mosquitoes in malaria transmission, kick-starting modern malaria research and attempts to understand and control the disease. This early 20th century work culminated in the Global Malaria Eradication campaign of the 1950s - 1960s. Unfortunately, in the wake of this unsuccessful campaign, efforts towards the treatment and elimination of malaria waned. Today, recognition of both the health and economic cost of uncontrolled malaria transmission has led to a re-invigorated effort to control, and ambitiously, eradicate malaria from human populations (2, 3). While current techniques for reducing malaria burden such as indoor residual spraying, use of insecticide-treated mosquito nets and post diagnosis drug treatments may prove effective in eliminating malaria from areas of low or intermittent transmission, there is wide acceptance that these approaches alone will not be sufficient to block malaria transmission in high intensity areas (4). Development of new technologies will thus play a vital role in future initiatives, with one of the leading focuses being vaccination.

1.1.1. Malaria Life Cycle

Plasmodium parasites have a multi-stage life cycle split across the female *Anopheles* mosquito (definitive host) and the vertebrate host (Figure 1-1). The life cycle can be split into three major stages.

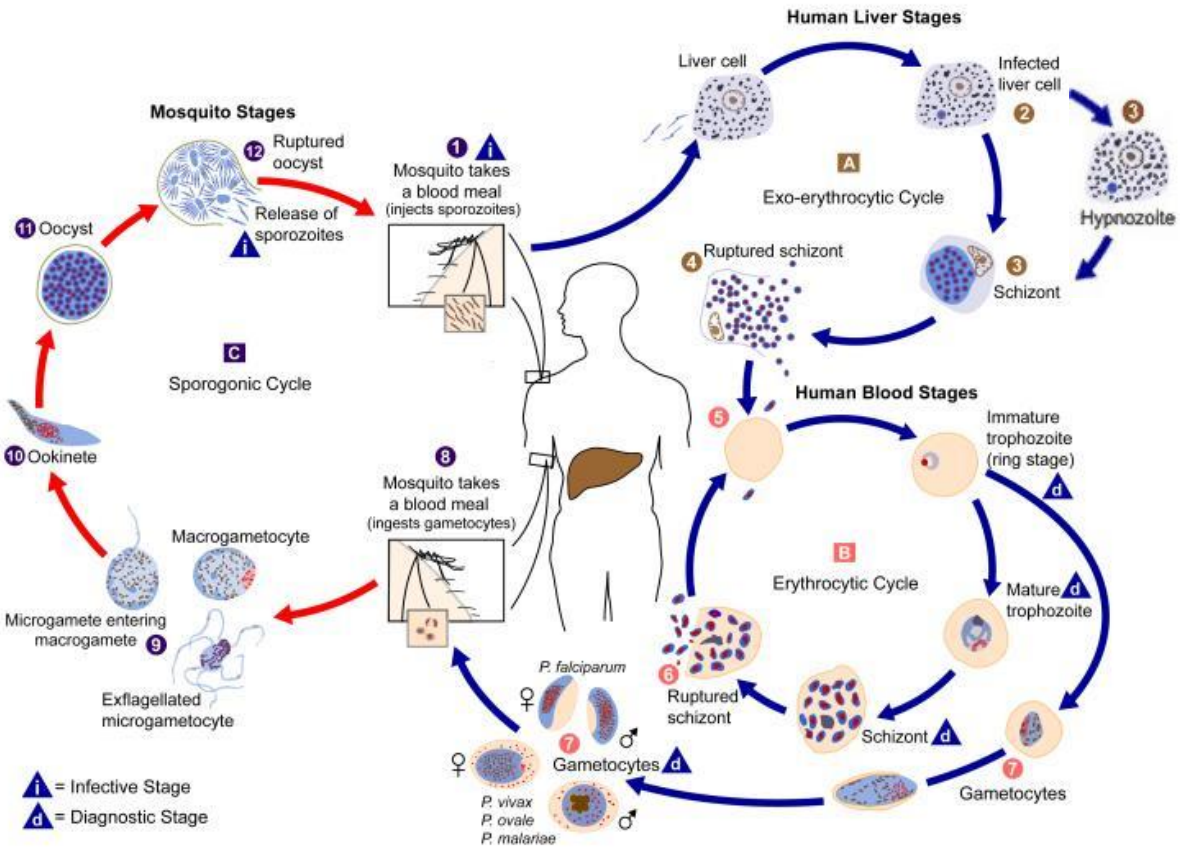

Figure 1-1. *Plasmodium* life cycle.
The multi-stage life cycle of *Plasmodium* parasites involves stages in both the human host (blue arrows) and the female *Anopheles* mosquito (red arrows). Adapted from (5).

Pre-erythrocytic stage: As an infected female *Anopheles* mosquito takes a blood meal, it injects sporozoites, the infective, motile stage of the malaria parasite, into the dermis of the vertebrate. The infectious inoculum only represents a fraction of the parasite load in the mosquito salivary glands and is typically about 15 sporozoites for *P. falciparum* (although this has been reported as high has 1000) (6, 7). Sporozoites then migrate away from the bite

site over the course of an hour or more with approximately 70% finding their way into the blood, and the remainder entering the lymphatic system (8, 9). Those in the blood stream make their way to the liver and exit the circulation predominantly through Kupffer cells lining the sinusoids (10). Sporozoites can be found in the liver as soon as two minutes after introduction to the circulation (11). Several hepatocytes are traversed by breaching their plasma membranes followed by rapid repair before the parasite finally infects a hepatocyte via the formation of a parasitophorous vacuole (12). Once a hepatocyte is infected the parasite multiplies over several days to form 1000s of merozoites, the erythrocyte infective form of the parasite. Eventually, the infected hepatocyte buds off vesicles of several thousand infective merozoites (merosomes) into the blood which can stay intact for over an hour (13, 14).

Erythrocytic stage: The erythrocytic stage of malaria is responsible for the pathology associated with disease, with ongoing replication of the parasite approximately every 48 hours (depending on the species) leading to the cyclical nature of fevers. Infection and replication in the blood is mediated by merozoites, ~1μm long cells which are highly specialised for the invasion of erythrocytes. Once released into the circulation, it takes less than one minute for a merozoite to find a cell to invade. Upon contact between any part of the merozoite and an erythrocyte, the merozoite quickly reorients itself onto its apical end. This allows the deployment of specialised invasion organelles, namely the rhoptries and micronemes, to initiate the invasion event. An irreversible tight junction forms between the merozoite and the erythrocyte, signifying commitment to invasion, which moves around the merozoite as it moves into the host cell via an actin-myosin motor anchored to the merozoite inner-membrane complex (15). Assuming that invasion efficiency is similar *in vivo* to that observed *in vitro*, the entire invasion process occurs in 30 s (16) meaning that in total the merozoite is only exposed, outside the erythrocyte, for <2 min. Within 5 h of invasion, the

parasite will have developed into a ring and have started exporting proteins to the erythrocyte membrane (17). Replication of the parasite at this stage of the life cycle is asexual, with nuclear division occurring by cytokinesis and only occurring once the parasite is inside the erythrocyte. The parasite develops through early and late trophozoite stages before becoming a schizont with 16-32 (for *P. falciparum*) discernible new merozoites. When the new merozoites are mature, the erythrocyte ruptures expelling them into the plasma. These merozoites go on to infect new erythrocytes, thus forming an exponential growth phase within the parasite life cycle.

Sexual stage: Instead of continuing within this asexual replicative cycle, a small percentage of parasites in the blood become sexual cells, or gametocytes. This is essential for malaria parasites to be transmitted through the mosquito. Recently, PfAP2-G has been identified as the transcriptional switch controlling sexual differentiation, and it is suggested that stochastic activation could explain biological gametocyte levels (18, 19). Alternatively, it is also possible that the PfAP2-G switch is activated by exosome mediated cell-cell communication between infected erythrocytes (20). When a female *Anopheles* mosquito feeds on an infected vertebrate, erythrocytes containing mature gametocytes are taken up (along with asexual forms of the blood-stage parasite which will ultimately die). The change in temperature and pH experienced by parasites as they enter the mosquito gut causes the gametocytes to lyse their encasing erythrocyte and form gametes. The male gamete exflagellates and moves through the blood meal to make contact with, and fuse to, a female gamete for fertilisation. Over 18-24 h, the resultant zygote develops into an ookinete which traverses the mosquito midgut epithelium and implants between the midgut epithelium and the basal lamina. Here, the ookinete differentiates into an oocyst in which, over the course of 6-10 days, sporozoites develop (21, 22). Mature sporozoites asynchronously rupture from the oocyst and migrate to

the salivary glands ready to infect a new vertebrate upon mosquito feeding, thus completing the life cycle.

1.1.2. *Plasmodium falciparum*

Of the five *Plasmodium* species that infect humans, *P. falciparum* is the most prevalent (23), with an estimated 220 million cases, and over 0.6 million deaths every year (2, 24). The majority of the mortality burden is borne by children under the age of five in sub-Saharan Africa as well as pregnant women, although it also occurs across the tropics of South America and Asia (Figure 1-2). Furthermore, in Africa alone, the burden of disease is estimated to have an economic cost of over US$ 12 billion annually (3).

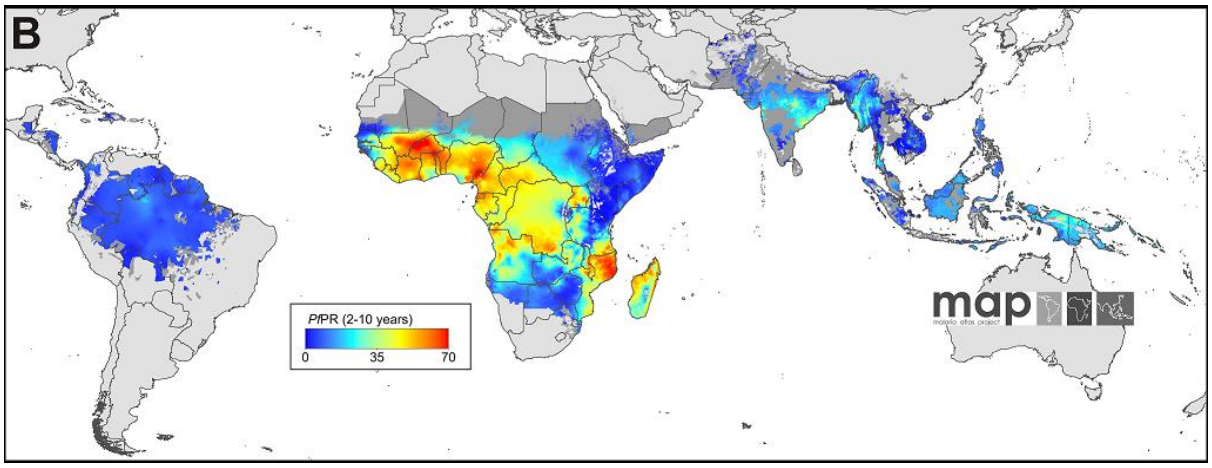

Figure 1-2. 2010 spatial distribution of *P. falciparum* endemicity

Estimates of the annual mean parasite rate (PfPR) in children aged 2-10 years within areas of stable *P. falciparum* transmission. Medium grey areas depict areas of unstable transmission (*P. falciparum* annual parasite incidence (*Pf*API) < 0.1 per 1,000 per annum) and light grey where there is no risk of malaria (*Pf*API = 0 per 1,000 per annum) (25).

As a result of the high burden of disease and level of mortality, *P. falciparum* has been by far the most studied of the five human malaria species. The development of techniques for long term *in vitro* culture of *P. falciparum* in erythrocytes during the 1970s (26) further

accelerated work on *falciparum* malaria and has been vital in understanding the parasite's invasion biology and subsequent development of anti-malarial drugs and vaccine candidates.

1.1.3. *Plasmodium vivax*

P. vivax is the most geographically widespread of the *Plasmodium* species to infect humans with up to 2.5 billion people at risk and 80 million clinical cases each year particularly across South America and South-East Asia (Figure 1-3). Infection leads to an incapacitating, relapsing disease with symptoms including acute respiratory distress syndrome, vicious paroxysms, fever, severe anaemia, and in extreme cases, death (27).

The *P. vivax* life-cycle differs from that of *P. falciparum* in two important ways. Firstly, *P. vivax* is able to stay dormant in the liver for anything from several weeks to years after initial infection meaning that relapses of the disease are possible after leaving a malaria infected area (28). This is achieved via a specialised form of the pre-erythrocytic stage parasite known as the hypnozoite. What causes a subset of parasites to become hypnozoites instead of progressing along the normal development pathway and dividing into merozoites, and the subsequent trigger for a parasite to escape dormancy and cause a new wave of infection, remains unknown (29). Secondly, once in the blood, *P. vivax* merozoites almost exclusively infect reticulocytes (30). Again, the exact receptors and interactions that lead to this reticulocyte restriction remain unknown. While both *P. falciparum* and *P. vivax* have at least one member within each of the two major protein families involved in erythrocyte invasion, the erythrocyte binding-like (EBL) and the reticulocyte binding-like proteins, unlike *P. falciparum* which has multiple redundant micronemal EBL proteins (EBA-175, 140, 181 and EBL-1) it can utilise for erythrocyte invasion (31, 32), *P. vivax* relies on an essential interaction between the Duffy antigen receptor for chemokines (DARC) on the erythrocyte surface and the parasite's Duffy binding protein (DBP) (33). The necessity of this interaction

is exemplified by the virtual disappearance of *P. vivax* from sub-Saharan African and Papua New Guinean populations where Duffy blood group negativity has arisen (Figure 1-3) (34-36).

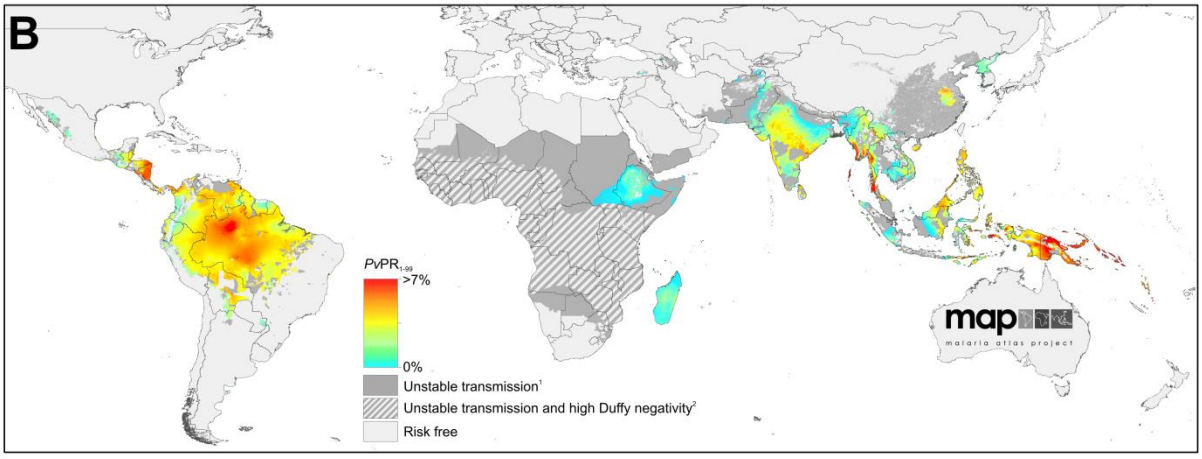

Figure 1-3. 2010 spatial distribution of *P. vivax* endemicity

Estimates of the annual mean parasite rate (PvPR) in people aged 1-99 years within areas of stable *P. vivax* transmission. Medium grey areas depict areas of unstable transmission (*P. vivax* annual parasite incidence (*Pv*API) < 0.1 per 1,000 per annum) and light grey where there is no risk of *P. vivax* malaria (*Pv*API = 0 per 1,000 per annum). Striped areas indicate locations where Duffy negativity is predicted to be >90% (37).

Despite the significant burden of disease caused by *P. vivax*, it has been overlooked for many decades. Yet if new ambitious calls to eradicate malaria are to be met, it is obvious that strategies involving *P. vivax* will be essential. A major hindrance to the study of *P. vivax* to date has been that, unlike *P. falciparum*, long term *in vitro* cultures of *P. vivax* parasites are not possible (38). The development of a reproducible *in vitro* culture technique for *P. vivax* would be a significant breakthrough in the field and would greatly assist the acceleration of studies into *P. vivax* biology and prevention.

1.2. Pathogenesis of Malaria

Only about 1% of malaria infections result in severe disease, with disease progression being influenced by both parasite factors such as species, multiplication rate and antigenic variation, as well as host pre-existing immunity, age and genetic traits. Most infections result in an uncomplicated mild cyclic fever which resolves as the body's immune system eliminates the disease, but can also include headaches, fatigue, vomiting and nausea. However, in non-immune individuals, especially children under the age of five, disease can progress to severe malaria, an often fatal condition encompassing cerebral malaria, metabolic acidosis, and severe anaemia (39, 40).

An important feature of *Plasmodium* biology is its ability to cause infected red blood cells (iRBC) to adhere to the vascular endothelium, which likely evolved as a way to avoid being cleared in the spleen. While causal mechanisms of iRBC sequestration in pathology remain debated, sequestration mediated by the interaction between parasite antigen PfEMP1 and host endothelial protein C receptor has been associated with severe disease (41). Resultant obstruction of blood flow through capillaries may reduce blood flow in the brain resulting in neuronal death and coma as typical in cerebral malaria. Additionally the high concentration of iRBCs and free haem from lysed red blood cells (RBCs) at the site of sequestration may lead to high levels of proinflammatory cytokines as well as reactive oxygen species (ROS) being produced by host immune cells, thus causing damage to the blood brain barrier and leading to cerebral oedema (40, 42). Similarly in the periphery, obstruction of microvasculature by sequestered iRBCs could reduce oxygen delivery and thus lead to hypoxia in downstream tissues. The resultant metabolic acidosis is the most important determinant of survival and has been related to the development of respiratory distress (39, 43). Finally, severe anaemia is a common manifestation of malaria infection. Anaemia is

likely not only to result from the lysis of iRBCs, but more importantly from the haemolysis of uninfected RBCs (44); a concurrent impairment in erythropoiesis driven by cytokines such as tumour necrosis factor α (TNFα) and interferon γ (IFN-γ) released in response to schizont rupture; and hepcidin upregulation restricting dietary iron uptake and locking iron within macrophages (45-47). Increased deposition of complement protein C3b on uninfected erythrocytes in malaria infected children has been suggested as a mechanism for the increased clearance of uninfected RBCs (48).

Importantly, malaria pathogenesis is often complicated by the presence of co-infections, making the range of symptoms and progression of disease even more diverse than that described here.

1.3. Models for studying malaria

Non-human *Plasmodium* species have been essential in the study of malaria and the testing of vaccine candidates. In particular, rodent malaria models have been extensively utilised. There are four species of rodent malaria (*P. berghei*, *P. chabaudi*, *P. vinckei* and *P. yoelii*) and a number of different strains within these species. Some strains cause lethal disease (e.g. *P. berghei ANKA* and *P. yoelii YM*) in various strains of laboratory mouse, while infections with others are naturally resolved. Like the human malaria species, different rodent malarias vary in their morphology, cell invasion preference and pathologies, and thus are suited to different study types. The two lethal strains mentioned here are the most commonly used for vaccine studies. Importantly, the role of Fc-dependent immune mechanisms in protection against these two species differs, with *P. berghei* being controlled by Fc-dependent mechanisms (49), while protection against *P. yoelii* infection is Fc-independent, or at least independent of functional γ-chain signalling (50). Thus results must be carefully interpreted in the context of the chosen model when conducting vaccine and other immunological studies.

The utility of mouse models for studying human malaria immunology and vaccine development remains debated (51). Not only must differences in parasite species be considered, but also important fundamental differences between human and murine immunological processes can make results difficult to extrapolate. However due to the ability to use multiple different parasite species in combination with different mouse strains (especially genetically modified mice), rodent malaria models continue to constitute powerful tools for studies on malaria immunology, pathology and vaccine development.

1.4. Genetic Resistance to Malaria

There are a number of genetic traits which have been associated with reduced rates of malarial disease in human populations. One example is glucose-6-phosphate dehydrogenase (G6PD) deficiency which affects over 400 million people worldwide and leaves erythrocytes more susceptible to damage by reactive oxygen species. The abundance of this X-linked trait is attributed to the fact that heterozygote females and hemizygote males are protected from severe malaria (52). Like G6PD deficiency, many additional genetic polymorphisms influencing immune pathways and processes have been implicated in affecting malaria disease progression (53). However, genetic traits affecting cell phenotype and morphology are also capable of affecting disease progression. As mentioned in Section 1.1.3, Duffy negativity has arisen across much of sub-Saharan Africa protecting the population from *P. vivax* disease progression (35, 36). Probably the most well studied genetic trait affecting malaria is sickle cell trait (HbS). While homozygosity (SS) of the trait results in anaemia and a relatively severe pathology, heterozygosity (AS) is associated with protection from malaria (54). This protection is likely imparted by a combination of impaired invasion, and reduced growth of parasites in affected RBCs (55). The relative abundance of sickle cell trait in malaria endemic areas highlights the selective pressure imparted by malaria infection.

1.5. Immunity to Malaria

Along with genetic factors affecting cellular morphology, the host immune system is the most important factor determining the outcome of malaria infection. Upon entering the human body, the malaria parasite is subject to multiple waves of the human immune response which attempt to pacify the pathogen. Both innate and adaptive immune responses play pivotal roles in the response to malaria infection.

1.5.1. Innate immunity

The innate immune system provides the first line of defence against infection once physical barriers such as the skin are breached. This defence system acts very rapidly to give a broadly specific effector response. Importantly however, no long-lasting immunological memory is conferred from the innate immune system. It is likely that innate immunity to malaria acts to control parasite density and is effective against multiple parasite strains, but that acquired adaptive responses are required to completely control and eliminate the parasite (56, 57).

1.5.1.1. Toll-like receptors

Pathogens are initially recognised by germline-encoded pattern recognition receptors such as Toll-like receptors (TLR) which signal through MyD88 and/or MAP kinases to activate NF-κB and subsequent regulation of immune and inflammatory genes (58, 59). The roles of TLRs in *Plasmodium* recognition and disease progression are not completely understood. TLRs are, however, thought to recognise *Plasmodium* infection in two ways. Firstly, different parasite glycosylphosphatidylinositol (GPI) motifs are recognised by TLR2/TLR1, TLR2/TLR6 heterodimers and to a lesser extent by TLR4 (60). Genetic variants which reduce the expression of TLR1 and TLR6 have been associated with increased incidence of malaria (61) highlighting the potential importance of this recognition pathway. However, it is thought

that GPI may contribute to severe disease by inducing a proinflammatory response, initiated by TLR signalling, which contributes to advanced clinical pathology (62). Secondly, TLR9 is activated during the blood-stage of the malaria life cycle by CpG motifs present in *Plasmodium* DNA. Importantly, parasite DNA binds to haemozoin (the waste product from digestion of haemoglobin) which is targeted to the endosome and thus brings the parasite DNA in contact with TLR9 to allow activation (63, 64). Again, polymorphisms in TLR9 have been associated with an increased risk of malaria highlighting the importance of TLR recognition in disease progression (65).

1.5.1.2. Complement system

The serum complement system represents an important part of the innate immune system. Activation via innate pattern recognition receptors or adaptive immune response-induced antibody, initiates a cascade involving over 30 plasma and cell surface proteins (66, 67). There are three described pathways by which complement based immunity can be activated: the alternate pathway whereby continuous hydrolysis of complement protein C3 produces C3b which can covalently bind microbial cell surface carbohydrates or proteins initiating further activation; the mannose-binding lectin pathway which relies on recognition of microbial pathogen associated molecular patterns by mannose-binding lectin associated proteases thus activating the complement cascade; and the classical pathway which is activated by antibodies induced through adaptive immune processes. All three pathways converge at the formation of a C3 convertase and cleavage of C3 leading to opsonisation with C3b. Subsequent formation of the C5 convertase leads to the formation of the membrane attack complex (MAC) via deposition of C5b-9. Importantly, the complement cascade can be deactivated by heating test serum to 56^{o}C for 30 min, greatly assisting the study of

complement and its role in different immune processes and diseases in *ex-vivo* experiments (68, 69).

It seems that a fine balance between complement activation and regulation is important for the pathogenesis of malaria infection. Indeed complement activation occurs during malaria infection (70-72), and can be activated by parasite-specific antibodies (73). The importance of complement in immunity to malaria is supported by genetic studies which associate reduced complement activation ability with higher parasitaemias in patients (74). In addition to MAC formation, complement activation has been shown to induce macrophage phagocytosis of iRBCs and thus potentially assist in the control of disease (75, 76). However, in some circumstances, complement activation may detrimentally affect disease outcome. This may manifest due to associated inflammatory response activation or increased cytoadhesion between iRBCs and endothelial cells (71, 77). Indeed, high-level complement activation has been associated with cerebral malaria (70), and a reduced ability to activate complement has been seen to improve severe clinical outcomes (78). Furthermore, complement-mediated immunity directed toward iRBC, especially in the absence of adequate regulatory proteins, has been implicated in an increased chance of anaemia (75, 76, 79, 80). Thus it remains unclear exactly what level of complement activation is desired for optimal disease outcome.

It is likely, however, that the malaria parasite itself utilises host complement regulatory factors to increase its chances of survival (71). Almost all host cells possess complement regulatory proteins to prevent self-cell destruction under normal physiological conditions (66, 67). Host CD59, a complement regulatory protein, has been shown to be important in preventing lysis of iRBC and thus helping the parasite evade the immune system (81). Furthermore, in the midgut of the mosquito, where complement remains active for

approximately 1 h, *P. falciparum* gametes express PfGAP50 which binds Factor H, a human protein which deactivates C3b and prevents complement-based lysis (82). Preliminary evidence also suggests that MSP3-family proteins on the merozoite may preferentially bind IgM, shielding the merozoite from efficient complement deposition (83).

1.5.1.3. Innate immune cells

A number of different cell types contribute to the innate immune response against pathogens, however, their specific involvement in immunity to malaria has been widely debated and is still the focus of much research (57). Non-phagocytic cells such as eosinophils, basophils and masts cells are particularly important in the protection of epithelial surfaces and are also involved in inflammation and allergy (84). They are particularly effective against parasites, releasing histamine upon pathogen recognition (85, 86). Natural killer (NK) cells are also non-phagocytic with cytotoxic effects mediated through granzyme and perforin release as well as cytokine producing effector functions initiated upon contact with target cells (87). IFN-γ produced by NK cells upon contact with iRBC has been shown to be essential for immunity to *P. chabaudi* malaria (88), and inherent differences in NK cell reactivity have been suggested to play a role in differing susceptibilities of humans to *P. falciparum* infection (89).

Sharing properties of both NK cells and T cells, NK T cells recognise glycolipids presented on antigen presenting cell (APC) CD1d and are activated to secrete IFN-γ and other cytokines within the first hours of infection (90). Despite being present in high numbers in the liver, NK T cells do not appear to effect immunity to pre-erythrocytic malaria, but instead may be important in assisting antibody production important for blood-stage immunity (91). In fact, NK T cell activation may be detrimental to individuals infected with malaria, with early NK T cell IFN-γ induction in mouse models promoting cerebral malaria pathology (92). The

same observation has been made with γδ T cells, with γδ knockout mice being resistant to the development of cerebral malaria (93). γδ T cells bridge the innate and adaptive immune systems. They recognise a broad array of antigens but do not require peripheral maturation or clonal expansion, instead acquiring their effector phenotype during thymic maturation. Unlike the αβ T cell receptor (TCR), the γδ TCR is not restricted to the recognition of peptides bound to major histocompatibility (MHC) molecules (94). Soluble schizont derived non-peptide antigens thus stimulate γδ T cell polyclonal expansion during *P. falciparum* infection (95, 96), which may play an important role in controlling blood-stage replication rates *in vivo* given γδ T cells ability to inhibit parasite growth *in vitro* (97).

There are also a number of phagocytic cells which are involved in innate immunity including macrophages, dendritic cells (DC) and neutrophils. While a number of effector functions of these cell types are stimulated by innate signals such as pattern recognition receptors, in many cases they also constitute an important link between innate and adaptive immunity. Macrophages, for example, have been reported to recognise parasite antigens expressed on iRBCs, such as PfEMP1 with scavenger receptor CD36, leading to induction of phagocytosis (98, 99). However, macrophages also have the ability to present malarial antigens to the adaptive immune system, inducing $CD4^+$ T cell IFN-γ production (100, 101). In fact DCs are professional APCs providing one of the most important links between innate and adaptive immunity. They are the only cell capable of inducing a primary immune response and subsequent immunological memory. They have a high phagocytic capacity, taking up antigens in the periphery before migrating to the lymphoid organs and presenting them on MHC molecules along with co-stimulatory molecules to activate both T and B cells (102, 103). Aside from their role as APCs, the role that DCs play in *P. falciparum* immunity is complex and still being elucidated (104). While blood-stage parasite products have been reported to induce DC maturation (105), it has also been shown that *P. falciparum* infected

erythrocytes are capable of preventing DC maturation and subsequent T cell activation (106). While this tension is yet to be resolved, it is possible that DC activation early in infection is important for initial control of parasitaemia, while down-regulation of proinflammatory signals later in infection helps to prevent severe pathologies.

Neutrophils

Neutrophils, or polymorphonuclear cells (PMN), are one of the innate immune system's most important cellular components. Neutrophils are capable of destroying microbes in four major ways: phagocytosis, the release of granules, respiratory burst, and the production of neutrophil extracellular traps (NETs). The ferocity of PMNs' antimicrobial activities also commonly leads to host cell damage and thus the control and efficient clearance of neutrophils from sites of inflammation is very important (107). As such, neutrophils are programmed to die by apoptosis, and macrophages play an important role in the clearance of apoptotic neutrophils to resolve inflammation (108).

In a process regulated by the rate of neutrophil apoptosis in the periphery, some 1-2 x 10^{11} PMNs are generated each day in the bone marrow of an adult human and upon emerging, circulate for 6-8 h (109). Inflammatory signals generated at a site of infection prompt proximal endothelial cells, especially in post-capillary venules, to express adhesion molecules which are recognised by PMNs causing them to adhere and roll along the endothelium before eventually migrating across the endothelium and into the site of inflammation (109, 110). Once at the site of inflammation, neutrophils have an important role in recruiting and activating other cells types. They express cytokines such as CCL3, CCL12 and TNFα which attract and activate DCs, monocytes and NK cells. They are also capable of activating the proliferation and maturation of T cells and B cells with subsequent T cell production of IFN-γ capable of prolonging neutrophil lifespan (107, 110). Neutrophils' primary function,

however, is in the direct killing of microbes. Efficient phagocytosis is triggered by TLR, Fc gamma receptor (FcγR) or complement receptor recognition of pathogens. PMNs constitutively express all TLRs (except TLR3), and FcγRIII (CD16) surface expression is upregulated upon PMN adhesion to endothelium meaning the cells are highly susceptible to activation once in the tissue (110).

In addition, neutrophils possess an array of granules containing proteins with anti-microbial and tissue digesting activities. These granules are classified into three groups based on their contents and the time during granulocyte differentiation at which they are made (109). Primary, or azurophil, granules contain myeloperoxidase (MPO) which is important for respiratory burst; secondary (specific) granules contain proteins such as lactoferrin which is capable of binding free iron which is essential for some bacterial growth (111) and flavocytochrome b_{558} which is essential for respiratory burst; and tertiary granules which contain gelatinase, a proteinase important for the degradation of all major components of the extracellular matrix (112). Activation of granule release is thus a powerful mechanism for destroying both cells and connective tissue.

As well as releasing anti-microbial granules, and of particular importance to this Thesis, neutrophils utilise respiratory burst to kill invading pathogens. This involves an abrupt, non-mitochondrial reduction of O_2 which can be stimulated by large particles such as bacteria and yeast, molecules involved in cell chemotaxis, bioreactive lipids, and antibodies (113). NADPH-oxidase is the multi-component complex which mediates respiratory burst. It is made up of cytosolic $p47^{phox}$, $p67^{phox}$, $p40^{phox}$, Rac2, Cdc42 and p29 peroxiredoxin, and membrane $gp91^{phox}$, $p22^{phox}$ and Rap1A. Together, membrane bound $gp91^{phox}$ and $p22^{phox}$ heterodimerise to form flavocytochrome b_{558} which functions to transfer electrons generated by the reduction of NADPH at the cytosolic surface across the plasma membrane to be

donated to molecular oxygen, either in the phagolysosome or the extracellular environment (114). Upon adhesion of neutrophils to endothelial cells, neutrophils enter a primed state where specific granules fuse with the plasma membrane inserting further b_{558} into the membrane. Final activation results in the cytosolic components of the NADPH oxidase complex assembling with the membrane bound components at the plasma membrane (Figure 1-4). The resultant electrons transferred across the plasma membrane are accepted by molecular oxygen to form O_2^-. O_2^- can then react to generate a number of further ROS including hydroxyl radicals (OH^-), ozone (O_3), $^1O_2$ and hydrogen peroxide (H_2O_2) via granular enzyme MPO (113, 114). The exact mechanisms by which ROS kill microbes remain debated, however likely processes include the damaging of biomolecules and enzymes, especially those bound to iron-sulphur clusters, by O_2^- and H_2O_2 which causes metabolic defects; and DNA base oxidation and the carbonylation of proteins by hydroxyl radicals (115, 116).

Finally, activated neutrophils are capable of forming NETs which can trap and kill bacteria. This process is dependent on signals generated through NADPH oxidase and ultimately leads to PMN cell death (117). NETs contain a number of granule proteins as well as histones, with chromatin comprising the major structural component (118). NETs are able to capture pathogens and eliminate them due to their high concentration of anti-microbial peptides (119).

The role of neutrophils in malarial immunity remains debated, although they have been shown to be important in animal challenge models (120). Phagocytosis of both free merozoites (121) and iRBCs (122) has been shown to inhibit parasite growth *in vitro* (123, 124), but its relevance *in vivo* remains unknown. Indeed, despite neutrophils' ability to effectively phagocytose gametocytes and gametes, phagocytosis does not appear to play a

significant role in naturally-acquired transmission blocking activity (125). Probably of most relevance is the PMN derived respiratory burst, given the susceptibility of *P. falciparum* parasites to ROS (126, 127).

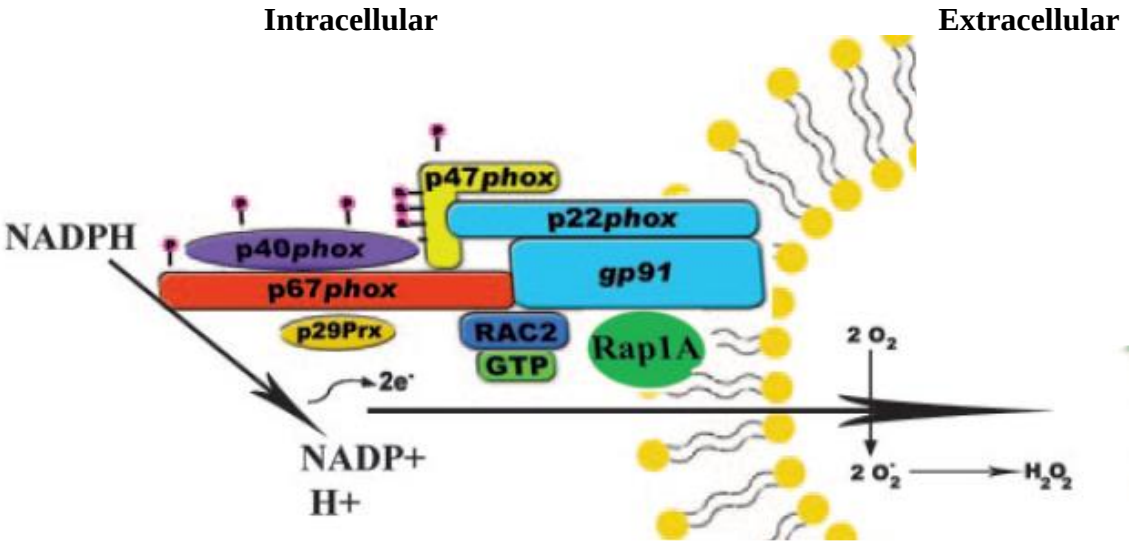

Figure 1-4. Activated NADPH oxidase complex

Representative image showing the NADPH oxidase complex as it would exist in an activated PMN. All components which exist in the cytosol of a resting neutrophil have translocated to the plasma membrane and complexed with b_{558} (light blue) allowing electron transfer across the membrane and the generation of O_2^-. O_2^- is capable of producing further ROS. Adapted from (114).

1.5.2. Adaptive Immunity

In the cases where the innate immune system is not sufficient to overcome an invading pathogen, the adaptive immune system is activated. Innate immune mechanisms play a vital role in this activation (128). Importantly, adaptive immunity is highly specific and is capable of producing long lasting memory. Adaptive immune responses are responsible for naturally-acquired immunity (NAI) to malaria and are the target of vaccination.

1.5.2.1. T cells

The cellular arm of the adaptive immune system comprises T lymphocytes which are activated by the presentation of antigen by APCs on MHC molecules along with other co-stimulatory molecules. T cells are characterised by their surface expression of the T cell receptor/CD3 complex, as well as either CD4 or CD8.

The cell type activated by an antigen relies largely on the source of that antigen. Exogenous particles that are internalised by APCs enter the endocytic pathway and are broken down into peptide fragments by enzymes such as cathepsins (129). MHC class II (MHC II) molecules assembled in the ER bind to the invariant chain and are transported to the late endosomal compartment. The resultant compartment containing antigen peptide fragments and membrane-bound MHC II-invariant chain complex is termed the MHC II containing compartment (MIIC). In the MIIC, chaperone HLA-DM assists the exchange of invariant chain peptide with antigen peptide into the MHC II peptide binding groove. MHC II, bound to its antigen peptide, is then transported to the plasma membrane enabling the antigen to be presented to immune effector cells (130). $CD4^+$ T cells recognise antigen presented on MHC II molecules, and in the presence of co-stimulatory molecules are activated. Once activated, $CD4^+$ T cells act primarily to recruit and activate other cell types.

$CD4^+$ T cells can be further broken down into, among others, Th1, Th2, Th17, T follicular helper (T_{FH}), and T regulatory (Treg) cell subsets according to their cytokine expression profiles. In the presence of interleukin (IL)-12 and IFN-γ, naïve $CD4^+$ T cells will develop into Th1 cells characteristically secreting IFN-γ, IL-2, TNF-α and TNF-β (131, 132). Th1 cells are important in the recruitment and activation of macrophages, NK cells and $CD8^+$ T cells, as well as facilitating the production of opsonising and complement fixing antibodies (133). Th2 cells are activated in the presence of IL-4 and secrete IL-4, IL-5, IL-10 and IL-13.

They are particularly efficient in attracting histamine-producing cells as well as promoting the production of IgE and are thus typically associated with immunity against helminths and other extracellular parasites (131). Th17 cells produce large amounts of pro-inflammatory cytokine IL-17 and are stimulated by TGF-β and IL-6. IL-17 is capable of mediating tissue inflammation and signalling the proliferation and maturation of neutrophils as well as their subsequent homing to sites of infection (134, 135). Indeed reduced neutrophil recruitment due to dysfunctional IL-17 signalling has been implicated in disease progression in mouse models of *Candida* (136). T_{FH} cells express CXCR5 and are important for the formation of germinal centres (GC) within the B cell follicles of secondary lymphoid organs. Activated T_{FH} cells induce B cell differentiation and proliferation to initiate GC formation and then play an important role in ongoing B cell survival. Continual T_{FH} derived survival signalling via CD40L, IL-4, IL-21 and PD-1 is essential for GC maintenance and thus the development of plasma cells capable of secreting high-affinity, isotype-switched antibody (137). Importantly for the prevention of excessive T cell activation and subsequent tissue damage, Tregs act to suppress T cell responses via direct cell contact signalling of apoptosis and the production of immunosuppressive cytokines (138).

Unlike $CD4^+$ T cells, $CD8^+$ T cells are activated when they recognise antigen peptides on MHC class I (MHC I) molecules. MHC I molecules are expressed on all nucleated cells. Endogenous proteins which are degraded into peptides within the cytosolic proteasome are transported to the lumen of the endoplasmic reticulum where they associate with MHC I. The MHC I/peptide complex is then transported through the Golgi to the plasma membrane via the secretory pathway (139). It is also possible for $CD8^+$ T cells to recognise exogenous antigen through cross-presentation onto MHC I molecules which occurs primarily in DCs (140). Activated $CD8^+$ T cells directly kill infected target cells by the secretion of cytokines

such as IFN-γ and TNF-α, ligation of Fas (CD95) by Fas ligand, or the release of cytotoxic granules containing perforin and granzymes (141).

Given that RBCs do not express MHC molecules, T cell derived immunity to malaria is unlikely to affect the erythrocytic stage of malaria as supported by normal courses of blood-stage infection in $CD8^+$ T cell knockout mice (142). $CD4^+$ T cells may play an indirect role in immunity to blood-stage malaria as evidenced in the widely used *P. chabaudi chabaudi* mouse model (143), however, T cell inducing vaccines have so far failed to impact blood-stage growth rates (144, 145). It is, however, widely accepted that T cell immunity can play an important role in vaccine-induced immunity to the pre-erythrocytic stages of infection. In contrast, little evidence exists that adaptive cellular immunity significantly contributes to NAI at the liver-stage in humans, however vaccine-induced T cell responses have been shown to protect animals from malaria and have been associated with protective outcome following experimental vaccination of humans (146, 147). While $CD8^+$ T cells secreting IFN-γ seem to be the key effectors in T cell-mediated immunity to liver-stage malaria (148), $CD4^+$ T cells likely play a role in maintaining a sustained $CD8^+$ T cell response (149). $CD8^+$ T cell derived IFN-γ may bind hepatocyte receptors to induce intracellular changes that prevent parasite growth (150) as well as recruiting IL-12 secreting DCs and macrophages which have been shown to be important for protection against disease, at least in the mouse model (151).

1.5.2.2. B cells and Antibodies

The humoral arm of the adaptive immune system involves B cells which secrete antibodies. Progenitor B cells in the bone marrow undergo genetic rearrangement of their heavy and light chain genes before the expression of immunoglobulin (Ig) molecules (in the form of IgM) on their surface as functional B cell receptors (BCR). These immature B cells are then able to leave the bone marrow and migrate to the peripheral lymphoid organs. Upon binding antigen

for which the particular B cell's BCR is specific, the B cell migrates to the T cell zone of the secondary lymphoid organs enabling the cell to interact with antigen-primed T cells (152). The antigen bound to the BCR is internalised and cleaved into peptides for presentation on the B cell surface in MHC II molecules. This allows $CD4^+$ T cells which recognise the antigen to provide T cell help, signalling both the B cells and T cells to proliferate. Upon activation, B cells undergo somatic hypermutation and class switching, processes mediated by the enzyme activation induced cytidine deaminase, which leads to the introduction of point mutations in the variable regions of Ig genes. This is important for ensuring that antibodies have high affinity for the antigens they recognise. During proliferation, B cells differentiate into short lived plasma cells or enter the germinal centre reaction to form long-lived plasma cells and memory B cells (153). Memory B cells are capable of differentiating into plasma cells upon re-encountering antigen and constitute an important part of long term immunological memory. Plasma cells, or antibody secreting cells, produce large quantities of immunoglobulin and are capable of producing high affinity IgG, IgA and IgE.

Immunoglobulins, or antibodies, are simply the secreted form of the BCR. Their structure was described in the 1970s (154) and since then the importance of this structure in antibody immune function has been well characterised (Figure 1-5). They consist of two identical heavy chains which determine the class of the antibody, and two identical light chains classed as either κ or λ depending on their genetic origin. The heavy and light chains are linked by disulfide bridges. Each of the heavy and light chains have a variable domain (V_H and V_L respectively) as well as constant domains. The folding of the antibody structure brings together the V_H and V_L to form the antigen binding site which is highly specific and, unlike T cell receptors, can recognise conformational epitopes on antigens. The immunoglobulin is structured so that there are two antigen binding regions (Fab) and a single constant region (Fc) (155). Antibodies are capable of imparting their anti-microbial activity in a number of

ways. They can simply bind to antigens and block them from interacting with their intended target effectively neutralising the pathogen; they may opsonise a pathogen, binding to its surface and signalling it to be ingested by phagocytes; or through binging to a pathogen, antibodies may signal through their Fc domain to activate complement pathways, or Fc receptors (FcR) on immune cells to initiate antibody dependent cellular cytotoxicity (ADCC) (156).

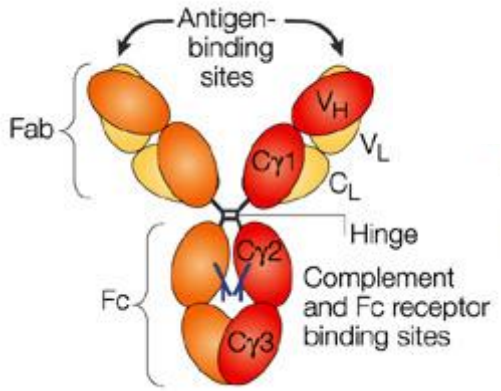

Figure 1-5: Immunoglobulin structure

Immunoglobulins consist of two identical heavy chains and two identical light chains linked by disulfide bridges. Each light chain (yellow) is comprised of a constant domain (C_L) and a variable domain (V_L) and each heavy chain (red and orange) has three (IgD, IgG and IgA) or four (IgM and IgE) constant domains ($C_{1\text{-}3/4}$) and a single variable domain (V_H). In human IgG molecules, as represented here, the Fab and Fc domains are separated by a flexible hinge region. Adapted from (155).

IgG is the most common isotype found in the body with the longest serum half-life. Based on differences of the constant regions of the heavy chain which affect hinge flexibility, among other properties, IgG has been stratified into four subclasses (IgG1-4 in humans and IgG1, IgG2a, IgG2b, IgG3 in mice; Table 1-1). The different constant regions affect a subclass' downstream effector functions, for example by affecting their ability to bind C1q and thus activate the classical complement cascade (in humans IgG3>IgG1>IgG2), and by affecting

the FcRs they bind to and activate (human IgG1 and IgG3 bind all FcγR classes but IgG2 only binds FcγRII) (157).

Table 1-1. Antibody classes and their effector functions

Class	Heavy chain	Subclass	Primary function
IgG	γ	Humans: IgG1, IgG2, IgG3, IgG4 Mice: IgG1, IgG2a, IgG2b, IgG3	Neutralisation, opsonisation, complement activation, induction of phagocytosis, ADCC
IgA	α	Humans: IgA1, IgA2	Dimeric, mucosal immunity, transport across the epithelium, neutralisation, induction of phagocytosis
IgM	μ		Pentameric, natural antibody, neutralisation, opsonisation, complement activation
IgE	ε		Mast cell and basophil activation
IgD	δ		Naïve follicular B cell antigen receptor

It is likely that the humoral immune response utilises many of these antibody effector functions to fight malaria. While some evidence exists that antibodies may play a role in pre-erythrocytic NAI (158), numerous studies have focused on the role of antibody-mediated immunity against the blood-stage of malaria infection. It is known that antibodies are critical for immunity against blood-stage infection from passive transfer studies (159, 160). These studies show that antibody-mediated immunity can be naturally-acquired over the course of multiple exposures to malaria. The exact mechanisms by which this NAI imparts its effect, and against which antigens it acts, remain highly debated with many studies having drawn

associations between antibody responses to certain antigens and their role in protective immunity (161-164). Strong evidence suggests that antibodies to parasite antigens expressed on the surface of iRBCs play an important role in NAI (165-168), further supported by the evolution of high levels of antigenic variation and polymorphism within parasite antigens expressed on the iRBC surface (169, 170). Antibodies directed against iRBC surface proteins, likely opsonise the iRBC signalling it for clearance by circulating phagocytes.

Antibodies are also capable of binding merozoite antigens to prevent the invasion of new blood cells. Antibodies directed to a number of merozoite antigens have been associated with NAI. Of particular interest have been merozoite surface protein (MSP) 1 (171, 172), apical membrane antigen 1 (AMA1) (162), MSP3 and glutamine rich protein (GLURP) (173). Traditionally, however, it has been difficult to compare results between separate cohorts, and where it has been possible, associations between antigen-specific antibody titre and clinical protection are often contradictory. A recent meta-analysis of 33 studies has indicated that antibody responses against $MSP1_{19}$ and MSP3 associated with protection from disease (164). Furthermore, it may be important to consider whether individuals have attained a certain protective threshold of antibody to a given antigen, rather than simply a minimally detectable response (174); or whether individuals have antibody responses to multiple antigens (175).

Invasion blocking activity of naturally acquired antibodies is typically measured using the assay of growth inhibition activity (GIA; Section 1.7.1). Inhibitory activity, as measured by this assay, is detectable in populations from endemic regions (176-178), however, the importance of this activity in reducing disease incidence is unclear (179).

As well as simply blocking parasite invasion, antibodies have also been implicated in protection from malaria infection through the activation of different cell types via their FcRs. This follows from reports showing that protective antibodies from individuals with NAI

incapable of imparting GIA, are able to kill parasites *in vitro* if co-incubated with monocytes (Section 1.7.2)(180). Furthermore, the ability of serum from individuals with NAI to induce Fc-dependent neutrophil activation has been shown to correlate with protection from *P. falciparum* malaria (181).

1.5.3. Fc Receptors

Receptors that mediate antibodies' effect on immune cells were first identified in 1966 (182), and now form a vital part of our understanding of humoral immune effector mechanisms. FcRs are expressed by numerous cells of haematopoietic origin which recognise and bind the Fc fragment of antibodies. FcμR, FcαR and FcεR play important roles in mediating cellular responses to stimulus from IgM, IgA and IgE respectively, and the neonatal FcR (FcRn) is important for transferring humoral immunity between the mother and foetus, as well as preventing the degradation of serum IgG and is thus a major determinant of IgG half-life (183). Type I FcRs including the FcRs which are responsible for recognising IgG (FcγRs) bind IgG Fc in its open conformation, close to the antibody hinge region. In contrast, type II FcRs including DC-SIGN and CD23 bind the Fc region in its closed conformation, a conformation induced by Fc sialylation, between the antibody heavy chain domains C_2 and C_3 (184). Importantly, the binding of IgG to both type I and type II FcRs requires the presence of a core glycan group on the highly conserved Fc glycan site Asn297. Modifications to this glycan act as critical regulators of IgG-FcR binding (184). In this section I focus on FcγRs, though many of the principles discussed apply equally to other FcR types.

With the exception of FcγRIIIb (CD16b), the FcγRs are a family of type I transmembrane glycoproteins consisting of several activating receptors and a single inhibitory receptor (Figure 1-6). Activating receptors with transmembrane domains signal via a cytosolic

immunoreceptor tyrosine-based activation motif (ITAM) composed of a twice-repeated YxxL sequence. These receptors fall into two categories: firstly, receptors with a ligand binding α-chain and a separate ITAM containing signal transduction domain (often the common γ-chain for example); and secondly, single chain receptors capable of signal transduction without association with a separate signal transduction domain (human FcγRIIa [CD32a] and FcγRIIc [CD32c]). FcγRIIIb, which is attached to the plasma membrane of neutrophils by a GPI anchor, lacks an ITAM and signals via association with other FcRs. Importantly, there also exists an inhibitory receptor, FcγRIIb (CD32b), which is capable of countering the activation signals from other FcRs. Like the other FcγRII group members, it is a single chain IgG receptor, however, it contains a immunoreceptor tyrosine-based inhibition motif (ITIM) which has only a single YxxL sequence instead of an ITAM (185).

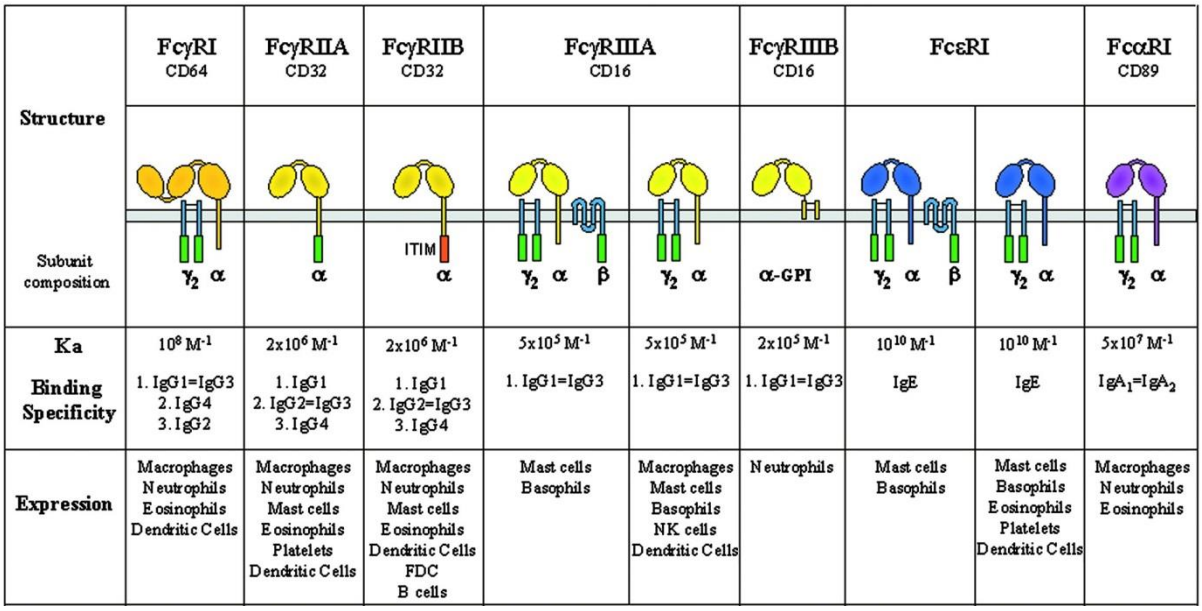

Figure 1-6: Human Fc receptors

Human Fc receptors' structure, binding affinity and specificity for different Ig subtypes, and the cell type on which they are expressed. Lobes on α-chain structures represent Ig-like binding domains. Green rectangles indicate ITAMs while red represents the FcγRIIb ITIM. Adapted from (186).

In general, the nomenclature of FcRs is defined by numbering them according to their affinity for IgG with FcγRI (CD64) being the only known high affinity FcR in both humans and mice with an affinity to human IgG1 and IgG3, and mouse IgG2a respectively of 10^8-10^9 M^{-1}. The other receptors have up to 1000 fold lower affinity for IgGs but generally recognise a broader range of IgG subclasses (186, 187). The higher affinity for IgG exhibited by FcγRI is mediated by a third Ig-like domain in the ligand binding α-chain compared with lower affinity FcγRs which possess only two Ig-like domains (188). Activation of FcRs requires the aggregation of receptors on the cell surface. Due to slight conformational changes and the asymmetry of the Ig Fc domain, each FcR can only bind a single antibody Fc (189, 190), and thus not even FcγRI, which is normally saturated with IgG, can be activated by physiological monomeric IgG. Instead there is a requirement for the presence of immune complexes (IC) to activate FcR signalling.

Upon binding Fc fragments of an immune complex, FcRs become cross-linked which initiates downstream signalling (Figure 1-7). Cross-linking of FcRs induces the phosphorylation of tyrosines on γ-chain ITAMs by SRC family kinases. This initiates signalling which ultimately leads to the activation of immune cells to impart their effector functions. Importantly, SYK dependent pathways stimulated by FcγRs have been shown to be crucial in IgG mediated respiratory burst (191). SYK recruitment of PI3K catalyses the transient production of PI3P proximal to FcR aggregation (192). The generated PI3P binds $p40^{phox}$ (Figure 1-4) ensuring it is retained at the site of IC-mediated activation so that it can localise with, and activate, the NADPH complex for ROS production (193, 194). PI3P dependent activation of RAC has also been shown to be vital for oxidative burst, with RAC forming a complex with $P67^{phox}$ allowing efficient NADPH electron transfer (195).

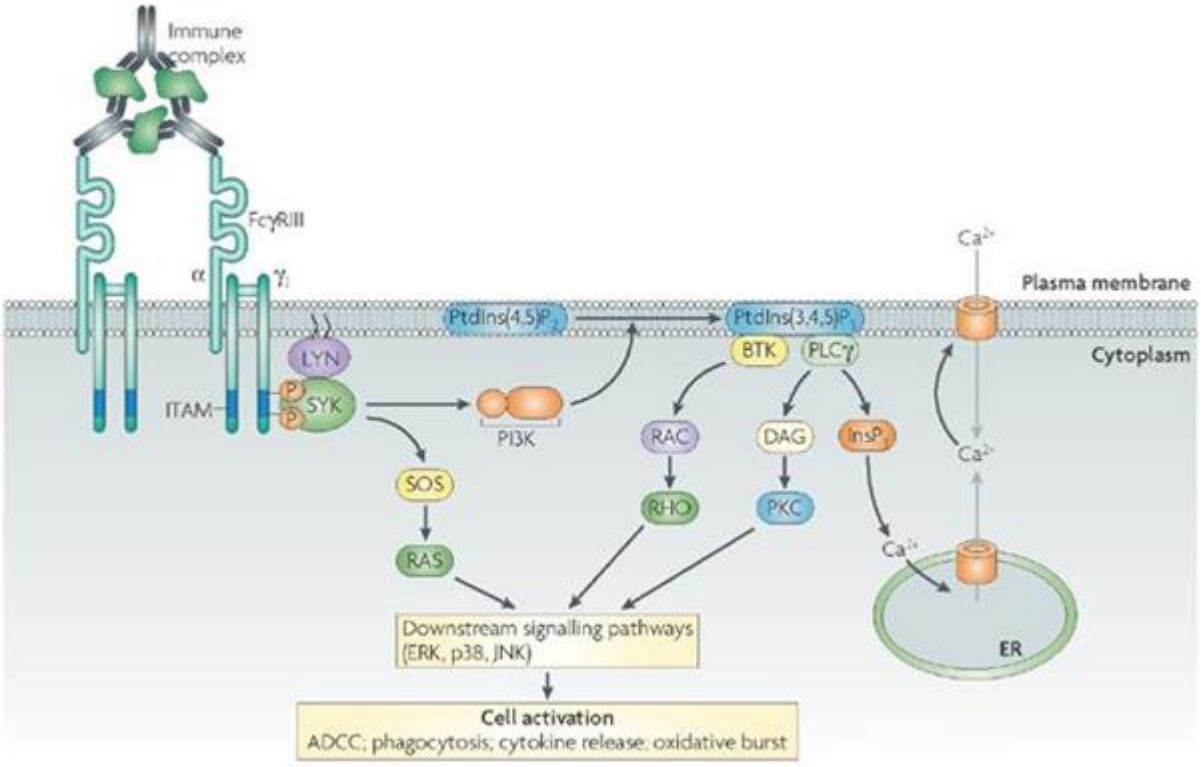

Figure 1-7: Signalling pathways triggered by cross-linking of activating FcγRs

Cross-linking of FcγRs by immune complexes results in ITAM phosphorylation by SRC family kinases. This recruits and allows the docking of SYK family kinases which are able to activate downstream signalling molecules such as phosphoinositide 3-kinase (PI3K) and son of sevenless homologue (SOS). PI3K creates membrane docking sites for Bruton's tyrosine kinase (BTK) and phospholipase Cγ (PLCγ), allowing the PLCγ dependent activation of pathways inducing endoplasmic reticulum (ER) Ca^{2+} release. SOS activation is also important for cellular activation signalling via the Ras-Raf-MAPK pathway. Figure and legend adapted from (156).

FcγRIIb is the only known inhibitory FcγR and plays an important role in regulating the immune response. It is present on all leukocytes except NK cells and T cells. Co-ligation of FcγRIIb and either an ITAM-containing FcR or the BCR results in phosphorylation of the FcγRIIb ITIM by LYN kinase and the subsequent recruitment of SRC-homology-2-domain-containing inositol-5-phosphatase (SHIP). SHIP can then hydrolyse membrane PIP3 and thus abrogates ITAM activation (196). This prevents Ca^{2+} mobilisation and thus blocks Ca^{2+} dependent processes such as degranulation, phagocytosis and ADCC. Similarly, ITIM

phosphorylation can block B cell proliferation via blocking of BCR induced Ras/MAPK activation pathway (Figure 1-8A) (197). This may not prevent B cell activation in all cases, but instead give B cells a higher threshold of IC stimulation for activation. FcγRIIb is also capable of signalling immune cell apoptosis upon cross-linking of multiple FcγRIIb receptors. This signalling pathway is independent of the receptor's ITIM but results from the recruitment of BTK (Figure 1-8B). Importantly, this apoptotic signal is prevented by the recruitment of SHIP upon co-ligation with the BCR or other ITAM containing receptors and has been implicated with the maintenance of B cell specificity following somatic hypermutation (198).

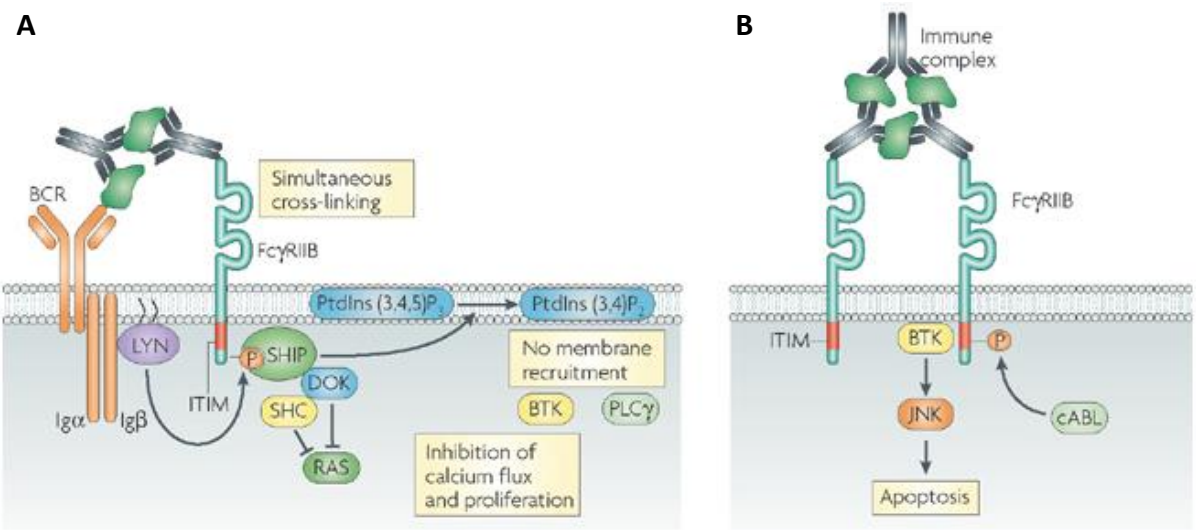

Figure 1-8: Inhibitory FcR signalling

The inhibitory FcγRIIb is capable of preventing cell activation in a number of ways. (A) Crosslinking of activating receptors such as the BCR or activating FcRs and inhibitory FcγRIIb leads to LYN dependent phosphorylation of the ITIM. Subsequent recruitment of SHIP enables the hydrolysis of phosphatidylinositol-3,4,5-triphosphate (PtdIns(3,4,5)P_3) into PtdIns(4,5)P_2 which prevents BTK and PLCγ recruitment. (B) Crosslinking of FcγRIIb only induces B cell apoptosis through ITIM-independent pathways involving cABL family kinases. Adapted from (156).

In reality, activatory and inhibitory receptors are co-expressed on many cell types. Importantly, a threshold between both activatory and inhibitory signalling must be achieved before the initiation of cellular triggering. IgG subclasses differ in their ability to activate this threshold due to their unequal affinities for different FcRs. For example, murine cytophilic antibody subclasses, IgG2a and IgG2b, have far higher affinities for activatory FcRs than the inhibitory FcγRIIb, with activatory to inhibitory (A/I) ratios of 70 and 7 respectively. In contrast, murine IgG1 has an A/I ratio of 0.1 indicating a higher relative affinity for the inhibitory FcR (199, 200). These properties fundamentally affect different IgG subclasses' ability to induce cellular immune activation.

Due to the high degree of inter-species variability in IgG subclass number and characteristics, it is difficult to draw parallels between FcRs of different species. However, due to the utility of mouse models in studying FcR immune mechanisms, some comparisons have been made between human and mouse receptors. Importantly, human FcRs have a much lower affinity for IgG than their mouse counterparts. Mice lack activating FcγRII as present in humans, but the inhibitory FcγRIIb is highly conserved between mice and humans. Instead, the murine FcγRIII is probably most analogous to human FcγRIIa despite the difference in ITAM domains. Mice also possess an FcγRIV which functions similarly to human FcγRIIIa. Mouse monocytes and macrophages express all activating and inhibitory FcγRs whereas neutrophils mainly express FcγRIIb, FcγRIII and FcγRIV. Like in humans, B cells express the inhibitory FcγRIIb (156). Human B cells, however, also express FcRL4 and FcRL5 which bind to complexed IgA and IgG respectively (201).

FcR dependent immune mechanisms have been implicated in immunity to malaria. This has come largely from two lines of evidence. Firstly, the use of Fc γ-chain knockout ($\gamma^{-/-}$) mice and transgenic mice with human FcRs, and secondly associations between FcR

polymorphisms in human populations and susceptibility to malaria infection. As the common γ-chain is required for surface expression and signal transduction of FcγRI, III and IV, $\gamma^{-/-}$ mice lack the ability to activate normal FcγR functions. This model has been used to show that FcRs play a critical role in resistance to *P. berghei* (49), although the opposite has been shown for protection against *P. yoelii* infection (50). Supporting the results seen in *P. berghei* infection, passive transfer of an anti-*P. falciparum* $MSP1_{19}$ mAb into mice transgenic for human FcγRI has been shown to protect against *P. berghei* with *P. falciparum* $MSP1_{19}$ (202), and FcγRIIb deficient mice have been shown to better control *P. chabaudi chabaudi* infection than wild type controls (203). In contrast, mice transgenic for FcαRI were not protected from challenge with *P. berghei* with *P. falciparum* $MSP1_{19}$ when passively transferred with human IgA recognising *P. falciparum* $MSP1_{19}$ (204). In humans, the effect of FcR polymorphisms, especially in FcγRIIa, on malaria infection is well documented and strongly supports the notion that FcRs are important in immunity to malaria (205-211).

1.6. Vaccines

Vaccines have been one of the most cost-effective and instrumental tools in the prevention and control of infectious diseases available to modern medicine. Vaccination aims to stimulate the immune system to mount a response against a pathogen or pathogen subunit and in so doing, create long-lasting immunological memory. On subsequent infections by the pathogen against which a person has been vaccinated, this immunological memory will assist in the mounting of a rapid immune response capable of fighting the present infection. The effect of vaccination was first formally shown by Edward Jenner in the late 18^{th} century where an individual inoculated with the cowpox virus derived protection against the smallpox variola virus (212). From these beginnings, routine vaccination grew culminating with the successful eradication of smallpox declared in 1980 (213). While smallpox remains the only

human infectious disease to be eradicated by means of vaccination (rinderpest, a viral disease of cattle, was also declared as eradicated in 2011 (214)), vaccination campaigns have played essential roles in reducing rates of morbidity and mortality of numerous diseases around the world such as measles, rubella, diphtheria and polio. However, there is still an urgent need for vaccines against some of the world's biggest killers including human immunodeficiency virus (HIV), tuberculosis and malaria.

Early vaccines predominantly consisted of live-attenuated or killed organisms (215), and for malaria, one of the most efficacious vaccines to date has involved whole irradiated sporozoites (216). However due to logistical limitations, the utility of whole sporozoite vaccines remains unlikely. Since the successful development of the recombinant protein hepatitis B vaccine in the 1980s (217), the development of other subunit vaccines has been a major focus, and is potentially a more realistic strategy for malaria vaccine development. The major limitations of this strategy are the difficulty of inducing effective durable immunity against a single target; the difficulty of producing correctly folded recombinant proteins, and the fact that these proteins are often poorly immunogenic, so require adjuvants or structural modifications to increase their immunogenicity; and the stage-specificity of vaccines against pathogens with complex life-cycles. A good example is the current leading malaria vaccine RTS,S which is based on *P. falciparum* circumsporozoite protein (CSP). To attain the exceptionally high antibody levels required for protection, CSP is incorporated into a hepatitis B surface antigen (HBsAg) particle involving a complicated manufacturing procedure and is delivered in a potent adjuvant called AS01 (218, 219). Even then, the vaccine must still be given on multiple occasions to attain protective antibody titres.

1.6.1. Viral Vectored Vaccines

Viral vectors work by infecting cells and delivering gene sequences, which are then transcribed and translated resulting in the expression of antigen within the host cell. The generation of intracellular protein activates the endogenous antigen-processing pathway and thus the direct presentation of antigen peptides on the cell surface in MHC I molecules. Gene secretion or cell apoptosis are likely mechanisms by which antigen is made available to MHC II presentation pathways and cross presentation within DCs. For this reason, viral vectors are able to induce robust cellular immune responses (146). In addition, genes for membrane anchored or secreted proteins delivered by viral vectors have been shown to induce strong antibody responses (220).

Adenoviruses are well characterised dsDNA viruses (34-43kb) which are easy to manipulate and thus lend themselves well to a vaccine delivery platform (221). Adenoviruses used as vectors have been engineered firstly to be replication deficient in human cells through the deletion of the E1 region which is essential for viral replication, and secondly to be able to accept larger transgene inserts via the removal of E3, an immunomodulatory region. Many adenovirus vaccines have been based on human adenovirus serotype 5 (AdHu5). However the high prevalence of pre-existing immunity against AdHu5 within the adult population (~40% in the U.S. and 80% in Africa) (222) has an impact on the immunogenicity of AdHu5 based vaccines and thus their clinical utility (223). As a result, the use of rarer human adenovirus serotypes such as AdHu35 and non-human adenovirus serotypes such as chimpanzee adenovirus 63 (ChAd63) has become common. Some, but not all, of these alternative vectors have been shown to be efficient in inducing strong cellular and humoral immune responses, comparable to AdHu5 (144, 224).

Poxviruses are large enveloped dsDNA viruses with genomes 180-300kb (and thus capable of accommodating large transgene inserts) which replicate in the cytoplasm. Their use as vectors developed out of the original use of cowpox virus to vaccinate individuals against the highly related variola virus which caused smallpox. This was extended to the use of replication competent vaccinia virus which was used throughout the WHO's campaign to eradicate smallpox. Due to safety concerns, an attenuated vaccinia virus, restricted to replication in a limited number of mammalian cell lines, was made by passaging the virus over 570 times in chick embryo fibroblast cells causing the virus to lose over 15% of its genome (225). This virus, named modified vaccinia virus Ankara (MVA) has since been used extensively to immunise people against smallpox and other diseases as a viral vector carrying a transgene. MVA has been utilised to generate malaria vaccine candidates targeting the liver-, blood- and mosquito-stages of disease, inducing strong $CD8^+$ T cell responses as well as serum IgG (226-228).

1.6.2. Prime-Boost Regimes

The magnitude and persistence of an immune response elicited by a single subunit vaccine immunisation is often insufficient to derive any clinical protection against disease. Furthermore, repeated immunisations with a transgene expressed from the same vector often leads to a significant anti-vector immune response, limiting the transgene immunogenicity. As such, heterologous prime-boost regimes were developed that utilise two separate vaccine vectors administered sequentially, expressing the same transgene (229). Initial use of a DNA prime followed by an MVA boost showed good levels of T cell induction (230), however the use of an adenovirus prime followed by an MVA boost has proven to be the most potent regime for inducing high frequencies of antigen specific $CD8^+$ T cells and high titre antibodies (144, 220, 226, 231-233). Importantly, the interval between each immunisation

seems to be crucial in the overall immunogenicity with a longer interval (~8 weeks) being optimal (232, 234).

For blood-stage malaria, where vaccination aims to elicit high titre antibodies rather than T cells, the effective $CD8^+$ T cell inducing ability of an MVA boost may not be necessary. Instead, recent developments have suggested the utility of adenoviral prime – protein-in-adjuvant boost regimes in inducing high titre antibody responses, comparable to 2-3 immunisations of recombinant protein-in-adjuvant (235-237). However a recent study in non-human primates with a leading blood-stage malaria vaccine candidate showed greater antibody induction and protection from *P. falciparum* challenge using an adenovirus-prime – MVA boost regime than one with an adenovirus prime – protein-in-adjuvant boost (Douglas *et al*. submitted).

1.6.3. Blood-Stage Malaria Vaccines

While the most advanced vaccine in the current development pipeline, RTS,S, is a pre-erythrocytic stage vaccine, and despite the fact that many others are currently being studied (reviewed in (238)), here I will focus on vaccines against the erythrocytic stage of malaria infection. The aim of vaccines against the blood-stage of malaria is to interrupt the life-cycle of the parasite and thus prevent disease of the host – either by inducing sterilising immunity, or by allowing for control and clearance of parasitaemia coupled with reduced transmission. As such, vaccines typically target a single antigen, or combination of antigens, present on the blood-stage parasite thought to be important to its survival. Often the selection of these targets is based on serological data from individuals with NAI, however there is an increasing acceptance that “non-natural” immune targets may constitute some of the best vaccine candidates. In the cases where vaccines target candidates identified from individuals with

NAI, vaccine-induced immunity may be able to be boosted by subsequent infections of the parasite leading to long term clinical protection.

While there is now significant pre-clinical work being conducted on a number of blood-stage antigens, the vast-majority of clinical work to date has focussed on two antigens, MSP1 and AMA1 (239). Unfortunately, success of these candidates in the clinic has been limited (144), however an AMA1 vaccine formulated with the adjuvant AS02A has shown strain-specific efficacy in a cohort of Malian children (240). Despite the lack of clinical efficacy associated with vaccines targeting these merozoite antigens, they remain two of the best characterised blood-stage antigens and thus important models for vaccine development studies.

Combination B is another vaccine candidate which has been tested in clinical trials. It consists of ring-infected erythrocyte surface antigen (RESA), MSP1 and MSP2 formulated in adjuvant. This vaccine was found to reduce parasite density in one of two groups of Papua New Guinean children in a Phase IIb trial, though this efficacy was MSP2 allele specific (241). Another vaccine, SPf66, which consisted of a multi-epitope, multi-peptide vaccine construct was found to have limited clinical efficacy after multiple field trials and so was deemed not worthy of further development (242).

Looking forward, a vaccine based on MSP3 as a long synthetic peptide is currently being investigated. Surveillance of the 45 volunteers enrolled in a Phase Ib trial in Burkina Faso following the primary endpoints indicated a reduction in clinical malaria rates in vaccine recipients (243). Also, reticulocyte-binding protein homologue 5 (RH5) has recently emerged as a promising anti-merozoite vaccine candidate showing cross-strain parasite neutralisation *in vitro* (244) and protective efficacy in non-human primates (Douglas *et al*. submitted).

1.7. Identifying New Blood-Stage Malaria Vaccine Targets

Promising early results from new vaccine candidates, such as RH5, highlight the need to identify new candidate antigens. However, for blood-stage malaria, no *in vitro* assay or animal model has been able to reliably predict clinical efficacy in humans. Thus there is an urgent need for the development and validation of new assays to assist in the discovery of new vaccine targets.

1.7.1. Assay of Growth Inhibitory Activity

Currently the 'gold standard' *in vitro* assay for assessing the effectiveness of vaccine-induced or naturally-acquired antibodies against blood-stage parasites, the assay of GIA, measures antibodies' cell-independent ability to neutralise parasites, and thus block their ability to invade or grow within erythrocytes (179, 245, 246). Most commonly, the assay involves mixing purified IgG from recipients of test vaccines or individuals with NAI with *P. falciparum* parasites in an *in vitro* culture and monitoring parasite growth across a single cycle of growth. GIA has been associated with decreased risk of malaria, however a low specificity of this association limits the predictive ability of GIA with clinical protection (247). While it seems highly likely that antibody GIA-type neutralisation is an important effector mechanism for some anti-malarial antibodies, vaccine candidates selected on the basis of promising GIA induction have so-far shown limited efficacy in clinical trials. For example, the highest levels of GIA yet induced in humans by vaccination was reported for the AMA1/AS02A protein-based vaccine candidate (see Section 1.6.3). In this case, immunised volunteers showed high levels of *in vitro* GIA (77% mean at 4 mg/mL purified IgG) but failed to exhibit any significant clinical efficacy against controlled human malaria infection with homologous 3D7 clone parasites (248). Intriguingly, the same vaccine was reported to induce strain-specific efficacy in a Phase IIb field trial in Malian children (240), however the

number of 3D7-type parasite infections was small, and it remains unreported as to whether protection was associated with *in vitro* GIA.

1.7.2. Antibody-Dependent Cellular Inhibition

Antibody-dependent cellular inhibition (ADCI) relies on the cooperation of serum IgG and blood monocytes. The assay of ADCI is very similar to the assay of GIA, however monocytes are added to the parasite culture (249). The assay was developed from the observation that IgG from individuals with NAI, when passively transferred, could impart protection, but had little GIA *in vitro*. In this case, the addition of blood monocytes to the assay induced high levels of strain transcending parasite inhibition, agreeing with the clinical data (180, 250). ADCI activity relies on IgG3 and IgG1 recognition of merozoite surface proteins and subsequent engagement of both FcγRIIa and FcγRIIIa to induce the release of monocyte soluble factors such as TNF-α. TNF-α release is capable of arresting parasite growth at the single nucleus stage (251, 252). Using this assay, MSP3 (253), GLURP (254), and serine repeat protein (SERP) (255) have been identified as potential vaccine candidates. While a vaccine targeting MSP3 has entered clinical trials (256), comprehensive data associating ADCI with clinical outcome in a vaccine trial is not available. In addition, a critical issue of poor assay reproducibility has prevented the widespread uptake of the ADCI assay as a vaccine development tool by the malaria research community.

1.7.3. Antibody-Dependent Cellular Cytotoxicity

Antibody-dependent cellular cytotoxicity (ADCC) is mediated by NK cells, predominantly through FcγRIIIa signalling, and has been studied extensively in the field of tumour immunotherapy (257). Given the demonstrated role of NK cells in immunity to *P. chabaudi* (88), the potential role of NK cells in susceptibility to *P. falciparum* malaria (89), and the fact that the assay is already used widely in the field of antibody-mediated tumour killing, the

ADCC assay may indeed be a useful tool for the investigation of FcR-dependent immunity in malaria. Unfortunately, no work to date has been done with ADCC and *P. falciparum*.

1.7.4. Phagocytosis Assays

The most common and widely used phagocytosis assay for studies on malaria is a flow cytometry based assay which assesses human monocytic THP-1 cells' ability to phagocytose free merozoites (258). The assay is FcR dependent and has been shown to have good inter-assay reproducibility. Sera from individuals with NAI induce higher rates of THP-1 phagocytosis than non-immune controls and this activity has been associated with reduced risk of clinical malaria (259, 260). Other assays describing phagocytosis of iRBCs (261), and phagocytosis mediated by neutrophils (262) have been reported. These assays all show potential utility, but have yet to be extensively applied to malaria vaccine development.

1.7.5. Antibody-Dependent Respiratory Burst

The antibody-dependent respiratory burst (ADRB) assay assesses antibodies' ability to activate neutrophils to produce ROS. Oxidative burst is measured by means of a luminol-based chemiluminescent reaction. Sera from immune individuals have recently been shown to be able to induce ROS production both intra- and extra-cellularly in a process dependent on FcγRIIa (263). Furthermore, ADRB activity has been associated with clinical protection in a single study based in Senegal (181). ADRB is a major focus of this Thesis, and until now, has not been applied to the field of malaria vaccine development.

1.7.6. *P. vivax* Assays

Unlike *P. falciparum*, long term *in vitro* cultures of *P. vivax* parasites are not possible (38), and as such, alternative and innovative methodologies must be utilised to assess the function of antibodies induced by vaccination. The development of human red blood cell adapted *P.*

knowlesi and the possibility for development of parasite lines transgenic for *P. vivax* proteins presents one such methodology enabling GIA-like assays (264). A simple binding assay has also been described which assesses antibodies' ability to block the essential interaction between DARC and DBP (265) allowing the assessment of vaccine-induced antibodies to mediate this activity.

1.8. Thesis Aims

Given that the updated 2030 Malaria Vaccine Technology Roadmap is calling for a vaccine to exert 75% efficacy over at least two years, for both *P. falciparum* and *P. vivax* (266), it is clear that new strategies for identifying vaccine candidates are needed. This requires assays capable of assessing immunity to blood-stage malaria, whether induced by vaccination in pre-clinical studies or early clinical trials, or from naturally-immune individuals, which are also capable of predicting subsequent clinical efficacy. Unfortunately, the assays currently used in the field have not been able to reliably achieve this.

As described in this Introduction, ROS is an important mediator of immunity against intra-cellular pathogens and cytophilic antibodies are capable of inducing neutrophils to produce ROS via FcR dependent mechanisms. Given that initial reports indicate an association between antibody mediated ROS production and clinical efficacy against *P. falciparum* malaria, and that numerous FcR polymorphisms have been associated with the clinical outcome of malaria infection, it is reasonable to hypothesise that an assay measuring antibodies ability to induce ROS production in response to malaria parasites, or particular parasite antigens, would be a useful tool in the study of vaccine-induced, and naturally-acquired, immunity to blood-stage *P. falciparum* malaria.

In addition, the development of assays to be used in studies of *P. vivax* vaccine candidates is also essential if the Malaria Vaccine Technology Roadmap milestones are to be met. Given

that the interaction between *P. vivax* DBP and DARC is known to be essential for parasite invasion, the development of assays assessing this interaction are vital.

This Thesis thus set out to address the challenges above with the following overall aims:

1.8.1. Aims

- To develop and characterise the ADRB assay, assessing antibodies' ability to induce neutrophil ROS production against malarial antigens and whole malaria parasites in both murine and human models.
- To investigate the association between ADRB activity and protection against clinical malaria.
- To establish, and demonstrate the use of, a *P. vivax* DARC-DBP binding inhibition assay in the context of a human vaccine clinical trial.

CHAPTER 2

MATERIALS AND METHODS

2. MATERIALS AND METHODS

2.1. Solutions

ACK Lysis Buffer: 8.29 g NH_4Cl (0.15 M), 1 g $KHCO_3$ (1 mM), 37.2 mg Na_2EDTA in 800 mL H_2O. pH was adjusted to 7.4 with HCl before making a final solution up to 1 L with H_2O.

Complete *P. falciparum* Culture Medium: 45 mL of incomplete culture medium, 5 mL of pooled heat-inactivated filter sterilised human serum and 50 µL of 10 mg/mL gentamicin.

Coomassie Brilliant Blue Stain: 1.2 g coomassie blue, 300 mL methanol, 60 mL acetic acid: made up to 500 mL in H_2O.

ELISA Development Buffer: 16 mL H_2O, 4 mL 5x development buffer, 1 tablet pNPP-20 mg (Note: light sensitive, make buffer in foil covered container).

HisTrap Protein Binding Buffer: 20 mM NaH_2PO_4, 300 mM NaCl, 20 mM imidazole, pH 7.4

HisTrap Protein Elution Buffer: 20 mM NaH_2PO_4, 300 mM NaCl, 500 mM imidazole, pH 7.4

IgG purification binding buffer: 0.144 M Na_2HPO_4, 0.056 M NaH_2PO_4, pH 7.2 in H_2O.

IgG purification elution buffer: 0.1 M Glycine pH 2.7: 7.5 mg glycine was dissolved in 800 mL H_2O and pH adjusted to 2.7 with concentrated HCl – made up to 1 L with H_2O.

Incomplete *P. falciparum* Culture Medium: 2.97 g HEPES, 0.025 g Hypoxanthine and 5 mL 100x L-glutamine solution added to 500 mL RPMI liquid and stirred for at least an hour. Final product filter sterilised.

Loading dye: 0.4% orange G, 15% Ficoll® 400, 10 mM Tris-HCl (pH 8.0), 50 mM EDTA (pH 8.0): made up with H_2O.

Neutrophil Buffer: 100 mL Hanks Buffered Salt Solution (HBSS; Sigma-Aldrich, UK), 1 g D-(+)- Glucose Hybri Max, 0.1 g BSA. Filter sterilised.

PBS/Tween 0.01M (PBS/T): (Sigma P3563): NaCl 0.138 M, KCl 0.0027 M, pH 7.4 Tween 0.05%: made by dissolving sachets in H_2O.

Phosphate buffered saline (PBS): 0.01 M (Sigma P4417): NaCl 0.138 M, KCl 0.0027 M, pH 7.4: made by dissolving tablets in H_2O.

Tris-acetate-EDTA (TAE) buffer: Made up from 50x concentrate with H_2O (Fisher BP1332-1)

Digestion Buffer: 50 mM Tris pH 8.0, 2 mM NaCl, 10 mM EDTA, 1% SDS, 1 mg/mL proteinase K.

2.2. Molecular Biology

2.2.1. Agarose Gels

DNA products were separated on 1% agarose gels (unless otherwise stated) with SYBR Safe (1:10,000) in Tris-acetate-EDTA (TAE) buffer by electrophoresis (100 V, 55 min). Samples were loaded in loading dye (1:6) and visualised on a transilluminator. Band size was determined against SmartLadder (Eurogentec) or GeneRuler 1kb (Thermo Scientific) DNA ladders which were run on each gel. For cloning, bands were excised and DNA extracted using the published QIAquick Gel Extraction Kit Protocol.

2.2.2. Mouse genotyping

The genotype of $\gamma^{-/-}$ and CD32b$^{-/-}$ mice was confirmed by PCR. To extract DNA, ear punches (~1.5 mm diameter) were collected and suspended in 20 µL digestion buffer and incubated at 55^{o}C for 20 min, vortexed vigorously and incubated again for 20 min at 55^{o}C. The reaction volume was then made up to 200 µL with H_2O and heated to 99^{o}C for 5 min. Upon cooling PCR reactions were carried out using Expand High Fidelity PCR (Roche). Separate mixtures were made as outlined below for each sample which included 5 µL of DNA extracted from ear punches. Primers oIMR0618, oIMR0619 and oIMR0620 were used to genotype CD32b$^{-/-}$ mice and oIMR0618, oIMR0621 and oIMR0622 for $\gamma^{-/-}$ mice (Table 2-1) as previously described (267). 25 µL of Mix 1 and Mix 2 were combined immediately prior to subjecting the reaction to thermal cycling conditions according to manufacturer's instructions and an annealing temperature of 65^{o}C. A mouse of known genotype, and a reaction containing template DNA were included each time as positive and negative controls respectively. Products were run on 3% agarose gels as outlined in 2.2.1 and bands inspected to ascertain genotype as follows: CD32b$^{-/-}$ = 232 bp, CD32b$^{+/-}$ = 232 bp and 161 bp, CD32b$^{+/+}$ = 161 bp; $\gamma^{-/-}$ = 260 bp, $\gamma^{+/-}$ = 260 bp and 224 bp, $\gamma^{+/+}$ = 224 bp.

Mix 1

1 µL Deoxynucleotide mix. 10 mM of each dNTP

1.5 µL of each primer (x3)

5 µL Template DNA

14.5 µL H_2O

Mix 2

5 µL Expand High Fidelity buffer, 10x without $MgCl_2$

0.75 µL Expand High Fidelity enzyme

8 µL 25 mM $MgCl_2$

11.25µL H_2O

Table 2-1: Oligonucleotide primers used in genotyping of $\gamma^{-/-}$ and CD32b$^{-/-}$ mice

Primer	Sequence
oIMR0618	CTCGTGCTTTACGGTATCGCC
oIMR0619	AAACTCGACCCCCCGTGGATC
oIMR0620	TTGACTGTGGCCTTAAACGTGTAG
oIMR0621	ACCCTACTCTACTGTCGACTCAAG
oIMR0622	CTCACGGCTGGCTATAGCTGCCTT

2.2.3. Restriction digest

20 µL digest reactions were set up as below and incubated at 37ºC for 2 h.

1 µL Total NEB Restriction Enzyme(s)

2 µL (10x) NEB restriction buffer

(2 µL 10x bovine serum albumin (BSA) if required)

x µL Plasmid DNA (0.5-1.0 µg)

x µL sterile distilled H_2O

$\sum$ = 20 µL

2.2.4. Ligation

Digested DNA fragments were isolated from agarose gels and purified using QIAgen MinElute gel extraction kits according to manufacturer's instructions. Ligation reactions were then set up as follows and incubated at room temperature (RT) for 15 min.

6 µL Insert

2 µL Plasmid backbone

1 µL 10x T4 ligase buffer

1 µL T4 DNA ligase

2.2.5. Circular Polymerase Extension Cloning (CPEC)

In cases where restriction digest cloning was not optimal, CPEC was used. PCR amplification and gel extraction were used to attain linearised template DNA into which each construct was to be inserted. Primers to amplify the construct for insertion were designed with the addition of approximately 20mer overlapping homology regions with the template DNA (268, 269). Importantly, homology regions were designed to have a high Tm (68-70^{o}C). The insert was thus PCR amplified and gel extracted.

150 ng of template DNA was then mixed with a molar equivalent of insert, 15 µL 2x Phusion HF Master Mix, and H_2O to make a total volume of 30 µL. The reaction mixture was then subjected to the following thermal cycling conditions.

98°C	30 s	
98°C	10 s	x20
70-55°C (0.1 °C s^{-1})	3 min	
55°C	30 s	
72°C	3 min	
72°C	5 min	

2.2.6. Bacterial Transformation

10-20 µL high efficiency DH5α *Escherichia coli* were thawed on ice before adding 1 µL of plasmid DNA from ligation, In-Fusion cloning, or CPEC reactions. Cell-DNA mixture was then incubated on ice for 15 min before heat shock at 42°C for 45 s and a further 2 min on ice. Cells were then plated onto LB agar plates containing selection antibiotics. For bacteria transformed with plasmids encoding a Kanomycin resistance gene, bacteria were incubated in 100 µL SOC medium at 37°C for 1 h prior to plating. Plates were then incubated overnight at 37°C to allow colonies to grow.

2.2.7. Colony PCR

A sterile pipette tip was touched onto a single bacterial colony and then dipped into a PCR tube containing 12 µL of the below PCR mix. Each tip was then ejected into LB broth with antibiotic for culturing as described in Section 2.2.8.

1 µL each primer (x2)

10 µL 1.1x ReadyMix PCR Master Mix (Thermo Scientific)

The reaction was then thermally cycled under the following conditions

98°C 10 min

98°C 30 s
50°C 2 min } x10
72°C 3 min

98°C 10 s
50°C 30 s } x25
72°C 2 min

Oligonucleotide primers were designed for each construct to anneal outside of the gene of interest and amplify across the inserted gene. PCR products were run on 1% agarose gels and analysed by size.

2.2.8. DNA production

Plasmid DNA was produced by seeding LB broth cultures with single colonies from agar plated *E. coli* transformations or pre-prepared bacterial glycerol stocks. Antibiotics were added to cultures at 1:1000 (Ampicillin) or 1:2000 (Kanamycin and Zeocin). Cultures were incubated at 37°C in a shaking incubator at 225 rpm for 16-24 h. 1 mL culture was mixed 1:1 with 70% glycerol and stored at -80°C for future culturing and DNA preparations. The remaining bacteria were then pelleted by centrifugation at 6000 x *g* for 10 min. Cells were then lysed and DNA extracted as outlined by QIAGEN Mini-, Midi-, Maxi-, and EndoFree Plasmid Maxi-Kit protocols. DNA was eluted in H_2O and concentration determined by

Nanodrop. Sequences were confirmed by outsourcing to Source Bioscience's Sanger sequencing service.

2.2.9. Phenol-chloroform extraction

Residual salt in DNA preparations can reduce transfection efficiency by interfering with DNA/transfection reagent complex formation. Thus to remove salt from DNA preparations after QIAGEN purification, DNA was subjected to phenol-chloroform extraction. DNA was mixed with an equal volume of phenol in a phase-lock tube and spun at 13,000 x *g* for 5 min at 4^{o}C. The DNA layer was then taken and the above process repeated sequentially with phenol-chloroform-isoamylalcohol and then chloroform-isoamyalcohol. DNA was then attainted by precipitation with 70% ethanol before dissolving in H_2O.

2.3. Protein Production

2.3.1. Protein production in *E. coli*

P. yoelii MSP1 19 kDa (PyMSP1$_{19}$), *P. yoelii* MSP1 33 kDa (PyMSP1$_{33}$) and *P. falciparum* MSP1 19 kDa (PfMSP1$_{19}$) (3D7/ETSR allele)-GST fusion proteins as well as GST control were produced in an *E. coli* expression system and purified on GST-affinity chromatography columns as described in J136 (Appendix 1) (232). Protein expression was confirmed by Nanodrop and Coomassie Blue staining (Section 2.3.5). Recombinant PyMSP1$_{19}$ fused to IMX108 (mouse complement C4 binding protein, C4bp) (270) was kindly provided by Dr F. Hill (Imaxio, France). *P. vivax* DBP_RII produced in *E. coli* was kindly provided by Dr Chetan Chitnis (ICGEB).

2.3.2. Protein production in HEK293 cells

A transient HEK293 expression system was used to express DARC.His as well as DBP_RII. Constructs were cloned into expression plasmids as described in Chapter 6 and transfected into HEK293E cells for protein expression as detailed in protocol J238 (Appendix 2).

Culture supernatants were then harvested after centrifugation and adjusted to 300 mM NaCl for purification by affinity chromatography. Cell pellets were treated with 1% n-Dodecyl β-D-maltoside (Sigma) to lyse cells and release internal proteins, before the centrifugation of the disrupted pellet and the harvesting of cell lysate "supernatant". Adjusted supernatants were passed over either a HisTrap Excel column (Sigma, UK) or a HiTrap TALON column (GE Healthcare) and eluted with 500mM imidazole for His-tagged proteins; or supernatant of expression cultures containing proteins with the C-tag purification tag (C-terminal four amino acids: E-P-E-A) were affinity purified using a nanobody affinity resin called CaptureSelect C-tag Affinity Matrix (Life Technologies).

2.3.3. Protein production in *Drosophila* S2 cells

P. vivax DBP_RII constructs were expressed in a *Drosophila* S2 insect stable cell line system. Stable transfections were set up for each protein to be expressed as detailed in protocol J314 (Appendix 3). Once an expression cell line was established and stocks frozen down, cultures were scaled up to approximately 1 L for protein expression. Supernatants were harvested and subjected to tangential flow filtration before purification of proteins. Proteins were affinity purified using C-tag purification tags as described in Section 2.3.2.

2.3.4. Western Blot

Supernatants and purified protein fractions were analysed by Western Blotting to confirm the presence of protein as described in protocol J119 (Appendix 4). Anti-5xHis and protein

specific primary antibodies (where available) were used to detect proteins followed by donkey anti-mouse-AP secondary antibodies.

2.3.5. Coomassie Blue Staining

Coomassie Blue staining was used for the detection of nonspecific protein. As described in J119 (Appendix 4) for Western blotting, samples were run by SDS-PAGE on BioRad Mini-PROTEAN TGX precast gels for 1 h at 100 V with a 10-250 kDa Protein ladder (New England Biolabs). Gels were then washed 3x in H_2O before being stained with Coomassie Brilliant Blue (BioRad Laboratories) for 1 h. Gels were then washed in H_2O for 4x15 min before a final overnight wash in H_2O.

2.4. Immunology

2.4.1. Animals

All procedures were performed in accordance with UK Animals (Scientific Procedures) Act Project Licence and were approved by the University of Oxford Animal Care and Ethical Review Committee. 6–8 week old wild-type (WT) female BALB/c ($H\text{-}2^d$), C57BL/6 ($H\text{-}2^b$) and Tuck Ordinary (TO) outbred mice were sourced from Harlan, UK. BALB/c Fc-gamma common chain knockout ($\gamma^{-/-}$) (271) and C57BL/6 CD32b knockout ($CD32b^{-/-}$) (Jackson Laboratory: 002848) mice were provided from the Queen's Medical Centre, Nottingham, UK and bred at the Wellcome Trust Centre for Human Genetics, University of Oxford, UK. Knockout mouse genotypes were confirmed by PCR (272, 273). Mice were anesthetised with Isoflo (Abbot Animal Health, UK) before immunisation. Immunisation of ZiKa rabbits was outsourced to BioGenes GmbH.

2.4.2. Immunisations

Recombinant human adenovirus serotype 5 (AdHu5) and chimpanzee adenovirus serotype 63 (ChAd63) vectors were administered at 1.5 x 10^9 infectious units (ifu), and modified vaccinia virus Ankara (MVA) vectors at 1 x 10^7 plaque forming units (pfu) unless otherwise stated. When immunising mice, virus vectored vaccines were formulated in endotoxin free low phosphate PBS (Gibco-Invitrogen, UK) and injected intramuscularly (i.m.) in a total volume of 50 µL split equally between each *musculus tibialis*. Adenovirus-prime MVA-boost immunisation regimes were administered eight weeks apart (Ad-M).

Protein vaccines were formulated in Adju-Phos® adjuvant (Brenntag Biosector, Denmark), Addavax™ (Invitrogen) or Abisco-100 (Isconova) and given i.m. at three week intervals (PP or PPP); or as a single 10 or 20 µg dose in adjuvant preceded eight weeks earlier with an adenovirus prime (AP).

2.4.3. Human Serum Samples

UK adult serum and plasma samples (pre- and post-vaccination) were obtained from healthy malaria-naïve adult volunteers receiving immunisation with ChAd63-MVA viral vectored vaccines encoding either *P. falciparum* MSP1 (PfMSP1) or *P. vivax* DBP_RII. These volunteers were enrolled in either Phase I (VAC036, VAC051) or Phase IIa (VAC039) malaria vaccine clinical trials with appropriate informed consent, and regulatory and ethical approvals, as previously reported (144). Sera were tested pre-immunisation (Day 0 or UK) and following ChAd63-MVA immunisation (but the day before controlled human malaria infection for VAC039 [Day C-1]). Where applicable, serum was heat inactivated by heating to 56^{o}C for 30 min.

Kenyan adult sera were collected during adult cross-sectional surveys between 2006 and 2008 from the villages surrounding the Chonyi area in Kilifi, Kenya that experiences moderate malaria transmission with an entomological inoculation rate of 10 – 100 infective bites/person/year; these adults are considered to have substantial naturally-acquired immunity as evidenced by the decline in clinical episodes of malaria with age (274). Hyper-immune serum from this cohort was pooled and used as a positive control in relevant assays. Scientific and ethical approvals for the Kenyan serum samples were granted by the Kenya National Scientific and Research Ethics Committees, respectively, SSC No. 1131. The samples were kindly provided by Dr Faith H. Osier and Prof Kevin Marsh (KEMRI-Wellcome, Kilifi, Kenya).

Malian plasma samples were collected from volunteers in the villages of Kenieroba and Fourda, Mali as part of a cohort study conducted by National Institute of Allergy and Infectious Diseases (NIAID, NIH, USA). The approval of the human study was obtained from the Ethical Review Committees of the Faculty of Medicine, Pharmacy, and Dentistry at the University of Bamako (Mali) and the NIAID (IRB no. 08-I-N120). Individual written informed consent was obtained from all participants.

2.4.4. Cell preparations

2.4.4.1. Preparation of mouse neutrophils

Mouse neutrophils were isolated from bone marrow extracted from the femurs and tibias of 6-20 week old BALB/c, C57BL/6, (Harlan, UK), $\gamma^{-/-}$ and $CD32b^{-/-}$ (Oxford, UK) mice using Percoll (Sigma Aldrich, UK) density gradients and resuspended in neutrophil buffer at 10 x 10^6 PMNs/mL. Purified cells were confirmed to be $Ly6C^{int}$ and $CD11b^{+}$ by flow cytometry and purity was assessed by Giemsa stained slides. To investigate the role of FcR signalling in

ADRB activity, PMNs were incubated for 15 min at 4°C with either rat anti-mouse CD16/32 mAb (clone 93; eBioscience, UK), or control rat IgG (Sigma Aldrich, UK).

2.4.4.2. *In vivo* depletion of mouse neutrophils

In order to deplete neutrophils, mice were injected intraperitoneally (i.p.) with 0.5 mg 1A8 rat mAb (Bio X Cell, USA) (275, 276) one day prior to, and three days following challenge with *P. yoelii* iRBCs. Control animals were given 0.5 mg control rat IgG (Sigma Aldrich, UK) i.p. at the same time points. Depletion was monitored at one and seven days after challenge in the blood and spleen of an additional group of animals as Section 2.4.7 by flow cytometry. The percentage depletion attained was calculated using the number of PMNs ($Ly6C^{int}$ $CD11b^{+}$ granulocytes) per lymphocyte in a mouse treated with control rat IgG compared to the number of PMNs/lymphocyte in a 1A8 treated mouse as follows:

$$\%\ Depletion = 100 \times \left(1 - \left(\frac{(PMNs/lymphocyte)_{1A8}}{(PMNs/lymphocyte)_{Rat\ IgG}}\right)\right)$$

2.4.4.3. Preparation of human neutrophils

Human polymorphonuclear neutrophils (PMNs) were isolated from whole blood collected in EDTA vacutainers (BD Bioscience). 4 mL blood was layered upon 5 mL polymorphprep (Axis-Shield Diagnostics) and centrifuged at 450 x *g* for 40 min. The band containing PMNs was isolated and washed in neutrophil buffer (HBSS, 1% glucose, 0.1% BSA). Contaminating RBCs were lysed with ice cold 0.2% NaCl added for 20 s before the restoration of isotonic conditions. Cell viability was confirmed by Trypan blue (Sigma-Aldrich, UK) exclusion and purity determined by Giemsa stained slide before suspension in neutrophil buffer at 1 x 10^7 PMNs/mL. Cell viability was >99% for all experiments. Giemsa stained slides were examined under a 100x oil immersion objective on a Leica DM2000

microscope and PMN purity assessed in at least 5 fields of view. If PMN purity was <95%, final dilution in neutrophil buffer was adjusted to ensure a final suspension of 1 x 10^7 PMNs/mL. If PMN purity was below 75% due to red blood cell contamination, the RBC lysis step was repeated.

2.4.5. Antibody-Dependent Respiratory Burst (ADRB) Assay

2.4.5.1. Mouse ADRB Assay

Two methodologies were used to assess mouse PMN ADRB activity.

i) Recombinant protein coated plates:

100 µL PyMSP1_{19}-GST or PfMSP1_{19}-GST protein at 10 µg/mL (unless otherwise stated) was adsorbed onto Nunc opaque Maxi-sorp 96-well plates (Thermo Scientific) at RT overnight. Plates were then washed three times with PBS and blocked for 1 h with Casein block solution (Pierce, UK) before a second wash. 100 µL serum diluted 1:100 in PBS (unless otherwise stated), or epitope matched anti-PfMSP1_{19} mouse IgG1 and IgG2a mAbs (277) at 8.3 µg/mL, was then added and incubated for 1 h at 37ºC. Within 2 min of a final wash of the assay plate in PBS, 50 µL isoluminol (Sigma Aldrich, UK) (0.04 mg/mL) and 50 µL of mouse cells at 1 x 10^7 PMNs/mL (unless otherwise stated) were added to each well and luminescence – in relative light units (RLU) – resulting from ROS released by PMNs reacting directly with isoluminol, was read each minute for 1 h using a Varioskan Flash luminometer. The maximum RLU output over the one hour period was determined and used for analysis (Figure 2-1).

ii) *P. yoelii* Parasitophorous vacuolar membrane-Enclosed Merozoite Structures (PyPEMS) in solution:

ADRB activity was assessed by adding 20 µL PyPEMS (see Section 2.5.3) and 5 µL neat sera, to each well of a half-area opaque 96-well plate (Fischer Scientific, UK) and incubating at 37°C for 1 h, before addition of neutrophils and isoluminol as above.

For both assays, RLU readouts were indexed against a positive reference serum from Ad-M PfMSP1 immunised, Ad-M PyMSP1$_{42}$ immunised or twice Py17XNL challenged mice for the PfMSP1, PyMSP1 and PyPEMS assays respectively.

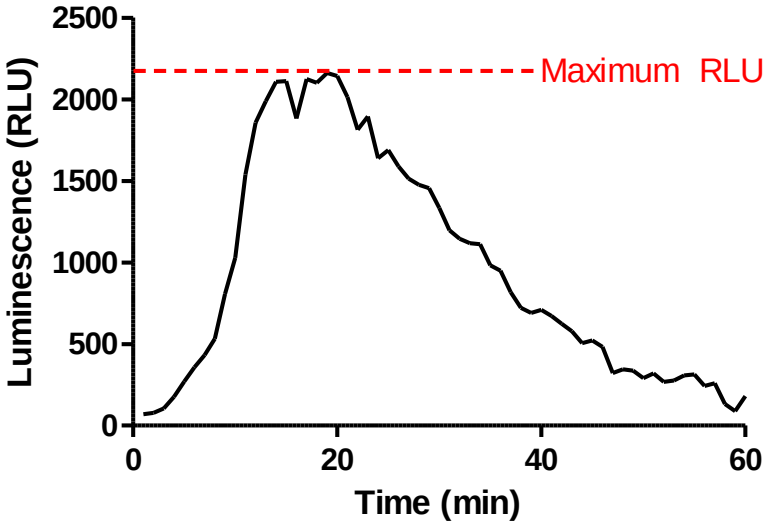

Figure 2-1. Measuring ADRB activity

Typical luminescence trace from a single sample produced by the luminometer for the ADRB assay.

2.4.5.2. Human ADRB assay

i) Recombinant protein coated plates:

100 µL recombinant GST-PfMSP1$_{19}$ (ETSR allele) fusion protein at 10 µg/mL was adsorbed onto Nunc opaque Maxi-sorp 96-well plates (Thermo Scientific) at RT overnight. Plates were then washed three times with PBS and blocked for 1 h with Casein block solution (Pierce, UK) before a second set of 3x washes. 100 µL serum (or plasma where specified) diluted 1:50 in PBS (unless stated otherwise), or an epitope matched anti-PfMSP1$_{19}$ human IgG1, IgG3 or IgA mAb (a kind gift from Prof. Richard Pleass, Liverpool School of Tropical Medicine) at stated concentrations, was then added and incubated for 1 h at 37^{o}C. Within 2 min of a final wash of the assay plate in PBS, 50µL isoluminol (Sigma Aldrich, UK) (0.04 mg/mL) and 50µL of isolated human PMNs at 1 x 10^7 PMNs/mL were added to each well and luminescence was read every 2 min for 1 h.

ii) *P. falciparum* PEMS coated plates:

100 µL *P. falciparum* PEMS (see Section 2.5.1) at 18.5 x 10^5 schizonts/mL was adsorbed onto Nunc opaque Maxi-sorp 96-well plates at RT overnight. Plates were then washed three times with PBS and blocked for 1 h with Casein block solution (Pierce, UK) before a second set of 3x washes. 100 µL serum diluted 1:50 in PBS (unless stated otherwise) was then added and incubated for 1 h at 37^{o}C. Within 2 min of a final wash of the assay plate in PBS, 50 µL isoluminol (0.04 mg/mL) and 50 µL of isolated human PMNs at 1 x 10^7 PMNs/mL were added to each well and luminescence was read every 2 min for 1 h.

2.4.6. Enzyme Linked Immunosorbent Assay (ELISA)

Total IgG ELISAs were carried out using a standardised ELISA methodology (232, 278). Antibody units (AU) were determined by comparison to a standard curve diluted two-fold

down the plate of pooled immune sera for relevant antigen/species combinations. OD was read at 405 nm (OD_{405}) using a BioTek EL 800 Microplate Reader (BioTek, UK). Naïve mouse serum or malaria-naïve human sera were used as negative controls on all plates. Plates were developed until positive control samples reached an OD_{405} of 1.0 and this point was defined as 1 AU, with antibody units being read off the resulting curve (278).

Serum total IgG endpoint ELISAs were carried out as described previously (232). Endpoint titres were defined as the dilution at which sample absorbance reached 3 standard deviations (SD) greater than the OD_{405} for serum from a naïve sample. A standard positive serum sample and naïve serum sample were included as controls for each assay.

Antigen-specific mouse IgG1 and IgG2a responses were also determined with a standardised ELISA method, as previously described (279). Briefly, 96 well plates were coated with *P. yoelii* $MSP1_{19}$-IMX108 protein to avoid measuring responses to GST in mice immunised with $PyMSP1_{19}$-GST. Standard curves were made with purified mouse IgG1 and IgG2a mAb (eBioscience, UK) starting at a concentration of 20 µg/mL and diluted 3-fold. After blocking, test serum was added in duplicate wells and incubated for 2 h before washing. Biotin anti-mouse IgG1 or IgG2a (Becton Dickinson Ltd) was then added for 1 h followed by washing and incubation with Extravidin Alkaline Phosphatase (Sigma-Aldrich, UK) for 30 min. Plates were then developed using the same reagents as for total IgG ELISA and isotype units (IU) calculated as for total IgG AU.

2.4.7. Flow cytometry

2.4.7.1. Mouse neutrophil staining

Whole mouse blood was collected from tail veins into 200 µL 10 mM EDTA in PBS and spleens harvested, crushed and passed through a 70 µm cell strainer before treatment with

ACK lysis buffer to lyse RBCs. Whole blood samples were also lysed in a similar manner. After washing, lymphocyte and splenocyte samples were resuspended in 200 µL and 7 mL 0.1% BSA in PBS (PBS/BSA) respectively. 150 µL of the resulting cell suspensions were surface stained for 30 min at 4ºC with Alexa Fluor 700-labelled anti-CD11b (clone M1/70), APC-labelled anti-Ly6C (clone HK1.4), and PerCPCy5.5-labelled anti-CD8α (clone 53-6.7) (all anti-mouse mAbs supplied by eBioscience). Cells were then washed twice in 150 µL PBS/BSA and resuspended in 200 µL PBS/BSA. Samples were run on an LSRII flow cytometer (BD Bioscience, USA) with stopping gates set at 100,000 $CD8^+$ events for splenocyte samples and 10,000 $CD8^+$ events for lymphocyte samples. Granulocytes were gated by forward and side scatter and neutrophils identified as the $CD11b^+$ $Ly6C^{int}$ granulocyte population. Data were analysed using FlowJo v8.8.7.

2.4.7.2. Human neutrophil staining

Whole blood was collected from healthy volunteers in EDTA vacutainers (BD). PMNs were isolated as above and resuspended in 500 µL 0.1% BSA in PBS (PBS/BSA). 150 µL of the resulting cell suspension was surface stained for 30 min at 4ºC with PE-Cy7-labelled anti-CD16 (clone 3G8), FITC-labelled anti-CD32 (clone 3D3) and PerCPCy5.5-labelled anti-CD64 (clone 10.1) (all anti-human mAbs supplied by BioLegend). Cells were then washed twice in 150 µL PBS/BSA and resuspended in 200 µL PBS/BSA. Samples were run on an LSRII flow cytometer with stopping gates set at 1 x 10^6 total events. Neutrophils were identified as the $CD16^+$ granulocyte population.

2.4.8. DBP_RII binding inhibition assay

To determine the ability of antibodies against DBP_RII raised in mice and humans to block the interaction DBP_RII and DARC, a binding inhibition assay was conducted (265). DARC protein consisting of the first 60 amino acids of the Fy^b variant of DARC (ABA10433.1),

with cysteines 4, 51 and 54 mutated to alanine (280), followed by a thrombin cleavage site, a biotin acceptor peptide and a 6 histidine tag (DARC.His), was coated onto a 96-well clear Nunc Maxi-sorp plate (Thermo Scientific) at 1 μg/mL overnight at 4°C. Test sera at various dilutions were then incubated with 0.05 μg/mL of recombinant DBP_RII at RT for 30 min. The DBP_RII protein used contained C-terminal PK and C-tag purification tags and consisted of amino acids 194-522 of the Salvador I strain (DQ156512.1) DBP with its three N-glycosylation sites mutated (T64A, S160A, T229A). After 30 min incubation, DBP_RII and test sera were added to the DARC.His coated plates. Bound DBP_RII was detected with serum from rabbits taken 70 days after immunisation with Ad-M DBP_RII (1:1000) followed by a secondary AP-conjugated goat anti-rabbit IgG antibody (1:1000). The amount of antibody required to block half the DARC-DBP_RII binding (IC_{50}) was determined by comparing the OD_{405} of a test antibody dilution series with that of a DBP_RII naïve control. Plates were allowed to develop for approximately 1 h until a control containing DBP_RII which had not been incubated with any serum reached an OD_{405} equal to 1.0. All samples were run in duplicate unless otherwise stated.

2.5. Parasitology

2.5.1. *P. falciparum* PEMS

P. falciparum 3D7 clone parasites were routinely maintained in culture with RBCs from healthy UK O^+ donors and in the presence of pooled human AB serum from healthy UK volunteers as previously described (244). To obtain PEMS, cultures were synchronised with D-sorbitol to lyse mature parasites and enrich ring stages (281) on two occasions approximately 42 h apart. Approximately 30 h following the second D-sorbitol treatment, late trophozoites and early schizonts were isolated upon a 65% isotonic Percoll density gradient. Infected cells containing late-stage parasites were then cultured for a further 2-8 h with 10

μM Epoxysuccinyl-L-leucylamido(4-guanidino)butane (E64) (282, 283). Once the culture was confirmed to contain >95% fully segmented schizonts by Giemsa staining, infected cells were washed in PBS before dilution to 18.5 x 10^5 schizonts per mL. The resulting suspension was vortexed vigorously, aliquoted and frozen to rupture the red cell membranes and release merozoites.

2.5.2. *P. falciparum* merozoite lysate

The supernatant of a 20 mL *in vitro* culture of *P. falciparum* at 10% haematocrit and 10-15% parasitaemia was harvested and replaced daily and centrifuged at 830 x *g* to pellet and discard RBCs. After 10 days, pooled supernatant was centrifuged at 1500 x *g* for 25 min to pellet free merozoites (Mz). The Mz pellet was washed twice in PBS and resuspended in 500 μL PBS. The resulting suspension was vortexed vigorously and freeze-thawed in aliquots to form a lysate. Anti-Mz immune sera was generated by immunising BALB/c mice subcutaneously (s.c.) once with 50 μL Mz lysate formulated in 50 μL complete Freund's adjuvant followed by two further s.c. immunisations of 50 μL Mz lysate in 50 μL incomplete Freund's adjuvant at three week intervals. Serum was harvested 21 days later.

2.5.3. *P. yoelii* PEMS

Two TO mice were inoculated i.p. with 100 μL lethal *P. yoelii* YM iRBCs and monitored until blood-stage parasitaemia reached 30-50%. Blood was taken and cultured for 24 h at 8% haematocrit and 37°C to allow parasites to mature to late schizonts. Infected cells were then isolated on a 65% Percoll gradient, washed, and resuspended in PBS before freezing to lyse the RBCs and release the merozoites.

2.5.4. *P. yoelii* blood-stage challenge

Lethal (strain YM) and non-lethal (strain 17XNL) *P. yoelii* were used to infect experimental animals by intravenous (i.v.) injection with 10^4 or 10^6 pRBCs. Blood-stage parasitaemia, calculated as percentage of infected RBCs, was monitored from day three post-challenge by microscopic examination of Giemsa-stained thin blood smears. Mice whose blood smears had no observable parasites in 50 fields of view were considered uninfected, and those which reached the humane end-point of 50% infected RBCs were culled.

2.5.5. Electron Microscopy

PEMS preparation was allowed to settle onto 13 mm glass coverslips coated with 1% 40 kDa linear polyethylenimine Max (Polysciences Inc.) for 1 h. Supernatant was removed and replaced with primary fixative (2.5% glutaraldehyde in 0.1 M PBS) for incubation overnight at 4°C before washing with 0.1 M sodium cacodylate buffer (pH 7) and further incubation in 1% tannic acid in 0.1 M sodium cacodylate buffer for 1 h at RT. Samples were washed again 3x 10 min in sodium cacodylate buffer, then incubated in secondary fixative (1% osmium tetroxide, 0.1 M sodium cacodylate buffer, pH 7) for 1 h at RT. Samples were rinsed 2x 5 min with H_2O, then taken through an ethanol dehydration series as follows: 50% ethanol for 15 min, 70% ethanol overnight at 4°C, 90% and 95% ethanol for 15 min each and then 100% ethanol for 3x 30 min. Samples were dried in a Touismis Auto Samdri-815 critical point drier, with a purge time of 15 min. Coverslips were mounted cell side up onto aluminium stubs using carbon tape. Samples were coated with approximately 10 nm gold/palladium in a BioRad E5100 Series II sputter coater, then imaged using the secondary electron detector on a JEOL JSM-6390 at 5 kV, spot size 30, working distance 5 mm.

2.6. Statistical Analysis

Statistical analyses were carried out using Prism v.5.03 (Graphpad, USA), JMP 11 (SAS Institute, USA) and R (version 2.15.2; in collaboration with Dr Michael Fay and Dr Kazutoyo Miura from the National Institute of Allergy and Infectious Diseases). Comparisons between two groups were conducted using Mann-Whitney tests, or Wilcoxon matched-pairs signed rank test when data were paired. Comparisons between three or more groups were assessed by means of a Kruskal-Wallis test (independent groups) or a Friedman test (paired data/repeated measures of samples). Post-hoc Dunn's multiple comparison tests were used to identify contributing factors to significant Kruskal-Wallis or Friedman tests. Correlations were tested using Spearman's rank correlation (r_s). Parasitaemia was analysed using an area under the curve (AUC) analysis, and correlations were tested using Spearman's rank correlation. Two-way ANOVAs were used to assess intra- and inter-assay variability for the mouse ADRB assay by analysing the effect of sample, and that of assay run respectively, as well as determining each factors' relative contribution to measured variance.

In the human ADRB assay (Chapter 4) PMN donor effects were tested for using a linear regression on log max RLU, using a likelihood ratio test comparing the model with main effects for sample and plate to the model that additionally has PMN donor effects. The test was repeated after adjusting for day instead of plate. To test for a plate effect it was not possible to use similar methods since each PMN donor was tested on only one plate. Instead, a permutation test was performed. Specifically, the second PMN donor on each plate was permutated, and for each permutation fit the linear regression of log max RLU by sample and plate, ordered the 24 permutations by the F-statistic of the "plate" effects, and the p-value is the proportion of all 24 F-statistics that are greater than or equal to the original.

Interclass correlation coefficient (ICC) analysis (284) was used to assess the repeatability of measurements under the same conditions in the cases in which samples were tested in duplicate. To determine the effect of PMN donor, a linear regression (using sample and PMN donor as main effects) on each response was run, and the total proportion of the variance explained by the model (R^2), was partitioned into R^2 due to sample (R^2_s), and R^2 due to donor (R^2_d) using hierarchical partitioning (285). Confidence intervals (CI) were calculated using a non-parametric bootstrap with the percentile intervals using 2000 replications (286, 287). Assumptions of normality of the residuals from linear models were checked graphically using kernel density estimation. For comparing the singlets versus duplicates R^2 values from the model with sample only included for the two methods were compared. $R^2_{s\ Dup}$ with the response equal to the average of the replicates was measured, as was $R^2_{s\ Sing}$ by including both replicates and calculating the R^2 in the usual way as data. This is like averaging the $R^2_{\ s\ Sing}$ values from repeatedly randomly selecting one replicate.

For associations with clinical protection in Chapter 5, nominal logistic fit analysis, or ordinal logistical fit analysis was used model parameters involved in whether or not an individual experienced clinical malaria, or to model the number of malaria episodes experienced throughout the transmission season. In these analyses, LogLikelihood (LL) values were utilised to indicate how well a model fit the data. LL tests were then conducted to assess whether the addition of a factor statistically improved a model.

Two-sided *P*-values <0.05 were considered significant.

CHAPTER 3

ANTIBODY-DEPENDENT RESPIRATORY BURST ACTIVITY IN A MOUSE MALARIA CHALLENGE MODEL

3. ANTIBODY-DEPENDENT RESPIRATORY BURST ACTIVITY IN A MOUSE MALARIA CHALLENGE MODEL

3.1. Introduction

Despite blood-stage malaria being a target for vaccination efforts for several decades, a lack of *in vitro* assays to assess vaccine-induced immunity contribute to a relatively incomplete understanding of how antibody-mediated protection is conferred *in vivo* in humans. While GIA assay-based assessment of anti-malarial antibody responses has become commonplace, increasing attention has been directed towards the ability of cytophilic antibodies to initiate cellular immune responses in response to merozoite antigens as a result of Fc-dependent signalling, and their subsequent ability to induce anti-malarial blood-stage immunity.

An interest in the role of cytophilic antibodies recognising merozoite antigens on blood-stage malaria immunity led to the development of an assay assessing antibody-dependent cellular inhibition (ADCI) which describes monocytes as key effectors in antibody-dependent anti-malarial cellular activity (250). Fc-gamma receptor IIa (FcγRIIa)/CD32a and FcγRIII/CD16 signalling activates human monocytes to release TNFα in response to the opsonisation of merozoites by cytophilic IgG1 and IgG3 antibodies (251, 252, 288). Polyclonal antibodies that showed ADCI activity *in vitro* were also reported to confer protection when passively transferred to non-immune humans (180), although no causal link was formally demonstrated between anti-merozoite ADCI and protective outcome. Despite these reports, however, the ADCI assay has been notoriously difficult to reproduce and as a result, has not established itself as a mainstream tool for anti-merozoite vaccine candidate antigen screening. Nevertheless, the contribution of FcRs to the mediation of blood-stage malaria immunity should not be discarded. While conflicting reports occur as to the role of FcR-dependent mechanisms in protection against *P. yoelii* rodent malaria (50, 289), IgG antibody-dependent FcR activity has been shown to play an important role in control of infections by both *P.*

berghei XAT (49) and *P. berghei* transgenic for the *P. falciparum* 19 kDa C-terminus of MSP1 ($PfMSP1_{19}$) (202), whilst the inhibitory FcγRIIb/CD32b is reported to affect *P. chabaudi* parasite clearance and disease outcome (203).

While the role of monocytes as effectors of antibody Fc-dependent anti-merozoite activity remains under investigation, neutrophils represent an alternative and plausible candidate cell population for clearing blood-stage parasites given their high phagocytic efficiency and their ability to generate ROS. In particular, a fast clearance of *P. falciparum* in Gabonese children has been correlated with high ROS production (290). Additionally, the antibody-dependent respiratory burst (ADRB) assay, which measures neutrophil ROS production in response to opsonised merozoites, has recently been associated with protection against clinical malaria in an endemic population (181). Conversely, assays measuring GIA in the serum of naturally-exposed humans have not established a clear association with clinical disease outcome, with studies being divided in their support for a role of GIA in naturally-acquired immunity (179). The association of ADRB with natural clinical protection provides a new opportunity to assess a largely neglected mechanism by which antibodies could be controlling blood-stage malaria infection. In this Chapter, the mechanisms of action underlying ADRB activity in the mouse model, and the contribution of ADRB activity in mediating *P. yoelii* rodent malaria challenge outcome in both MSP1-vaccinated and naïve non-immunised mice are investigated.

3.2. Results

3.2.1. ADRB assay development

Neutrophil respiratory burst activity (NADPH oxidase activation) induced by mouse sera was initially assessed using neutrophils enriched from mouse bone marrow, and recombinant protein coated onto a plate, according to published methodologies (289, 291). Briefly, plates coated with 10 µg/mL PfMSP1$_{19}$-GST protein were incubated with sera from naïve or immunised mice before the addition of mouse neutrophils at 1 x 10^7 cells/mL and the monitoring of respiratory burst activity. To establish the assay, sera from BALB/c mice immunised with viral vectors AdHu5 and MVA (Ad-M) encoding PfMSP1 were used which were known to be reactive against PfMSP1$_{19}$-GST protein (231). Percoll separation was used to enrich neutrophils to >95% as determined by examination of Giemsa stained slides. The isolated cell population was confirmed as Ly6C^{int} CD11b^{+} granulocytes by flow cytometry (Figure 3-1). Results in a previous study were indexed according to a positive reference serum which was included each time the assay was run (181). This approach was also applied here, using a pool of positive antigen-specific serum (see Chapter 2, Section 2.4.5.1). As such, results in this Chapter are presented in indexed relative light units (iRLU), where

$$Indexed\ RLU\ (iRLU) = \frac{Absolute\ maximum\ RLU\ of\ test\ sample}{Absolute\ maximum\ RLU\ of\ reference}$$

Respiratory burst activity was induced when the recombinant PfMSP1$_{19}$ antigen was coated onto the assay plate at a concentration ≥ 5 µg/mL, while the same concentrations of antigen present in solution failed to induce a response (Figure 3-2). Coated protein likely forms an array, not present when the antigen is in solution, which causes FcR on the neutrophil surface to co-localise and thus initiate activatory γ-chain signalling and the respiratory burst (185, 292, 293).

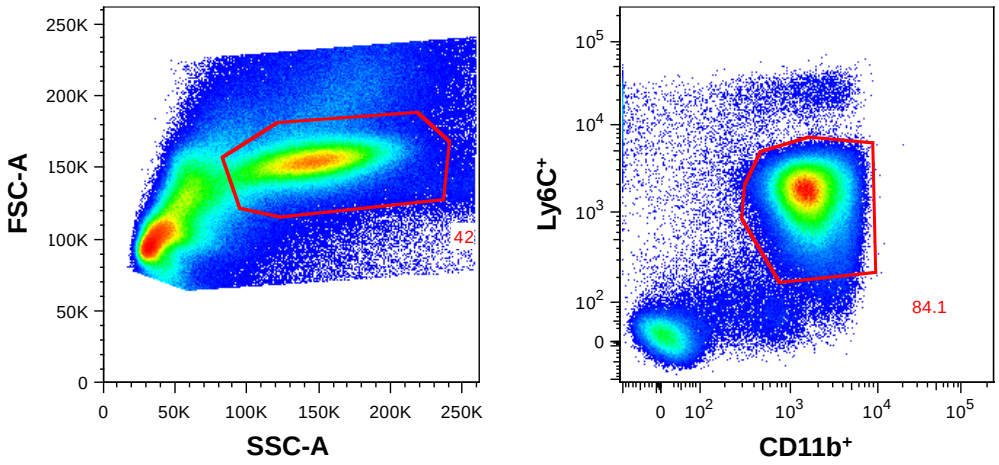

Figure 3-1: Mouse neutrophils isolated on Percoll density gradient

Bone marrow was extracted from the femurs and tibias of mice, and PMNs isolated on Percoll density gradients. Cells were surface stained with anti-CD11b, anti-Ly6C, and anti-CD8α. Events were acquired until 10,000 (in the case of blood samples) or 100,000 (spleen samples - as shown here) $CD8^+$ events had been measured. (A) Granulocytes, were gated by forward (FSC-A) and side scatter (SSC-A) profiles. (B) PMNs were then defined as the Ly6Cint CD11b+ population.

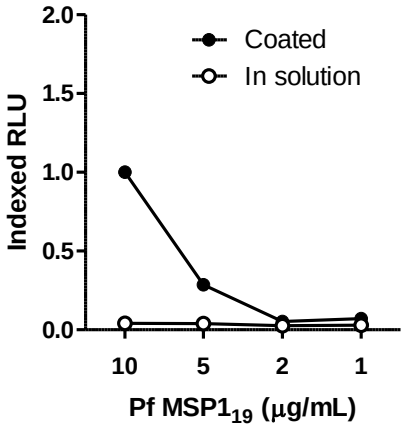

Figure 3-2: Respiratory burst activity against protein coated plate versus protein in solution

ADRB activity induced by sera diluted 1:25 in PBS from Ad-M PfMSP1 immunised BALB/c mice, and neutrophils enriched to 1 x 10^7 PMNs/mL from the bone marrow of naïve BALB/c mice. Varying concentrations of $PfMSP1_{19}$-GST protein were either coated onto plates or added in solution. Points represent mean of two assay replicates for each sample.

After coating separate wells of the assay plate with two different antigens (GST and PfMSP1$_{19}$-GST), respiratory burst activity induced by a panel of different sera was tested. The panel of sera included five different samples from mice immunised with Ad-M PfMSP1 (231); *P. falciparum* Mz in Freund's adjuvant (thus containing PfMSP1$_{19}$ as well as many other antigens); Ova (279); a transmission-blocking malaria vaccine candidate Pfs25 (228); and GST, as well as serum from non-immunised mice (Naïve). Positive ADRB activity was induced by sera only when the immunisation antigen matched the antigen coated onto the assay plate (Figure 3-3), confirming the specificity of the assay.

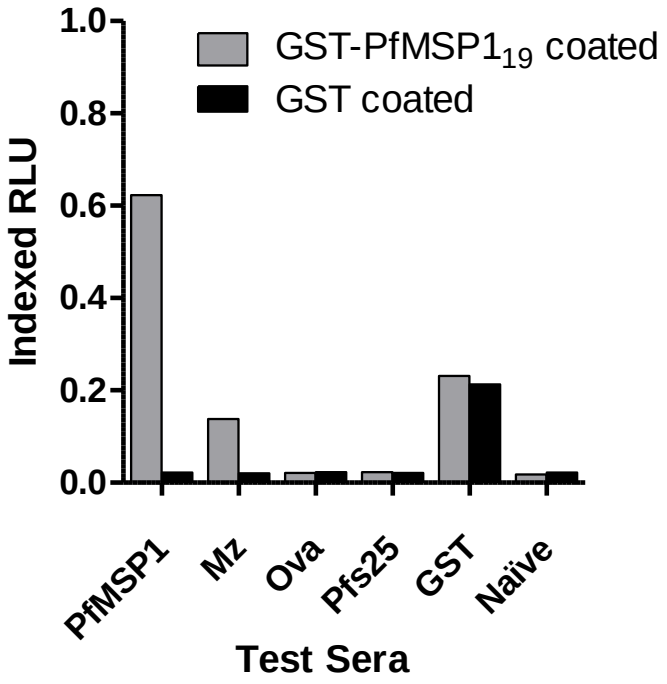

Figure 3-3: ADRB antigen specificity

The assay plate was coated with either GST (black) or PfMSP1$_{19}$-GST (grey) recombinant protein at 10µg/mL. Bars indicate ADRB (all indexed against PfMSP1 positive sera on PfMSP1$_{19}$-GST coated plate) induced by sera taken from mice immunised with PfMSP1, *P. falciparum* merozoites in Freund's adjuvant (Mz), Ovalbumin (Ova), Pfs25, GST, or with no prior immunisation (Naïve). Bars represent mean of two assay replicates for each sample (n = 1).

Additionally, the magnitude of the iRLU response decreased with decreasing coating antigen concentration (Figure 3-2), increasing serum dilutions and reduced cell numbers in each well (Figure 3-4). As such a set of assay conditions were established for further experiments, as follows: antigen coated on the assay plate at 10μg/mL, serum diluted 1:100 in PBS, and 50μL neutrophils added to each well at 1 x 10^7 PMNs/mL. The use of maximal assay conditions with a mid-range serum dilution (1:100) ensured that both higher and lower assay responses could be detected for test sera.

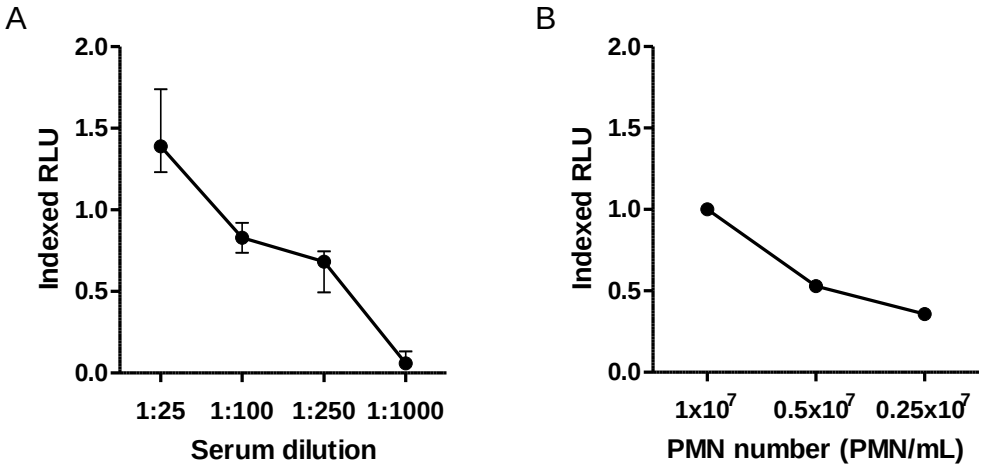

Figure 3-4: Assay parameters: Serum dilution and cell number

ADRB induction by anti-PfMSP1 sera (A) at increasing serum dilutions (points represent mean ± SEM of 6 independent samples), and (B) at a constant serum dilution of 1:100 with decreasing numbers of cells per well (50μL cells added at presented cell number/mL; points represent mean of two assay replicates for each sample).

Using these assay conditions and a PfMSP1$_{19}$-GST coated plate, assay variability was also determined. To assess intra-assay variability, a single pool of serum derived from eight Ad-M PfMSP1 immunised BALB/c mice, was tested for induction of ADRB activity in eight separate wells with neutrophils from a single donor mouse on each of two days (Figure 3-5A). Inter-assay variability was determined by assessing ADRB activity elicited by serum from each of the eight Ad-M PfMSP1 immunised BALB/c mice on six different days (i.e.

with a different neutrophil donor each day). While intra-assay variability was not significant (Two-way ANOVA $F_{7,7} = 0.70$, $P = 0.67$), there was significant inter-assay variability (Two-way ANOVA $F_{5,54} = 23.08$, $P < 0.0001$) although assay repeat (or different neutrophil donor) accounted for less than 5% of the observed variance compared with over 93% resulting from differences between the vaccine response in the test samples as determined by R^2 analysis (Figure 3-5B).

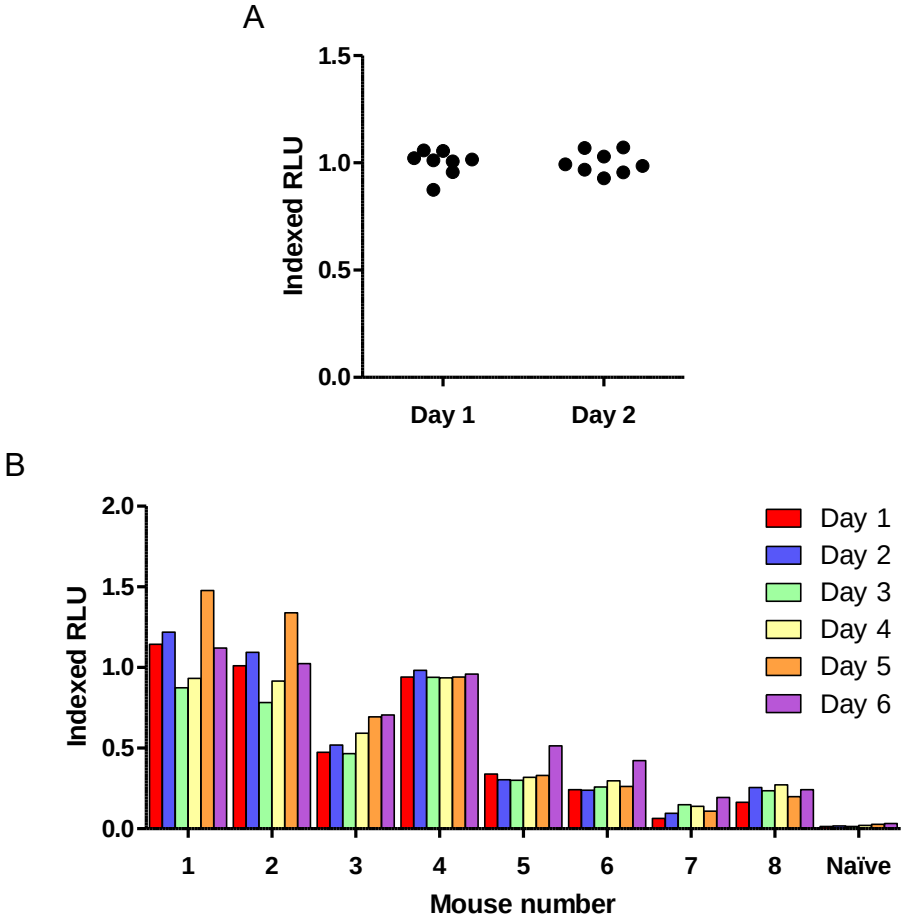

Figure 3-5: Intra- and inter-assay variability

(A) Serum pooled from six Ad-M PfMSP1 immunised mice was tested in 8 replicate wells on two days to assess intra-assay variability. (B) Serum from eight Ad-M PfMSP1 immunised mice and one naïve mouse was tested on six separate days in the assay to assess inter-assay variability. Bars and points represent mean of two assay replicates for each sample.

3.2.2. Role of FcR-mediated pathways in ADRB induction

Having established the assay, the role of FcR-mediated pathways in inducing ADRB activity was investigated using both γ-chain knockout ($\gamma^{-/-}$), and FcγRIIb knockout ($CD32b^{-/-}$) mice. The number of neutrophils added to each well was kept constant between groups by counting the number of cells using a hemocytometer and assessing the percentage purity of neutrophils by Giemsa stained slide, before adjusting accordingly. In this case, ADRB activity was measured against $PyMSP1_{19}$-GST protein (using serum from mice immunised with PyMSP1-based vaccines). The response induced by neutrophils from wild type (WT) mice in response to serum of BALB/c mice immunised i.m. with Ad-M $PyMSP1_{42}$ (median = 0.62 iRLU) was ablated when using neutrophils enriched from the bone marrow of $\gamma^{-/-}$ mice (median = 0.06; *P* = 0.03) (Figure 3-6A). Additionally, pre-incubation of WT neutrophils with anti-CD16/32 mAb ablated their ability to induce ADRB activity (Figure 3-6B). On the other hand, neutrophils isolated from the bone marrow of C57BL/6 mice lacking the inhibitory FcγRIIb were able to induce higher ADRB (median = 2.40 iRLU) than those isolated from WT mice (median = 1.00 iRLU; *P* = 0.03) (Figure 3-6C). Thus it appears that ADRB activity is dependent upon γ-chain-mediated pathways, whilst regulation occurs via CD32b. Furthermore, given mice lack CD32a (294-296) (the activatory FcγRII), and given the ablation of ADRB with anti-CD16/32 mAb, CD16/FcγRIII appears likely to mediate ADRB induction in the mouse system.

3.2.3. Role of mouse IgG isotypes in ADRB induction

Having shown the importance of FcRs in the induction of ADRB, I next looked to determine the contribution of different IgG isotypes to ADRB activity. Chimeric mouse IgG1 and IgG2a mAbs against the C1 epitope of $PfMSP1_{19}$ were thus expressed in HEK293 and CHO cell lines respectively (277). Purified antibodies of each isotype at 8.3µg/mL induced

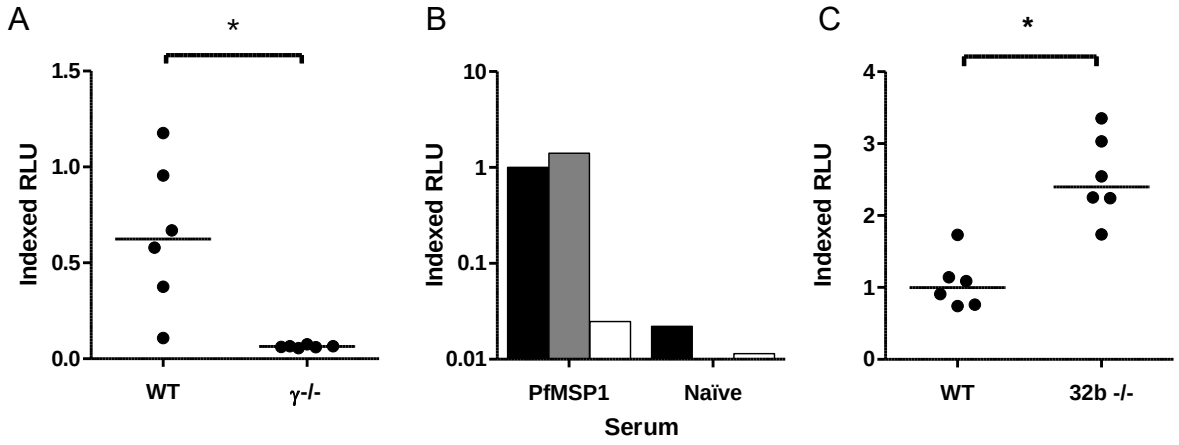

Figure 3-6: The role of Fc-receptors in ADRB activity

Serum was collected from BALB/c and C57BL/6 mice immunised with Ad-M PyMSP1$_{42}$. Assays were set up with 10µg/mL PyMSP1$_{19}$-GST (A, C) or PfMSP1$_{19}$-GST (B) coated plates, 50µL per well of neutrophils at 1 x 10^7 PMNs/mL, and serum diluted 1:100 in PBS run in duplicate wells. Neutrophils were isolated from the bone marrow of wild type BALB/c and C57BL/6 mice, plus $\gamma^{-/-}$ and CD32b$^{-/-}$ knockout mice on the same genetic backgrounds respectively. ADRB induction was assessed by: (A) BALB/c and $\gamma^{-/-}$ PMNs in response to sera from BALB/c mice immunised with Ad-M PyMSP1$_{42}$; (B) BALB/c PMNs in response to sera from Ad-M PfMSP1 immunised, or naïve, BALB/c mice (on at PfMSP1$_{19}$-GST coated plate), where PMNs had been pre-incubated with neutrophil buffer (black), control rat IgG (grey), or anti-CD16/32 mAb (white); (C) C57BL/6 and CD32b$^{-/-}$ PMNs in response to sera from C57BL/6 mice immunised with Ad-M PyMSP1$_{42}$. * $P < 0.05$ (Wilcoxon matched-pairs signed rank test). Bars and points represent means of two replicates for each sample, and medians on dot plots are represented by lines.

indistinguishable levels of ADRB activity against PfMSP1$_{19}$-GST (Figure 3-7). Additionally, mice immunised i.m. with either a PyMSP1$_{42}$ adenovirus prime – PyMSP1$_{19}$-GST protein-in-Adju-Phos® boost regime (AP), or a three dose PyMSP1$_{19}$-GST protein-in-Adju-Phos® regime (PPP) (279), induced the same total IgG titre against PyMSP1$_{19}$ as measured by endpoint ELISA (Figure 3-8A), but different profiles of IgG isotypes (Figure 3-8B). AP immunisation resulted in a balanced isotype response with equivalent induction of IgG1 and IgG2a. In contrast, PPP immunisation resulted in an IgG1 dominated response with negligible levels of IgG2a being induced, as shown previously for the Adju-Phos® adjuvant (279). ADRB activity was assayed using serum from mice immunised with these two vaccination regimes and no difference was observed (P = 0.39) (Figure 3-8C), in agreement with the epitope-matched chimeric mAbs. These data suggest that the mouse IgG1 and IgG2a isotypes can both elicit equivalent ADRB activity from neutrophils.

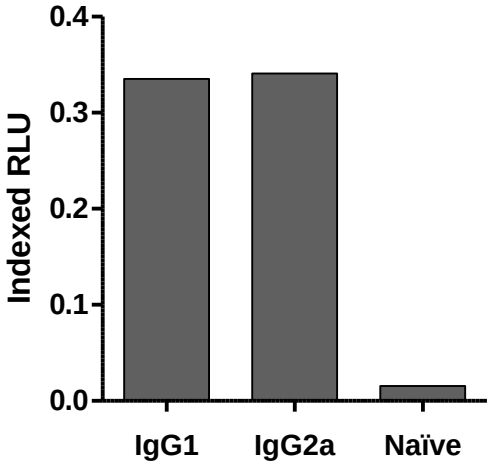

Figure 3-7: Isotype mAbs and ADRB induction

ADRB plates were coated with 10µg/mL PfMSP1$_{19}$-GST and ADRB induction by BALB/c PMNs in response to mouse isotype-specific chimeric anti-PfMSP1$_{19}$ mAbs at 8.3µg/mL was assessed. Bars represent means of two replicates for each sample.

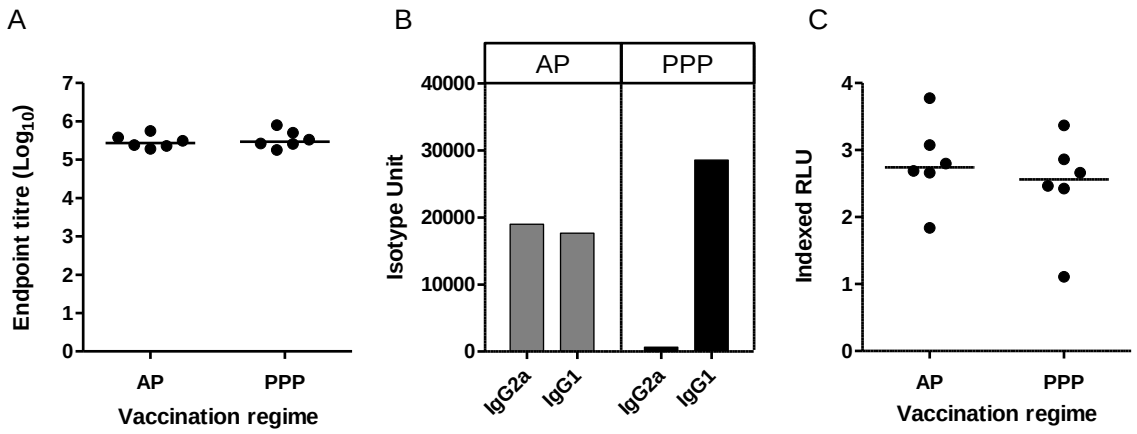

Figure 3-8: Role of immunisation-induced isotypes in ADRB induction

BALB/c mice were immunised with three doses of PyMSP1$_{19}$-GST with Adju-Phos® (PPP) or one dose AdHu5-PyMSP1$_{42}$ followed by one dose PyMSP1$_{19}$ with Adju-Phos® (AP). (A) PyMSP1$_{19}$ endpoint ELISA titres against PyMSP1$_{19}$-IMX108 (to avoid detection of antibodies raised against the GST tag present in the protein vaccine) coated plates; (B) IgG1 and IgG2a isotype-specific ELISA titres against the same protein as total IgG; and (C) ADRB activity using BALB/c PMNs; were determined. Bars and points represent means of two replicates for each sample, and medians on dot plots are represented by lines.

3.2.4. FcRs and efficacy against *P. yoelii* challenge

One of the goals of utilising this assay was to assess the ability of activity measured in the assay to associate with protective efficacy against blood-stage malaria infection. The previous data showed that ADRB activity was dependent on γ-chain signalling in the mouse model. Given it is well established that PyMSP1-based vaccine efficacy in the *P. yoelii* blood-stage challenge model is antibody-mediated (232, 297), the impact of FcR-modifications on challenge outcome in vaccinated and *P. yoelii* infected mice was assessed. Vaccine doses were chosen based on prior experience with this model to allow for improved or reduced vaccine efficacy to be observed. Immunisation i.m. with Ad-M PyMSP1$_{42}$ induced the same levels of anti-PyMSP1$_{19}$ antibodies in both WT and $\gamma^{-/-}$ BALB/c mice at all time-points (Figure 3-9A). The presence or absence of FcR signalling thus had no impact on viral vectored vaccine antibody immunogenicity. All mice were subsequently challenged with 10^4

lethal *P. yoelii* strain YM iRBCs. The rate of survival was similar between WT and $\gamma^{-/-}$ groups in both vaccinated and naïve non-immunised control groups (Figure 3-10A). Area under the curve (AUC) analysis of day 3-5 parasitaemias for vaccinated mice showed no difference in parasite burden between WT and $\gamma^{-/-}$ groups ($P = 0.31$), although naïve mice showed a higher parasite burden in the WT group ($P = 0.002$; Figure 3-11A) indicating a small but significant delay in the knockouts reaching endpoint parasitaemia. Similarly, in WT and $CD32b^{-/-}$ C57BL/6 mice, antibody levels induced by vaccination did not differ at any time-point between groups (Figure 3-9B), nor was there any difference in challenge outcome survival rates (Figure 3-10B) or parasite burden (AUC analysis for days 3-5) for either vaccinated ($P = 0.93$) or naïve groups ($P = 0.13$) (Figure 3-11B).

Thus, despite the inability of $\gamma^{-/-}$ mice to induce ADRB, the vaccinated mice were still able to control parasitaemia indicating that vaccine-induced efficacy in this model is unlikely ADRB or γ-chain-dependent. Likewise the ability of $CD32b^{-/-}$ mice to induce higher ADRB did not enhance vaccine-mediated control of parasitaemia. Taken together, all of these initial protection data suggested that γ-chain-mediated effector functions (including ADRB activity as measured in vaccinated mice) are not essential in determining the outcome of primary challenge in the murine *P. yoelii* model, neither in vaccinated nor control mice.

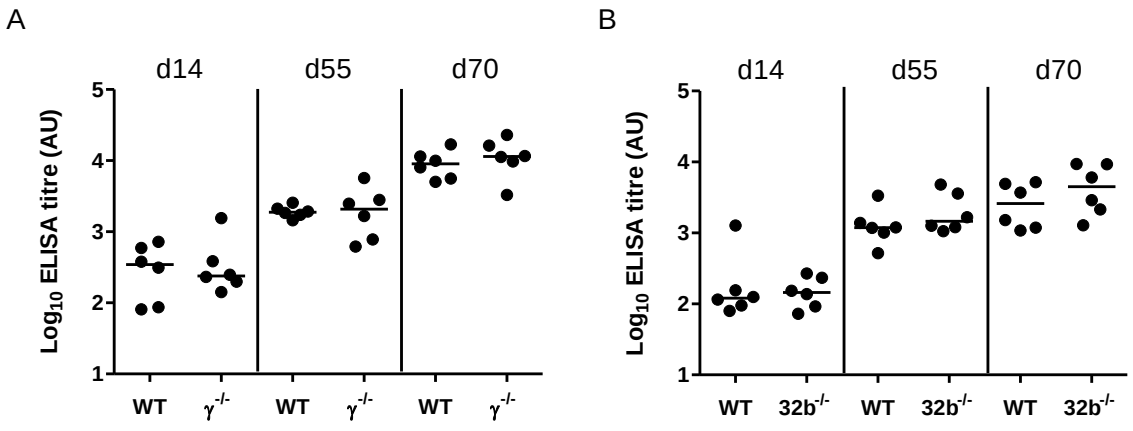

Figure 3-9: Immunogenicity of Ad-M PyMSP1$_{42}$

BALB/c, $\gamma^{-/-}$, C57BL/6 and CD32b$^{-/-}$ mice (n = 6 per group) were immunised i.m. with Ad-M PyMSP1$_{42}$. PyMSP1$_{19}$ ELISA titres were determined in (A) BALB/c and $\gamma^{-/-}$ mice, and (B) C57BL/6 and CD32b$^{-/-}$, at 14, 55 and 70 days post adenovirus immunisation (MVA boost occurred on day 56). Lines represent median values.

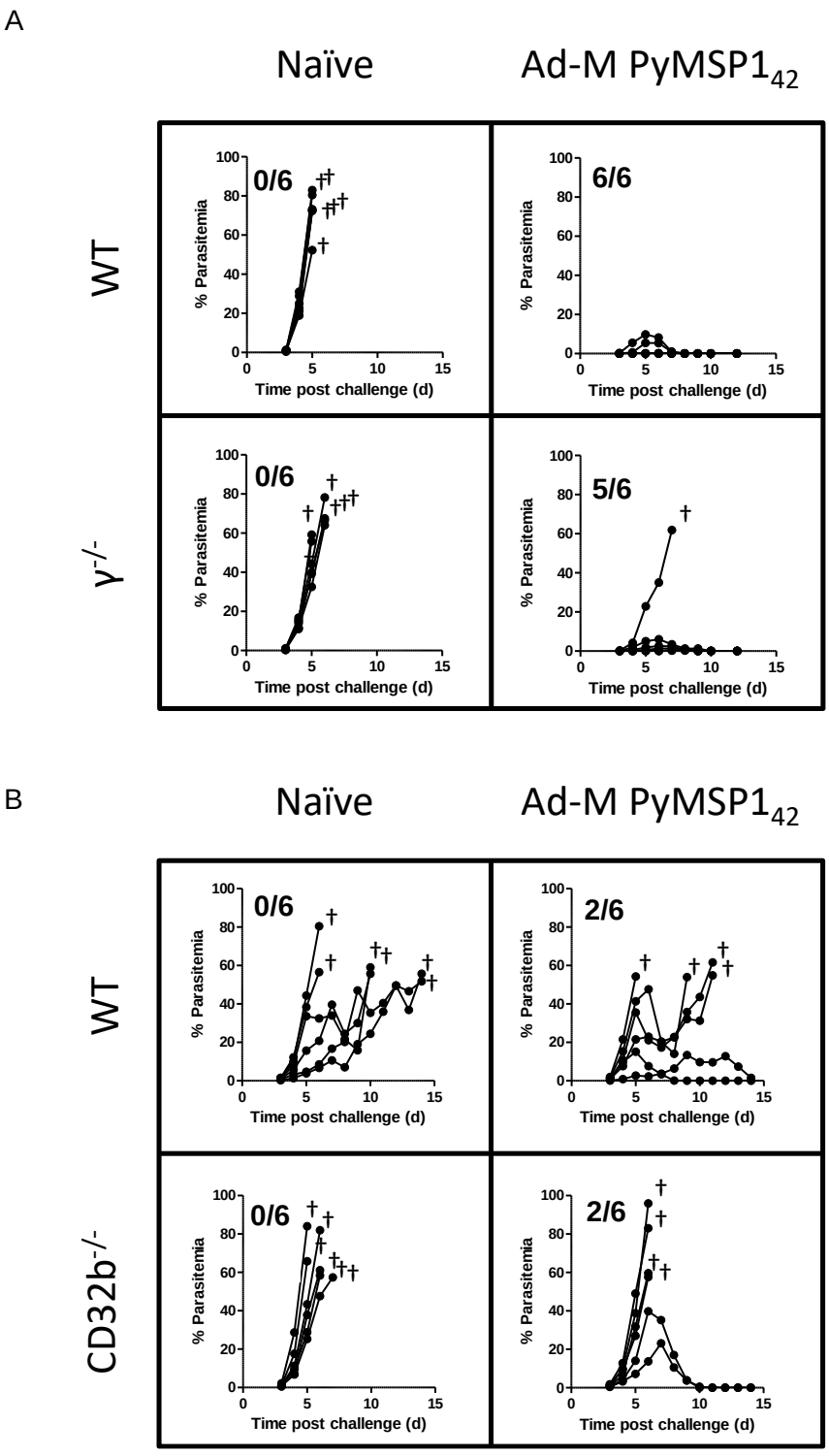

Figure 3-10: *P. yoelii* challenge outcome in WT and knockout mice

Mice from Figure 3-9 were challenged at day 70 i.v. with 10^4 *P. yoelii* YM iRBCs. Blood-stage parasitaemia is reported as the percentage of infected RBCs over time in (A) BALB/c and $\gamma^{-/-}$ groups, and (B) C57BL/6 and CD32b$^{-/-}$ groups. † indicates animal being culled after reaching the humane endpoint of 50% blood-stage parasitaemia.

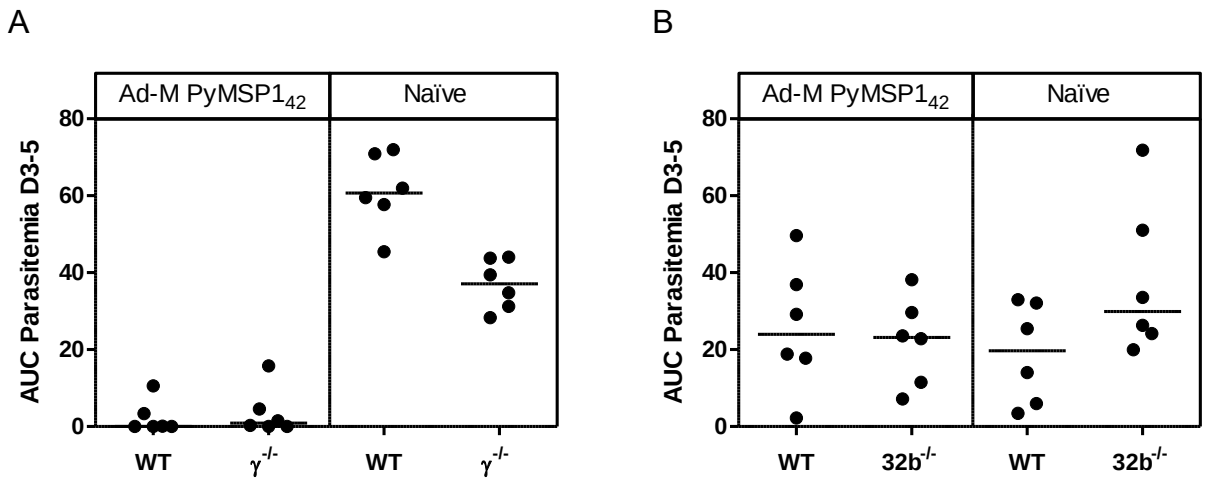

Figure 3-11: Area under the curve analysis of *P. yoelii* challenge

Area under the curve analysis for days 3-5 of challenge described in Figure 3-10 was conducted on (A) parasitaemia plots for BALB/c and $\gamma^{-/-}$ mice, and (B) plots from C57BL/6 and CD32b$^{-/-}$ mice. Lines represent median values.

3.2.5. Assaying ADRB with coated antigen versus whole merozoite

The ADRB assay methodology established above is not limited to use with MSP1$_{19}$ antigen, but can be used to assess functional antibody activity against any antigen under study once coated onto the plate (291, 298). It also does not permit assessment or comparison of the effectiveness of ADRB induction by antibodies binding to different antigens as presented in the context of the intact merozoite itself. In light of the negative challenge results above, it was therefore decided to assess the possibility of using whole malaria parasites in the assay rather than an array of recombinant MSP1$_{19}$ protein. While the vaccines used above induce serum antibodies that show ADRB responses against MSP1$_{19}$ protein coated onto the plate, it was wholly possible that the same vaccines do not induce functional ADRB from neutrophils via opsonisation of merozoites. The first challenge dataset supported this hypothesis, indicating that there was no association between ADRB activity as measured in the assay against PyMSP1$_{19}$ (Figure 3-6A,C) and vaccine efficacy. As such, the assay was established

to assess ADRB activity in response to *P. yoelii* YM merozoites (PyPEMS), and was shown to be reproducible in the same fashion as the PyMSP1$_{19}$ assay (Figure 3-12).

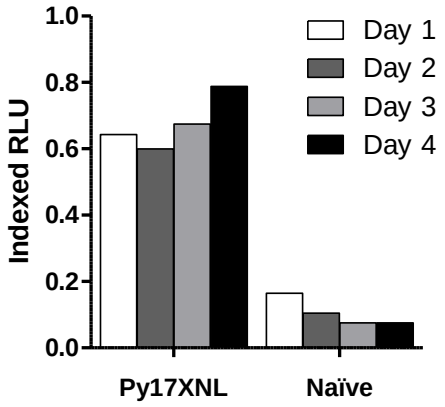

Figure 3-12: PyPEMS ADRB assay reproducibility

ADRB induction against PyPEMS was assessed using BALB/c PMNs in response to serum from a naïve BALB/c mouse, or one previously challenged with 10^6 Py17XNL iRBCs. ADRB activity was assessed on four separate days using four different PMN donors to assess inter-assay variability. Bars represent the mean of two assay replicates for each sample.

In order to investigate whether anti-PyPEMS ADRB was induced by immunisation, twelve WT BALB/c mice were first immunised i.m. with Ad-M PyMSP1$_{42}$ and then challenged with a non-lethal strain of *P. yoelii* (17XNL). Two weeks after the boost (time of challenge), sera from immunised mice showed both PyMSP1$_{19}$- and PyMSP1$_{33}$-specific antibody responses as measured by standardised ELISA. These responses were boosted slightly after challenge for both PyMSP1$_{19}$ (Wilcoxon signed rank test, P = 0.002) and PyMSP1$_{33}$ (Wilcoxon signed rank test, P = 0.004; Figure 3-13A). However, following vaccination, the sera did not lead to a significant induction of ADRB activity against PyPEMS (Figure 3-13B, white bars). In contrast, following challenge with 10^6 Py17XNL iRBCs and parasite clearance, serum from 5/12 mice did induce detectable levels of ADRB activity against *P. yoelii* merozoites (Figure 3-13B, black bars).

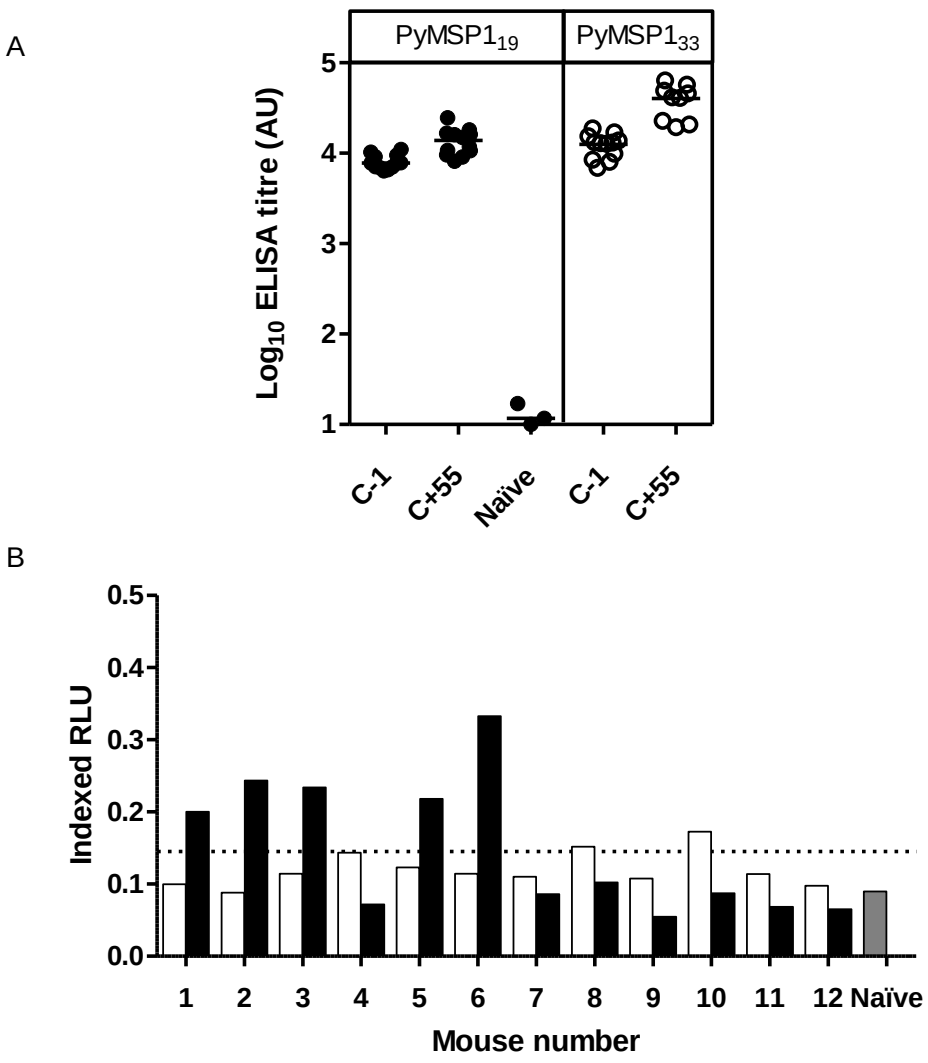

Figure 3-13: Impact of *P. yoelii* challenge on PyMSP1 ELISA titre and PyPEMS ADRB

Twelve WT BALB/c mice were immunised i.m. with Ad-M PyMSP1$_{42}$, before being challenged i.v. with 10^6 *P. yoelii* 17XNL iRBCs. (A) PyMSP1$_{19}$ (●) and PyMSP1$_{33}$ (○) antibody titres were assessed by standardised ELISA in mice two weeks after boost (one day before challenge; C-1), and 55 days after challenge (C+55). PyMSP1$_{19}$ titres for serum from three naïve non-immunised control mice are also shown. (B) ADRB activity induced by BALB/c PMNs (1 x 10^7 PMN/mL) against *P. yoelii* PEMS was determined using sera (neat) from both the C-1 (white bars) and C+55 (black bars) time-points. Background cut-off, defined as 3 SD above the mean of the level of ADRB activity induced by naïve BALB/c mouse serum (*n*=4) in the same assay (grey bar), is indicated by the dotted line. Lines on dot plots represent medians, bar charts represent mean of two assay replicates.

This induction of ADRB activity could be a result of boosting pre-existing antibody titres against PyMSP1$_{42}$, or an induction of antibody responses against *de novo* parasite antigens. It seemed more likely that the resultant activity is due to recognition of new antigens as there was no correlation between PyMSP1$_{19}$- or PyMSP1$_{33}$-specific total IgG ELISA titre and anti-merozoite ADRB activity after challenge (r_s = 0.44, P = 0.15; r_s = 0.07, P = 0.86 respectively), or when the pre- and post-challenge data were pooled (PyMSP1$_{19}$: r_s = 0.09, P = 0.67; PyMSP1$_{33}$: r_s = -0.04, P = 0.85) (Figure 3-14).

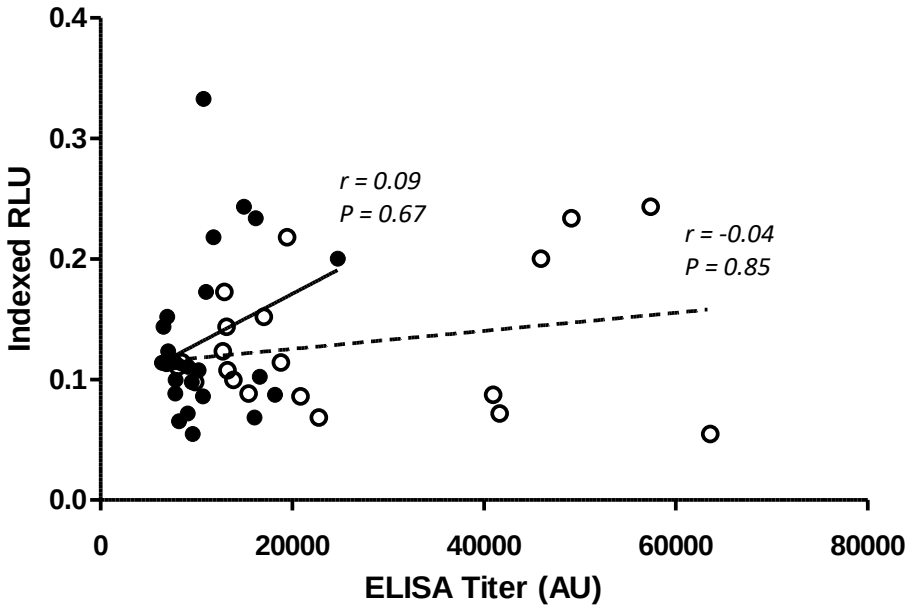

Figure 3-14: Correlation between PyMSP1 ELISA titre and PyPEMS ADRB

PyMSP1$_{19}$ (●) and PyMSP1$_{33}$ (○) ELISA titres from mice described in Figure 3-13 were plotted against pre- and post-challenge anti-PyPEMS ADRB activity. Spearman's rank correlations shown on scatter plot for *P. yoelii* PEMS ADRB with PyMSP1$_{19}$ (solid line) and PyMSP1$_{33}$ (broken line) ELISA titres.

3.2.6. ADRB activity and secondary parasite exposure

The above data suggested that functional anti-merozoite ADRB activity was detectable in the *P. yoelii* model following vaccination and a non-lethal primary parasite exposure. It was therefore sought to assess whether anti-merozoite ADRB activity could contribute to protective efficacy following secondary parasite exposure, given the activity in serum was now detectable. To address this, in addition to the 12 immunised WT mice described in Figure 3-13, six $\gamma^{-/-}$ mice were also immunised and challenged with non-lethal parasites in the same manner, while a matching 18 mice were challenged without prior immunisation (Figure 3-15A). Following primary challenge, AUC analysis of blood-stage parasitaemia demonstrated that vaccination achieved significant protection (Mann Whitney test) in both the WT (n = 12 vs 12; P = 0.001) and $\gamma^{-/-}$ (n = 6 vs 6; P = 0.002) groups. Intriguingly, $\gamma^{-/-}$ mice also controlled parasitaemia better than WT mice in both vaccinated (P = 0.004) and naïve (P = 0.002) groups (Figure 3-15B). On day 55 after the primary *P. yoelii* 17XNL challenge (between 35 and 49 days post parasite clearance), and in agreement with the previous observation, serum from 18/35 mice elicited positive ADRB activity against PyPEMS (when tested with neutrophils from WT mice) (Figure 3-16). The induction of this serum activity was comparable and equally distributed across the immunised and non-immunised groups, again suggesting this activity was independent of $PyMSP1_{42}$ vaccine-induced responses. It was also hypothesised that ADRB induction may occur as a result of accumulative parasite exposure in which case ADRB activity against *P. yoelii* merozoites would be expected to correlate with parasite exposure as measured by AUC analysis of blood-stage parasitaemia, however, no such correlation was seen (r_s = 0.08, P = 0.66; Figure 3-17).

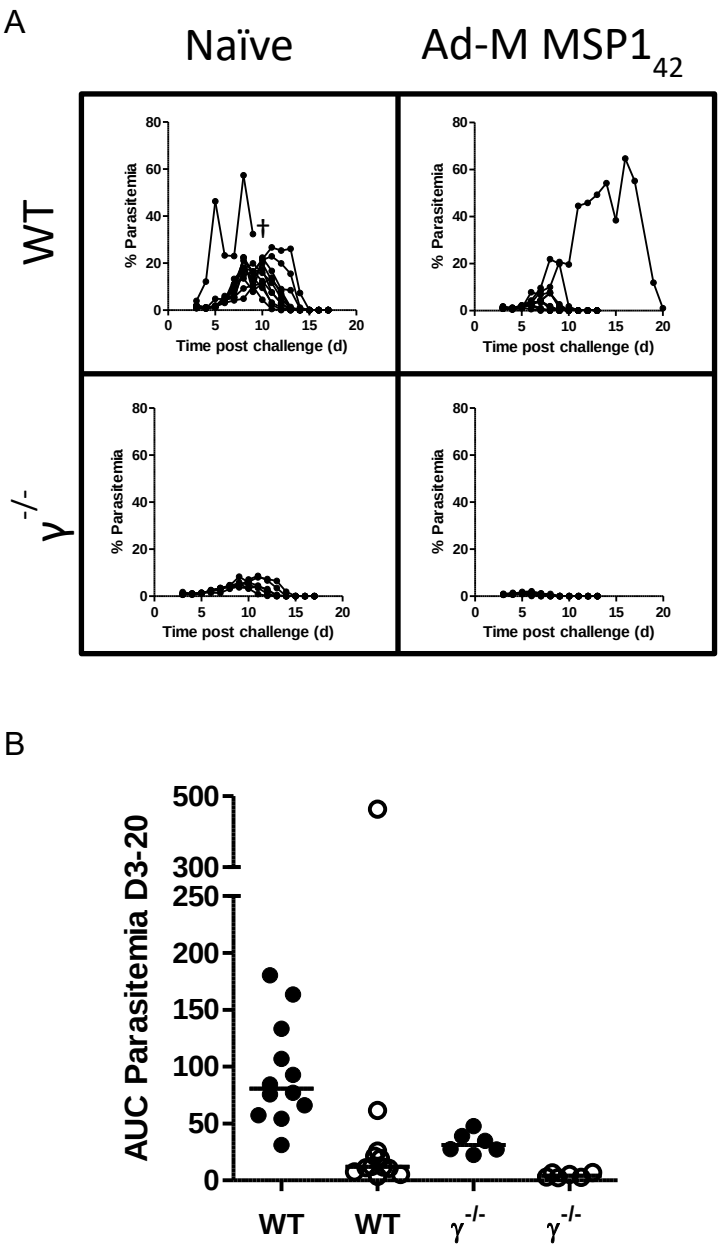

Figure 3-15: Py17XNL challenge of BALB/c and $\gamma^{-/-}$ mice

BALB/c or $\gamma^{-/-}$ mice were immunised i.m. with Ad-M PyMSP1$_{42}$ and challenged two weeks later with 10^6 *P. yoelii* 17XNL iRBCs. (A) Blood-stage parasitaemias in both BALB/c and $\gamma^{-/-}$ groups are reported as the percentage of infected RBCs. (B) AUC analysis of parasitaemia between day 3 (D3) and D20 was conducted for naïve/non-vaccinated (●) and immunised (○) groups. Lines on dot plots represent medians. †Animal being culled after reaching the humane end-point.

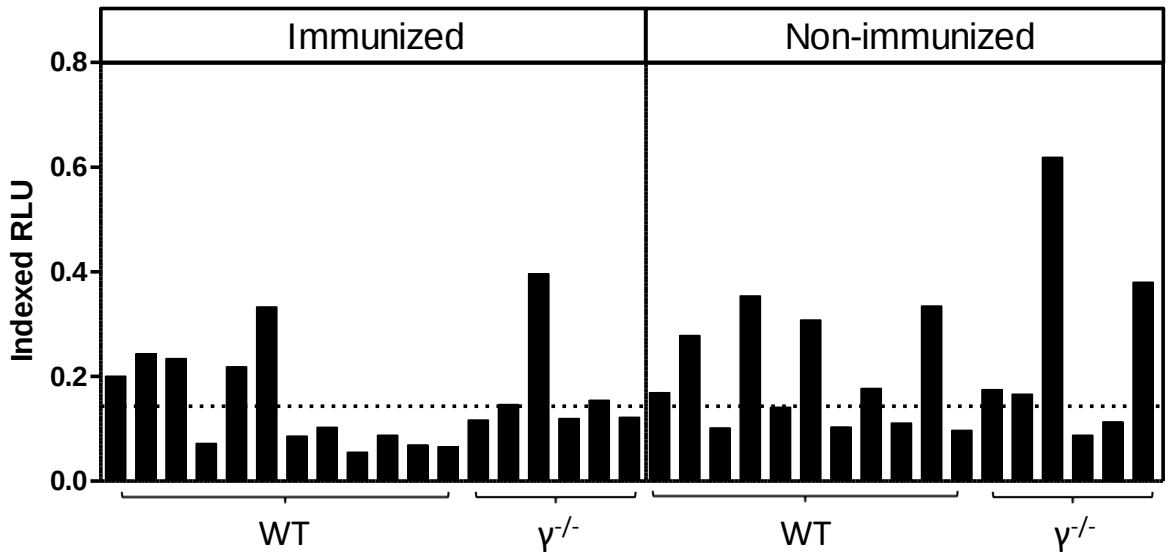

Figure 3-16: Post-malaria challenge ADRB activity

Fifty-five days after Py17XNL challenge, ADRB activity of mouse serum against *P. yoelii* PEMS was assessed as described in Figure 3-13B. Bars represent mean of two replicates.

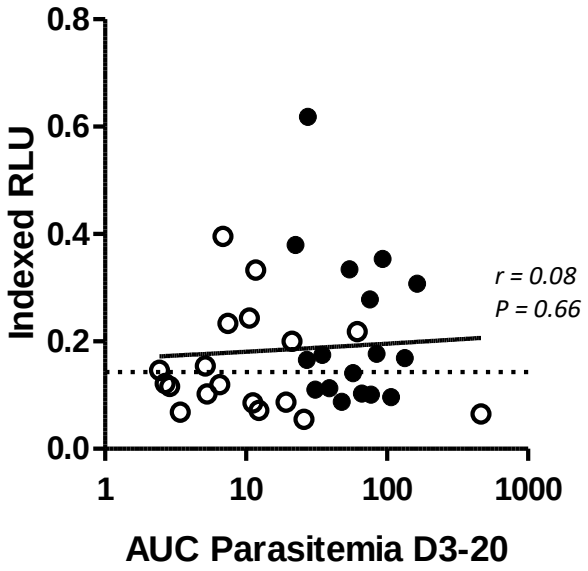

Figure 3-17: Correlation between parasite burden and ADRB activity

After Py17XNL challenge, anti-*P. yoelii* PEMS ADRB activity was assessed as described in Figure 3-13B and plotted against AUC calculated between D3-20. Line represents Spearman's rank correlation.

To ascertain whether an induction of anti-merozoite ADRB activity had any effect on challenge outcome, all 35 mice were re-challenged eight weeks after the initial non-lethal challenge with 10^6 lethal *P. yoelii* YM iRBCs. One day before challenge, and three days following challenge, one group of six mice in each of the immunised and non-immunised WT groups was injected i.p. with 0.5mg 1A8 mAb, a neutrophil depleting agent (275, 276). All other mice received a comparable dose of control rat IgG at the same time-points. Neutrophil depletion (PMN^-) was confirmed in both the blood and the spleen of additional control mice at days 1 and 7 post-challenge by flow cytometry. The blood neutrophil population was depleted by 90% over this time-course. On day one post-challenge a high level of depletion was visible in the spleen (>80%) however this population had largely reappeared by day 7 (Figure 3-18).

Following lethal secondary challenge, 66% of all mice were sterilely protected with no parasites being observed in the blood over the course of the monitoring period. There was no difference in parasite burden between the three immunised groups (WT, PMN^- and $\gamma^{-/-}$) as determined by one-way ANOVA (P = 0.40) (Figure 3-19), although it may remain impossible to ascertain potential differences in the face of such high levels of protective efficacy afforded by the preceding vaccination and *P. yoelii* 17XNL challenge. On the other hand, there was a significant difference between non-immunised groups (P = 0.008) due to a greater parasite burden experienced by $\gamma^{-/-}$ mice than non-immunised WT mice as measured by AUC between days 3 and 6. Neutrophil depleted mice, in contrast, experienced a similar infectious burden to non-depleted WT mice (Dunn's multiple comparison test; Figure 3-19). It should also be noted that all mice that received 1A8 treatment had completely cleared and/or prevented parasitaemia by day 6 (during the time of maximum PMN depletion). In fact, only 2/11 mice treated with 1A8 developed any detectable parasitaemia following secondary challenge.

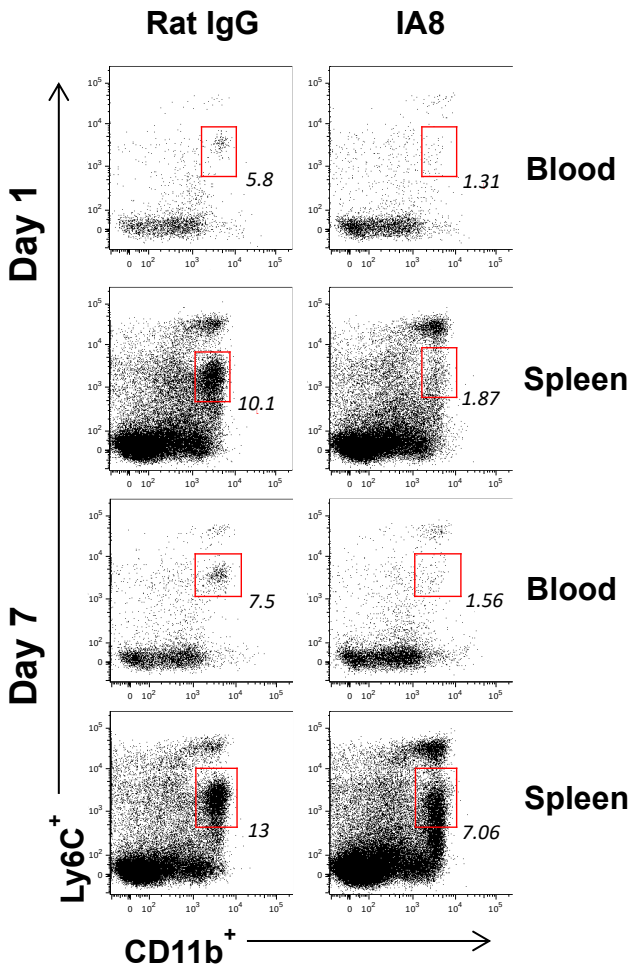

Figure 3-18: *In vivo* neutrophil depletion

BALB/c mice were given either 0.5mg 1A8 or 0.5mg control rat IgG i.p. at day -1 and day 3. Representative flow plots show granulocytes from both the blood and the spleen of treated mice. Flow data acquisition was normalised by setting stopping gates at 10^4 or 10^5 $CD8^+$ cells for blood and spleen samples respectively. Boxes and numbers indicate the neutrophil population and their percentage make-up of the granulocyte population.

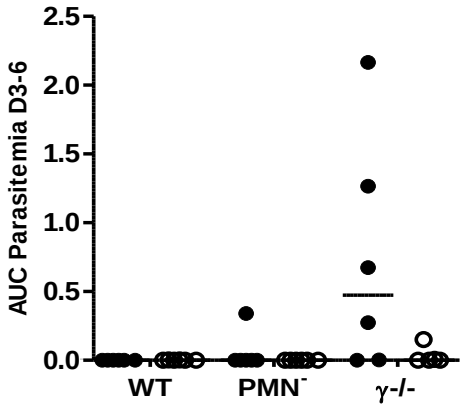

Figure 3-19: Role of Fc signalling and neutrophils on secondary challenge outcome

BALB/c or $\gamma^{-/-}$ mice were immunised i.m. with Ad-M PyMSP1$_{42}$, challenged at week 10 with 10^6 *P. yoelii* 17XNL iRBCs, and then re-challenged at week 18 with 10^6 *P. yoelii* YM iRBCs. One day prior to, and three days after secondary challenge, six BALB/c and six $\gamma^{-/-}$ mice were given 0.5mg 1A8 i.p. (PMN^{-}) and all other mice, WT and $\gamma^{-/-}$, were given 0.5mg i.p. control rat IgG. Figure 3-18 thus represents inferred PMN depletion in challenged mice. Dots show AUC analysis of parasitaemia for days 3-6 following secondary challenge of non-immunised (●) and immunised (○) groups. Lines on dot plots represent medians.

Thus overall it appears that the FcR common γ-chain signalling may play a role in the control of parasitaemia during secondary infection of some mice that did not receive a prior effective vaccine, although this control is not mediated by neutrophils. It should also be noted that the $\gamma^{-/-}$ mice here experiencing reduced control of secondary parasitaemia exhibited the lowest levels of parasite exposure (and the highest degree of innate protection) in the preceding *P. yoelii* 17XNL challenge (Figure 3-15A,B). However, the induction of serum anti-PyPEMS ADRB activity post-challenge (Figure 3-16) was comparable to the WT non-immunised mice, suggesting similar induction of anti-malarial responses in these mice despite the slightly lower parasite burden in the primary challenge.

Despite the lack of association between ADRB activity and challenge outcome in this model, ADRB activity following the secondary *P. yoelii* exposure was also assessed in the 13 mice

showing the highest ADRB response after primary challenge. Serum ADRB activity was enhanced by parasite exposure (Figure 3-20), showing higher levels in comparison to after primary challenge (Figure 3-16). To further address antigen-specificity in the assay, sera were depleted using the recombinant PyMSP1 proteins (Figure 3-20). As expected, assays using plates coated with recombinant PyMSP1$_{19}$ or PyMSP1$_{33}$ protein demonstrated an antigen-specific effect of antibody depletion upon ADRB activity (Figure 3-21). When tested using PyPEMS, depletion of PyMSP1$_{19}$ antibodies did not significantly decrease the sera's ability to induce ADRB activity (Friedman test; Dunn's multiple comparison test), however, PyMSP1$_{33}$ antibody depletion reduced ADRB activity against *P. yoelii* PEMS similarly in both immunised and non-immunised mice suggesting that, after secondary challenge, the PyMSP1$_{33}$ region of the PyMSP1 antigen is a target of ADRB-inducing antibodies.

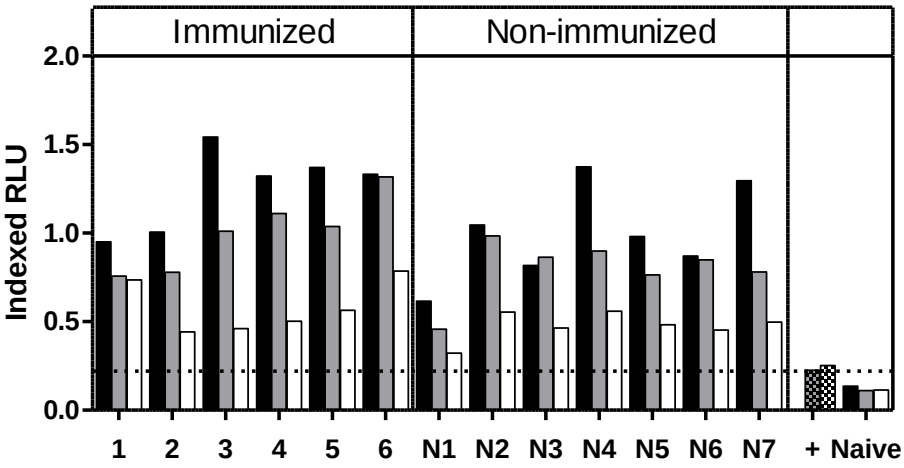

Figure 3-20: Contribution of anti-PyMSP1$_{42}$ antibodies to post-secondary challenge anti-PyPEMS ADRB activity

BALB/c or $\gamma^{-/-}$ mice were immunised i.m. with Ad-M PyMSP1$_{42}$, and challenged as in Figure 3-19. Fourteen days post second challenge, anti-*P. yoelii* PEMS ADRB activity was assessed in mouse serum pre-incubated with PBS (no depletion; black), or depleted of PyMSP1$_{19}$- (grey) or PyMSP1$_{33}$-specific (white) antibodies. Chequered bars (+ = positive reference serum) represent background ADRB activity of depleted sera without any antigen coated onto the plate. Results with naïve BALB/c mouse serum are also shown.

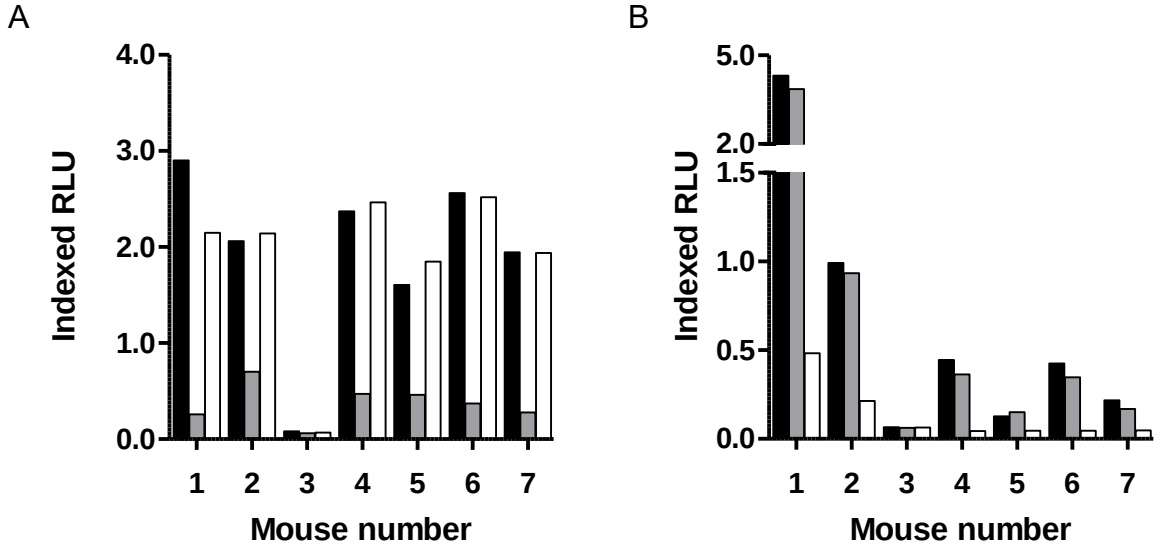

Figure 3-21: Confirming PyMSP1 antibody depletion protocol

ADRB induction was assessed by BALB/c PMNs on either (A) $PyMSP1_{19}$ or (B) $PyMSP1_{33}$ coated plates in response to sera from BALB/c mice immunised with Ad-M $PyMSP1_{42}$ which was pre-incubated with PBS (no depletion; black), or depleted of $PyMSP1_{19}$ (grey) or $PyMSP1_{33}$ (white) antibodies. Bars represent the mean of two replicates for each sample.

3.3. Discussion

Here, the assessment of the ADRB assay in the mouse model is reported and applied, for the first time, to the field of malaria vaccine development.

Initial work confirmed antigen-specificity and established the assay parameters when using recombinant antigen arrayed on the plate. These assay conditions used a minimal volume of serum and allowed for both an increase and decrease in ADRB activity to be observed with minimal intra-assay variability. Although some inter-assay variability was noted when repeatedly using the same sample on freshly isolated PMNs, the inherent differences between individual samples were greater and thus reliably observed between assay replicates. This mouse ADRB assay also allowed for the roles of γ-chain-mediated antibody signalling to be assessed. Mice have three classes of activatory FcγRs (I, III, IV) which signal through the common γ-chain immunoreceptor tyrosine-based activation motifs (ITAMs) (294). The work reported here has shown a dependency on these receptors for ADRB induction, given ablation of this activity when using PMN from $\gamma^{-/-}$ mice. More specifically, it was concluded that ADRB activation is FcγRIII (CD16)-mediated given that FcγRI (CD64) is not constitutively expressed on mouse neutrophils (299, 300) and thus is unlikely to contribute to ADRB (a result supported by the ablation of ADRB activity by a CD64-irrelevant mAb (anti-CD16/32)), and that mice lack the activatory FcγRIIa (CD32a) (294, 296). ADRB induction, however, is not only induced by CD16, but is regulated by FcγRIIb (CD32b) given enhanced levels of activity were observed when using PMN from $CD32b^{-/-}$ mice. It is unlikely that CD32b regulation results from interference with other antibody-FcR binding, but rather results from intracellular immunoreceptor tyrosine-based inhibitory motif (ITIM) signalling which initiates the recruitment of inositol phosphatase SHIP and impedes CD16 signal transduction (196, 301, 302).

The human IgG1 and IgG3 cytophilic isotypes have been reported to be essential for the induction of ADCI activity against the *P. falciparum* parasite and specific antigens such as MSP3 (253, 288, 303), whilst a human IgG1 mAb against $PfMSP1_{19}$, but not an epitope-matched IgA, have been reported to protect against transgenic *P. berghei* in humanised mice (202, 204). Similarly, the cytophilic mouse isotype IgG2a has been reported to be important for protective immunity against blood-stage *P. berghei* (304) and *P. yoelii* (305, 306). However, in these experiments both the IgG1 and IgG2a isotypes appeared comparable in their ability to induce ADRB activity from PMN – either using serum skewed towards specific isotype profiles by use of different vaccine immunisation regimes (279), or by using chimeric epitope matched mAbs (277). I was unable to express sufficient quantities of chimeric epitope-matched mouse IgG2b and IgG3 (data not shown) and so it remains to be determined whether these isotypes could also function in a similar manner. Notably mAbs of both these isotypes have been shown to afford efficacy against blood-stage *P. yoelii* (289, 307). However, given mouse IgG1 and IgG2a are reported to signal via CD16 (294, 308) and tend to be the dominant IgG isotypes in serum, these data suggest that total antigen-specific IgG antibody titre in mice is likely to closely correlate with ADRB induction.

In addition to using the ADRB assay to assess antibody-receptor interactions, mouse malaria models provide an invaluable tool for assessing protective outcome. Initial studies indicated that serum from $PyMSP1_{42}$ vaccinated mice could reliably induce ADRB activity from neutrophils in the assay when recombinant $PyMSP1_{19}$ antigen was arrayed on the plate. Despite neutrophils from $\gamma^{-/-}$ mice lacking the ability to produce ROS in the context of the ADRB assay, and $CD32b^{-/-}$ mouse neutrophils having an increased ability to produce ROS, no difference was seen in primary *P. yoelii* challenge outcome following immunisation of these mice (which mounted comparable immune responses to WT controls in response to viral vector immunisation as seen in a previous study (272)). I also observed little difference

in protective outcome between non-immunised WT and CD32b$^{-/-}$ C57BL/6 mice following lethal *P. yoelii* challenge, unlike that reported for *P. chabaudi* infection on the BALB/c background (203). However, it became apparent following further investigation that these immunised animals did not have antibodies capable of inducing ADRB against *P. yoelii* PEMS. ROS production by PMNs has been widely tested in the literature using such methodology (291, 298, 309-311), but these data highlight the importance of using native parasites in such an assay set-up. Previous work on ADCI activity suggests that it is not overly surprising that C-terminal MSP1 ($MSP1_{42}$) immunisation did not induce anti-parasite cellular activation, given that investigation of antibody-dependent monocyte activation has identified other antigenic targets such as GLURP (254), SERP (255), MSP3 (312) and MSP1 block 2 (313). Due to the likely similarity in antibody action between ADCI and ADRB, the aforementioned targets may also represent those playing dominant roles in eliciting anti-merozoite ADRB activity. The lack of detectable anti-PyPEMS ADRB activity post-$PyMSP1_{42}$ vaccination was thus in agreement with the challenge data showing no bearing on an initial challenge in the knockout mice, and moreover these data would suggest that the mechanism by which the $PyMSP1_{42}$ vaccine protects is not γ-chain-mediated. Importantly these data also suggested that anti-$PyMSP1_{19}$ IgG responses may not be sufficient to induce ADRB activity, which would make sense given the closeness of this moiety to the parasite surface and the fact the antigen may not be accessible to antibodies until the MSP1 molecule is processed during red blood cell invasion (314, 315). However, it remained possible that throughout the course of a challenge infection the animal could acquire *de novo* anti-parasite antibodies capable of inducing ADRB, but this would be unlikely given the short infection period investigated here with the highly lethal YM strain of *P. yoelii*. I thus switched to the use of a non-lethal model, in order to assess post-challenge antibody responses.

In this case, following a non-lethal strain 17XNL primary infection, almost 50% of mice acquired anti-*P. yoelii* PEMS serum ADRB activity. This induction was irrespective of prior $PyMSP1_{42}$ vaccination status and did not correlate with antibody titres against $PyMSP1_{19}$ or $PyMSP1_{33}$, again suggesting the activity to be independent of this antigen. However, it was then possible to re-assess the importance of FcR and anti-PyPEMS ADRB activity in protection against secondary *P. yoelii* challenge. In this case, when mice were depleted of neutrophils, they were still able to control parasitaemia suggesting that these cells are not key effectors in controlling secondary infection in the *P. yoelii* model, despite measurable ADRB activity. Nevertheless, data from non-vaccinated $\gamma^{-/-}$ mice in the same experiment alluded to a contribution of γ-chain-mediated signalling in controlling secondary exposure to *P. yoelii* malaria in mice, and the possibility that this efficacy is mediated through a non-neutrophil cell group. There have been numerous reports of monocytes playing an important role in parasite killing through ADCI (180, 249-251, 256) or phagocytosis of infected RBCs. It would seem possible that in the absence of vaccine-induced responses against $PyMSP1_{42}$, that other antigen-specificities acting against the merozoite and/or infected RBC may play a more dominant role in effective immunity.

Overall, this data support the evidence that *P. yoelii* malaria infection is controlled largely by γ-chain-independent activity (50), especially given that both immunised and non-immunised $\gamma^{-/-}$ mice performed better than WT litter mate controls in the challenge experiments. Interestingly, ADRB serum activity was again enhanced by secondary infection (with a likely increased contribution from anti-$PyMSP1_{33}$ antibodies). Even though no association was established with protection against *P. yoelii*, these data suggest that other antigen targets of anti-PEMS ADRB activity remain to be established. They also suggest this activity increases with repeated malaria exposure thus adding weight to the original report of association of this activity with clinical immunity against *P. falciparum* (181).

The development of new functional antibody assays remains vital for pre-clinical malaria vaccine development. With relative ease, the principles of this assay could be transferred to assessment of ADRB activity using *P. falciparum* PEMS and human neutrophils, thus overcoming the limitations in extrapolating results from *P. yoelii* challenges in mice to humans and *P. falciparum*. Thus, in Chapter 4, I build upon the development of the ADRB assay described here to establish a standardised protocol for assessing the ADRB activity of human serum with neutrophils isolated from human donors.

CHAPTER 4

STANDARDISATION OF THE ADRB ASSAY WITH HUMAN NEUTROPHILS AND *PLASMODIUM FALCIPARUM*

4. STANDARDISATION OF THE ADRB ASSAY WITH HUMAN NEUTROPHILS AND *PLASMODIUM FALCIPARUM*

I am very grateful to Dr Kazutoyo Miura and Dr Michael Fay who have helped to conduct the statistical analysis for this Chapter as part of an ongoing collaboration.

4.1. Introduction

The development of efficacious vaccines against malaria promises to be one of the most cost effective strategies for achieving significant reductions in global health burden and realising the possibility of eradication (316). However despite this burden of disease, the immunological mechanisms which confer protection against malaria *in vivo* in humans remain highly debated and poorly understood (317), and thus vaccine development strategies often suffer from a lack of informed immunological guidance.

Sustained interest in vaccines against the blood-stage of malaria infection has demanded assessment of antibody function against merozoite and infected red blood cell (iRBC) expressed antigens. While it is largely accepted that parasite antigens expressed on the surface of the iRBC are particularly important for naturally-acquired immunity (NAI) (317), differential expression profiles, and high levels of polymorphism in RBC surface expressed genes between different parasite strains, mean that the majority of blood-stage vaccine efforts have not focused on these targets. Instead merozoite proteins, in particular those involved in the erythrocyte invasion process, have been the focus of vaccine development efforts (15, 239). To this end, the assay of growth inhibitory activity (GIA) – one that assesses anti-merozoite antibodies' ability to block parasite invasion into the human erythrocyte and/or parasite growth inside the erythrocyte, has been used to direct many blood-stage vaccine development efforts. While the assay of GIA seeks to measure one important mechanism by which vaccine-induced antibodies can block parasite proliferation (essentially cell-

independent antibody neutralisation), such a mechanism remains to be formally associated with protection following human vaccination (318) and even then, would likely represent a 'non-natural' form of immunity given the relatively poor association between GIA and clinical outcome in the context of studies of NAI (179).

Consequently, there is significant interest in assays that can guide the development of vaccines that may afford antibody-mediated protection via alternative mechanisms to GIA, and which may help researchers to better understand mechanisms of natural malaria immunity. For example a number of protocols for conducting phagocytosis assays have been described assessing the ability of immune sera to initiate monocyte or neutrophil phagocytosis of either merozoites (259, 260) or iRBCs (124, 261, 319). In addition, the antibody-dependent cellular inhibition (ADCI) assay, in which monocytes are the effectors of antibody Fc-dependent signaling and subsequent anti-malarial cellular activity has been described (250). Polyclonal antibodies isolated from the serum of immune African volunteers have been shown to elicit ADCI activity *in vitro*, and these same antibodies were reported to control malaria infection when passively transferred into non-immune humans (180). However, despite the potential utility of this assay, historically it has proved problematic with regard to demonstrating reproducibility and development of a standardised protocol for use by the malaria community, and thus the assay has been largely under-explored as a vaccine antigen screening tool. More recent work seeking to address this problem, may in time facilitate wider uptake of this approach (320).

The ADRB assay using *P. falciparum* parasites, human neutrophils and human antibodies has also been described (181, 321) but, like the ADCI assay, lacks a formal qualification, thus limiting its immediate utility as a vaccine screening or NAI investigative tool. The ADRB assay's assessment of the ability of anti-merozoite antibodies to activate

neutrophils/polymorphonuclear cells (PMNs) via Fc receptors (FcR) to produce ROS relies on a mechanism distinct from assays which assess antibody-induced neutrophil phagocytosis of either merozoites or iRBCs (124, 262, 289, 322). Although I have shown that the ADRB assay does not associate with protection against *P. yoelii* rodent malaria (Chapter 3)(323), ADRB activity has been strongly associated with a reduction in *P. falciparum* clinical disease in naturally-exposed individuals in Senegal (181) lending support to the utility of a reproducible, standardised protocol for a human neutrophil-based assay for use by the malaria research community. In fact, the production of ROS is known to be effective in attenuating growth of intracellular parasites (324-326) including *P. falciparum* (290, 327). This is further supported in mouse models incapable of producing superoxide which experience accelerated malaria parasite multiplication rates (328). ADRB activity is thus a plausible mediator of protection against *P. falciparum* malaria, supporting the reported association with clinical protection (181).

Given the reported association between ADRB activity and clinical disease, a reliable protocol for the assay would allow it to be used more broadly in pre-clinical and clinical vaccinology as well as epidemiological assessment of NAI. The assay has three major components: *P. falciparum* merozoites, human PMNs, and human serum. In this chapter I define optimal parameters for each of these components. In addition I assess both intra- and inter-assay reproducibility in order to define an optimal protocol for testing serum samples for ADRB activity. Using the protocol developed, I show that a cohort can be quickly and efficiently characterised. I thus provide a standardised protocol for conducting the ADRB assay with human PMNs so that the assay can be used by other laboratories for malaria vaccine development and the evaluation of NAI.

4.2. Results

4.2.1. Effector cell number and purity

Initially PMNs were prepared from whole blood from healthy UK adult donors as described in Chapter 2. The number and purity of freshly isolated PMNs were assessed before addition to the assay in order to meet basic quality control standards. Immediately following the completion of the PMN isolation protocol, cell preparations were examined by Giemsa stained slides (Figure 4-1) and cellular purity determined as percentage PMNs. A cell preparation of >95% PMNs was typical from counting 1000 total cells (data not shown). Typical contaminates were RBCs and monocytes. If ≥25% cells were RBCs, the RBC lysis step was repeated. If ≥25% cells were monocytes, the cell preparation was discarded. A preparation of >75% PMNs was considered sufficient to conduct the assay. After adjusting for PMN purity in the cell preparation, the assay was conducted with 100 µL cell suspension in each well at 1 x 10^7 PMN/mL in accordance with previous versions of the assay (181, 323). Cells were normally used in the assay within 5 minutes of suspension in PMN buffer and no later than 30 minutes; and within 2 hours (maximum 4 hours) of phlebotomy. Typically, enough cells for a complete 96-well assay plate could be isolated from 25 mL whole blood.

4.2.2. *P. falciparum* PEMS number and purity

The assay was conducted with *P. falciparum* PEMS isolated as described in Chapter 2. PEMS were counted as schizonts before rupturing and suspended at 18.5 x 10^5 schizonts/mL – the concentration used in the assay. Once suspended in PBS at the correct concentration, PEMS were frozen to rupture the parasitophorous vacuole and release the merozoites. PEMS suspensions were stored at -20^{o}C for up to 1 year before use. Aliquots were thawed once, the day prior to the assay being conducted, and 100 µL coated onto each well of the assay

plate(s) which were then left overnight at room temperature. During assay development, the PEMS suspension used to coat plates was confirmed to contain free merozoites by scanning electron microscopy (SEM) (Figure 4-2), while no such structures were visible in a non-infected RBC preparation (data not shown).

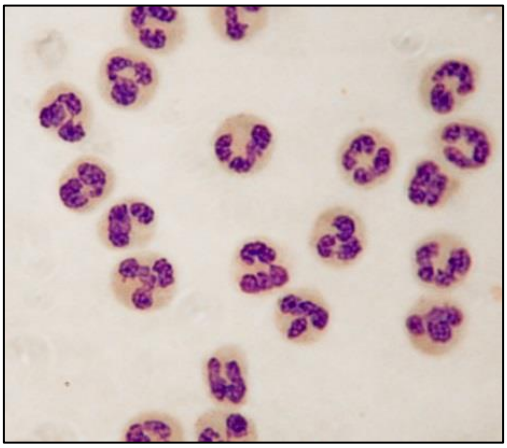

Figure 4-1: PMN preparation

PMNs were isolated from whole blood and confirmed to be >75% pure by Giemsa stained slide. 100 µL of cell suspension was added to each well of the assay at 1 x 10^7 PMNs/mL.

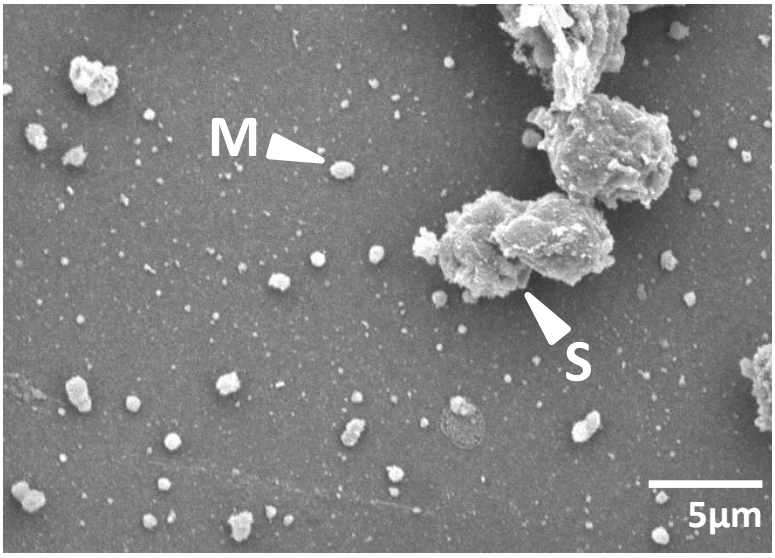

Figure 4-2: PEMS preparation used in ADRB assay

Scanning electron micrograph of PEMS preparation showing both merozoites (M) and schizonts (S).

4.2.3. Assay readout: Maximum RLU

Luminescent readings were taken from each well of the 96-well assay plate for 1000 ms every two minutes for 1 hour (Figure 4-3) and from the resulting data the following parameters were calculated: maximum RLU; area under the curve (0-60min); area under the curve (4-20min); and average RLU (0-30min). The analyses described below were comparable between all outputs (data not shown), however for consistency with the limited number of previous studies related to this assay (181, 323), it was decided to progress using maximum RLU as the assay output (referred to as RLU throughout the rest of the text).

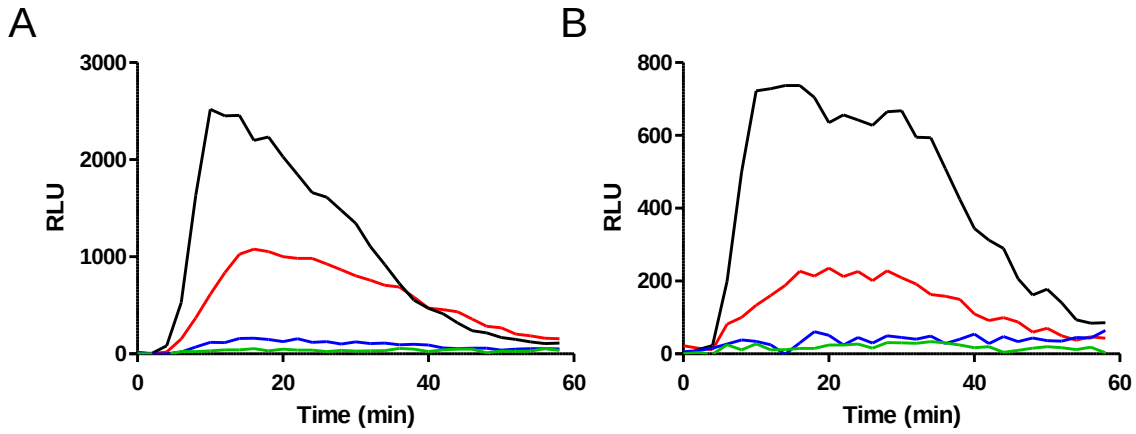

Figure 4-3: Example luminescence traces from ADRB assay

Luminescence of individual wells in the ADRB assay was measured every two minutes for one hour. (A) and (B) each show four example traces from two separate experiments using different PMN donors. Black – positive control, Red – test sample with positive ADRB activity, Blue – UK negative control, Green – test sample with negative ADRB activity.

4.2.4. Effect of serum parameters on ADRB activity

Given the ADRB assay aims to assess the activity of human antibodies against *P. falciparum* blood-stage parasites, it was important to assess how different concentrations and preparations of test serum would affect ADRB activity. Respiratory burst activity induced by

a pool of hyper-immune Kenyan sera (tested in duplicate) decreased with increasing serum dilutions, whilst a pool of sera from malaria-naïve UK adults failed to induce ADRB activity at dilutions of 1:25 or more (Figure 4-4A). Given this result, it was decided to conduct all future assays with serum diluted 1:50. This was sufficient to observe high level responses from ADRB positive serum without using large volumes of serum (2 µL required per well).

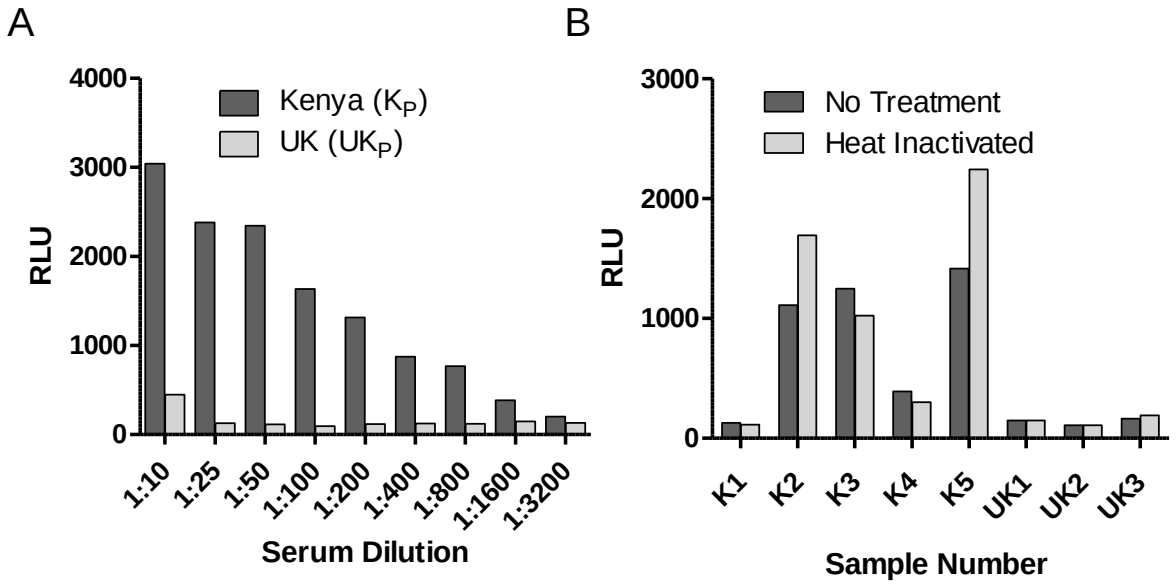

Figure 4-4: Serum parameters affecting ADRB activity

Assay parameters were determined using a plate coated with 18.5 x 10^5 schizonts/mL and serum from malaria-naïve UK volunteers and Kenyan adults. (A) ADRB activity induced by pooled serum from Kenyan (K_p) and UK adults (UK_p) was tested at different serum dilutions and is reported as maximum RLU. (B) ADRB activity induced by sera (5 Kenyan and 3 UK individual sera) diluted 1:50 before and after heat inactivation. Bars represent the mean of duplicate wells tested with the same PMN donor.

Using the defined serum dilution of 1:50, I also assessed whether the ADRB activity was induced independent of complement. The results showed that there was no significant difference between respiratory burst induction from serum subjected to heat-inactivation compared to non-heat-inactivated samples (Wilcoxon sign rank test: $P = 0.74$; Figure 4-4B). In a related series of experiments using a malaria protein-based (as opposed to PEMS-based)

assay (323), I also showed that there was no difference in induction of ADRB activity from plasma and serum taken from the same volunteers previously immunised with a candidate malaria vaccine targeting the *P. falciparum* merozoite surface protein 1 (PfMSP1) antigen (Figure 4-5A) (144); suggesting that the presence of clotting factors or lithium heparin anticoagulant does not affect the assay output. Using the same assay setup, I also showed that ADRB activity was induced differently by epitope-matched chimeric anti-PfMSP1 monoclonal antibodies of different human isotypes (202, 204), such that IgA>IgG3>IgG1 (Figure 4-5B).

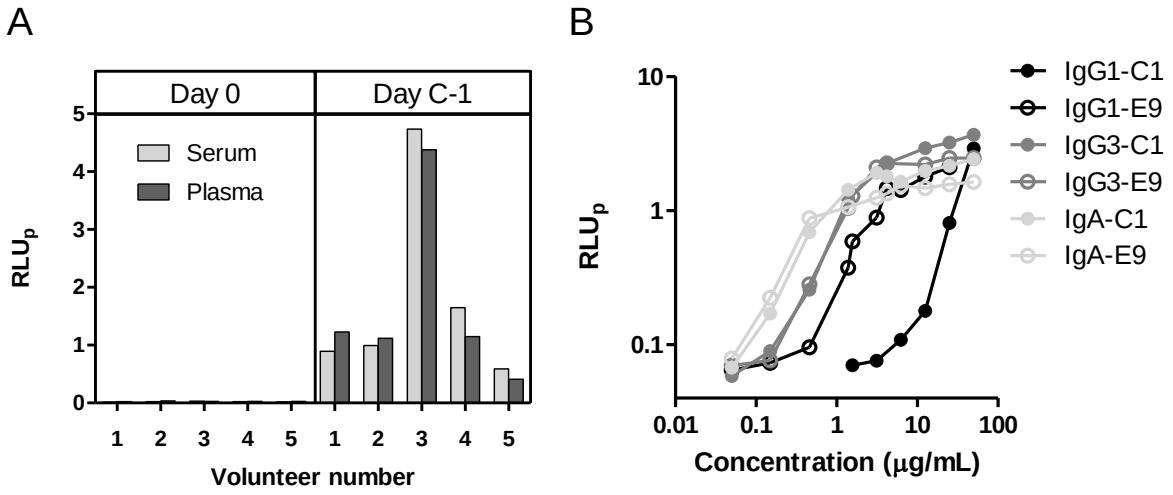

Figure 4-5: Effect of clotting factors and antibody isotype on ADRB activity

ADRB activity induced on a plate coated with 10 μg/mL GST-PfMSP1$_{19}$ by (A) sera (light) and plasma (dark) diluted 1:50 from volunteers both before (Day 0) and after (Day C-1) ChAd63-MVA PfMSP1 immunisation, and (B) by chimeric human epitope-matched IgG1 (black), IgG3 (dark grey) and IgA (light grey) mAbs against the C1 and E9 epitopes of PfMSP1$_{19}$ at a range of concentrations. All samples are indexed against a pool of hyper-immune serum as described in Section 4.2.6.2 and reported as indexed RLU (RLU$_p$). Bars and dots represent the mean of two assay replicates.

4.2.5. ADRB activity is dependent on *P. falciparum* PEMS

Having established that malaria hyper-immune sera from Kenyan adults induced ADRB activity, whilst sera from malaria-naïve UK adults did not, it was important to establish that this activity was specific to the malaria parasite and not a potential reaction to RBCs (in this case isolated from healthy UK adults). Both uninfected RBC and PEMS from malaria iRBC cultures were thus produced and 100 µL of either suspension coated onto plates at 18.5 x 10^5 schizonts (or RBC)/mL. Upon coating plates with PEMS, serum from Kenyan adult volunteers (with significant levels of prior malaria exposure) elicited ADRB activity. This activity was not induced when coating a plate with uninfected RBC (Figure 4-6). In addition, no ADRB activity was elicited by sera collected from malaria-naïve UK volunteers against either PEMS-coated or RBC-coated plates.

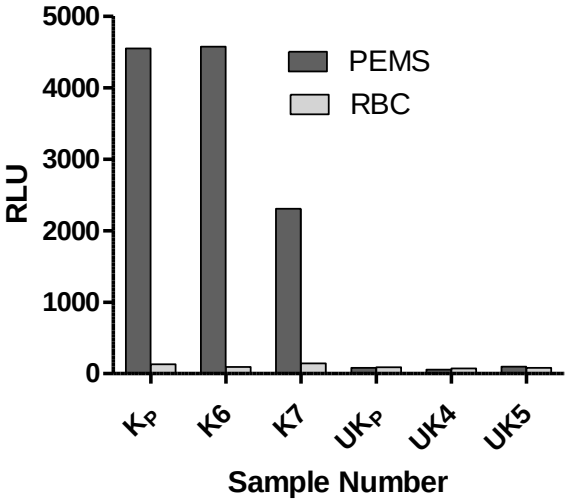

Figure 4-6: Specificity of ADRB activity to malaria parasites

Assay parameters were determined using a plate coated with 18.5 x 10^5 schizonts/mL and serum from malaria-naïve UK volunteers and Kenyan adults. ADRB activity induced by a pool of sera from Kenyan adults and two individual Kenyan volunteers, and a pool of UK, malaria-naïve adults and two individual UK volunteers was assessed using plates coated with either PEMS (dark) or uninfected RBCs (light). Bars represent the mean of duplicate wells tested with the same PMN donor.

4.2.6. Reproducibility

Reproducibility in the ADRB assay was assessed using a small cohort of serum or plasma from 13 African adults and serum from 10 malaria-naïve UK adults. All samples were assayed in duplicate such that with the 23 test samples and the positive control (see below), the whole cohort could be run in 48 wells (half a plate). This layout was replicated on each plate with PMNs from two different healthy UK adult donors and assayed in parallel. This experimental setup was run on three consecutive days, with two plates being run on one day, and thus each sample was run with eight independent PMN preparations (Figure 4-7). As above, all sera and plasma were diluted 1:50 and not heat-inactivated, 100 µL PMNs were added at 1 x 10^7 PMNs/mL, and PEMS were coated onto plates at 18.5 x 10^5 schizonts/mL.

4.2.6.1. Intra-assay reproducibility

For each serum sample tested with each PMN donor (n = 184) duplicate readings were compared to each other (Figure 4-8). Interclass correlation coefficient (ICC) analysis (284) showed that measuring activity by maximum RLU was highly repeatable under the same conditions (ICC = 0.973). Given this I asked whether it was necessary to test samples in duplicate as, for the purposes of high throughput of samples, it would be beneficial to only have to test samples in singlet upon an individual assay plate.

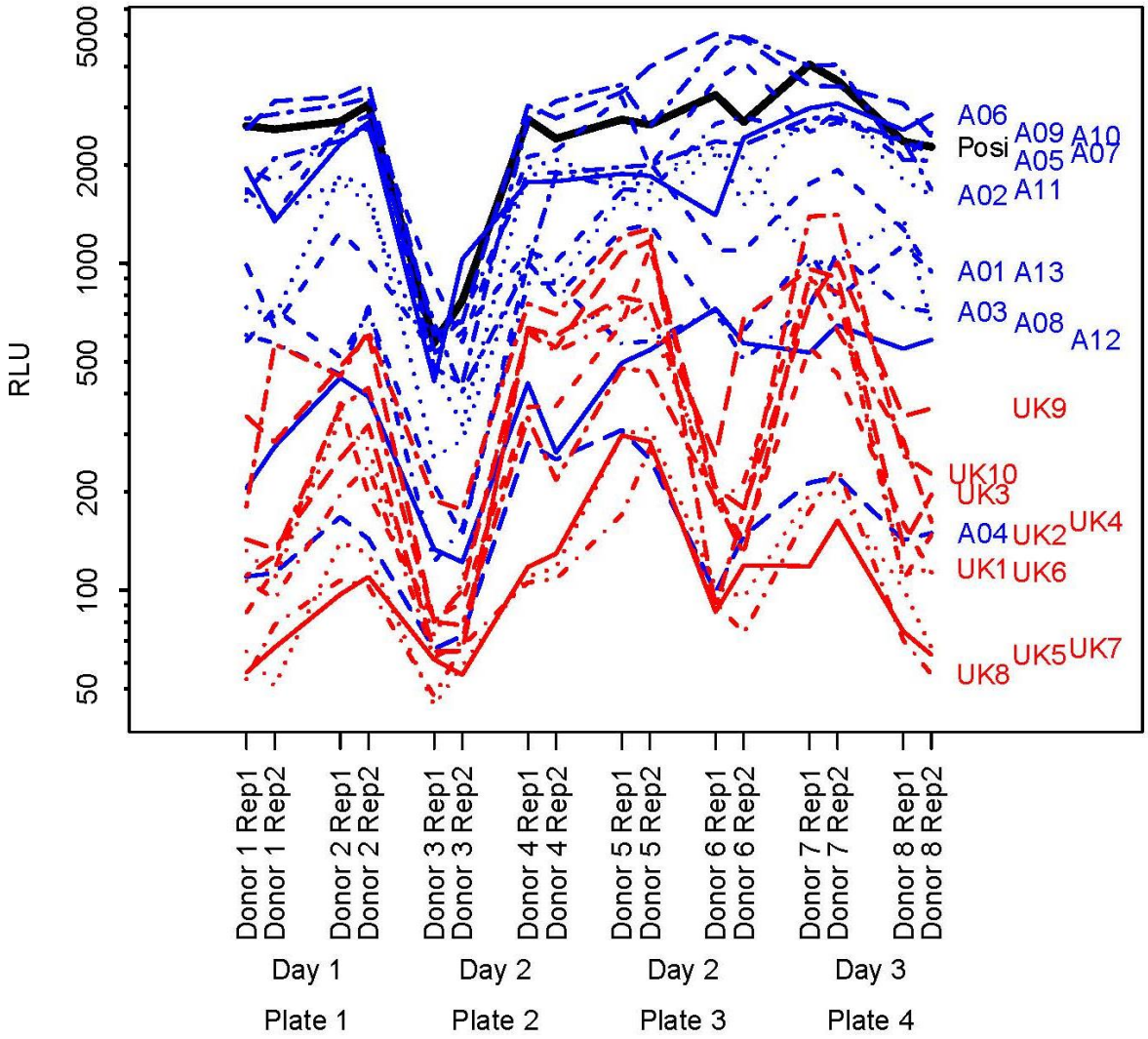

Figure 4-7: Raw ADRB assay data from repeats with multiple PMN donors

ADRB activity against PEMS was determined for 13 malaria-endemic African and 10 malaria-naïve UK serum or plasma samples using 8 different neutrophil donors. Samples were diluted 1:50, randomised on PEMS coated plates and were all measured in duplicate.

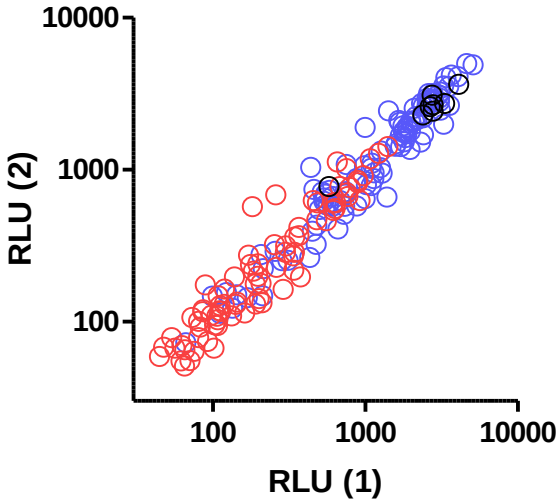

Figure 4-8: Relationship between intra-assay replicates

ADRB activity against PEMS was determined for 13 malaria-endemic African and 10 malaria-naïve UK serum or plasma samples using 8 different neutrophil donors (*n* = 184) in duplicate. Duplicate values for maximum RLU achieved by each sample in each assay were plotted against each other. Blue = African samples, red = UK sample, black = positive hyper-immune pool. ICC = 0.973.

To address the singlet versus duplicate question, R^2 values from linear models with sample included only (R_s^2), using either singlets ($R_{s\,Sing.}^2$) or duplicates ($R_{s\,Dup.}^2$) were compared. Ideally, R_s^2 will be close to 1, because the only variability in the measured responses will be due to differences in the samples, and there will be no variability due to differences in PMN donors, plates, day, or replicate. Comparing $R_{s\,Sing.}^2$ and $R_{s\,Dup.}^2$ enables us to see how much the variability due to replicates can be reduced, and thus the R_s^2 be maximised (there will however, still be unavoidable variability due to PMN donors present). For duplicates, the average of the two replicates as a response was used, so there will be less total variability in the responses compared to using a single replicate as the response. Thus, the proportion of that total variability explained by the sample in the model (i.e. $R_{s\,Dup.}^2$) will necessarily be

larger than that proportion for the single replicate, $R^2_{s\,Sing.}$. The important question is how much improvement does using duplicates give? To answer this the percent increase was used,

$$100 \times \frac{R^2{}_{s\ Dup.} - R^2{}_{s\ Sing.}}{R^2{}_{s\ Sing.}}$$

This analysis showed that the % increase in R^2_s due to testing samples in duplicate was less than 7% for all data when assessing African samples only whether analysed as total values (RLU), indexed values (RLU_p) as described in Section 4.2.6.2, or log transformed data. When UK samples were included in the analysis, measuring samples in singlet reduced R^2_s by less than 4% compared to R^2_s when measuring samples in duplicate (Table 4-1), thus confirming the assay could be acceptably performed in singlet.

Table 4-1: Singlets vs duplicates

Comparison of R^2 from the linear models explained by sample effects only (R^2_s) for samples measured in either singlet or duplicate wells using either: malaria-endemic African samples only, or both malaria-endemic African and malaria-naïve UK samples combined. The percentage increase in R^2_s between testing samples in duplicate and testing singlets is also shown (as calculated in the text).

	African			**African + UK**		
	Singlets	Duplicates	% Increase	Singlets	Duplicates	% Increase
RLU	0.622	0.635	2.14	0.734	0.745	1.45
Log_{10} RLU	0.690	0.704	2.04	0.734	0.744	1.36
RLU_p	0.787	0.840	6.68	0.860	0.893	3.81
Log_{10} RLU_p	0.888	0.913	2.88	0.847	0.863	1.85

4.2.6.2. Inter -assay reproducibility

The raw assay readout in terms of maximum RLU varied significantly by donor. The effects of donor are significant even after accounting for day or plate effects (Friedman test: $P < 0.001$, see also Figure 4-7). As I needed to prepare fresh human neutrophils each day, there is no way to measure actual day-to-day variation other than as the effect of PMN donor. I thus focus on donor effects for the analysis of inter-assay variability. Using a permutation test, no significant plate effects were found after accounting for donor effects ($P = 1.00$). Notably, during the assay development I had observed that PMN Fc receptor expression profile on $CD16^+$ granulocyte populations (Figure 4-9) of 5 tested healthy UK adult volunteers fell into two distinct groups which may potentially contribute to the inter-donor variation observed here, with some volunteers expressing either low (Figure 4-9D) or high (Figure 4-9E) levels of CD32.

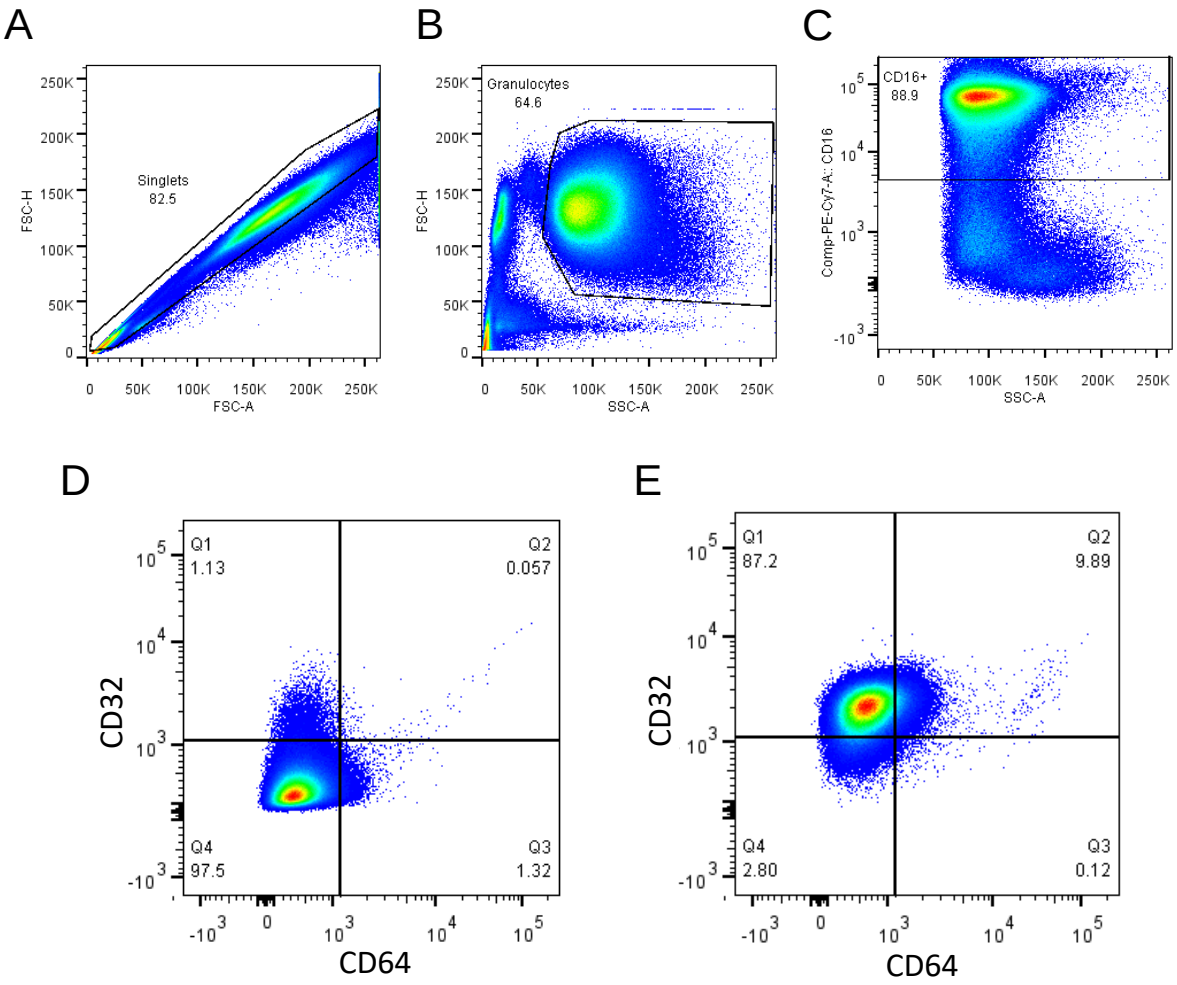

Figure 4-9: Assessment of FcR on human PMNs

Whole blood was taken from healthy UK volunteers, and PMNs isolated on polymorphprep gradients. Cells were surface stained with anti-CD16, anti-CD32, and anti-CD64. One million events were acquired in total. (A) Singlets were gated by forward scatter-area (FSC-A) and -height (FSC-H) profiles. (B) Granulocytes were then gated by FSC-A and side scatter-area (SSC-A) profiles. (C) PMNs were then defined as the $CD16^{+}$ population and were characterised with regard to their CD32 and CD64 expression levels. Representative plots from individuals who exhibited either (D) $CD32^{lo}$ or (E) $CD32^{hi}$ phenotypes.

Potential strategies for indexing data to compensate for PMN donor variation were thus investigated using the cohort of 13 African and 10 UK samples. In accordance with previous iterations of this assay in both mice (323) and humans (181), a positive control sample was defined and included on each assay plate against which test samples, under exactly the same conditions, were indexed (RLU_p) such that:

$$RLU_p = \frac{RLU_{test\ sample}}{RLU_{positive\ control}}$$

This positive control consisted of a pool of hyper-immune Kenyan adult sera with sufficient volume to run over 1000 plates. Similar to non-indexed data, intra-assay reproducibility for RLU_p was high (ICC = 0.926) and the assay could be acceptably run with singlets (Table 4-1). Values for all data as a proportion of the ADRB activity of the mean of the 10 malaria-naïve UK serum samples (RLU_n) were also calculated. To assess inter-assay reproducibility the African samples only were first considered, since it was difficult to index by the mean of the negative (UK) controls if the measurement of the negative control samples as well was required in the same assay. In order to measure how well this indexing (i.e., using RLU_p that divides by positive control max RLU, or using RLU_n that uses a negative control) removes the variability due to PMN donor, the R square from the model with sample and PMN donor included were partitioned into two parts: the percent due to PMN donor (%$\mathbf{R^2_{donor}}$) and the percent due to sample (%$\mathbf{R^2_{sample}}$ = 100-%$\mathbf{R^2_{donor}}$). In addition Log_{10} RLU_p and Log_{10} RLU_n were considered. This analysis showed that %$\mathbf{R^2_{donor}}$ was smaller when indexed against the positive control, as compared to indexing against the UK samples (Table 4-2). Both RLU_p and Log_{10} RLU_p perform similarly well (Table 4-2).

Table 4-2: Variation due to PMN donor effect

ADRB activity against PEMS was determined for 13 malaria-endemic African and 10 malaria-naïve UK serum or plasma samples using 8 different neutrophil donors. The Table reports percentage of assay output R^2 explained by donor effects on African samples only, or both African and UK samples after no indexing (RLU); indexing against a positive hyper-immune Kenyan pool (RLU_p); indexing against the mean of the 10 malaria-naïve UK samples (RLU_n); and log transformation of data. Parentheses indicate 95% CIs.

Assay Readout	African (% R^2_{donor})	African + UK (% R^2_{donor})
RLU	24.5 (17.8-33.8)	12.5 (9.5-17.6)
Log_{10} RLU	25.9 (18.7-34.9)	19.4 (15.7-24.0)
RLU_p	3.5 (2.4-10.2)	1.4 (1.2-4.6)
Log_{10} RLU_p	2.0 (1.7-7.4)	5.3 (3.6-9.5)
RLU_n	44.3 (35.3-52.1)	18.7 (13.8-24.9)
Log_{10} RLU_n	27.8 (21.6-35.6)	6.8 (4.8-10.9)

When UK samples (negative controls) were included in the analysis, the same trend was generally seen: the positive control gives lower values of $\%\mathbf{R^2_{donor}}$ than either no indexing or indexing by the negative control. As a result, the stock of pooled hyper-immune Kenyan serum was continued as the control against which all further samples were indexed.

In addition to indexing by the positive control, I could additionally repeat the analysis on different PMN donors to reduce the dependence of the results on PMN donor. Increasing the number of PMN donors will increase the reproducibility, but how many are reasonably enough? To answer this question, simple simulations were done assuming that the errors due to PMN donor (on the Log_{10} RLU_p) are normally distributed (this assumption appeared

reasonable based on some graphical analysis; not included). To compare different numbers of donors, I compared the width of confidence intervals based on the t-distribution (which is used for normal data).

The lengths of the 95% CIs were then compared between assay outputs using different numbers of replicates/donors (n = 2, 3, ... ,8) by simulating 1000 data sets. There was a substantial decrease in the length of CIs between data simulated with samples evaluated with two donors compared to three (Table 4-3). Additional replicates had a decreasing impact on the reduction of CI length. Considering the level of donor effect I can reduce by adding further PMN donor replicates, and considering the practicality of conducting the assay with many PMN donors, it was determined that three replicates/donors should be sufficient for most applications.

Table 4-3: Optimising the number of PMN donors

Table shows the mean length of the 95% CI using different numbers of donors, as a percentage of the length of the 95% CI calculated using only two donors. These calculations are based on the normality assumption (deemed reasonable by graphical methods, not shown), and were done by simulation using 1000 replications.

Number Donors	95% CI length (% n=2)
2	100.0
3	30.4
4	20.3
5	16.1
6	13.9
7	12.3
8	11.2

4.2.7. ADRB cohort analysis

A standardised protocol for determining the ADRB activity for a sample was thus adopted: plates coated with 100 µL PEMS at 18.5 x 10^5 schizonts/mL; 100 µL PMNs at 1 x 10^7 PMNs/mL; un-treated serum or plasma diluted 1:50; samples measured in singlet with three different PMN donors after which data were indexed against a positive control which was included on each plate; all data being log transformed; and the mean of the three indexed and log transformed data points was then reported. Using this protocol, a cohort of serum samples, separate from the one used in the studies above, from 39 Kenyan adults and 47 UK malaria-naïve adults was assessed. Sera from the Kenyan adults induced significantly higher ADRB activity than sera from UK volunteers ($P < 0.0001$; Figure 4-10A). I also assessed whether ADRB activity correlated with PEMS-specific ELISA titre. When the Kenyan samples were plotted there was a significant but relatively weak relationship ($r_s = 0.57$, $P = 0.0001$; Figure 4-10B), with samples of mean ELISA response (370 AU) showing a high variation – from maximal to minimal ADRB activity as measured in this cohort. I also tested a subset of these sera using the alternative protein-based assay methodology using recombinant $PfMSP1_{19}$ antigen (Figure 4-11). These data showed a strong and highly significant correlation between ADRB activity and ELISA titre. Overall, these data suggest that the PEMS-based assay, as undertaken here, is suitable for testing for anti-merozoite ADRB activity in the sera of malaria-exposed individuals, and can yield extra information on the functionality of the antibody response that is complementary to those obtained by PEMS-based ELISA.

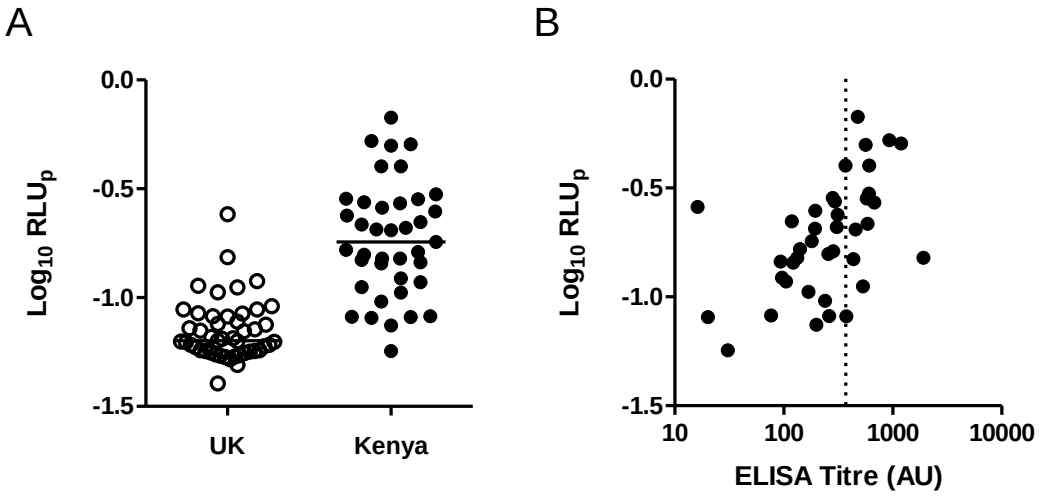

Figure 4-10: Assessment of ADRB activity in a cohort of Kenyan and UK adults

Serum was collected from adults from both Kenya and the UK. (A) ADRB activity induced by sera from UK (open circles n = 47) and Kenyan adults (closed symbols; n = 39) and is reported as Log_{10} RLU_p. (B) Anti-PEMS total IgG ELISA titre was plotted against Kenyan anti-PEMS ADRB activity (r_s = 0.57, P = 0.0001). Lines on dot plots represent medians. Dotted line indicates mean ELISA response (370 AU).

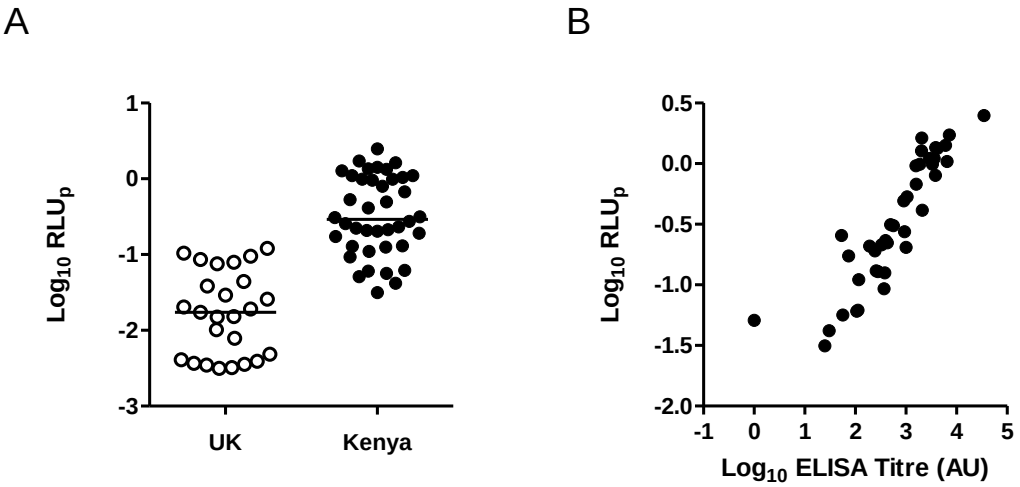

Figure 4-11: Assessment of ADRB activity in a cohort of Kenyan and UK adults on an $MSP1_{19}$ coated plate

Serum was collected from adults from both Kenya and the UK. Each sample was measured in singlet with three independent PMN donors. (A) ADRB activity induced on a GST-$PfMSP1_{19}$ coated plate by sera diluted 1:50 from UK (open circles n = 25) and Kenyan adults (closed symbols; n = 40). (B) Anti-$PfMSP1_{19}$ total IgG ELISA titre was plotted against Kenyan anti-$PfMSP1_{19}$ ADRB activity (r_s =0.92, P < 0.0001). Lines on dot plots represent medians.

4.3. Discussion

This study optimises and describes a protocol for conducting the ADRB assay to assess antibody reactivity against blood-stage malaria parasites. While a protocol for this assay has been previously reported (181, 321), this is the first time the ADRB assay has been standardised for reproducibility. I have also used this protocol upon a study cohort of 86 individuals showing that it could easily be applied to the immunological assessment of NAI or vaccine-induced responses from cohorts of individuals enrolled in epidemiological studies or clinical trials.

I was able to show a significant difference between ADRB activity induced by sera from malaria-naïve UK adults and that from malaria-exposed Kenyan adults. While the malaria-naïve cohort tested here could be used as a reference for future ADRB studies, I would recommend that at least a single 'negative' sample be run on each assay plate as a quality control measure to ensure that background responses are minimised.

When investigating whether any prior processing of samples was required before they could be tested in the assay, I found that assay output was independent of any effects mediated by complement. This was confirmed by heat inactivation of serum which did not affect the ability of serum from hyper-immune or malaria-naïve volunteers to induce ADRB activity. While the involvement of complement proteins in PMN activation and ROS release has been described (329, 330), it is possible that complement-dependent activity is mediated predominantly by a single IgG subclass (331), and subsequently, when stimulating PMNs with polyclonal sera, subclasses which do not activate complement pathways may still be able to activate PMNs by alternate pathways (e.g. CD32) making the effect of complement proteins indistinguishable. Despite this, when I did look at individual isotypes in a related $PfMSP1_{19}$ protein-based ADRB assay, purified monoclonal antibodies (and thus samples

lacking complement) of different isotypes induced similar activation profiles to those previously described (331) with IgA>IgG3>IgG1.

I next aimed to address a key limitation in the field of cell-based assays: optimising assay reproducibility, and in particular, inter-assay variability. Guidelines for assay validation, as outlined in the International Conference on Harmonisation Harmonised Tripartite Guidelines Q2(R1) state the importance of assessing reproducibility for any assay to be widely used in research (332). The impact of a highly reproducible assay to the field cannot be understated, as shown by the extensive use of standardised ELISAs in the field of malaria vaccine development (278). It was apparent that a significant source of inter-assay variation in the ADRB assay resulted from using PMNs isolated from different donors and even from the same donor at different times. Plate-to-plate variation, tested by using the same PMN prep on different plates, was not directly assessed, although the permutation test indicated that this was not necessary. Differences in PMN FcR expression profile may account for some of this difference, especially given the importance of human CD32 in ADRB (321). I observed donors with both $CD32^{hi}$ and $CD32^{lo}$ PMN phenotypes. It is unknown whether these phenotypic differences reflect genetic polymorphisms in CD32 genes (leading to differential expression or differential binding of flow cytometry antibodies), or simply differences in *in vivo* inflammatory environments at the time of phlebotomy resulting in differential CD32 expression (333). Whether individuals with a $CD32^{hi}$ phenotype are capable of inducing a higher overall ADRB level *in vivo* remains unknown and is not able to be tested without a personalised assay format matching donor serum and PMNs (which remains, for now, not possible). Adding support to the argument that differential CD32 expression, or at least differences in CD32 signalling activity, may lead to heightened ADRB levels *in vivo*, are the numerous associations between CD32 polymorphisms and clinical malaria outcome (205, 208, 209, 211).

In the context of the ADRB assay, where the primary focus is to assess the potential of antibodies to activate neutrophils, I found that despite neutrophil donor phenotype providing a possible source of inter-assay variation, inter-assay variability could be optimised by testing each sample with three neutrophil donors. Given that, in many laboratories, one of the limiting factors for high throughput of this assay will be the number of neutrophil donors available, I suggest that excluding certain donors based on their PMN phenotype is not practical, and I was able to attain acceptable reproducibility without doing so.

Having defined the assay parameters, I assessed ADRB activity in a cohort of samples from Kenyan and UK adult volunteers. I also compared these to ELISA titres. When I used a related assay which assessed responses against recombinant protein instead of blood-stage malaria parasites, like the PEMS-based assay, Kenyan sera induced higher activity that UK sera and ADRB activity strongly correlated with $PfMSP1_{19}$ antigen-specific IgG ELISA titres. A similar result was observed with anti-PEMS ADRB activity, when correlated against PEMS-specific IgG ELISA titre. Importantly, however, a complete range of ADRB responses were elicited from samples with an equivalent PEMS-specific IgG ELISA titre of 370AU, suggesting that valuable extra information should be gained by assaying for ADRB activity when seeking to associate immunological parameters with protection and/or clinical outcome. In this case, it appears that the presentation of antigens on the surface of the parasite is important in the induction of functional activity and cannot be assessed holistically with traditional ELISA-based methods. A recent study on ADRB adds further weight to the importance of antigen type and presentation in the assay, reportedly effecting the cellular location of respiratory burst (321). Work involving a different assay in the field of blood-stage malaria, the GIA assay, has also shown the importance of assessing functional activity of human sera instead of ELISA titre alone, despite the association between IgG titre and GIA activity for some antigens (334, 335).

While I have applied the assay method developed here to blood-stage malaria, it could similarly be used to assess antibody induced PMN activation against any antigen or pathogen. The PEMS-specific ADRB assay is not overly labor intensive and can be used to screen large cohorts quickly. Using this protocol, 50 samples are comfortably assayed in a day. The two major limiting factors on even higher throughput in the protocol in my hands was PEMS production, which I overcame by setting up large cultures (up to 150mL) of parasites for harvesting, and sourcing blood donors for isolation of fresh PMNs. Importantly I show that both serum and plasma can be used in the assay without affecting the result, thus negating the need to source specifically prepared samples from the clinic.

I thus describe a standardised protocol for the ADRB assay, providing a valuable tool for the assessment of NAI and vaccine development. The current paucity in pre-clinical assays available for assessing the function of either vaccine-induced or naturally-acquired antibodies presents a major problem in the study of immunity against blood-stage malaria. Due to this paucity, the field to date has relied on assessing cell-independent anti-merozoite activity using the GIA assay. In more recent years, other cell-based phagocytic assays have also been described (259, 260), and thus the ADRB assay, as presented here, should complement the use of the GIA neutralisation assay and newer phagocytic assays in studies of immunity to, and vaccination against, blood-stage malaria. In the next Chapter, I will use the ADRB assay to assess the association between ADRB activity and clinical protection and compare it to other commonly used assays in the field.

CHAPTER 5

ASSOCIATION OF ADRB ACTIVITY WITH CLINICAL PROTECTION AND IMMUNOLOGICAL ASSAYS

5. ASSOCIATION OF ADRB ACTIVITY WITH CLINICAL PROTECTION AND IMMUNOLOGICAL ASSAYS

I am very grateful to Dr Kazutoyo Miura who has helped to conduct the statistical analysis for this Chapter as part of an ongoing collaboration.

5.1. Introduction

Having developed and standardised the ADRB assay for use with human PMNs and *P. falciparum* PEMS, it is now important to assess its utility as a tool for the assessment of NAI. The ADRB assay has been previously associated with protection against clinical malaria (181) however this result has yet to have been replicated. Furthermore, how the ADRB assay compares to other assays used in the field is currently unknown. Thus it is of particular importance to assess the ADRB assay and any association it may have with immunity to malaria in the context of other assays which exist in the field such as the GIA assay, the surface reactivity assay (SRA) (336), and ELISAs against merozoite antigens.

A number of studies have shown that exposure to *P. falciparum* in endemic regions is associated with the acquisition of antibodies capable of inducing GIA (176-178), however the association with subsequent protection against clinical disease has been less clear (179). While some studies have reported an association between GIA and protection from blood-stage parasitaemia (337), others dispute this (338, 339). Similarly, when using clinical malaria as an endpoint, there is disagreement as to whether GIA associates (247), or does not associate (177, 340) with protection.

In other studies, individuals in endemic regions have been shown to acquire antibodies that recognise variant erythrocyte surface antigens via a SRA-type assay (341-343). A number of studies have associated the presence of antibodies reactive to variant surface antigens with clinical benefit (165, 168, 344). In a Sudanese cohort, the presence of antibodies against a

Ghanaian parasite isolate surface variant protein associated with protection, but data for other isolates were less convincing (165). In contrast, recognition of this parasite isolate did not associate with protection in a Ghanaian cohort however other isolates did (168). Thus, while SRA-type assays are potentially useful for assessing NAI, they are dependent on knowing, and having access to, parasite isolates *in vitro* that are representative of local circulating strains with respect to variant surface antigen expression. Given the additional complication that the parasite isolate needed for the assay may change over time, further optimisation is required before SRA can be used universally across cohorts.

The investigation of NAI using ELISAs against different merozoite antigens is prolific (172, 174, 340, 345-347). Evidence as to whether individual antigens correlate with protection is contradictory, and as such the contribution of responses against any given antigen to NAI remains debated (164). As an example, antibodies recognising $MSP1_{19}$ have been associated with protection in a Ghanaian cohort (173) but not in Kenyan children (345). However, meta-analysis of 33 studies associating IgG titre with malaria risk by Fowkes *et al*. (164) found that, despite discrepancies in individual studies, overall, people with antibodies to $MSP1_{19}$ and MSP3 (C-terminal region) had a reduced risk of malaria. The effect of other antigens such as AMA1, GLRUP, MSP1 (N-terminal region) and MSP2 on reducing the risk of malaria were less clear. However, instead of considering antibody responses to a particular antigen on a continuous scale, it may instead be valuable to determine whether or not an individual's response exceeds a "protective threshold" (174). Such an analysis would require comparison to a universal standard, however it would enable more robust comparisons of different cohorts between which total antigen-specific IgG responses are likely to differ.

A major limitation of the majority of previous studies is that they have focused on only single antigens when characterising naturally immune cohorts by ELISA. It is however likely that

the utility of using ELISAs for the assessment of NAI comes from assessing responses to a number of different antigens (175, 345). Given the ease of conducting ELISAs, it is feasible to conduct these against multiple antigens, however in some cases the ability to produce recombinant antigen is prohibitive. While ELISAs against multiple antigens are thus potentially useful, it is often difficult to combine results from multiple antigens into a meaningful output for use in cohort analyses. Some headway in this regard has been made in a recent study, where individuals were categorised by the number of antigens to which they had antibody responses (up to a maximum of 5) and this variable used to assess potential protective efficacy (175). This analysis showed that a cumulative response against combinations of antigens that were, on their own, somewhat protective, was capable of completely explaining protective efficacy. Repetition of this type of analysis on other cohorts is now required to determine whether this finding is broadly applicable.

Thus, while a number of assays currently exist for the assessment of NAI, evidence is unclear as to their utility for predicting clinical outcome, or in the case of the ADRB assay, the single reported study has simply not been replicated, so it is impossible to comment on its validity. In this Chapter, I thus assess ADRB activity in a cohort of children from Kenieroba, Mali which have been previously characterised for GIA activity and recognition of variant surface antigens via a SRA. For the purposes of this Chapter, I will refer to GIA, SRA and ADRB, as native-antigen assays. In addition to these native-antigen assay readouts, comprehensive ELISA data exists for this cohort and thus ADRB activity will be compared to ELISA responses. As defined in Chapter 4, all analyses are carried out using the ADRB readout of Log_{10} RLU_p and are referred to simply as ADRB.

5.2. Results

5.2.1. ADRB activity in a cohort from Mali

The standardised protocol for performing the ADRB assay on human samples described in Chapter 4 was applied to a cohort of plasma samples collected from 255 volunteers in the villages of Kenieroba and Fourda, Mali immediately prior to the transmission season in both 2009 and 2011 (348). 230 samples were assayed from 2009 (range = -1.48 – -0.04; Appendix 5-1) and 219 from 2011 (range = -1.52 – 0.11; Appendix 5-2). Of these, ELISA and GIA data was collected for 216 of the 2009 samples, and 194 of the individuals had paired plasma samples from both 2009 and 2011 (Table 5-1). For the assaying of these cohorts, a single batch of *P. falciparum* PEMS was prepared so that all samples were assessed with the same preparation of PEMS. Samples were run over 17 plates each with a fresh preparation of PMNs isolated from one of 13 PMN donors.

Table 5-1: Population demographics of the Mali cohort used in immunological analyses

Cohort Year	Number	Sex		Age			Hb Type	
		Male	Female	Lo	Med	Hi	Non-AS	AS
2009	216	114	102	79	81	56	149	67
2011	194	103	91	72	74	48	133	61

Age categories: Lo - 3-5 y; Med = 6-8 y; Hi = 9-11 y

Non-AS: Both AA and AC haemoglobin (Hb) type

5.2.2. ADRB and host factors

Out of the 255 individuals assayed, 194 individuals had ADRB activity assayed in both 2009 and 2011 plasma samples (Appendix 5-3, Analysis group 1). ADRB activity elicited by plasma from individuals in 2009 correlated with their ability to induce ADRB activity in

2011 (r_s = 0.59, P <0.0001; Figure 5-1), and a paired analysis indicated that the level of ADRB induced by an individual did not change significantly between the two sampling periods (P = 0.41), and this was consistent across children of different ages. As such, further analyses were conducted with samples from the 2009 cohort only, as a more complete immunological characterisation exists for these samples.

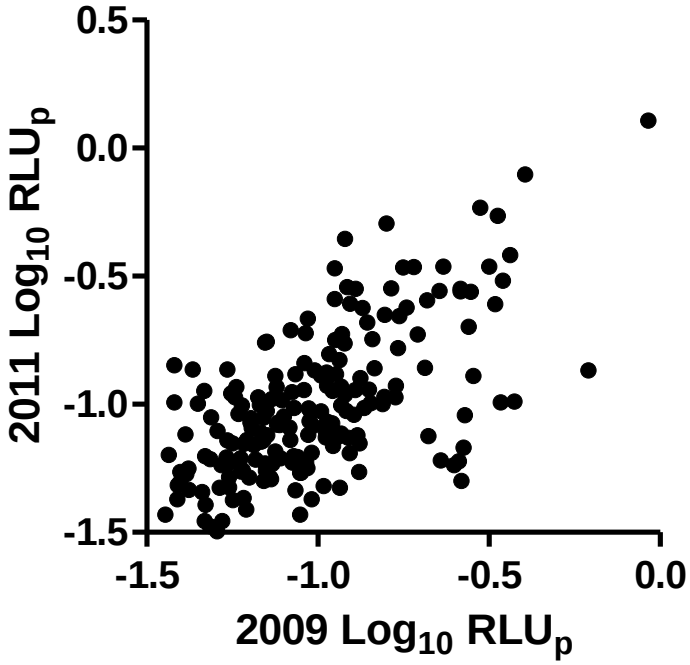

Figure 5-1: ADRB activity compared between 2009 and 2011

ADRB activity elicited against *P. falciparum* PEMS was determined for 194 plasma samples collected from volunteers in Mali before the transmission seasons in both 2009 and 2011 (r_s = 0.59, P <0.0001). Samples were assayed at a plasma dilution of 1:50.

To assess the impact of individual host factors such as age, haemoglobin (Hb) type and sex on ADRB activity, a subset of 216 samples were used (Appendix 5-3, Analysis group 2). Volunteers were stratified into age categories (Hi = 9-11 y, Med = 6-8 y, Lo = 3-5 y). Plasma from children in the Lo age category had significantly lower ability to induce ADRB activity than either Med (P = 0.003) or Hi (P < 0.0001) aged children (Figure 5-2A). No difference,

however, was seen in the ability to induce ADRB activity between children of non-AS (i.e., either AA or AC Hb types) or AS Hb types (P = 0.22; Figure 5-2B).

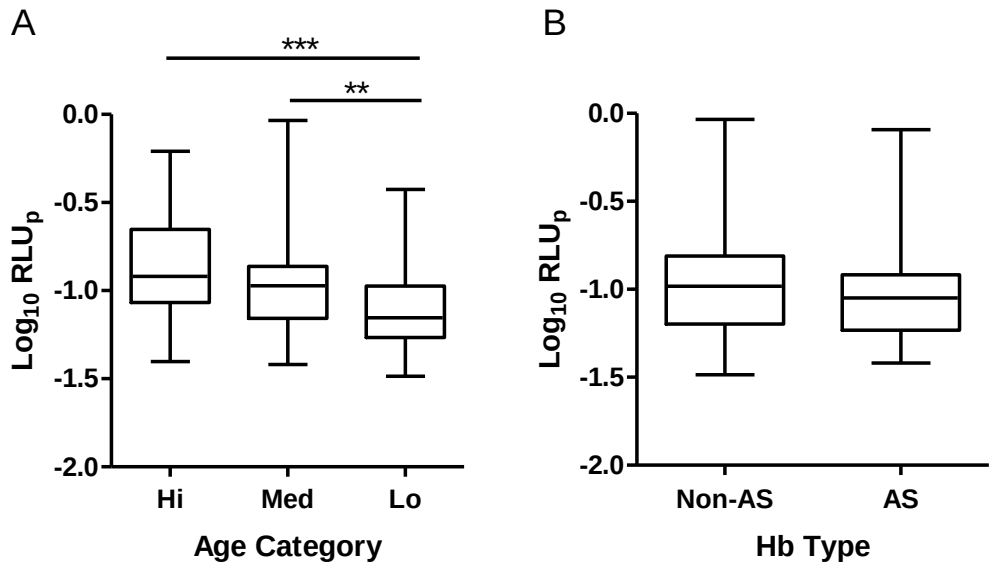

Figure 5-2: ADRB activity and host factors

ADRB activity elicited against *P. falciparum* PEMS by plasma diluted 1:50 from (A) individuals classed by age (Hi = 9-11 y [n = 56], Med = 6-8 y [n = 81], Lo = 3-5 y [n = 79]), or (B) individuals classed by Hb type (non-AS [n = 149], AS [n = 67]. Whiskers represent range. ** P = 0.003, *** P < 0.0001 (Dunn's test).

5.2.3. ADRB and clinical protection

Following collection of plasma samples, volunteers were monitored throughout the transmission season (June – December) for episodes of clinical malaria. Clinical malaria was defined in treatment seeking individuals as a temperature ≥37.5°C and the presence of any density of asexual parasites visible by microscopic examination of thick blood films as previously described (348). Using the 216 samples from Analysis group 2 (Appendix 5-3), associations between ADRB and clinical malaria were assessed.

Firstly, a nominal logistic fit analysis was used to model parameters associated with an individual's likelihood of experiencing clinical malaria. In this analysis, the LogLikelihood

(LL) value is an indicator of how well the model fits the data, with LL values closer to zero indicating better models. An LL test was then conducted to assess whether the addition of a factor statistically improves the model. To start, a model was constructed using both age and Hb type (non-AS, AS) to explain yes/no malaria (Table 5-2). Inclusion of age and Hb type significantly improved the fit of the model to the data ($P < 0.0001$). The addition of ADRB activity further improved the model ($P = 0.0007$) with an odds ratio (OR) of 0.13 (95% CI 0.04 – 0.43). Thus, after adjusting for the effect of age and Hb type on susceptibility to clinical malaria, ADRB is associated with clinical immunity with a rise of 1 Log_{10} RLU_p reducing the risk of malaria by 87% (95% CI: 57 – 96%).

Table 5-2: Modelling clinical malaria outcome with immunological parameters from Analysis group 2.

Model Variable	Yes/No Malaria			Number Clinical Episodes		
	LL	df	P	LL	df	P
Hb type/Age	-127.88	3	< 0.0001	-298.04	3	0.0002
ADRB	-122.13	4	0.0007	-294.63	4	0.009
GIA	-127.85	4	0.81	-297.96	4	0.69

Secondly, and for comparison with a previous study (181), an ordinal logistic fit analysis was conducted using the number of malaria episodes experienced throughout the transmission season (Table 5-2). Again, after accounting for age and Hb type, ADRB significantly associated with the number of malaria episodes ($P = 0.009$). Incident rate ratio analysis showed that a unit rise in Log_{10} RLU_p reduced the number of episodes by 73% (95% CI: 27 – 90%). Joos *et al*. conducted their analysis with ADRB data bisected into either above or below their mean response. I thus conducted the above analysis with ADRB classed as above or below the median response, and in these cases ADRB significantly explained yes/no

malaria (LL = -124.19, *df* = 4, *P* = 0.007; OR = 0.42 [0.22 – 0.79]), but not number of clinical episodes (LL = -296.79, *df* = 4, *P* = 0.11).

In summary, ADRB activity as a continuous variable is able to explain whether or not an individual experiences clinical malaria, and also the number of episodes experienced by an individual within the transmission season.

5.2.4. ADRB versus other native-antigen assays

The cohort assessed in this Chapter has been previously characterised for GIA activity and reactivity against erythrocyte surface antigens from a number of parasite strains in a SRA (336). Here I use the ADRB data generated on this cohort to compare these native-antigen assay readouts.

Using the 216 samples from Analysis group 2 (Appendix 5-3), ADRB activity correlated with GIA activity against the 3D7 strain of *P. falciparum* (r_s = 0.42, *P* < 0.0001; Figure 5-3A). Similarly, using the 164 samples from Analysis group 3 (Appendix 5-3) for which I have SRA data, ADRB correlated with SRA (r_s = 0.56, *P* < 0.0001; Figure 5-3B).

GIA and SRA were then added into the models for clinical protection using Analysis groups 2 and 3 respectively. Addition of GIA as a factor to explain whether or not an individual experienced clinical malaria did not significantly improve the model beyond that which included age and Hb type (*P* = 0.81), nor did it improve the model of number of clinical episodes experienced (*P* = 0.69; Table 5-2). Similarly, SRA failed to explain whether or not a clinical episode was experienced (*P* = 0.67; c.f. ADRB *P* = 0.001) or the total number of clinical episodes per individual (*P* = 0.14; c.f. ADRB *P* = 0.01) over the models explaining these factors with Hb type and age (Table 5-3).

Thus, despite moderate correlations between ADRB and both GIA and SRA, ADRB was the only native-antigen assay tested capable of explaining clinical outcome in this cohort.

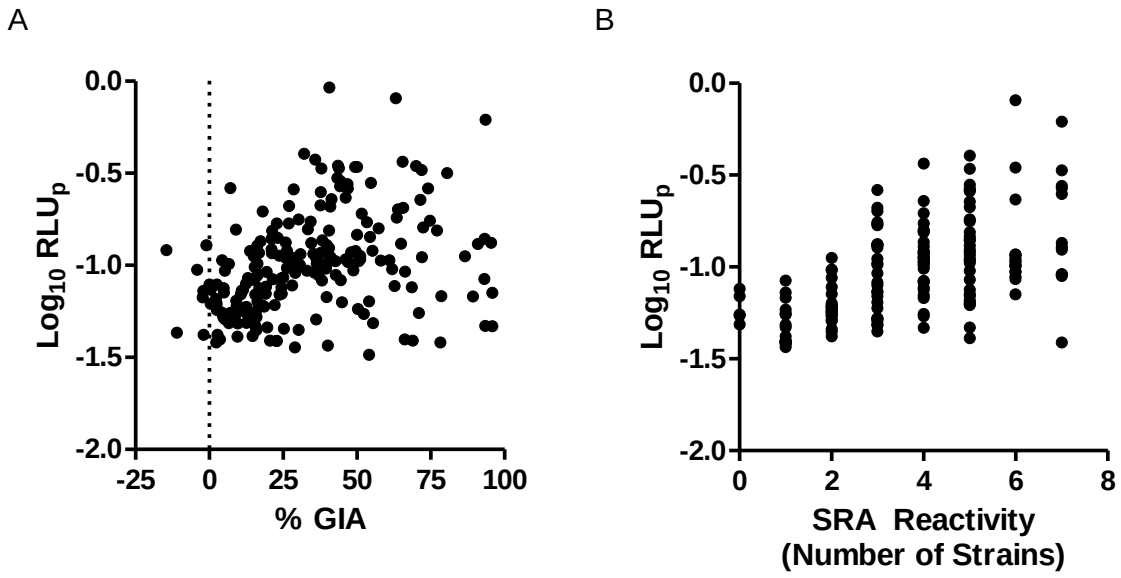

Figure 5-3: Correlations between ADRB activity and other native-antigen assays
ADRB activity induced against *P. falciparum* PEMS by human plasma diluted 1:50 plotted against (A) GIA activity (349) induced by purified human IgG at 10 mg/mL (n = 216; r_s = 0.42, P < 0.0001), and (B) number of parasite strains recognised by plasma in the SRA (336) (n = 164; r_s = 0.56, P < 0.0001).

Table 5-3: Modelling clinical malaria outcome with immunological parameters from Analysis group 3.

Model Variable	Yes/No Malaria			Number Clinical Episodes		
	LL	df	P	LL	df	P
Hb type/Age	-93.59	3	< 0.0001	-226.29	3	< 0.0001
ADRB	-88.3	4	0.001	-223.31	4	0.01
SRA	-91.11	10	0.67	-220.78	10	0.14

5.2.5. ADRB activity versus ELISA titres

One of the most commonly used assays in the assessment of NAI is the ELISA, and thus ADRB was compared to ELISA titres for a number of antigens within this cohort. For this analysis, the 216 samples of Analysis group 2 were used.

ADRB correlated with ELISA titres for 3D7 strain antigens AMA1 (r_s = 0.68, P < 0.0001), erythrocyte-binding antigen 175kDa (EBA-175) (r_s = 0.66, P < 0.0001), $MSP1_{42}$ (r_s = 0.60, P < 0.0001) and MSP2 (r_s = 0.61, P < 0.0001) (Figure 5-4). For modelling purposes, these ELISA titres were combined into an ELISA rank score. Thus for each sample, the ELISA rank score was calculated as the sum of each antigen's ELISA rank score, where:

$$Antigen\ ELISA\ rank\ score = -\frac{Rank\ of\ test\ sample - Median\ rank}{Maximum\ rank}$$

For example, if 161 of the 216 samples had a detectable level of antibody by ELISA for antigen X, the samples would be ranked 1-161, and all samples below the detection limit would be assigned a rank of 162. The median rank of this data set would thus be 108.5, and the maximum rank would be 162. Thus for a sample ranked 10^{th}:

$$Antigen\ X\ ELISA\ rank\ score = -\frac{10 - 108.5}{162}$$

$$= 0.608$$

Similar to individual antigens, the ELISA rank score correlated with ADRB activity (r_s = 0.77, P < 0.0001; Figure 5-5).

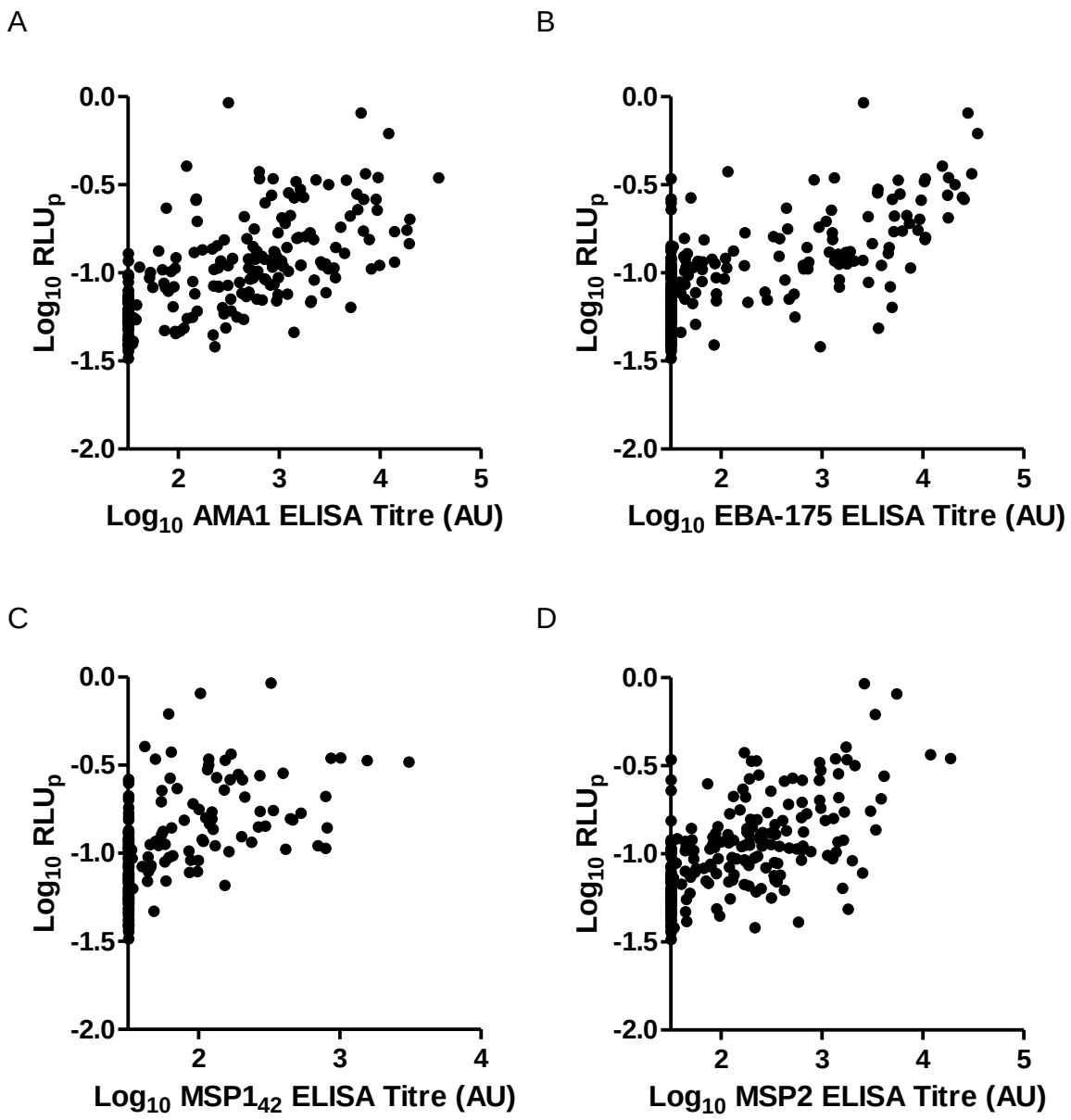

Figure 5-4: Correlations between ADRB activity and ELISA titres

ADRB activity induced against *P. falciparum* PEMS by human plasma diluted 1:50 (*n* = 216) plotted against antigen-specific ELISA titres for (A) AMA1 (r_s = 0.68, P < 0.0001), (B) EBA-175 (r_s = 0.66, P < 0.0001), (C) $MSP1_{42}$ (r_s = 0.60, P < 0.0001) and (D) MSP2 (r_s = 0.61, P < 0.0001). All ELISA responses below the limit of detection (44 ELISA units) were assigned a value of 22 ELISA units (348).

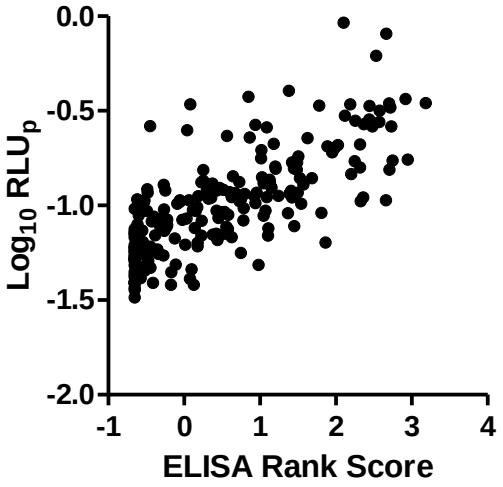

Figure 5-5: Correlation between ADRB activity and ELISA rank score

ADRB activity induced against *P. falciparum* PEMS by human plasma diluted 1:50 (*n* = 216) plotted against ELISA rank score calculated by combining the rank scores for each of the four antigens tested ($r_s = 0.77$, $P < 0.0001$).

As with the native-antigen assays, clinical outcome was modelled with ELISA data. Including ELISA rank score significantly improved the model explaining whether or not an individual experienced clinical malaria, over the model including only age and Hb type (LL = -117.04, *df* = 4, $P < 0.0001$). Using each individual antigen's ELISA titre instead of the ELISA rank score also explained yes/no malaria (LL = -115.77, *df* = 7, $P < 0.0001$), but it did not seem to generate a drastically improved model when compared to ELISA rank score. Similarly, both ELISA rank score (LL = -287.86, *df* = 4, $P < 0.0001$) and individual antigen ELISA titres (LL = -281.50, *df* = 7, $P < 0.0001$) significantly improved the model explaining number of malaria episodes. The addition of ADRB to models including either individual ELISA titres, or ELISA rank score, did not help further explain any measures of clinical outcome ($P > 0.4$ for all comparisons).

In addition to the association with ADRB reported above, in this cohort, models of both yes/no malaria, and the number of clinical episode experienced could be explained by ELISA data.

5.3. Discussion

In this Chapter, I utilised the standardised method developed in Chapter 4 for the ADRB assay, to assess NAI and clinical outcome in a cohort from Mali.

The strong relationship between ADRB activity induced by an individual between 2009 and 2011 indicated that children with low responsiveness remained low across transmission seasons. This is in agreement with published ELISA data for this cohort (348). However, it may have been expected that total ADRB response would increase between the two sampling periods given that I also showed differences in the ability to induce ADRB activity between different age categories within the 2009 data set. However, no such difference was seen. This may be explained by the distribution of children between age categories. The differences observed in ADRB induction between age categories was due to the Lo age category having lower ADRB inducing ability than the Med and Hi age categories, but there was no difference between Med and Hi age groups. Thus the movement of children from Med age to Hi age would not be expected to cause any significant change in measured ADRB activity. With 137 of the 216 children assayed being in the Med and Hi age categories in 2009, it is thus not surprising that I am unable to see a difference between the 2009 and 2011 ADRB cohorts. Given my further analysis which suggests that ADRB activity associates with protection from clinical malaria, this observation suggests that children under the age of 5 would be particularly susceptible to infection, in agreement with widely accepted epidemiological data (24, 350, 351).

It has been previously reported, that Hb type affects the induction of antigen-specific antibody responses (348). This observation holds true for the ELISA rank score as calculated here (data not shown). Despite this, and the relationship shown here between antibody titre and ADRB activity, no difference was seen in individuals' ability to induce ADRB activity

based upon their Hb type. Perhaps small changes in circulating antibodies as a result of Hb type are insufficient to affect ADRB induction, or alternatively, reduction in circulating antibody of a specific antigen specificity may be compensated for by antibodies against another antigen still capable of inducing ADRB. This raises the issue that we currently do not know what antigens are responsible for ADRB induction. While all four antigens reported here correlate with ADRB, it is possible that they merely reflect an individual's reactiveness, and actually represent a correlate of a different, ADRB inducing antigen(s).

Importantly, here I present the first comparison between ADRB and other native-antigen assays commonly used in assessments of NAI and vaccine development. The PEMS in the ADRB assay contains free merozoites, red cell membrane fragments from lysed schizonts, as well as some whole un-ruptured schizonts. Thus it is reasonable to think that there may be some overlap between ADRB activity and one, or both of GIA (a non-iRBC surface antigen specific output) and SRA (measuring reactivity to infected erythrocyte surface antigens). Indeed ADRB correlated with both GIA and SRA, however r_s values were low reflecting the wide spread of data. Once again, this begs the question as to whether different antigens are involved for the different activities measured by the different assays. Another possibility is that the ADRB assay is capable of teasing out subtle differences in an antibody's ability to signal via its Fc region, a function irrelevant to GIA and SRA. In this case, antibodies bound to the same antigen in both the ADRB assay and the GIA assay, for example, could produce different results. However if the increase in ADRB activity measured in the assay due to antibodies with high efficiency Fc-signalling rather than low efficiency Fc-signalling is minor, individuals with high overall antibody titres, but poor Fc-signalling ability, may still activate a stronger respiratory burst response than individuals with low overall titres but high Fc-signalling efficiency. Thus, to some extent, absolute amount of antibody would likely be

able to overcome subtle differences in FcR activation, explaining the weak correlation observed here between FcR-dependent and -independent assays.

The next important question was to assess the utility of these assays for association with NAI. In the cohort presented here, I show that ADRB is the only native-antigen assay capable of explaining immunity against clinical disease in terms of i) whether or not an individual experienced malaria, and ii) the number of clinical episodes experienced by individuals within the transmission season. This is contrary to a similar cohort from a village only 90 km north of Kenieroba, where GIA was seen to associate with the dichotomous variable of whether or not an individual experienced malaria, but not with the number of episodes experienced (247).

It is somewhat surprising that SRA data do not associate with clinical outcome given the assumed importance of antibodies to infected erythrocyte surface proteins in malarial immunity (165, 166, 168). It is possible, however, that the number of isolates recognised by an individual as reported here, is less relevant than whether or not an individual recognises the local isolates to which they are exposed. Thus, despite no association with protection reported here, other iterations of the SRA may indeed prove to be useful tools in assessing NAI.

Aside from the comparison of ADRB to other native-antigen assays, a major aim of this work was to attempt to replicate the previous association of ADRB activity and clinical immunity (181). While I did find that ADRB correlated with protection in this cohort, there are a number of important differences between the study presented here and that done by Joos *et al*.. Firstly, in the Joos cohort, they do not find any association between Hb type and clinical outcome. Thus their data is modeled using age only before the addition of ADRB to the model, compared to both age and Hb type as reported here. Secondly, when assessing the

impact of ADRB on their modelled data, they use a dichotomised readout of either above or below their mean value of ADRB index = 250 (this equates to -0.60 in Log_{10} RLU_i, where i refers to indexing data with their positive control). Using this cutoff they find a difference in cumulative number of clinical cases in several age groups. The best comparator to this study here is to look at the number of clinical cases experienced by each individual within the transmission season. Since our data is not normally distributed, the median was chosen as a more scientifically valid cutoff than the mean. Under these conditions, ADRB was not able to explain the number of clinical episodes experienced by individuals.

While it may thus appear as though the Joos study has not been replicated here, some important differences in the cohorts should be considered. Firstly, the Senegalese cohorts involved people of much greater age, with a mean age of 24.0 and 28.6 for the two cohorts studied. In both their study, and here, age was seen to influence ADRB activity. As such, the mean of their ADRB data, and thus the cutoff they use to assess protective immunity, is likely much higher than the median response for the data set presented here (mean age 6.6). Indeed if I use the 75^{th} percentile as the cutoff in the Kenieroba cohort, ADRB does associate with the number of clinical episodes experienced by individuals (data not shown). Secondly, as both studies use different positive controls against which to index their data, it is not possible to compare ADRB responses directly. Thus, while not directly comparable, this work supports the association of ADRB with clinical protection presented by Joos *et al.*.

Finally it seemed logical to ask which assay, or combination of assays, is best for assessing NAI. While ADRB was the only native-antigen assay to associate with protection in this cohort, ELISA titres also predicted immunity. This has been reported previously with the set of antigens reported here (345). In all cases, modelling the data with either the four individual ELISA titres or the ELISA rank score, explained clinical outcome better than ADRB. While I

attempted here to use ELISA rank score to explain immunity to malaria, it was always at least as good, if not better, to use each of the individual ELISA titres in the models. Given the generation of the ELISA rank score still requires four separate assays to be conducted, for modelling the data against clinical outcome, individual ELISA titres seem to be best. This strategy, however, may not be effective in explaining clinical outcome in other populations where the distribution of antibody responses is different. For a more reliable and universal assessment of the contribution of ELISA titres to clinical outcome, it is likely that a standardised protective threshold needs to be defined for each antigen or combination of antigens (174). Using data dichotomised in this way, Osier *et al*. are able to combine responses against a number of antigens to explain clinical outcome (175). People with responses to three or more of their top five ranking individually protective proteins (PF3D7_1136200, MSP2, RhopH3, P41, and MSP11) saw protective efficacy rise to 100%. Similar to my analysis of ELISA rank score, potentially valuable information is lost when dichotimising data, i.e. a response just above the threshold is treated exactly the same as a very high responder. It remains to be seen whether the association with protection reported by Osier *et al*. will apply in other cohorts, however, it may be necessary to consider the inclusion of continuous variable data from individuals above the pre-defined threshold instead of simply categorising them as above or below threshold.

In summary, in this cohort from Mali, the combination of measurement of AMA1, $MSP1_{42}$, MSP2 and EBA-175 using ELISAs is the best predictor of clinical outcome. Taking threshold titres into consideration may make ELISA-based associations with protection more reproducible (174), however, even then, it remains to be seen whether assessments of ELISA titre would be effective in predicting clinical outcome across all populations. In future studies, it will be interesting to test whether ADRB activity associates with protection in a cohort in which ELISA titres do not explain clinical outcome. In this Chapter, I show that the

ADRB assay associates with clinical outcome in a cohort completely distinct to where it has been tested before. This single assay thus provides a useful tool for the assessment of NAI, and to date appears to be useful in explaining clinical protection.

CHAPTER 6

ASSESSMENT OF ANTIBODIES' ABILITY TO BLOCK *P. VIVAX* DUFFY BINDING PROTEIN FROM BINDING DARC

6. ASSESSMENT OF ANTIBODIES' ABILITY TO BLOCK *P. VIVAX* DUFFY BINDING PROTEIN FROM BINDING DARC

6.1. Introduction

Having established the ADRB assay as a tool for the assessment of immunity against blood-stage *P. falciparum* and discussed its potential utility for vaccine development, the final results Chapter of this Thesis tackles the issue of developing blood-stage malaria vaccines against *P. vivax*. *P. vivax* has been overlooked for many decades, despite being the most widespread *Plasmodium* species geographically. Infection leads to an incapacitating, relapsing disease with symptoms including acute respiratory distress syndrome, vicious paroxysms, fever, severe anaemia, and in extreme cases, death. Despite increasing implementation of malaria control measures, with more than 100 million cases each year, the burden of this disease remains far too high (27, 37, 352, 353). While the updated 2030 Malaria Vaccine Technology Roadmap is calling for a vaccine to exert 75% efficacy over at least two years, for both *P. falciparum* and *P. vivax* (266), less than five vaccine candidates for *P. vivax* have been trialled. If this ambitious target is to be met, new approaches to malaria subunit vaccine design are urgently required, and *P. vivax* must emerge as a priority species for vaccine development.

Encouragingly, *P. vivax* relies on the essential interaction between Duffy binding protein (DBP) and the Duffy antigen receptor for chemokines (DARC) (33, 354), illustrated by the resistance to *P. vivax* of populations which are Duffy blood group negative (34). DBP is *P. vivax*'s sole member of the erythrocyte binding-like (EBL) family of proteins, although gene duplication events in field isolates may be giving rise to parasite strains with more than one DBP gene (355). DBP belongs to a micronemal family of proteins which bind erythrocyte receptors via Duffy binding-like (DBL) domains (356). DBL domains include a cysteine

rich region labelled “region II” with DBP region II (DBP_RII) containing 12 highly conserved cysteines (357). DBP_RII is responsible for binding to DARC on the erythrocyte surface (358).

While DARC is a complex multi-pass membrane protein, its interaction with DBP_RII has been localised to its N-terminal 60 amino acids. Furthermore, the sulfonation of tyrosine 41 of DARC is essential for DBP_RII binding (280). DBP_RII and DARC interact with a stoichiometry of 1:1, however dimerisation of DBP_RII is reported to be required for binding (359). Furthermore, DARC exists in two immunologically distinct alleles, Fy^a and Fy^b. Individuals an Fy^{a+b-} phenotype have been shown to be at reduced risk of clinical *P. vivax* malaria due to reduced capacity for binding of DBP to Fy^a and an increased ability of naturally acquired antibodies to block this interaction compared with Fy^b (360). Binding of DBP_RII and DARC is an essential step in the formation of a tight junction between the *P. vivax* merozoite and the erythrocyte and thus the initiation of invasion (361).

Given the essential nature of the interaction between DBP_RII and DARC for merozoite invasion, DBP_RII has been regarded a natural and leading target for *P. vivax* blood-stage vaccine development. However, the assessment of vaccine-induced antibody efficacy in pre-clinical models (and clinical samples) is difficult given that long term *in vitro* culture of *P. vivax* parasites is not possible (38) and thus GIA-type assays cannot be conducted. As such, alternative and innovative methodologies must be utilised to assess the function of antibodies induced by vaccination.

One such methodology has recently been described in the form of a binding inhibition assay which assesses the ability of vaccine-induced antibodies to block the DARC-DBP_RII interaction (265). It is hoped that showing that vaccine induced antibodies are able to block the DARC-DBP_RII interaction *in vitro* using this assay, would provide an indication that

the same vaccine-induced antibodies may be able to block the interaction, and thus *P. vivax* invasion, *in vivo*. In this Chapter, I thus aim to establish the DARC-DBP binding assay for use with both pre-clinical rodent serum samples as previously described, and apply it, for the first time, to human clinical trial sera, taking advantage of the first clinical trial conducted with DBP_RII. This trial, called VAC051, was a Phase Ia clinical trial, conducted in Oxford in 2012-13 using ChAd63 and MVA viral vaccines recombinant for DBP_RII. The DBP_RII vaccine construct consisted of the native DBP_RII sequence from the Sal I strain of *P. vivax* (362). In total 24 healthy UK adults were vaccinated with either ChAd63 alone, or using the ChAd63-MVA prime-boost regime. The vaccines showed a favourable safety profile, and demonstrated DBP_RII-specific T cell responses by ELISpot and serum IgG by ELISA (Payne *et al.*, in preparation; NCT01816113). In order to conduct a limited number of immunological characterisations described in this Chapter, a very small amount of DBP_RII protein produced in *E. coli* was kindly provided by Dr Chetan Chitnis (ICGEB). However, this protein was not available for the majority of studies and thus it was necessary to produce further DBP_RII as described below.

6.2. Results

In order to establish the DBP binding assay, it was necessary to optimise the production of both recombinant DARC and DBP proteins. Various genes encoding these proteins were thus cloned into expression vectors as described below. For the purposes of this Chapter, when describing expression constructs, the following abbreviations are used:

Abbreviation	Description
BAP	Biotin Acceptor Peptide (GLNDIFEAQKIEWHE)
BiP	17 amino acid *Drosophila* signal sequence
CD4	A 21 kDa epitope tag consisting of domains 3 and 4 from rat CD4 (363)
C-tag	A four amino acid C-terminal tag (EPEA)
His	A six histidine tag with affinity for bivalent Ni^{2+} and Co^{2+} metal ions
IMX313	An oligomerisation domain based on the chicken orthologue of human complement protein C4bp α-chain which auto-assembles into heptamers (272)
PK	A 14 amino acid epitope tag also known as V5 (GKPIPNPLLGLDST)
Strep	An eight amino acid tag (WSHPQFEK) with affinity towards Strep-Tactin (364)
TCS	Thrombin cleavage sequence (LVPRGS)
tPA	Human tissue plasminogen activator 32 amino acid leader sequence (232)

6.2.1. Expression of recombinant DARC N-terminus in HEK293 cells

Given the higher affinity of DBP_RII to the Fy^b allele of DARC (360), a gene encoding the first 60 amino acids of the Fy^b variant (ABA10433.1), followed by a TCS and a BAP was cloned using KpnI and BamHI into the adenovirus entry vector pENTR4 containing a tPA leader sequence and a His tag (Figure 6-1A). Cysteines 4, 51 and 54, which normally form disulphide bonds with the extracellular loops of DARC, were mutated to alanine (280). A 250 mL culture of suspension HEK293E cells was transfected with the plasmid encoding DARC.TCS.BAP.His (DARC.His) and allowed to grow for three days before the supernatant was harvested. After purification using a HisTrap Excel column (Sigma), and buffer exchange into PBS, the presence of purified protein was confirmed at the expected size of 9.8 kDa by Coomassie Blue stain and Western blotting with polyclonal rabbit anti-CD234 (AbD Serotec), however the presence of higher molecular weight bands indicated a level of aggregation (Figure 6-1). Recognition of DARC.His by mouse polyclonal IgG (Sigma) raised against amino acids 1 – 337 of DARC with a single mutation from the DARC.His protein sequence (D42G), also recognised the protein by Western blot and ELISA (data not shown). Furthermore, mass spectrometry conducted by collaborators Caroline Lenz and Matthew Higgins, confirmed that the protein was the expected size for DARC with two sulphated tyrosines (data not shown)(280). From the 250 mL expression culture, a yield of 3.45 mg of protein was purified giving an expression and purification efficiency of 14 µg/mL.

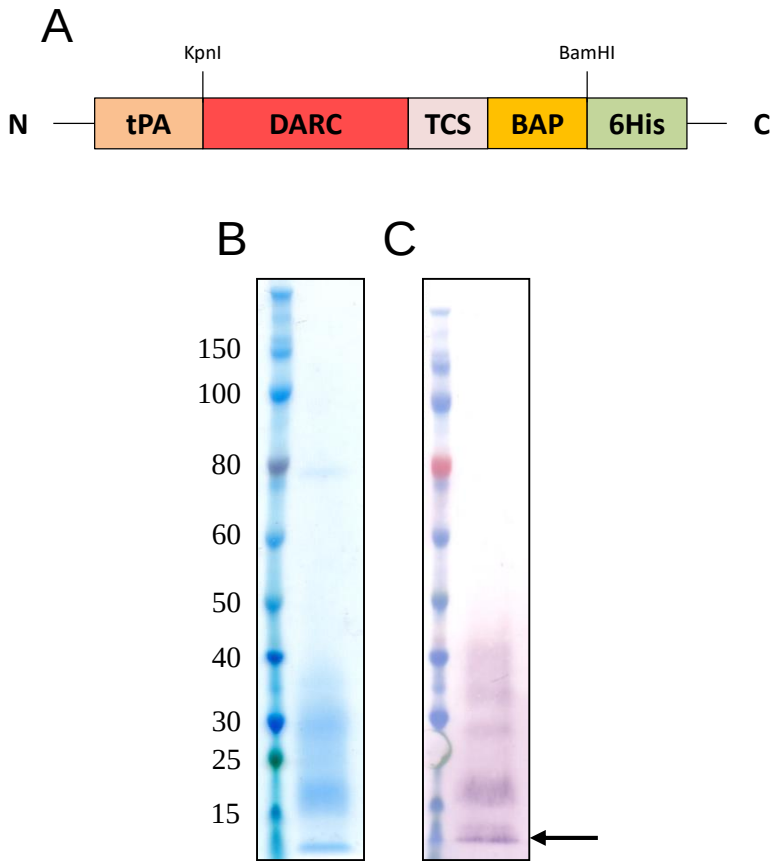

Figure 6-1: Expression of DARC.His in HEK293 cells

DARC was expressed by transient transfection of HEK293E cells. (A) Amino acids 1-60 of the Fy^b variant of human DARC fused to a TCS, BAP and His tag were cloned into expression vector pENTR4 with a tPA leader sequence. After three days of culture, supernatants were harvested and DARC.His purified on a HisTrap column. Purified protein samples were run on SDS PAGE under non-reducing conditions and detected with (B) Coomassie Blue stain, and (C) polyclonal anti-DARC antibody. Arrow indicates monomeric DARC.

6.2.2. Expression of recombinant DBP in HEK293E cells

In order to optimise the expression of DBP in HEK293E cells, six different constructs were generated (Table 6-1). All constructs were based on DBP from the Salvador I strain of *P. vivax* (DQ156512.1) with one construct encoding the full length DBP protein, and the other five consisting of amino acids 194-522 which make up DBP region II (RII). Among the constructs encoding DBP_RII, there were a number of differences. Firstly, the presence of C-terminal tags allowed the purification of proteins by different methods and had been previously shown to affect expression of certain *Plasmodium* proteins (Illingworth *et al., unpublished data*). Thus for initial expression studies a number of different tags were used. Secondly, while four of the five DBP_RII constructs were cloned into pENTR4, DBP_RII.CD4 was encoded within the pOPINTT plasmid. Unlike pENTR4 which has a long human Cytomegalovirus (CMV) immediate-early promoter which retains an intron, protein expression from the pOPINTT plasmid is driven by a short CMV promoter which lacks this intron. Thirdly, the native sequence of DBP_RII contains three N-linked glycosylation sequons that could be glycosylated following expression in mammalian cells. In the DBP_RII.PK.C-tag construct, these sites were mutated (T64A, S160A, T229A) to prevent the glycosylation of expressed protein and potentially better reflect the native, *Plasmodium* produced protein (365). Finally, four out of the six constructs were cloned using standard restriction enzyme cloning while cloning for the remaining two utilised seemless techniques such as PCR and circular polymerase extension cloning (CPEC) (269). In particular, the use of a BamHI restriction site at the C-terminal end of DBP_RII results in a residual two amino acids between the construct and the tag. While the impact of this on expression levels remains to be formally tested, anecdotal evidence from expression trials in our group suggests it is worth noting.

Table 6-1: DBP constructs used in HEK293 expression trials (see Appendix 6)

Construct	DBP	Tags	tPA	N-glycans	Plasmid	Cloning
DBP_RII	RII	none	+	+	pENTR4	Restriction enzymes
DBP_RII.His	RII	BAP, His	+	+	pENTR4	Restriction enzymes
DBP.His	Full length	BAP, His	+	+	pENTR4	Restriction enzymes
DBP_RII.CD4	RII	CD4, BAP, Strep	-	+	pOPINTT	Restriction enzymes
DBP_RII-313	RII	IMX313	+	+	pENTR4	Seemless
DBP_RII.PK.C-tag	RII	PK, C-tag	+	Mutated	pENTR4	Seemless

The six constructs were transfected into 30 mL cultures of suspension HEK293E cells and allowed to grow for three days before harvesting. Coomassie Blue staining of supernatants run on SDS PAGE under reducing conditions indicated low expression levels (Figure 6-2A). Faint bands were detectable for the full length DBP.His at approximately 80 and 100 kDa, running slightly lower than the anticipated 123 kDa protein (lane 3, Figure 6-2A). A distinguishable band was also present in the culture of DBP_RII.CD4 at the expected size of 63 kDa (lane 4, Figure 6-2A). A Western blot on the supernatants (under non-reducing conditions) using sera from mice immunised with ChAd63-MVA DBP_RII (de Cassan *et al.*, in preparation) to detect proteins, confirmed successful protein expression for DBP_RII (lane 1), DBP_RII.His (lane 2), DBP_RII.CD4 (lane 4) and DBP.PK.C-tag (lane 6) at their expected sizes of 39 kDa, 43 kDa, 63 kDa and 40 kDa respectively (Figure 6-2B). Western blot using the same detection antibody on proteins extracted from the cell pellets confirmed DBP.His (lane 3) and DBP_RII-313 expression without complete secretion (Figure 6-2C). This also provided evidence that DBP_RII-313 was forming multimers as would be expected due to the IMX313 oligomerisation domain.

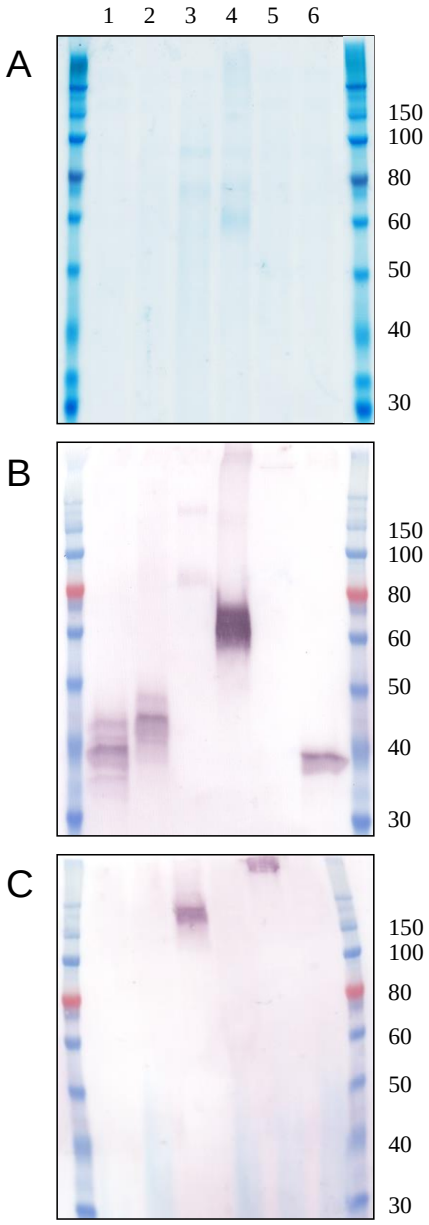

Figure 6-2: DBP protein expression trials in HEK293 cells

Expression vectors described in Table 6-1 were transfected into 30 mL cultures of suspension HEK293 cells. After three days, supernatants (A-B) and cell pellets (C) were harvested and run without prior treatment on SDS page: lane 1 = DBP_RII [expected size = 39 kDa], lane 2 = DBP_RII.His [43 kDa], lane 3 = DBP.His [123 kDa], lane 4 = DBP_RII.CD4 [63 kDa], lane 5 = DBP_RII-313 [316 kDa], lane 6 = DBP_RII.PK.C-tag [40 kDa]. (A) Coomassie gel showing total protein in supernatants. Western blots from (B) supernatants, and (C) cell pellets using polyclonal mouse-anti-DBP_RII serum for detection.

For use in the DBP binding assay, it was decided that a secreted protein with a C-terminal tag allowing purification was worth pursuing. Despite DBP.CD4 giving the highest expression levels as inferred from Western blot it was decided not to continue with this protein initially due to the potential for the large tag to interfere with potential binding to DARC. Thus I attempted to produce sufficient protein to conduct both ELISAs and the DBP binding assay using both the DBP_RII.His and DBP_RII.PK.C-tag constructs.

Firstly larger-scale DBP_RII.His expression was attempted. After several failed attempts to purify measurable quantities of protein, a six litre culture of HEK293 cells was transfected. After affinity chromatography using a HiTrap TALON column, there were still a number of non-DBP contaminants in the protein sample as seen by Coomassie Blue staining (Figure 6-3A). Size exclusion chromatography (SEC) was then carried out to obtain a more pure protein preparation (Figure 6-3B). The second fraction of the SEC elution was confirmed to be DBP by Western blot using serum from both ChAd63-MVA DBP_RII immunised mice (Figure 6-3C) and a penta-His antibody (Qiagen; Figure 6-3D). However, using this protocol, from the six litres of culture, less than 40 µg of protein was able to be purified as estimated by measuring optical density at 280 nm. In addition, it was noted that upon running the protein on SDS PAGE under reducing conditions, immune serum from mice was no longer able to recognise the protein (lane 6, Figure 6-3C).

I next attempted to produce DBP_RII.PK.C-tag. This construct was ideal for use in the DBP binding assay as it had its N-glycan sites mutated, reducing the possibility of glycosylation of the protein during mammalian cell expression interfering with its binding to DARC as has been described (366), and because the presence of the PK tag meant it may be possible to detect the protein in the DBP binding assay with an anti-V5 mAb.

Despite the results shown in the initial expression trials (Figure 6-2), I was unable to purify measurable protein from the supernatant of expression cultures. Instead, protein was extracted from the cells of a four litre expression culture. C-tag purification resulted in a reasonably pure protein preparation, however following subsequent SEC (Figure 6-4A), I was able to obtain pure DBP_RII.PK.C-tag (Figure 6-4). Similar to that seen with DBP_RII.His, reducing the protein prevented detection with DBP_RII immune mouse sera (Figure 6-4C). Unfortunately, the protein was not detectable using an anti-V5 antibody unless the protein had been reduced, suggesting that under its native confirmation, the PK tag is hidden within the protein structure (Figure 6-4D). This result was confirmed in the DBP binding assay whereby anti-V5 antibody was unable to detect DBP_RII.PK.C-tag in its native conformation (data not shown). From this expression culture, only 20 µg of protein was produced, however due to the relative purity and the small amount required to conduct the DBP binding assay, this was considered sufficient to proceed.

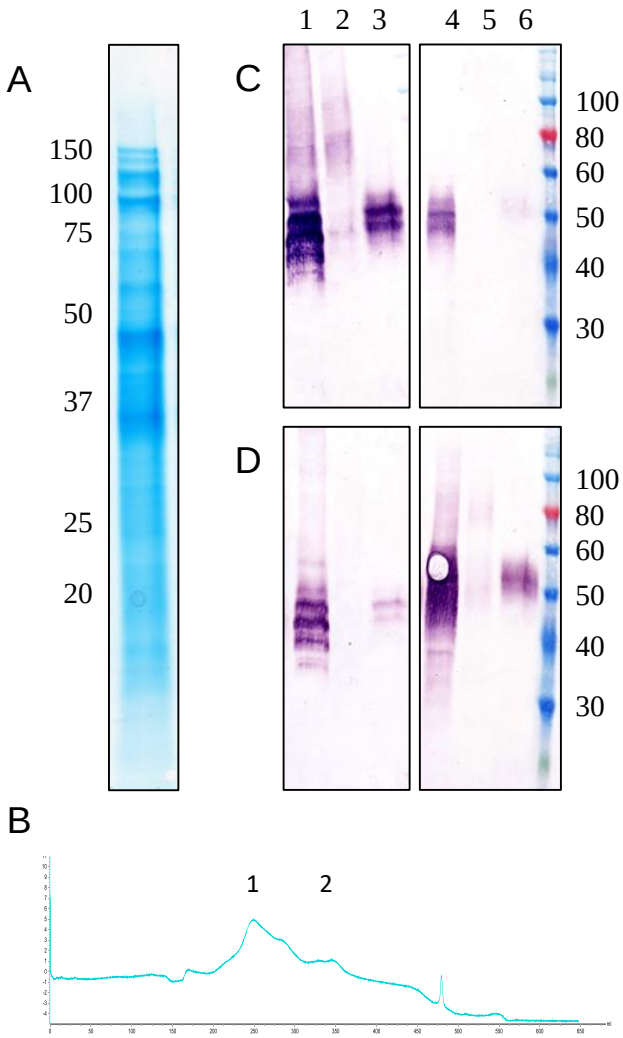

Figure 6-3: Expression of DBP_RII.His in HEK293 cells

The DBP_RII.His expression plasmid was transfected into six litres of suspension HEK293 cell culture. Supernatant was harvested three days post transfection and protein purified by affinity chromatography on a HiTrap TALON column followed by size exclusion chromatography (SEC). Purified proteins were run on SDS-PAGE. (A) Coomassie Blue protein stain on elution from HiTrap TALON column under reducing conditions. (B) SEC trace showing two protein peaks. Protein was detected by Western blotting with (C) serum from mice immunised with ChAd63-MVA DBP_RII and (D) anti-His antibody. Samples in lanes 1-3 were run under non-reducing conditions, and samples in lanes 4-6 were run under reducing conditions. Lane 1 = HiTrap TALON elution; lane 2 = peak 1 from SEC; lane 3 = peak 2 from SEC; lane 4 = HiTrap TALON elution; lane 5 = peak 1 from SEC; lane 6 = peak 2 from SEC.

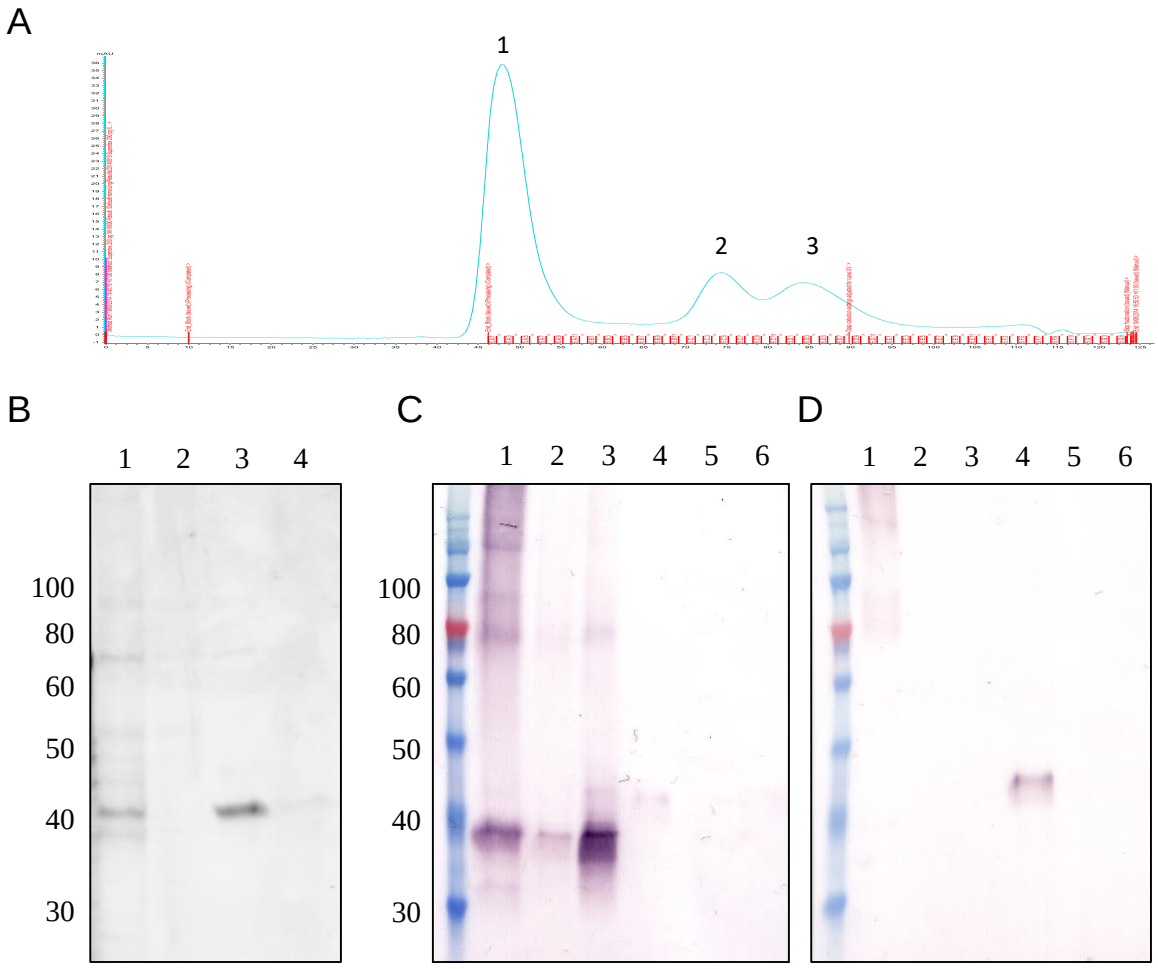

Figure 6-4: Expression of DBP.PK.C-tag in HEK293 cells

The DBP_RII.PK.C-tag expression plasmid was transfected into four litres of suspension HEK293E cell culture. Cells were harvested three days post transfection and protein purified by affinity chromatography using CaptureSelect C-tag affinity matrix followed by SEC. (A) SEC trace of CaptureSelect C-tag affinity matrix purified protein. Purified proteins were run on SDS PAGE. (B) Coomassie Blue protein stain on elution from: lane 1 - CaptureSelect C-tag affinity matrix; lane 2 - SEC peak 1; lane 3 - SEC peak 2; lane 4 - SEC peak 3. Protein was detected by Western blotting with (C) serum from mice immunised with ChAd63-MVA DBP_RII and (D) anti-V5 antibody. For (C) and (D) samples loaded on lanes 1-3 had no prior treatment, while samples in lanes 4-6 were run under reducing conditions. Lane 1 = SEC peak 1; lane 2 = SEC peak 2; lane 3 - SEC peak 3; lane 4 = SEC peak 1; lane 5 = SEC peak 2; lane 6 = SEC peak 3.

6.2.3. Development of the DARC-DBP binding assay

Having generated the proteins required for the DBP binding assay, it remained necessary to produce immune sera in mice (in order to test antibody blocking in assay development studies) and in rabbits (as a detection antibody for the assay). Both mice and rabbits were immunised with ChAd63-MVA DBP_RII and developed a detectable antibody response by ELISA against DBP_RII produced in *E. coli* and DBP_RII.His produced in HEK293 cells respectively (Figure 6-5). Serum from day 70 post ChAd63-MVA immunisation was pooled and used for assay development.

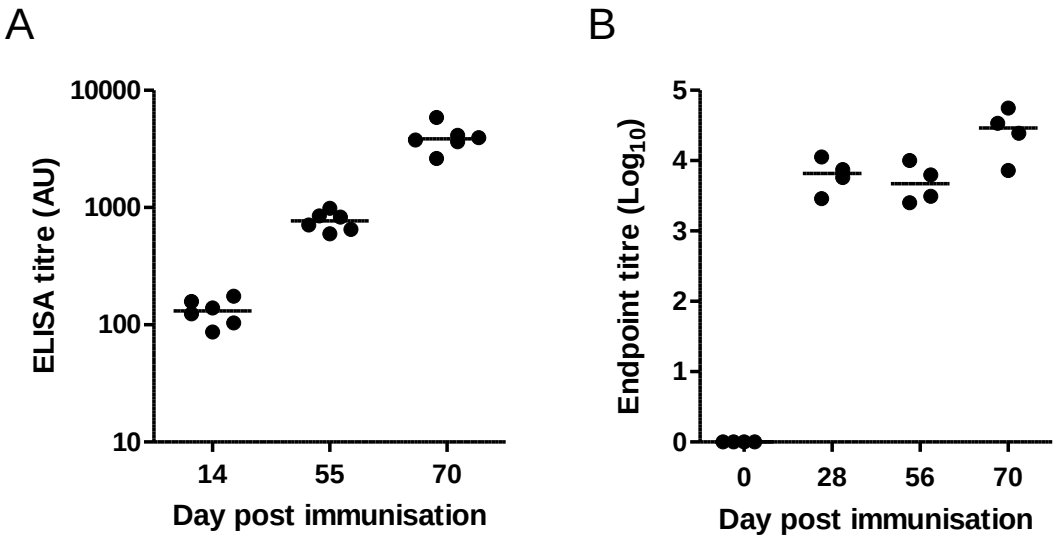

Figure 6-5: Generation of anti-DBP immune sera in mice and rabbits

Immune sera for optimising the DBP binding assay were generated in both mice and rabbits. (A) Six BALB/c mice were immunised i.m. with 1 x 10^8 ifu ChAd63 expressing DBP_RII (without any tags) followed eight weeks later by 1 x 10^7 pfu MVA expressing DBP_RII (without any tags). Serum was collected at 14, 55 and 70 days post initial ChAd63 immunisation. Antibody titre was determined using a standardised ELISA with a plate coated with 2 µg/mL DBP_RII.His produced in *E. coli* (367). (B) Four Zika rabbits were immunised i.m with the same viral vectors as used in mice at 4.1 x 10^8 ifu and 5 x 10^7 pfu respectively. Serum was harvested before immunisation (day 0) and 28, 56 and 70 days post adenovirus administration. ELISA titres were determined using an endpoint ELISA with plates coated with DBP_RII.His produced in HEK293 cells. Lines represent medians.

Using the components hence described, the DBP binding assay was conducted in a manner similar to that previously reported (265), with higher concentrations of detecting rabbit immune sera (1:1000) and secondary anti-rabbit IgG AP (1:1000). As mentioned above, I attempted to use an anti-V5 antibody conjugated to AP to detect DBP binding in the hope that this would avoid potential blockage of DBP detection antibody with primary immune sera, however like the Western blot result, anti-V5 did not recognise the DBP_RII.PK.C-tag protein. Instead I proceeded with the published protocol utilising rabbit anti-DBP sera as the detection reagent.

Under these conditions binding was detected only when both DBP_RII.PK.C-tag and DARC were present in assay wells, and this binding was completely abrogated by the pre-incubation of DBP_RII.PK.C-tag with pooled day 70 immune mouse sera diluted 1:100, while the preincubation of DBP_RII.PK.C-tag with naïve mouse sera had no effect on DBP-DARC binding (Figure 6-6).

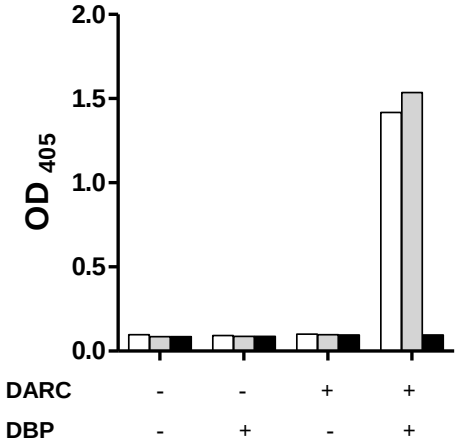

Figure 6-6: Optimisation of DBP binding assay with mouse serum

Maxisorp ELISA plates were coated with DARC.His at 1 µg/mL (+) or PBS (-). 0.025 µg/mL DBP.PK.Ctag (+) or PBS (-) was incubated for 1 h with PBS (white), serum from a naïve mouse diluted 1:100 (grey), or pooled day 70 serum from mice immunised with ChAd63-MVA DBP_RII diluted 1:100 (Black; Figure 6-5). Binding of DBP to DARC (represented by higher ODs) was detected with pooled ChAd63-MVA DBP_RII day 70 rabbit serum. Bars represent the average of triplicate wells.

6.2.4. Vaccine-induced antibodies in humans do not inhibit DBP binding DARC

After confirming the blocking activity of sera from mice immunised with ChAd63-MVA DBP_RII, I assessed the ability of human sera to block DBP binding to DARC after immunisation with the same vaccines. Volunteers received either single dose of ChAd63 encoding DBP_RII at 5 x 10^9 vp (Ad – Lo; n=4) or 5 x 10^{10} vp (Ad – Hi; n=4), or both a ChAd63 DBP_RII dose at 5 x 10^{10} vp followed eight weeks later by MVA DBP_RII at 1 x 10^8 pfu (AdM – Lo; n=7) or 2 x 10^8 pfu (AdM – Hi; n=8). Serum was collected from volunteers 84 days after initial ChAd63 immunisation. No volunteers receiving any of the immunisation regimes elicited substantial blockage of DBP binding at a serum dilution of 1:300, though there was a hint of blocking in volunteer 10 which remains to be repeated (Figure 6-7). By contrast, a positive control sample from a naturally immune Thai individual showed complete blocking of DBP binding at the same dilution.

To confirm that volunteers from the clinical trial had responded to the vaccine and produced antibodies against DBP_RII, an ELISA was conducted with a small subset of samples with the DBP_RII.PK.C-tag protein that was available. While volunteers from the groups receiving ChAd63 immunisation alone did not appear to sera-convert, all individuals tested from groups receiving both ChAd63 and MVA were positive for DBP_RII specific antibodies (Figure 6-8). Thus, despite the presence of antibodies to DBP_RII, sera from human vaccinees were unable to block DBP binding to DARC in stark contrast to the results observed in mice or with Thai sera.

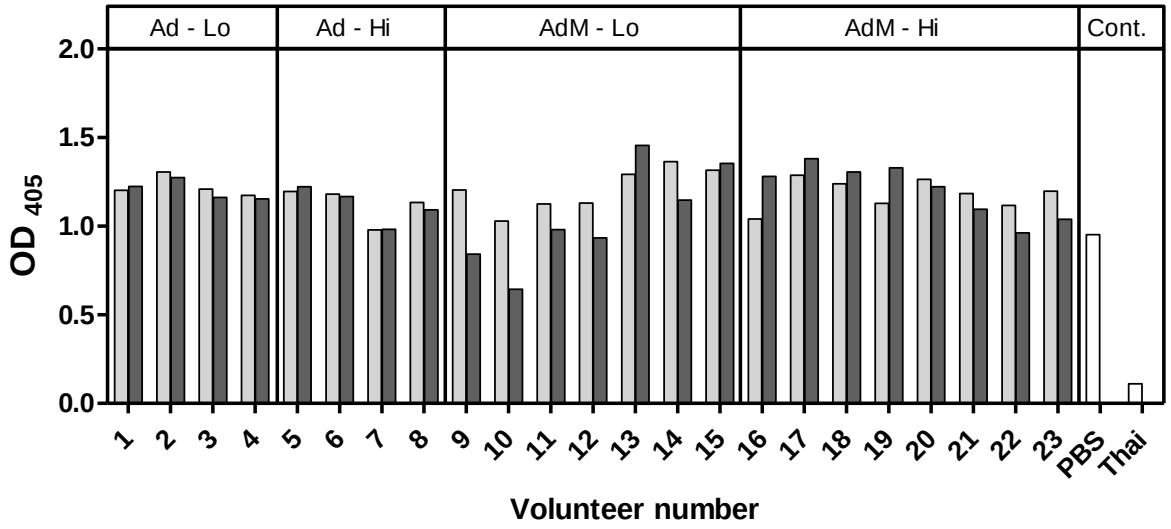

Figure 6-7: DBP binding assay with human serum from volunteers immunised with ChAd63-MVA DBP_RII

Healthy adult volunteers enrolled in a Phase Ia clinical trial were immunised with either a single dose of ChAd63 encoding DBP_RII at 5 x 10^9 vp (Ad - Lo) or 5 x 10^{10} vp (Ad - Hi), or both a ChAd63 DBP_RII dose at 5 x 10^{10} vp followed eight weeks later by MVA DBP_RII at 1 x 10^8 pfu (AdM - Lo) or 2 x 10^8 pfu (AdM - Hi). Serum was collected from volunteers before initial immunisation (light grey) and at 84 days after initial immunisation (dark grey). The ability of each serum sample to inhibit DBP binding at a dilution of 1:300 was assessed in the DBP binding assay. Low OD_{405} represents an inhibition of DARC-DBP binding. A negative control in the absence of any human sera (PBS) and a positive control of sera from a naturally exposed Thai adult were included. Bars represent the mean of samples run in duplicate.

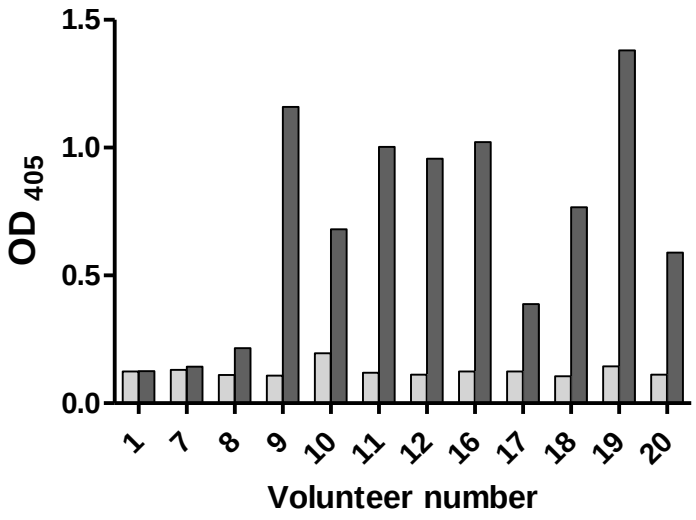

Figure 6-8: DBP_RII antibody responses following immunisation of human volunteers

DBP_RII specific antibody responses in the sera of adult volunteers (enrolled in a Phase Ia clinical trial as described in Figure 6-7) were determined in 12 of the 23 volunteers by ELISA on a plate coated with 0.1 µg/mL DBP_RII.PK.C-tag. Bars represent OD_{405} averages of duplicates for day 0 (light) and day 84 (dark) serum samples.

6.2.5. Improving DBP vaccines

Given the inability of vaccine-induced sera in humans to block DBP binding, it is clear that the vaccine must be improved. Due to limitations on the amount of protein available at present, an in-depth analysis of immunogenicity has yet to be finalised and remains on-going, however, one potential improvement for the vaccine would be to induce a higher antibody response. Previous work in our lab has shown that the fusion of some malarial proteins (232), but not others (272), to the oligomerisation domain IMX313 is capable of enhancing antibody responses following genetic immunisation (Llewellyn and Biswas, *unpublished data*). In addition, here I had already shown that DBP_RII-313 is capable of producing protein multimers (Figure 6-2C). As such, three doses of 50 µg of the DBP_RII-313 expression vector was administered i.m. into BALB/c mice at two week intervals and compared with the

same regime using the DBP_RII expression vector. No difference in antibody response between the two groups was observed at any time point (Dunn's test $P > 0.05$).

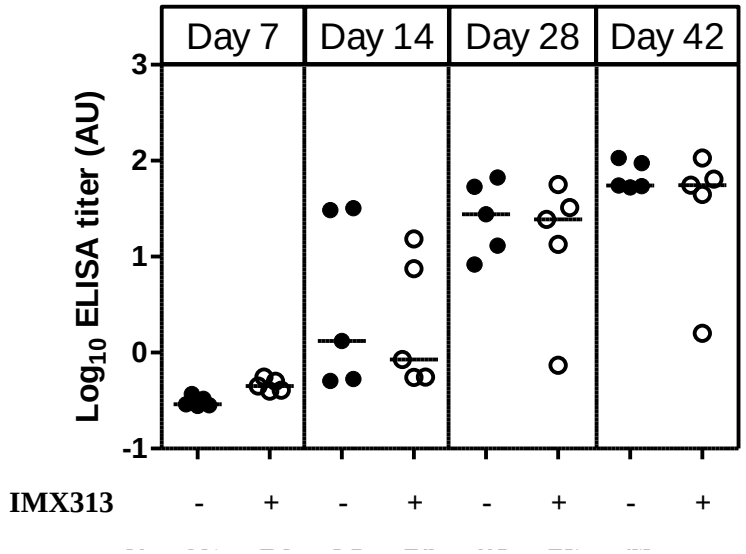

Figure 6-9: DNA immunisation of DBP_RII ± IMX313

Mice were immunised i.m. with 3 doses of 50 µg plasmid DNA encoding DBP_RII (-) or DBP_RII-313 (+) two weeks apart. Serum was collected at 7, 14, 28 and 42 days post initial DNA immunisation. Antibody titre was determined using a standardised ELISA with a plate coated with 2 µg/mL DBP_RII produced in *E. coli*.

Given the inability to induce a substantial improvement in immunogenicity using IMX313, I next attempted to mix the viral vectored vaccine with an adjuvant, Addavax. To assess the impact of adjuvant on immune response, both low and high dose viral vector regimes were administered with and without Addavax. Importantly, two weeks following MVA boost, there was a significant difference between groups (Kruskal-Wallis test, $P = 0.004$) with the groups receiving low dose ChAd63 and MVA inducing a significantly higher antibody titre following the mixing of the vaccine with Addavax compared to viral vectors without adjuvant (Dunn's multiple comparison test, $P < 0.05$; Figure 6-10). Thus, the mixing of adjuvant with ChAd63-MVA DBP_RII presents a possible clinically-relevant approach to enhance immunogenicity of the current vaccine.

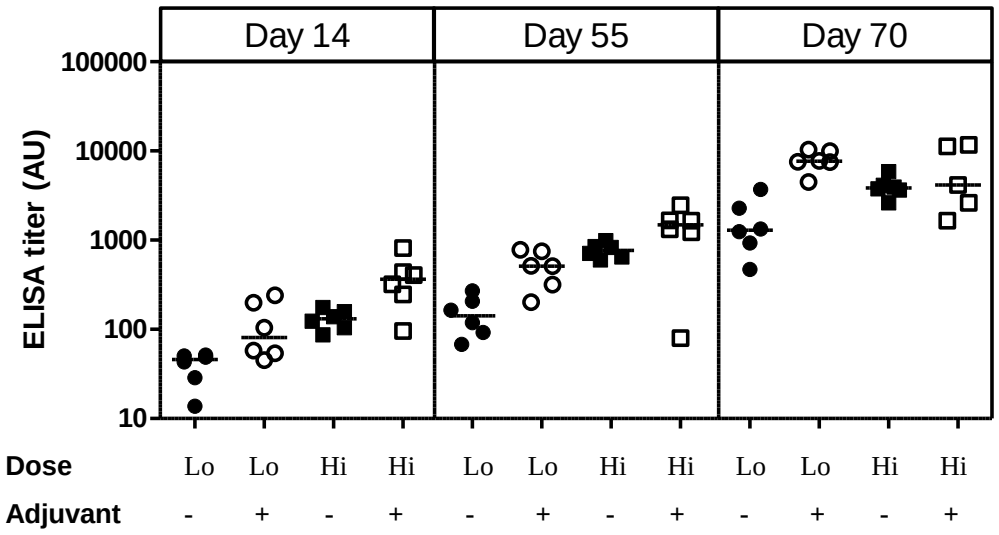

Figure 6-10: The combination of viral vectors and adjuvants to improve immunogenicity

BALB/c mice were immunised i.m. with viral vectors expressing DBP_RII with (+) or without (-) Addavax at the following doses: 1 x 10^6 ifu ChAd63 and boosted with 1 x 10^6 pfu MVA (Lo), or 1 x 10^8 ifu ChAd63 and boosted with 1 x 10^7 pfu MVA (Hi). Serum was collected at 14, 55 and 70 days post initial ChAd63 immunisation. Antibody titre was determined using a standardised ELISA with a plate coated with 2 µg/mL DBP_RII produced in *E. coli*.

Finally, different vaccine regimes were utilised to assess whether immunogenicity could be improved over the ChAd63-MVA DBP_RII regime described thus far. BALB/c mice primed with AdHu5 DBP_RII and boosted with MVA trended toward having a lower anti-DBP_RII antibody titre than mice primed with ChAd63 in a different experiment, although this was not significant by post-hoc Dunn's multiple comparison ($P > 0.05$). There was however a significant improvement in immunogenicity in groups receiving an AdHu5 prime and *E coli* produced protein in adjuvant boost, or two doses of protein in adjuvant compared to AdHu5-MVA immunisation ($P < 0.05$; Figure 6-11A).

Sera from mice receiving AdHu5-MVA, AdHu5-protein in adjuvant, and protein-protein regimes were thus assessed by the DBP binding assay. There was a significant difference between DBP binding inhibition as assessed by the dilution at which 50% of binding was

blocked (IC_{50}) between the three groups (Kruskal-Wallis test, P = 0.001) with post hoc analysis indicating a difference between AdHu5-MVA and AdHu5-protein in adjuvant groups ($P < 0.001$; Figure 6-11B & C). While the IC_{50} for ChAd63-MVA DBP_RII was not assessed for individual mice, analysis of a pool of sera from two weeks post MVA boost indicated that the IC_{50} of the pool was in excess of 8000. Furthermore, for the three vaccine regime groups tested, DBP binding inhibition was associated with DBP specific antibody titre (r_s = 0.66, P = 0.005), and thus ChAd63-MVA immunised mice could be expected to perform similarly to AdHu5-protein and protein-protein groups. Overall, these data show that, in mice, strategies for increasing the immunogenicity of vaccines can be utilised to improve DBP binding inhibition activity.

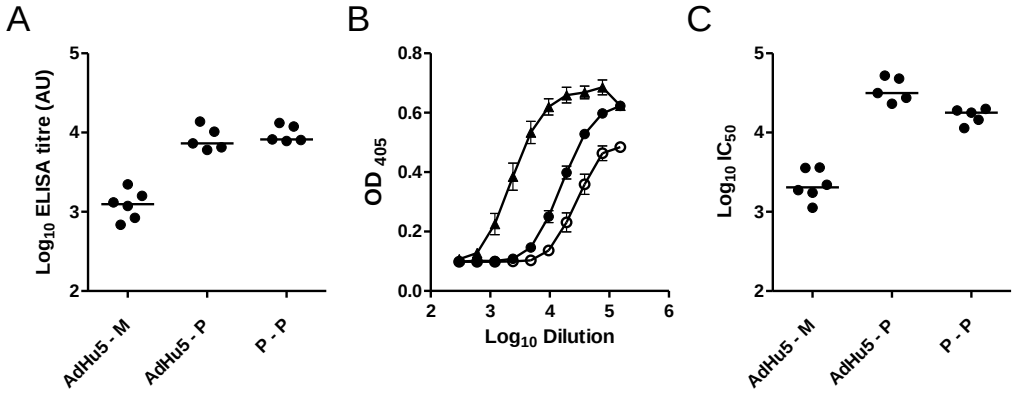

Figure 6-11: Antibody induction and the blocking of DARC-DBP binding by different immunisation regimes

BALB/c mice were immunised i.m with either two doses of 10 µg recombinant DBP_RII produced in *E. coli* formulated in Abisco three weeks apart (P – P) (n=5); one dose of 1 x 10^9 vp AdHu5 expressing DBP_RII followed eight weeks later by 10 µg DBP_RII in Abisco (AdHu5 – P) (n=5); or one dose of 1 x 10^9 vp AdHu5 expressing DBP_RII followed eight weeks later by 1 x 10^7 pfu MVA expressing DBP_RII (AdHu5 – M) (n=6). (A) Antibody titre was determined by standardised ELISA against DBP_RII expressed in *E. coli*. (B) Dilution curves from the DARC-DBP binding assay given as OD_{405} averages for mice receiving AdHu5 – M (n = 6, ▲), AdHu5 – P (n = 5, ○), and P – P (n = 5, ●). (C) The serum dilution required to block half the binding of DBP_RII to DARC in comparison to naïve BALB/c serum (IC_{50}) as measured in the DARC-DBP binding assay for the three different immunisation regimes.

6.2.6. Improvements to binding assay

Finally, in order for complete immunological characterisation of the clinical trial sera, as well as conducting ongoing work with the DBP binding assay, a more efficient protocol for producing DBP_RII protein must be developed. As such, I attempted to express DBP_RII.PK.C-tag in stably transfected S2 *Drosophila* cells. DBP_RII, with a BiP signal sequence, mutated N-glycan sites, and codon optimised for expression in *Drosophila* cells, was ordered and cloned into ExpreS^{2}ion Biotechnologies' proprietary expression vector pExpreS2-2 by CPEC also introducing the PK.C-tag at the C-terminus. A stable cell line was generated before a 900 mL expression culture was initiated. After seven days supernatant was harvested and protein purified by affinity chromatography and SEC. Protein was obtained from the second SEC peak and confirmed to be pure by Coomassie Blue stain (Figure 6-12A) and identified as DBP_RII by Western blot at the expected size of 40 kDa (Figure 6-12B). From the 900 mL culture, approximately 200 µg DBP_RII was purified representing an expression and purification efficiency of 0.22 µg/mL, an almost 50-fold improvement over HEK293 cells. S2 cell expression of DBP_RII thus presents a more promising strategy for the generation/optimisation of larger quantities of DBP_RII protein thus allowing complete immunological characterisation of the human clinical trial samples.

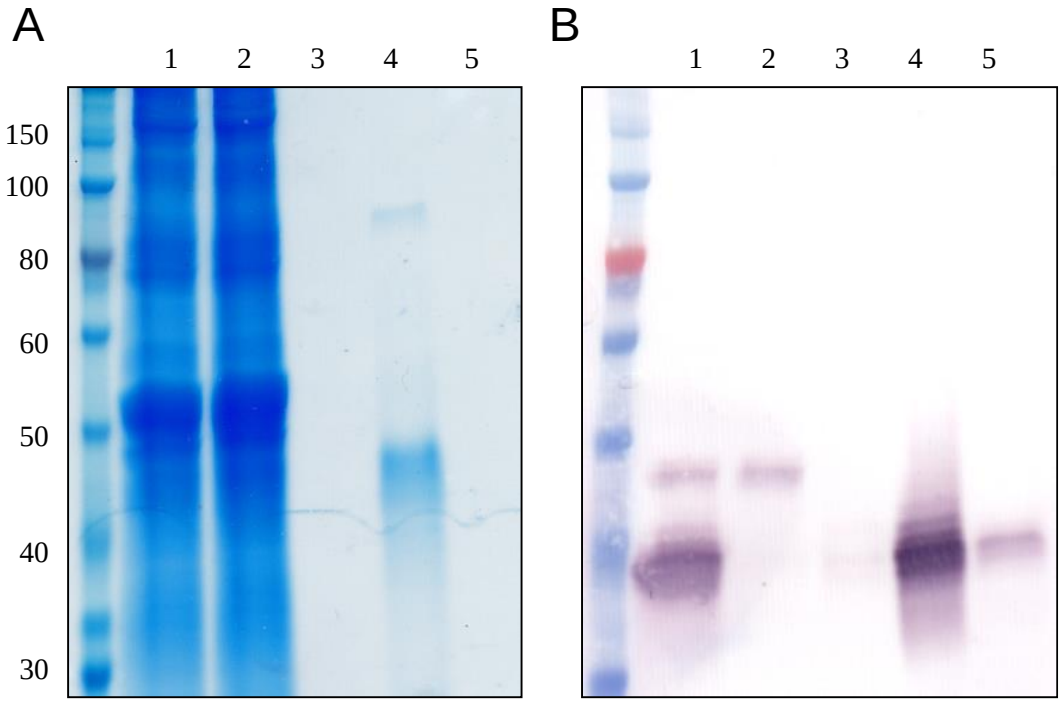

Figure 6-12: Expression of DBP.PK.C-tag in S2 cells

A stable S2 cell line expressing DBP_RII.PK.C-tag was generated. Supernatant was harvested after eight days of culture and protein purified by affinity chromatography using CaptureSelect C-tag affinity matrix followed by SEC. (A) Coomassie Blue stain of samples under reducing conditions, and (B) Western blot of non-reduced samples with serum from mice immunised with ChAd63-MVA DBP_RII. Lane 1 = S2 supernatant as applied to CaptureSelect C-tag affinity matrix; lane 2 = CaptureSelect C-tag affinity matrix flow through; lane 3 = SEC peak 1; lane 4 = SEC peak 2; lane 5 = SEC peak 3.

6.3. Discussion

In this Chapter I have described the preliminary establishment and optimisation of the DARC-DBP binding assay, and have applied it, for the first time, to human sera from a Phase I clinical trial. A major obstacle in the establishment of the assay was the expression of the component proteins. As previously described (280), DARC was easily expressed in HEK293 cells at the size expected with two sulphated tyrosines (280). DBP_RII protein, however, presented a far greater challenge. Previous studies have purified DBP_RII from inclusion bodies after expression in *E. coli* (359, 367). An optimised protocol using this system has been reported to give a protein yield of 16 mg/L (368), some 70 times more efficient than my expression trial in S2 cells (albeit with a slightly different protein construct). However, only a small number of laboratories around the world have been able to efficiently produce DBP_RII in this way, and on attempting to reproduce this protocol, collaborators in the Department of Biochemistry, University of Oxford, were unable to produce refolded DBP_RII protein. I did, however, receive a limited amount of *E. coli* produced DBP_RII as a kind gift from Dr Chetan Chitnis (ICGEB) with which some experiments in this Chapter have been conducted.

It is clear that the efficiency of protein expression reported here requires improvement, especially if sufficient quantities are to be generated for immunisation experiments, however, there is precedent for expressing DBP_RII in HEK293 cells (369). In contrast to my attempts to produce DBP_RII, in this previously described work, Sampath *et al*. utilise a high efficiency transfection procedure for the expression of a number of different glycoforms of the protein. The transfection protocol utilised by Sampath *et al*. has been shown to increase expression of soluble HIV Envelope proteins (370), and given that transfection efficiencies in the experiments presented in this Chapter were typically low (~15-20%), the high efficiency

technique provides a promising avenue for future improvement. Cell lines reported to be transfected with high efficiencies such as HEK293-6E could also be tried. In addition, further improvements to construct design such as N-glycan site mutation and codon harmonisation (371), coupled with the ease of producing large expression cultures – especially in the S2 expression system once a stable cell line has been generated – mean that large quantity protein production should be possible. Recent developments have suggested that isolating S2 monoclonal cell lines can result in up to a 20-fold increase in protein expression when compared with polyclonal cultures (Jin *et al*., *unpublished data*), providing another potential strategy improving protein expression.

Once sufficient protein had been generated to conduct the DBP binding assay, I tested the ability of sera from DBP_RII immunised mice to block DARC-DBP_RII binding. As has been previously reported (265), serum from mice receiving immunisation with *E. coli* produced protein in adjuvant was able to block DBP binding. In addition, mice receiving different immunisation regimes (ChAd63-MVA, AdHu5-MVA, AdHu5-Protein) also mounted responses capable of blocking DBP binding. Blocking appeared to occur in a DBP_RII antibody titre dependent manner, with IC_{50} titres ranging from 2,000 to over 10,000. This suggests that overall differences in antibody titre between immunisation regimes in mice play a more important role in receptor-ligand blocking activity than a difference in the quality of antibodies generated from different immunisation regimes. This observation, however, remains to be formally tested.

If we do assume that a higher anti-DBP_RII antibody titre would induce more DARC-DBP_RII binding inhibition, it would be desirable to produce more immunogenic DBP_RII vaccines. I thus attempted to improve the immunogenicity of the current ChAd63-MVA vaccine by formulating the viral vaccines with adjuvant. Importantly, immunogenicity of the

vaccine was improved in mice receiving a low dose of ChAd63-MVA DBP_RII when the viral vectors were mixed with the squalene-oil-in-water adjuvant, Addavax (a biosimilar of the MF59 adjuvant from Novartis (licensed for human use), and highly similar to the AS03 adjuvant from GSK (in clinical development)). Mice receiving a higher dose of viral vectors derived no benefit from the addition of Addavax, although it is possible that the high dose of this viral vector regime induced a maximal humoral response in the absence of the adjuvant (372). This has relevance to human vaccination given that an Addavax equivalent (MF59) is licenced for use in humans, and given the doses of viral vectors administered to humans are unlikely to induce the maximum possible humoral immune response. This mixing of adjuvants with viral vectored vaccines thus provides a legitimate strategy for improving immunogenicity of viral vectored vaccines in humans, and is being explored as part of the clinical trials programme at the Jenner Institute with our industrial collaborators Novartis and GSK as part of the MultiMalVax programme.

Nevertheless, it does seem likely that antibody quality, rather than simply titre, may play an important role in the inhibition of DBP binding. This is evident by the fact that human antibodies raised against the same vaccine as that used in mice did not block the DARC-DBP_RII interaction at all, whereas some level of blocking was measurable from mouse serum even when diluted 1:10,000. This presents an interesting question about the differences in immune response between humans and mice. While we know that the induction of antibodies from vaccination of humans, in terms of overall concentration, is often lower than that in animal models for similar vaccines (220)(Milne, *unpublished data*), given the relatively high IC_{50} results generated with mouse sera, it seems unlikely that this explains the complete absence of blocking imparted by human sera. We do know that sera from mice immunised with ChAd63-MVA DBP_RII only recognise non-reduced protein, and thus seems to be directed towards conformational epitopes. It is possible that a key conformational

epitope of DBP_RII is immunodominant in mice, but fails to induce a significant response in humans. The mapping of key inhibitory epitopes with mAbs generated from immune mice may thus provide a promising direction for future design of next generation immunogens.

These results clearly suggest that the human DBP_RII vaccine requires significant optimisation. If inhibitory epitopes could be identified, strategies to target vaccine responses to these epitopes could be employed. For example, the use of glycan masking has recently been used to focus the immune response in rabbits and mice to predicted inhibitory epitopes of DBP_RII (369). Furthermore, exciting advances in the field of epitope focused vaccine design, especially with the fusion of neutralising epitopes to particles (373), and the use of synthetic scaffolds as pioneered in the field of development of viral vaccines (374-376), provide novel techniques which could aid the development of an effective human DBP_RII vaccine.

Thus, while DBP_RII remains an exciting and promising vaccine target for blood-stage *P. vivax* malaria, significant improvements are likely still required. Ideally, an association of the DARC-DBP binding assay with clinical protection in a naturally immune cohort, as presented in Chapter 5 for ADRB, should be conducted to verify the use of the DBP binding assay in vaccine development. One study has suggested that very high levels of inhibition in the DARC-DBP binding assay are associated with delayed time to infection when determined by light microscopy (377). However, this association disappeared when using more sensitive diagnosis techniques, making the result difficult to interpret. Until more thorough associations are drawn between the DARC-DBP binding assay and clinical protection, the assay remains a valuable tool for the assessment of antibody-induced DARC-DBP_RII binding inhibition, and is an important step towards addressing the paucity of assays available for the study of immunity to *P. vivax* malaria.

CHAPTER 7

CONCLUDING REMARKS AND FUTURE DIRECTIONS

7. CONCLUDING REMARKS AND FUTURE DIRECTIONS

7.1. Summary

Blood-stage malaria vaccinology finds itself at a junction between an historical inertia created by obsessive work on a limited number of vaccine candidates, and the acceptance that promising new targets must be discovered and exploited before calls for an efficacious vaccine can be realised. Nevertheless, the historical failure to broaden the field's scope can be attributed in some part to the paucity of available pre-clinical assays with which candidate antigens can be robustly and reproducibly assessed for utility as vaccine candidates (378). Furthermore, the lack of such assays comes from a relatively incomplete understanding of how antibody-mediated protection against the blood-stage malaria parasite is conferred *in vivo* in humans.

In this Thesis, I describe the development of both the ADRB assay for *P. falciparum*, and the *P. vivax* DBP-DARC binding inhibition assay, for use in the assessment of naturally-acquired and vaccine-induced antibody responses. Both assays address key gaps in the field, enabling the reproducible assessment of γ-chain-dependent immune activation against *P. falciparum* blood-stage parasites, and the *in vitro* quantification of antibody-induced blockade of an essential receptor-ligand interaction in the *P. vivax* life cycle respectively. The use of these assays should help to direct future vaccine development efforts as well as forming useful tools to assess and understand NAI.

7.2. Conclusions

7.2.1. ADRB: From models for vaccine development to NAI in humans

Thorough standardisation of assay protocols is necessary in order for newly developed assays to be widely useful to the malaria community. The ADRB assay as presented in this Thesis

now provides such a protocol. Given that the assay can be used with very small amounts (< 10 µL) of serum or plasma (suitable for samples routinely collected in pre-clinical vaccine development studies and epidemiological studies), the assay can be easily applied to studies and cohorts which already exist, as well as being used in the immunological assessment of future work.

The ADRB assay was first established using a mouse model which, in turn, enabled the assessment of the contribution of FcR to the induction of ADRB activity, as well as a controlled investigation of the role of ADRB activity in malaria challenge outcome. In mice, ADRB activity was not required in order to attain vaccine-induced protection against lethal *P. yoelii* infection using vaccines based on PyMSP1$_{42}$. However, ADRB activity was elicited after non-lethal challenge of mice with *P. yoelii*, suggesting that antigen targets of anti-PEMS ADRB activity remain to be established. Given that an ADRB-inducing vaccine remains to be developed, it remains unknown as to whether such a vaccine would be able to protect mice, and indeed humans, from malarial challenge. It might be inferred from the fact that ADRB activity associated with clinical protection in a cohort of NAI, that an ADRB-inducing vaccine would be protective, however this requires formal testing.

The association of ADRB activity with clinical protection with the aforementioned cohort from Mali, reproduced a result previously reported in a Senegalese cohort (181). Interestingly, GIA and SRA activity did not correlate with clinical outcome in this cohort, alluding to the potential importance of antibody-dependent cellular activation in natural protection against *P. falciparum* malaria. Unlike GIA and SRA, ADRB activity was dependent on functional γ-chain signalling. In mice, this was shown to be particularly dependent upon activatory CD16 signalling. Given that mouse CD16 is thought to play a similar role to CD32a in humans, a dependency of ADRB activity on CD16 signalling in

mice agrees with the wealth of epidemiological data in humans suggesting that CD32a polymorphisms affect clinical outcome following malaria infection (205-211). Overall, the combination of FcR polymorphism data and clinical outcome, the susceptibility of *P. falciparum* to ROS (127), and now the repeated association of ADRB activity with clinical immunity, provide a persuasive argument for the role of respiratory burst in protection against *P. falciparum* malaria.

A key finding elucidated by the work in mice, however, was that despite differences in ability to control secondary infection between mice with or without functional FcR signalling, neutrophils were not responsible for these differences. This highlights a broader question as to the source of any actual protective efficacy. For many years Pierre Druilhe *et al.* have argued that antibody-induced activation of monocytes elicits protection. Indeed they have shown that in culture of *P. falciparum*, antibodies mixed with monocytes are capable of inhibiting parasite growth, while antibodies mixed with neutrophils are not (180, 250). It is thus possible that ADRB activity merely reflects antibodies ability to induce cellular responses, providing a reproducible *in vitro* surrogate for monocyte activation. Indeed, a possible marrying of these two lines of work comes in the suggested importance of macrophage produced ROS in anti-malarial activity (126). It is, however, important to be cautious when attempting to infer mechanisms from *in vitro* parasite cultures to *in vivo* interactions. While current evidence suggests that the production of ROS is a reasonable candidate as an important mechanism for anti-malarial immunity, other antibody-induced activities such as phagocytosis (121-124) may also play an important role. At this stage, it is impossible to state conclusively the mechanism involved in ADRB activity associated protection against malarial infection.

Through this work, the ADRB assay has emerged as a useful tool for the assessment of NAI. It remains to be seen whether it can be effectively applied to the field of vaccine development in humans. Importantly, studies on NAI, as presented in this Thesis, show that the ADRB assay is capable of measuring a type of anti-malarial activity which is distinct from that indicated by the GIA and SRA assays. Future work on vaccine development should consider GIA-, SRA-, and ADRB-type immunological mechanisms and thus the ADRB assay is in a unique position to complement the use of other assays in the field.

7.2.2. *P. vivax*: blocking the DARC-DBP_RII interaction

Given the Malaria Vaccine Technology Roadmap call for a vaccine to exert 75% efficacy over at least two years, for both *P. falciparum* and *P. vivax* (266), it is obvious that new approaches to malaria subunit vaccine design are urgently required, and *P. vivax* must emerge as a priority species for vaccine development. Given the unique opportunity of the first clinical trial with a *P. vivax* blood-stage vaccine candidate, vaccine-induced antibodies were assessed for their ability to block the interaction between DARC and DBP_RII in a binding assay (265). It is reasonable to believe that vaccine-induced antibodies capable of blocking the interaction between DARC and DBP_RII should be able to prevent *P. vivax* from invading host erythrocytes, and thus prevent disease, given the essential nature of this interaction (33), and early results in a cohort of NAI (377). However, despite inhibitory antibodies being induced by immunisation in mice, no such response was found in humans. Perhaps this results from a long co-evolution between *P. vivax* and humans, where *P. vivax* has evolved to direct human immune responses to non-inhibitroy epitopes, a selection pressure not imparted on mice which cannot be infected with *P. vivax*. Given that targeting DBP_RII as a vaccine candidate intends to impart protection via GIA-like invasion blocking activity, and that antibodies induced in humans were not able to block the DARC-DBP_RII

interaction, it is unlikely that this vaccine would have any efficacy against *P. vivax* challenge. It is of course possible that the vaccine induced antibodies could still affect some activity *in vivo* through ADRB-like mechanisms, however this remains to be tested.

A major hindrance to the field of blood-stage malaria study, illustrated in the attempts to produce DBP protein, is the difficulty of producing recombinant *Plasmodium* proteins. This has been noted previously, especially with respect to prokaryotic expression systems (379, 380). Here I achieved small amounts of protein expression using transiently transfected HEK293E cells, a system which has previously been used to express *Plasmodium* proteins with some success (381, 382). However, despite this, yields of DBP_RII were still very low. Improvements in yield were attained using a stable *Drosophila* S2 cell line (383, 384), providing a promising avenue for future protein production. The utility of this system for expression of *Plasmodium* proteins has been clearly demonstrated by the recent use of S2 cell lines in solving the structure of PfRH5 (384).

7.2.3. The use of mouse models in malaria research

In addition to the use of *in vitro* assays, the study of infectious diseases has benefited greatly from the use of a number of animal models which are able to approximate disease in humans. Mouse models in particular have played a valuable role in medical research, however the importance of noting differences between mice and humans when extrapolating results cannot be overstated. The work I have conducted clearly supports this caution. While the ability to induce ADRB activity was not required for protection against lethal *P. yoelii* infection in mice, ADRB activity did associate with protection in a human population. It is firstly important to recognise, however, that these two findings relate to different species of *Plasmodium*. Indeed, given that immunity against *P. yoelii* is known to be largely mediated by γ-chain-independent mechanisms (50), and that vaccines which can protect mice from *P.*

yoelii malaria do not protect humans when targeting the *P. falciparum* orthologues (144, 232), it is perhaps not surprising to see these conflicting results. Indeed, given the association presented here between protection against *P. falciparum* malaria and an Fc-dependent activity (ADRB), perhaps *P. berghei*, against which protection is thought to be Fc-dependent (49), would be a better tool for modelling *P. falciparum* immunity.

Even more interesting, is the difference in immune response between mice and humans to an identical vaccine as shown in my work on DBP. When administered to mice, antibodies induced were able to block DARC-DBP_RII binding, however antibodies raised against the same vaccine in humans were not capable of inhibitory activity. While there is a slim possibility this is due simply to titre, the fact that mouse antibodies at a high dilution were capable of blocking binding disputes this. Instead, I suggest that this result reflects a fundamental difference in immunology between the two species. While, in general, mice provide very good models for immunological research, differences between mouse and human immune systems have been widely reported (385). Without further investigation, it is difficult to suggest what might contribute to the differences seen in DBP_RII response between mice and humans. A reasonable hypothesis is that different epitopes are immunodominant in the two species, skewing the antibody response against DBP_RII in mice towards inhibitory epitopes, and the response in humans to non-inhibitory epitopes. Given the viral plasmids within the vaccine contain CpG motifs, perhaps the differences in TLR-9 distribution on the innate immune cells and antigen presenting cells between mice and humans (386, 387) affect the priming of immune responses and subsequent antibody affinity.

Immunological differences between mice and humans also have interesting implications for ADRB and anti-malarial activity. In adult humans, 50-70% of circulating immune cells are neutrophils compared to only 10-25% in mice (388), potentially affecting neutrophil-based

effector efficiency. Furthermore, incompletely understood differences in FcR biology may result in a difference in reactivity between mouse and human neutrophil populations.

Overall, due to the practicalities of using mice for malarial research, the number of infection models available, and the availability of models with genetic modification, mice will continue to be a valued tool for research in malaria. It is, however, important to be aware of inherent differences which make the extrapolation of results in mouse models to human clinical trials difficult, a problem which the development of *in vitro* assays should help to address.

7.3. Future Directions

7.3.1. Utilising the ADRB assay

Much of the intention of the work presented in this Thesis was to establish the ADRB assay as a tool which could be used widely for the assessment of NAI and for blood-stage malaria vaccine development. The assay has now been successfully conducted in three laboratories (181, 321) and associated with clinical protection in two independent studies, albeit only once with the standardised protocol described here. In terms of NAI, the assay will need to be applied to a number of additional cohorts before it can be concluded as to whether or not ADRB can out-perform the cohort-specific associations of protection seen with ELISAs. Importantly, assessing the ADRB assay and its association with clinical protection in a cohort for which ELISA titre does not predict clinical outcome remains to be conducted. Ideally the assay would be taken up and used within other groups, allowing future assessments of inter-laboratory reproducibility.

As mentioned, a key reason for the development of the ADRB assay was to help direct vaccine development. The blood-stage malaria vaccine group at the Jenner Institute is now in a unique position to do this. Through a project aimed at antigen screening using the GIA

assay, immune sera from mice have been generated against 28 merozoite proteins. By slightly adapting the protocol developed in this Thesis, to having a plate coated with *P. falciparum* PEMS and using mouse PMNs, these immune sera could be tested for their ability to induce ADRB activity. Any 'hits' would represent the first candidate antigen(s) identified using the ADRB assay, and potentially represent a class of vaccine distinct from the invasion blocking candidates developed to date (389, 390).

An interesting finding of this work was that different individuals had different FcR expression profiles upon their neutrophils. The effect that this has on subsequent neutrophil activation and malaria disease outcome is worth investigating.

While this Thesis has focused on malaria and the application of ADRB to *P. falciparum* in particular, the protocol developed here could be applied to any antigen or pathogen for the assessment of cytophilic antibody reactivity. Importantly, if sufficient merozoites could be generated for *P. vivax*, the ADRB assay could provide an important tool in assessing *P. vivax* NAI and in the development of *P. vivax* blood-stage vaccine candidates.

7.3.2. The development of *P. vivax* blood-stage vaccines

7.3.2.1. Engineering Improved Immunogens

Given the result presented in Chapter 6 showing that following DBP_RII immunisation human sera were incapable of blocking DARC-DBP binding, it is clear that there is much left to do. Firstly, and importantly, an investigation into the differences between the immune responses elicited in both mice and humans to the same vaccine is required. Basic ELISA-based methods would be useful for an initial characterisation of immune responses, assessing isotype profiles and antibody affinity. However, it seems most probable that differences in

inhibitory activity are a result of binding to different epitopes on DBP_RII. Thus, identifying the binding-inhibitory epitopes of DBP_RII should be a key priority moving forward.

One strategy for achieving this is by isolating inhibitory mAbs from mouse spleens, or human blood from immunised volunteers. While immunised volunteers did not exhibit any DARC-DBP_RII blocking activity, it may still be possible to isolate rare inhibitory mAb producing B cells. It is noteworthy that the most potent inhibitory mAbs directed against PfRH5 as measured in the GIA assay, are not capable of blocking the PfRH5-basigin interaction (384), and thus the lack of ability of immune sera to block the DARC-DBP_RII interaction, does not preclude isolated mAbs from having any functional activity. To isolate human mAbs, antibody secreting cells ($CD19^+$, $CD27^+$, $CD21^-$, $CD20^-$, $CD38^+$) taken seven days after booster immunisation, could be isolated from which V_H and $V\kappa$ genes from single cells could be amplified (391). Subsequent production of human mAbs using a HEK293 cell expression system would enable antibodies to be screened for antigen-specific binding properties.

If neutralising mAbs were generated, they could then be utilised in structural studies as has recently been done with the PfRH5 antigen (384). While the structure of DBP is known (392), such studies would represent the first structures of DBP in complex with neutralising human mAbs. In combination with the biological characterisation of the generated mAbs in the DARC-DBP binding assay, this work would provide a detailed molecular insight into the critical and protective molecular interactions between DBP and human binding-inhibitory antibodies. Furthermore, this information would be vital to the design and testing of a new panel of vaccine immunogens that focus on the induction of more potent and durable immunogenicity against key B cell epitopes. Such studies could involve structure-guided antigen truncations, or transferring mAb epitopes onto particle (373) or protein scaffolds, as reported for HIV (375, 376). How to test the utility of newly discovered immunogens without

immunising people, remains an issue. The recent development of DRAG mice which can be reconstituted with a human immune system is one promising avenue that could be explored in this endeavour (393).

7.3.2.2. Novel Invasion Assay Development

Upon the development of new vaccine candidates, it will be necessary to vigorously test the functional activity of elicited immune responses to justify progression to Phase IIa clinical trials. In terms of the DARC-DBP binding assay as presented in Chapter 6, an important iteration will be to conduct the assay with allelic variants of DBP_RII. Utilising recently obtained genomic sequence databases of DBP, variants could be expressed and used to assess antibody cross-strain receptor-ligand blocking. This would address the key obstacle of field isolate polymorphism associated with *P. vivax* vaccine design. Furthermore, antibody inhibitory activity could be assessed against the full-length DBP protein in the binding assay enabling the assessment of whether neutralising epitopes are shielded by natural protein folding.

The development of a GIA-type assay for *P. vivax* would also represent an invaluable tool for the study of *P. vivax* malaria. Recent progress in the adaptation of *P. knowlesi* to culture in human erythrocytes represents an exciting opportunity (264). Although not reticulocyte-restricted like *P. vivax*, by replacing *P. knowlesi*'s DBPα gene with *P. vivax* DBP (394), this parasite could enable the first *in vitro* functional readout of anti-*P. vivax* DBP antibodies without necessitating access to fresh *P. vivax* parasites. This work is currently in progress within the blood-stage group.

7.4. Final Remarks

The development of effective vaccines against both *P. falciparum* and *P. vivax* malaria remain an urgent global health priority. However, a thorough understanding of the mechanisms involved in immunity to malaria will be essential in guiding future vaccine development efforts. In this Thesis, I have thus explored the importance of Fc-dependent antibody function in immunity to *P. falciparum* blood-stage malaria, and the importance of reliable *in vitro* assays for the assessment of anti-merozoite antibody function. The tools developed here should not only provide guidance for the development of new blood-stage malaria vaccines, but should also play vital roles in the assessment of vaccine candidates once they have progressed to human trials.

REFERENCES

REFERENCES

1. Neghina, R., A. M. Neghina, I. Marincu, and I. Iacobiciu. 2010. Malaria, a journey in time: in search of the lost myths and forgotten stories. *The American Journal of the Medical Sciences* 340: 492-498.
2. Alonso, P. L., G. Brown, M. Arevalo-Herrera, F. Binka, C. Chitnis, F. Collins, O. K. Doumbo, B. Greenwood, B. F. Hall, and M. M. Levine. 2011. A research agenda to underpin malaria eradication. *PLoS Medicine* 8: e1000406.
3. Roll Back Malaria Partnership. 2008. The global malaria action plan for a malaria free world. RBM. Available: http://www.rollbackmalaria.org/gmap/gmap.pdf, Geneva.
4. Mendis, K., A. Rietveld, M. Warsame, A. Bosman, B. Greenwood, and W. H. Wernsdorfer. 2009. From malaria control to eradication: The WHO perspective. *Tropical Medicine & International Health* 14: 802-809.
5. Centers for Disease Control and Prevention. 2010. Malaria - Biology. CDC, Atlanta: http://www.cdc.gov/malaria/about/biology/.
6. Rosenberg, R., R. A. Wirtz, I. Schneider, and R. Burge. 1990. An estimation of the number of malaria sporozoites ejected by a feeding mosquito. *Transactions of the Royal Society of Tropical Medicine and Hygiene* 84: 209-212.
7. Vanderberg, J. P. 1977. *Plasmodium berghei*: Quantisation of sporozoites injected by mosquitoes feeding on a rodent host. *Experimental Parasitology* 42: 169-181.
8. Yamauchi, L. M., A. Coppi, G. Snounou, and P. Sinnis. 2007. *Plasmodium* sporozoites trickle out of the injection site. *Cellular Microbiology* 9: 1215-1222.
9. Amino, R., S. Thiberge, B. Martin, S. Celli, S. Shorte, F. Frischknecht, and R. Menard. 2006. Quantitative imaging of *Plasmodium* transmission from mosquito to mammal. *Nature Medicine* 12: 220-224.
10. Frevert, U., I. Usynin, K. Baer, and C. Klotz. 2006. Nomadic or sessile: can Kupffer cells function as portals for malaria sporozoites to the liver? *Cellular Microbiology* 8: 1537-1546.
11. Shin, S. C. J., J. P. Vanderberg, and J. A. Terzakis. 1982. Direct infection of hepatocytes by sporozoites of *Plasmodium berghei*. *The Journal of Protozoology* 29: 448-454.
12. Mota, M. M., G. Pradel, J. P. Vanderberg, J. C. R. Hafalla, U. Frevert, R. S. Nussenzweig, V. Nussenzweig, and A. Rodríguez. 2001. Migration of *Plasmodium* sporozoites through cells before infection. *Science* 291: 141-144.
13. Prudencio, M., A. Rodriguez, and M. M. Mota. 2006. The silent path to thousands of merozoites: the *Plasmodium* liver stage. *Nature Reviews Microbiology* 4: 849-856.
14. Sturm, A., R. Amino, C. van de Sand, T. Regen, S. Retzlaff, A. Rennenberg, A. Krueger, J.-M. Pollok, R. Menard, and V. T. Heussler. 2006. Manipulation of host hepatocytes by the malaria parasite for delivery into liver sinusoids. *Science* 313: 1287-1290.
15. Wright, G. J., and J. C. Rayner. 2014. *Plasmodium falciparum* erythrocyte invasion: combining function with immune evasion. *PLoS Pathogens* 10: e1003943.
16. Gilson, P. R., and B. S. Crabb. 2009. Morphology and kinetics of the three distinct phases of red blood cell invasion by *Plasmodium falciparum* merozoites. *International Journal for Parasitology* 39: 91-96.
17. Boddey, J. A., and A. F. Cowman. 2013. *Plasmodium* nesting: remaking the erythrocyte from the inside out. *Annual Review of Microbiology* 67: 243-269.
18. Kafsack, B. F. C., N. Rovira-Graells, T. G. Clark, C. Bancells, V. M. Crowley, S. G. Campino, A. E. Williams, L. G. Drought, D. P. Kwiatkowski, D. A. Baker, A. Cortes,

and M. Llinas. 2014. A transcriptional switch underlies commitment to sexual development in malaria parasites. *Nature* 507: 248-252.
19. Sinha, A., K. R. Hughes, K. K. Modrzynska, T. D. Otto, C. Pfander, N. J. Dickens, A. A. Religa, E. Bushell, A. L. Graham, R. Cameron, B. F. C. Kafsack, A. E. Williams, M. Llinas, M. Berriman, O. Billker, and A. P. Waters. 2014. A cascade of DNA-binding proteins for sexual commitment and development in *Plasmodium*. *Nature* 507: 253-257.
20. Regev-Rudzki, N., Danny W. Wilson, Teresa G. Carvalho, X. Sisquella, Bradley M. Coleman, M. Rug, D. Bursac, F. Angrisano, M. Gee, Andrew F. Hill, J. Baum, and Alan F. Cowman. 2013. Cell-cell communication between malaria-infected red blood cells via exosome-like vesicles. *Cell* 153: 1120-1133.
21. Bray, R., and P. Garnham. 1982. The life-cycle of primate malaria parasites. *British Medical Bulletin* 38: 117-122.
22. Sinden, R. E., and H. M. Gilles. 2002. The malaria parasites. In *Essential Malariology*, 4th ed. H. M. Gilles, and D. A. Warrell, eds. Arnold, London. 8-34.
23. Marois, E. 2011. The multifaceted mosquito anti-*Plasmodium* response. *Current Opinion In Microbiology* 14: 429-435.
24. World Health Organisation. 2013. World Malaria Report 2013. Geneva.
25. Gething, P. W., A. P. Patil, D. L. Smith, C. A. Guerra, I. Elyazar, G. L. Johnston, A. J. Tatem, and S. I. Hay. 2011. A new world malaria map: *Plasmodium falciparum* endemicity in 2010. *Malaria Journal* 10: 1475-2875.
26. Trager, W., and J. Jensen. 1976. Human malaria parasites in continuous culture. *Science* 193: 673-675.
27. Sina, B. 2002. Focus on *Plasmodium vivax*. *Trends in Parasitology* 18: 287-289.
28. Hulden, L., and L. Hulden. 2011. Activation of the hypnozoite: a part of *Plasmodium vivax* life cycle and survival. *Malaria Journal* 10: 1-6.
29. Mueller, I., M. R. Galinski, J. K. Baird, J. M. Carlton, D. K. Kochar, P. L. Alonso, and H. A. del Portillo. 2009. Key gaps in the knowledge of *Plasmodium vivax*, a neglected human malaria parasite. *The Lancet Infectious Diseases* 9: 555-566.
30. Kitchen, S. 1938. The infection of reticulocytes by *Plasmodium vivax*. *The American Journal of Tropical Medicine and Hygiene* 1: 347-359.
31. Persson, K. E. M., F. J. McCallum, L. Reiling, N. A. Lister, J. Stubbs, A. F. Cowman, K. Marsh, and J. G. Beeson. 2008. Variation in use of erythrocyte invasion pathways by *Plasmodium falciparum* mediates evasion of human inhibitory antibodies. *Journal of Clinical Investigation* 118: 342-351.
32. Cowman, A. F., and B. S. Crabb. 2006. Invasion of red blood cells by malaria parasites. *Cell* 124: 755-766.
33. Chitnis, C. E., and A. Sharma. 2008. Targeting the *Plasmodium vivax* Duffy-binding protein. *Trends in Parasitology* 24: 29-34.
34. Chitnis, C. E., and A. Sharma. 2008. Targeting the Plasmodium vivax Duffy-binding protein. *Trends Parasitol* 24: 29-34.
35. Miller, L. H., S. J. Mason, D. F. Clyde, and M. H. McGinniss. 1976. The resistance factor to *Plasmodium vivax* in blacks. The Duffy-blood-group genotype, FyFy. *New England Journal of Medicine* 295: 302-304.
36. Carter, R. 2003. Speculations on the origins of *Plasmodium vivax* malaria. *Trends in Parasitology* 19: 214-219.
37. Gething, P. W., I. R. Elyazar, C. L. Moyes, D. L. Smith, K. E. Battle, C. A. Guerra, A. P. Patil, A. J. Tatem, R. E. Howes, M. F. Myers, D. B. George, P. Horby, H. F. Wertheim, R. N. Price, I. Müeller, J. K. Baird, and S. I. Hay. 2012. A long neglected

world malaria map: *Plasmodium vivax* endemicity in 2010. *PLoS Neglected Tropical Diseases* 6: e1814.
38. Udomsangpetch, R., O. Kaneko, K. Chotivanich, and J. Sattabongkot. 2008. Cultivation of *Plasmodium vivax*. *Trends in Parasitology* 24: 85-88.
39. Miller, L. H., D. I. Baruch, K. Marsh, and O. K. Doumbo. 2002. The pathogenic basis of malaria. *Nature* 415: 673-679.
40. Miller, L. H., H. C. Ackerman, X.-z. Su, and T. E. Wellems. 2013. Malaria biology and disease pathogenesis: insights for new treatments. *Nature Medicine* 19: 156-167.
41. Turner, L., T. Lavstsen, S. S. Berger, C. W. Wang, J. E. V. Petersen, M. Avril, A. J. Brazier, J. Freeth, J. S. Jespersen, M. A. Nielsen, P. Magistrado, J. Lusingu, J. D. Smith, M. K. Higgins, and T. G. Theander. 2013. Severe malaria is associated with parasite binding to endothelial protein C receptor. *Nature* 498: 502-505.
42. Hunt, N. H., and G. E. Grau. 2003. Cytokines: accelerators and brakes in the pathogenesis of cerebral malaria. *Trends in Immunology* 24: 491-499.
43. Taylor, T. E., A. Borgstein, and M. E. Molyneux. 1993. Acid-base status in paediatric *Plasmodium falciparum* malaria. *Quarterly Journal of Medicine* 86: 99-109.
44. Jakeman, G., A. Saul, W. Hogarth, and W. Collins. 1999. Anaemia of acute malaria infections in non-immune patients primarily results from destruction of uninfected erythrocytes. *Parasitology* 119: 127-133.
45. Kwiatkowski, D. 1990. Tumour necrosis factor, fever and fatality in *falciparum* malaria. *Immunology Letters* 25: 213-216.
46. Felli, N., F. Pedini, A. Zeuner, E. Petrucci, U. Testa, C. Conticello, M. Biffoni, A. Di Cataldo, J. A. Winkles, C. Peschle, and R. De Maria. 2005. Multiple members of the TNF superfamily contribute to IFN-γ-mediated inhibition of erythropoiesis. *The Journal of Immunology* 175: 1464-1472.
47. Spottiswoode, N., P. E. Duffy, and H. Drakesmith. 2014. Iron, anemia and hepcidin in malaria. *Frontiers in Pharmacology* 5: 125.
48. Odhiambo, C. O., W. Otieno, C. Adhiambo, M. l. Odera, and J. A. Stoute. 2008. Increased deposition of C3b on red cells with low CR1 and CD55 in a malaria-endemic region of western Kenya: Implications for the development of severe anemia. *BMC Medicine* 6: 1-14.
49. Yoneto, T., S. Waki, T. Takai, Y.-i. Tagawa, Y. Iwakura, J. Mizuguchi, H. Nariuchi, and T. Yoshimoto. 2001. A critical role of Fc receptor-mediated antibody-dependent phagocytosis in the host resistance to blood-stage *Plasmodium berghei* XAT infection. *The Journal of Immunology* 166: 6236-6241.
50. Rotman, H. L., T. M. Daly, R. Clynes, and C. A. Long. 1998. Fc receptors are not required for antibody-mediated protection against lethal malaria challenge in a mouse model. *The Journal of Immunology* 161: 1908-1912.
51. Langhorne, J., P. Buffet, M. Galinski, M. Good, J. Harty, D. Leroy, M. M. Mota, E. Pasini, L. Renia, E. Riley, M. Stins, and P. Duffy. 2011. The relevance of non-human primate and rodent malaria models for humans. *Malaria Journal* 10: 23.
52. Ruwende, C., S. C. Khoo, R. W. Snow, S. N. R. Yates, D. Kwiatkowski, S. Gupta, P. Warn, C. E. M. Allsopp, S. C. Gilbert, N. Peschu, C. I. Newbold, B. M. Greenwood, K. Marsh, and A. V. S. Hill. 1995. Natural selection of hemi- and heterozygotes for G6PD deficiency in Africa by resistance to severe malaria. *Nature* 376: 246-249.
53. Cooke, G. S., and A. V. S. Hill. 2001. Genetics of susceptibitlity to human infectious disease. *Nature Reviews Genetics* 2: 967-977.
54. Allison, A. C. 1954. Protection afforded by sickle-cell trait against subtertian malarial infection. *British Medical Journal* 1: 290-294.

55. Pasvol, G., D. J. Weatherall, and R. J. M. Wilson. 1978. Cellular mechanism for the protective effect of haemoglobin S against *P. falciparum* malaria. *Nature* 274: 701-703.
56. Bruce, M. C., and K. P. Day. 2003. Cross-species regulation of *Plasmodium* parasitemia in semi-immune children from Papua New Guinea. *Trends in Parasitology* 19: 271-277.
57. Stevenson, M. M., and E. M. Riley. 2004. Innate immunity to malaria. *Nature Reviews Immunology* 4: 169-180.
58. Akira, S., S. Uematsu, and O. Takeuchi. 2006. Pathogen recognition and innate immunity. *Cell* 124: 783-801.
59. Kawai, T., and S. Akira. 2009. The roles of TLRs, RLRs and NLRs in pathogen recognition. *International Immunology* 21: 317-337.
60. Krishnegowda, G., A. M. Hajjar, J. Zhu, E. J. Douglass, S. Uematsu, S. Akira, A. S. Woods, and D. C. Gowda. 2005. Induction of proinflammatory responses in macrophages by the glycosylphosphatidylinositols of *Plasmodium falciparum*: cell signaling receptors, glycosylphosphatidylinositol (GPI) structural requirment, and regulation of GPI activity. *Journal of Biological Chemistry* 280: 8606-8616.
61. Leoratti, F. M. S., L. Farias, F. P. Alves, M. C. Suarez-Mútis, J. R. Coura, J. Kalil, E. P. Camargo, S. L. Moraes, and R. Ramasawmy. 2008. Variants in the Toll-like receptor signaling pathway and clinical outcomes of malaria. *Journal of Infectious Diseases* 198: 772-780.
62. Nebl, T., M. J. De Veer, and L. Schofield. 2005. Stimulation of innate immune responses by malarial glycosylphosphatidylinositol via pattern recognition receptors. *Parasitology* 130: S45-S62.
63. Parroche, P., F. N. Lauw, N. Goutagny, E. Latz, B. G. Monks, A. Visintin, K. A. Halmen, M. Lamphier, M. Olivier, D. C. Bartholomeu, R. T. Gazzinelli, and D. T. Golenbock. 2007. Malaria hemozoin is immunologically inert but radically enhances innate responses by presenting malaria DNA to Toll-like receptor 9. *Proceedings of the National Academy of Sciences* 104: 1919-1924.
64. Coban, C., K. J. Ishii, T. Kawai, H. Hemmi, S. Sato, S. Uematsu, M. Yamamoto, O. Takeuchi, S. Itagaki, N. Kumar, T. Horii, and S. Akira. 2005. Toll-like receptor 9 mediates innate immune activation by the malaria pigment hemozoin. *The Journal of Experimental Medicine* 201: 19-25.
65. Esposito, S., C. G. Molteni, A. Zampiero, E. Baggi, A. Lavizzari, M. Semino, C. Daleno, M. Groppo, A. Scala, L. Terranova, M. Miozzo, C. Pelucchi, and N. Principi. 2012. Role of polymorphisms of toll-like receptor (TLR) 4, TLR9, toll-interleukin 1 receptor domain containing adaptor protein (TIRAP) and FCGR2A genes in malaria susceptibility and severity in Burundian children. *Malaria Journal* 11: 10.1186.
66. Walport, M. J. 2001. Complement: first of two parts. *New England Journal of Medicine* 344: 1058-1066.
67. Carroll, M. C. 2004. The complement system in regulation of adaptive immunity. *Nature Immunology* 5: 981-986.
68. Ecker, E. E., L. Pillemer, and S. Seifter. 1943. Immunochemical studies on human serum: I. human complement and its components. *The Journal of Immunology* 47: 181-193.
69. Seifter, S., L. Pillemer, and E. E. Ecker. 1943. Immunochemical studies on human serum: II. *in vitro* studies on the stability of human complement and its components. *The Journal of Immunology* 47: 195-204.

70. Adam, C., M. Géniteau, M. Gougerot-Pocidalo, P. Verroust, J. Lebras, C. Gibert, and L. Morel-Maroger. 1981. Cryoglobulins, circulating immune complexes, and complement activation in cerebral malaria. *Infection and Immunity* 31: 530-535.
71. Roestenberg, M., M. McCall, T. E. Mollnes, M. van Deuren, T. Sprong, I. Klasen, C. C. Hermsen, R. W. Sauerwein, and A. van der Ven. 2007. Complement activation in experimental human malaria infection. *Transactions of the Royal Society of Tropical Medicine and Hygiene* 101: 643-649.
72. Wenisch, C., S. Spitzauer, K. Florris-Linau, H. Rumpold, S. Vannaphan, B. Parschalk, W. Graninger, and S. Looareesuwan. 1997. Complement activation in severe *Plasmodium falciparum* malaria. *Clinical Immunology and Immunopathology* 85: 166-171.
73. Healer, J., D. McGuinness, P. Hopcroft, S. Haley, R. Carter, and E. Riley. 1997. Complement-mediated lysis of *Plasmodium falciparum* gametes by malaria-immune human sera is associated with antibodies to the gamete surface antigen Pfs230. *Infection and Immunity* 65: 3017-3023.
74. Garred, P., M. A. Nielsen, J. A. L. Kurtzhals, R. Malhotra, H. O. Madsen, B. Q. Goka, B. D. Akanmori, R. B. Sim, and L. Hviid. 2003. Mannose-binding lectin is a disease modifier in clinical malaria and may function as opsonin for *Plasmodium falciparum*-infected erythrocytes. *Infection and Immunity* 71: 5245-5253.
75. Goka, B. Q., H. Kwarko, J. A. L. Kurtzhals, B. Gyan, E. Ofori-Adjei, S. A. Ohene, L. Hviid, B. D. Akanmori, and J. Neequaye. 2001. Complement binding to erythrocytes is associated with macrophage activation and reduced haemoglobin in *Plasmodium falciparum* malaria. *Transactions of the Royal Society of Tropical Medicine and Hygiene* 95: 545-549.
76. Helegbe, G. K., B. Q. Goka, J. A. Kurtzhals, M. M. Addae, E. Ollaga, J. K. Tetteh, D. Dodoo, M. F. Ofori, G. Obeng-Adjei, K. Hirayama, G. A. Awandare, and B. D. Akanmori. 2007. Complement activation in Ghanaian children with severe *Plasmodium falciparum* malaria. *Malaria Journal* 6: 165.
77. Stoute, J. A. 2005. Complement-regulatory proteins in severe malaria: too little or too much of a good thing? *Trends in Parasitology* 21: 218-223.
78. Cockburn, I. A., M. J. Mackinnon, A. O'Donnell, S. J. Allen, J. M. Moulds, M. Baisor, M. Bockarie, J. C. Reeder, and J. A. Rowe. 2004. A human complement receptor 1 polymorphism that reduces *Plasmodium falciparum* rosetting confers protection against severe malaria. *Proceedings of the National Academy of Sciences* 101: 272-277.
79. Stoute, J. A., A. O. Odindo, B. O. Owuor, E. K. Mibei, M. O. Opollo, and J. N. Waitumbi. 2003. Loss of red blood cell–complement regulatory proteins and increased levels of circulating immune complexes are associated with severe malarial anemia. *Journal of Infectious Diseases* 187: 522-525.
80. Waitumbi, J. N., B. Donvito, A. Kisserli, J. H. M. Cohen, and J. A. Stoute. 2004. Age-related changes in red blood cell complement regulatory proteins and susceptibility to severe malaria. *Journal of Infectious Diseases* 190: 1183-1191.
81. Wiesner, J., H. Jomaa, M. Wilhelm, H.-P. Tony, P. G. Kremsner, P. Horrocks, and M. Lanzer. 1997. Host cell factor CD59 restricts complement lysis of *Plasmodium falciparum*-infected erythrocytes. *European Journal of Immunology* 27: 2708-2713.
82. Simon, N., E. Lasonder, M. Scheuermayer, A. Kuehn, S. Tews, R. Fischer, Peter F. Zipfel, C. Skerka, and G. Pradel. 2013. Malaria parasites co-opt human factor H to prevent complement-mediated lysis in the mosquito midgut. *Cell Host & Microbe* 13: 29-41.

83. Wright, G. J. 2014. Identifying extracellular host-pathogen interactions using systematic protein interaction screens. In *Biology of Host-Parasite Interactions*. Gordon Research Conferences, Salve Regina University, Newport, RI.
84. Stone, K. D., C. Prussin, and D. D. Metcalfe. 2010. IgE, mast cells, basophils, and eosinophils. *Journal of Allergy and Clinical Immunology* 125: S73-S80.
85. Wedemeyer, J., M. Tsai, and S. J. Galli. 2000. Roles of mast cells and basophils in innate and acquired immunity. *Current Opinion in Immunology* 12: 624-631.
86. Urb, M., and D. C. Sheppard. 2012. The role of mast cells in the defence against pathogens. *PLoS Pathogens* 8: e1002619.
87. Smyth, M. J., E. Cretney, J. M. Kelly, J. A. Westwood, S. E. A. Street, H. Yagita, K. Takeda, S. L. H. v. Dommelen, M. A. Degli-Esposti, and Y. Hayakawa. 2005. Activation of NK cell cytotoxicity. *Molecular Immunology* 42: 501-510.
88. Mohan, K., P. Moulin, and M. M. Stevenson. 1997. Natural killer cell cytokine production, not cytotoxicity, contributes to resistance against blood-stage *Plasmodium chabaudi* AS infection. *The Journal of Immunology* 159: 4990-4998.
89. Artavanis-Tsakonas, K., and E. M. Riley. 2002. Innate immune response to malaria: rapid induction of IFN-γ from human NK cells by live *Plasmodium falciparum*-infected erythrocytes. *The Journal of Immunology* 169: 2956-2963.
90. Godfrey, D. I., S. Stankovic, and A. G. Baxter. 2010. Raising the NKT cell family. *Nature Immunology* 11: 197-206.
91. Vasan, S., and M. Tsuji. 2010. A double-edged sword: the role of NKT cells in malaria and HIV infection and immunity. *Seminars in Immunology* 22: 87-96.
92. Hansen, D. S., M.-A. Siomos, L. Buckingham, A. A. Scalzo, and L. Schofield. 2003. Regulation of murine cerebral malaria pathogenesis by CD1d-restricted NKT cells and the natural killer complex. *Immunity* 18: 391-402.
93. Yañez, D. M., J. Batchelder, H. C. van der Heyde, D. D. Manning, and W. P. Weidanz. 1999. γδ T-cell function in pathogenesis of cerebral malaria in mice infected with *Plasmodium berghei* ANKA. *Infection and Immunity* 67: 446-448.
94. Vantourout, P., and A. Hayday. 2013. Six-of-the-best: unique contributions of γδ T cells to immunology. *Nature Reviews Immunology* 13: 88-100.
95. Waterfall, M., A. Black, and E. Riley. 1998. $\gamma\delta^+$ T cells preferentially respond to live rather than killed malaria parasites. *Infection and Immunity* 66: 2393-2398.
96. Hviid, L., J. A. L. Kurtzhals, V. Adabayeri, S. Loizon, K. Kemp, B. Q. Goka, A. Lim, O. Mercereau-Puijalon, B. D. Akanmori, and C. Behr. 2001. Perturbation and proinflammatory type activation of $V\delta1^+$ γδ T cells in African children with *Plasmodium falciparum* malaria. *Infection and Immunity* 69: 3190-3196.
97. Elloso, M. M., H. C. van der Heyde, J. A. vande Waa, D. D. Manning, and W. P. Weidanz. 1994. Inhibition of *Plasmodium falciparum in vitro* by human gamma delta T cells. *The Journal of Immunology* 153: 1187-1194.
98. Serghides, L., T. G. Smith, S. N. Patel, and K. C. Kain. 2003. CD36 and malaria: friends or foes? *Trends in Parasitology* 19: 461-469.
99. McGilvray, I. D., L. Serghides, A. Kapus, O. D. Rotstein, and K. C. Kain. 2000. Nonopsonic monocyte/macrophage phagocytosis of *Plasmodium falciparum*–parasitized erythrocytes: a role for CD36 in malarial clearance. *Blood* 96: 3231-3240.
100. Luyendyk, J., O. R. Olivas, L. A. Ginger, and A. C. Avery. 2002. Antigen-presenting cell function during *Plasmodium yoelii* infection. *Infection and Immunity* 70: 2941-2949.
101. Quin, S. J., E. M. G. Seixas, C. A. Cross, M. Berg, V. Lindo, B. Stockinger, and J. Langhorne. 2001. Low CD4+ T cell responses to the C-terminal region of the malaria

merozoite surface protein-1 may be attributed to processing within distinct MHC class II pathways. *European Journal of Immunology* 31: 72-81.
102. Banchereau, J., F. Briere, C. Caux, J. Davoust, S. Lebecque, Y.-J. Liu, B. Pulendran, and K. Palucka. 2000. Immunobiology of dendritic cells. *Annual Review of Immunology* 18: 767-811.
103. Qi, H., J. G. Egen, A. Y. C. Huang, and R. N. Germain. 2006. Extrafollicular activation of lymph node B cells by antigen-bearing dendritic cells. *Science* 312: 1672-1676.
104. Wykes, M. N., and M. F. Good. 2008. What really happens to dendritic cells during malaria? *Nature Reviews Microbiology* 6: 864-870.
105. Coban, C., K. J. Ishii, D. J. Sullivan, and N. Kumar. 2002. Purified malaria pigment (hemozoin) enhances dendritic cell maturation and modulates the isotype of antibodies induced by a DNA vaccine. *Infection and Immunity* 70: 3939-3943.
106. Urban, B. C., D. J. P. Ferguson, A. Pain, N. Willcox, M. Plebanski, J. M. Austyn, and D. J. Roberts. 1999. *Plasmodium falciparum*-infected erythrocytes modulate the maturation of dendritic cells. *Nature* 400: 73-77.
107. Nathan, C. 2006. Neutrophils and immunity: challenges and opportunities. *Nature Reviews Immunology* 6: 173-182.
108. Savill, J., and C. Haslett. 1995. Granulocyte clearance by apoptosis in the resolution of inflammation. *Seminars in Cell Biology* 6: 385-393.
109. Borregaard, N. 2010. Neutrophils, from marrow to microbes. *Immunity* 33: 657-670.
110. Amulic, B., C. Cazalet, G. L. Hayes, K. D. Metzler, and A. Zychlinsky. 2012. Neutrophil function: from mechanisms to disease. *Annual Review of Immunology* 30: 459-489.
111. Adlerova, L., A. Bartoskova, and M. Faldyna. 2008. Lactoferrin: a review. *Veterinarni Medicina* 53: 457-468.
112. Hibbs, M. S., and D. F. Bainton. 1989. Human neutrophil gelatinase is a component of specific granules. *The Journal of Clinical Investigation* 84: 1395-1402.
113. Robinson, J. M. 2008. Reactive oxygen species in phagocytic leukocytes. *Histochemistry and Cell Biology* 130: 281-297.
114. Sheppard, F. R., M. R. Kelher, E. E. Moore, N. J. D. McLaughlin, A. Banerjee, and C. C. Silliman. 2005. Structural organization of the neutrophil NADPH oxidase: phosphorylation and translocation during priming and activation. *Journal of Leukocyte Biology* 78: 1025-1042.
115. Fang, F. C. 2011. Antimicrobial actions of reactive oxygen species. *mBio* 2: e00141-00111.
116. Slauch, J. M. 2011. How does the oxidative burst of macrophages kill bacteria? Still an open question. *Molecular Microbiology* 80: 580-583.
117. Fuchs, T. A., U. Abed, C. Goosmann, R. Hurwitz, I. Schulze, V. Wahn, Y. Weinrauch, V. Brinkmann, and A. Zychlinsky. 2007. Novel cell death program leads to neutrophil extracellular traps. *Journal of Cell Biology* 176: 231-241.
118. Brinkmann, V., U. Reichard, C. Goosmann, B. Fauler, Y. Uhlemann, D. S. Weiss, Y. Weinrauch, and A. Zychlinsky. 2004. Neutrophil extracellular traps kill bacteria. *Science* 303: 1532-1535.
119. Amulic, B., and G. Hayes. 2011. Neutrophil extracellular traps. *Current Biology* 21: R297-R298.
120. Pierrot, C., E. Adam, D. Hot, S. Lafitte, M. Capron, J. D. George, and J. Khalife. 2007. Contribution of T cells and neutrophils in protection of young susceptible rats from fatal experimental malaria. *The Journal of Immunology* 178: 1713-1722.

121. Trubowitz, S., and B. Masek. 1968. *Plasmodium falciparum*: Phagocytosis by polymorphonuclear leukocytes. *Science* 162: 273-274.
122. Laing, A. B., and M. Wilson. 1972. Remarkable polymorphonuclear phagocytosis of *P. falciparum*. *Transactions of the Royal Society of Tropical Medicine and Hygiene* 66: 523.
123. Brown, J., and M. Smalley. 1981. Inhibition of the in vitro growth of *Plasmodium falciparum* by human polymorphonuclear neutrophil leucocytes. *Clinical and Experimental Immunology* 46: 106-109.
124. Celada, A., A. Cruchaud, and L. H. Perrin. 1983. Phagocytosis of *Plasmodium falciparum*-parasitized erythrocytes by human polymorphonuclear leukocytes. *The Journal of Parasitology* 69: 49-53.
125. Healer, J., A. Graszynski, and E. Riley. 1999. Phagocytosis does not play a major role in naturally acquired transmission-blocking immunity to *Plasmodium falciparum* malaria. *Infection and Immunity* 67: 2334-2339.
126. Wozencraft, A., H. Dockrell, J. Taverne, G. Targett, and J. Playfair. 1984. Killing of human malaria parasites by macrophage secretory products. *Infection and Immunity* 43: 664-669.
127. Nnalue, N. A., and M. J. Friedman. 1988. Evidence for a neutrophil-mediated protective response in malaria. *Parasite Immunology* 10: 47-58.
128. Iwasaki, A., and R. Medzhitov. 2010. Regulation of adaptive immunity by the innate immune system. *Science* 327: 291-295.
129. Chapman, H. A. 2006. Endosomal proteases in antigen presentation. *Current Opinion in Immunology* 18: 78-84.
130. Neefjes, J., M. L. M. Jongsma, P. Paul, and O. Bakke. 2011. Towards a systems understanding of MHC class I and MHC class II antigen presentation. *Nature Reviews Immunology* 11: 823-836.
131. O'Garra, A., and N. Arai. 2000. The molecular basis of T helper 1 and T helper 2 cell differentiation. *Trends in Cell Biology* 10: 542-550.
132. Szabo, S. J., B. M. Sullivan, S. L. Peng, and L. H. Glimcher. 2003. Molecular mechanisms regulating Th1 immune responses. *Annual Review of Immunology* 21: 713-758.
133. Stevens, T. L., A. Bossie, V. M. Sanders, R. Fernandez-Botran, R. L. Coffman, T. R. Mosmann, and E. S. Vitetta. 1988. Regulation of antibody isotype secretion by subsets of antigen-specific helper T cells. *Nature* 334: 255-258.
134. Fossiez, F., O. Djossou, P. Chomarat, L. Flores-Romo, S. Ait-Yahia, C. Maat, J. J. Pin, P. Garrone, E. Garcia, S. Saeland, D. Blanchard, C. Gaillard, B. Das Mahapatra, E. Rouvier, P. Golstein, J. Banchereau, and S. Lebecque. 1996. T cell interleukin-17 induces stromal cells to produce proinflammatory and hematopoietic cytokines. *The Journal of Experimental Medicine* 183: 2593-2603.
135. Kolls, J. K., and A. Lindén. 2004. Interleukin-17 family members and inflammation. *Immunity* 21: 467-476.
136. Huang, W., L. Na, P. L. Fidel, and P. Schwarzenberger. 2004. Requirement of interleukin-17A for systemic anti-*Candida albicans* host defense in mice. *Journal of Infectious Diseases* 190: 624-631.
137. Crotty, S. 2011. Follicular helper CD4 T cells (T_{FH}). *Annual Review of Immunology* 29: 621-663.
138. Sakaguchi, S., T. Yamaguchi, T. Nomura, and M. Ono. 2008. Regulatory T cells and immune tolerance. *Cell* 133: 775-787.
139. Jensen, P. E. 2007. Recent advances in antigen processing and presentation. *Nature Immunology* 8: 1041-1048.

140. Amigorena, S., and A. Savina. 2010. Intracellular mechanisms of antigen cross presentation in dendritic cells. *Current Opinion in Immunology* 22: 109-117.
141. Wong, P., and E. G. Pamer. 2003. CD8 T cell responses to infectious pathogens. *Annual Review of Immunology* 21: 29-70.
142. van der Heyde, H. C., D. D. Manning, D. C. Roopenian, and W. P. Weidanz. 1993. Resolution of blood-stage malarial infections in $CD8^+$ cell-deficient β_2-$m^{0/0}$ mice. *The Journal of Immunology* 151: 3187-3191.
143. Stevenson, M., and M. Tam. 1993. Differential induction of helper T cell subsets during blood-stage *Plasmodium chabaudi* AS infection in resistant and susceptible mice. *Clinical and Experimental Immunology* 92: 77-83.
144. Sheehy, S. H., C. J. A. Duncan, S. C. Elias, P. Choudhary, S. Biswas, F. D. Halstead, K. A. Collins, N. J. Edwards, A. D. Douglas, N. A. Anagnostou, K. J. Ewer, T. Havelock, T. Mahungu, C. M. Bliss, K. Miura, I. D. Poulton, P. J. Lillie, R. D. Antrobus, E. Berrie, S. Moyle, K. Gantlett, S. Colloca, R. Cortese, C. A. Long, R. E. Sinden, S. C. Gilbert, A. M. Lawrie, T. Doherty, S. N. Faust, A. Nicosia, A. V. Hill, and S. J. Draper. 2012. ChAd63-MVA–vectored blood-stage malaria vaccines targeting MSP1 and AMA1: assessment of efficacy against mosquito bite challenge in humans. *Molecular Therapy* 20: 2355-2368.
145. Bijker, E. M., G. J. H. Bastiaens, A. C. Teirlinck, G.-J. van Gemert, W. Graumans, M. van de Vegte-Bolmer, R. Siebelink-Stoter, T. Arens, K. Teelen, W. Nahrendorf, E. J. Remarque, W. Roeffen, A. Jansens, D. Zimmerman, M. Vos, B. C. L. van Schaijk, J. Wiersma, A. J. A. M. van der Ven, Q. de Mast, L. van Lieshout, J. J. Verweij, C. C. Hermsen, A. Scholzen, and R. W. Sauerwein. 2013. Protection against malaria after immunization by chloroquine prophylaxis and sporozoites is mediated by preerythrocytic immunity. *Proceedings of the National Academy of Sciences* 110: 7862-7867.
146. Ewer, K. J., G. A. O'Hara, C. J. A. Duncan, K. A. Collins, S. H. Sheehy, A. Reyes-Sandoval, A. L. Goodman, N. J. Edwards, S. C. Elias, F. D. Halstead, R. J. Longley, R. Rowland, I. D. Poulton, S. J. Draper, A. M. Blagborough, E. Berrie, S. Moyle, N. Williams, L. Siani, A. Folgori, S. Colloca, R. E. Sinden, A. M. Lawrie, R. Cortese, S. C. Gilbert, A. Nicosia, and A. V. S. Hill. 2013. Protective CD8+ T-cell immunity to human malaria induced by chimpanzee adenovirus-MVA immunisation. *Nature Communications* 4: 2836.
147. Weiss, W. R., M. Sedegah, R. L. Beaudoin, L. H. Miller, and M. F. Good. 1988. $CD8^+$ T cells (cytotoxic/suppressors) are required for protection in mice immunized with malaria sporozoites. *Proceedings of the National Academy of Sciences* 85: 573-576.
148. Schofield, L., J. Villaquiran, A. Ferreira, H. Schellekens, R. Nussenzweig, and V. Nussenzweig. 1987. γ interferon, $CD8^+$ T cells and antibodies required for immunity to malaria sporozoites. *Nature* 330: 664-666.
149. Carvalho, L. H., G.-i. Sano, J. C. R. Hafalla, A. Morrot, M. A. C. de Lafaille, and F. Zavala. 2002. IL-4-secreting $CD4^+$ T cells are crucial to the development of $CD8^+$ T-cell responses against malaria liver stages. *Nature Medicine* 8: 166-170.
150. Schofield, L., A. Ferreira, R. Altszuler, V. Nussenzweig, and R. S. Nussenzweig. 1987. Interferon-gamma inhibits the intrahepatocytic development of malaria parasites in vitro. *The Journal of Immunology* 139: 2020-2025.
151. Doolan, D. L., and S. L. Hoffman. 1999. IL-12 and NK cells are required for antigen-specific adaptive immunity against malaria initiated by $CD8^+$ T cells in the *Plasmodium yoelii* model. *Journal of Immunology* 163: 884-892.

152. MacLennan, I. C. M., K.-M. Toellner, A. F. Cunningham, K. Serre, D. M. Y. Sze, E. Zúñiga, M. C. Cook, and C. G. Vinuesa. 2003. Extrafollicular antibody responses. *Immunological Reviews* 194: 8-18.
153. MacLennan, I. C. M. 1994. Germinal centers. *Annual Review of Immunology* 12: 117-139.
154. Huber, R., J. Deisenhofer, P. M. Colman, M. Matsushima, and W. Palm. 1976. Crystallographic structure studies of an IgG molecule and an Fc fragment. *Nature* 264: 415-420.
155. Woof, J. M., and D. R. Burton. 2004. Human antibody-Fc receptor interactions illuminated by crystal structures. *Nature Reviews Immunology* 4: 89-99.
156. Nimmerjahn, F., and J. V. Ravetch. 2008. Fcγ receptors as regulators of immune responses. *Nature Reviews Immunology* 8: 34-47.
157. Schroeder Jr, H. W., and L. Cavacini. 2010. Structure and function of immunoglobulins. *Journal of Allergy and Clinical Immunology* 125: S41-S52.
158. John, C. C., A. J. Tande, A. M. Moormann, P. O. Sumba, D. E. Lanar, X. M. Min, and J. W. Kazura. 2008. Antibodies to pre-erythrocytic *Plasmodium falciparum* antigens and risk of clinical malaria in Kenyan children. *Journal of Infectious Diseases* 197: 519-526.
159. Cohen, S., I. A. McGregor, and S. Carrington. 1961. Gamma-globulin and acquired immunity to human malaria. *Nature* 192: 733-737.
160. Sabchareon, A., T. Burnouf, D. Ouattara, P. Attanath, H. Bouharoun-Tayoun, P. Chantavanich, C. Foucault, T. Chongsuphajaisiddhi, and P. Druilhe. 1991. Parasitologic and clinical human response to immunoglobulin administration in *falciparum* malaria. *The American Journal of Tropical Medicine and Hygiene* 45: 297-308.
161. Polley, S. D., D. J. Conway, D. R. Cavanagh, J. S. McBride, B. S. Lowe, T. N. Williams, T. W. Mwangi, and K. Marsh. 2006. High levels of serum antibodies to merozoite surface protein 2 of *Plasmodium falciparum* are associated with reduced risk of clinical malaria in coastal Kenya. *Vaccine* 24: 4233-4246.
162. Polley, S. D., T. Mwangi, C. H. Kocken, A. W. Thomas, S. Dutta, D. E. Lanar, E. Remarque, A. Ross, T. N. Williams, G. Mwambingu, B. Lowe, D. J. Conway, and K. Marsh. 2004. Human antibodies to recombinant protein constructs of *Plasmodium falciparum* apical membrane antigen 1 (AMA1) and their associations with protection from malaria. *Vaccine* 23: 718-728.
163. Bull, P. C., B. S. Lowe, M. Kortok, C. S. Molyneux, C. I. Newbold, and K. Marsh. 1998. Parasite antigens on the infected red cell surface are targets for naturally acquired immunity to malaria. *Nature Medicine* 4: 358-360.
164. Fowkes, F. J. I., J. S. Richards, J. A. Simpson, and J. G. Beeson. 2010. The relationship between anti-merozoite antibodies and incidence of *Plasmodium falciparum* malaria: a systematic review and meta-analysis. *PLoS Medicine* 7: e1000218.
165. Giha, H. A., T. Staalsoe, D. Dodoo, C. Roper, G. M. Satti, D. E. Arnot, L. Hviid, and T. G. Theander. 2000. Antibodies to variable *Plasmodium falciparum*-infected erythrocyte surface antigens are associated with protection from novel malaria infections. *Immunology Letters* 71: 117-126.
166. Mackintosh, C. L., T. Mwangi, S. M. Kinyanjui, M. Mosobo, R. Pinches, T. N. Williams, C. I. Newbold, and K. Marsh. 2008. Failure to respond to the surface of *Plasmodium falciparum* infected erythrocytes predicts susceptibility to clinical malaria amongst African children. *International Journal for Parasitology* 38: 1445-1454.

167. Chan, J.-A., K. B. Howell, L. Reiling, R. Ataide, C. L. Mackintosh, F. J. I. Fowkes, M. Petter, J. M. Chesson, C. Langer, G. M. Warimwe, M. F. Duffy, S. J. Rogerson, P. C. Bull, A. F. Cowman, K. Marsh, and J. G. Beeson. 2012. Targets of antibodies against *Plasmodium falciparum*–infected erythrocytes in malaria immunity. *The Journal of Clinical Investigation* 122: 3227-3238.
168. Dodoo, D., T. Staalsoe, H. Giha, J. A. L. Kurtzhals, B. D. Akanmori, K. Koram, S. Dunyo, F. K. Nkrumah, L. Hviid, and T. G. Theander. 2001. Antibodies to variant antigens on the surfaces of infected erythrocytes are associated with protection from malaria in Ghanaian children. *Infection and Immunity* 69: 3713-3718.
169. Biggs, B. A., L. Gooze, K. Wycherley, W. Wollish, B. Southwell, J. H. Leech, and G. V. Brown. 1991. Antigenic variation in *Plasmodium falciparum*. *Proceedings of the National Academy of Sciences USA* 88: 9171-9174.
170. Brown, K. N., and I. N. Brown. 1965. Immunity to malaria: antigenic variation in chronic infections of *Plasmodium knowlesi*. *Nature* 208: 1286-1288.
171. Egan, A. F., J. Morris, G. Barnish, S. Allen, B. M. Greenwood, D. C. Kaslow, A. A. Holder, and E. M. Riley. 1996. Clinical immunity to *Plasmodium falciparum* malaria is associated with serum antibodies to the 19-kDa C-terminal fragment of the merozoite surface antigen, PfMSP-l. *Journal of Infectious Diseases* 173: 765-768.
172. Al-Yaman, F., B. Genton, K. J. Kramer, S. P. Chang, G. S. Hui, M. Baisor, and M. P. Alpers. 1996. Assessment of the role of naturally acquired antibody levels to *Plasmodium falciparum* merozoite surface protein-1 in protecting Papua New Guinean children from malaria morbidity. *The American Journal of Tropical Medicine and Hygiene* 54: 443-448.
173. Dodoo, D., A. Aikins, K. A. Kusi, H. Lamptey, E. Remarque, P. Milligan, S. Bosomprah, R. Chilengi, Y. D. Osei, B. D. Akanmori, and M. Theisen. 2008. Cohort study of the association of antibody levels to AMA1, MSP119, MSP3 and GLURP with protection from clinical malaria in Ghanaian children. *Malaria Journal* 7: 142.
174. Murungi, L. M., G. Kamuyu, B. Lowe, P. Bejon, M. Theisen, S. M. Kinyanjui, K. Marsh, and F. H. Osier. 2013. A threshold concentration of anti-merozoite antibodies is required for protection from clinical episodes of malaria. *Vaccine* 31: 3936-3942.
175. Osier, F. H., M. J. Mackinnon, C. Crosnier, G. Fegan, G. Kamuyu, M. Wanaguru, E. Ogada, B. McDade, J. C. Rayner, G. J. Wright, and K. Marsh. 2014. New antigens for a multicomponent blood-stage malaria vaccine. *Science Translational Medicine* 6: 247ra102.
176. McCallum, F. J., K. E. M. Persson, C. K. Mugyenyi, F. J. I. Fowkes, J. A. Simpson, J. S. Richards, T. N. Williams, K. Marsh, and J. G. Beeson. 2008. Acquisition of growth-inhibitory antibodies against blood-stage *Plasmodium falciparum*. *PLoS ONE* 3: e3571.
177. Perraut, R., L. Marrama, B. Diouf, C. Sokhna, A. Tall, P. Nabeth, J.-F. Trape, S. Longacre, and O. Mercereau-Puijalon. 2005. Antibodies to the conserved C-terminal domain of the *Plasmodium falciparum* merozoite surface protein 1 and to the merozoite extract and their relationship with *in vitro* inhibitory antibodies and protection against clinical malaria in a Senegalese village. *Journal of Infectious Diseases* 191: 264-271.
178. Bolad, A., I. Nebie, N. Cuzin-Ouattara, A. Traore, F. Esposito, and K. Berzins. 2003. Antibody-mediated *in vitro* growth inhibition of field isolates of *Plasmodium falciparum* from asymptomatic children in Burkina Faso. *American Journal of Tropical Medicine and Hygiene* 68: 728-733.

179. Duncan, C., A. V. S. Hill, and R. Ellis. 2012. Can growth inhibition assays (GIA) predict blood-stage malaria vaccine efficacy? *Human Vaccines & Immunotherapeutics* 8: 706-714.
180. Bouharoun-Tayoun, H., P. Attanath, A. Sabchareon, T. Chongsuphajaisiddhi, and P. Druilhe. 1990. Antibodies that protect humans against *Plasmodium falciparum* blood stages do not on their own inhibit parasite growth and invasion *in vitro*, but act in cooperation with monocytes. *The Journal of Experimental Medicine* 172: 1633-1641.
181. Joos, C., L. Marrama, H. E. J. Polson, S. Corre, A. M. Diatta, B. Diouf, J. F. Trape, A. Tall, S. Longacre, and R. Perraut. 2010. Clinical protection from *falciparum* malaria correlates with neutrophil respiratory bursts induced by merozoites opsonized with human serum antibodies. *PLoS ONE* 5: e9871.
182. Berken, A., and B. Benacerraf. 1966. Properties of antibodies cytophilic for macrophages. *The Journal of Experimental Medicine* 123: 119-144.
183. Roopenian, D. C., and S. Akilesh. 2007. FcRn: the neonatal Fc receptor comes of age. *Nature Reviews Immunology* 7: 715-725.
184. Pincetic, A., S. Bournazos, D. J. DiLillo, J. Maamary, T. T. Wang, R. Dahan, B.-M. Fiebiger, and J. V. Ravetch. 2014. Type I and type II Fc receptors regulate innate and adaptive immunity. *Nature Immunology* 15: 707-716.
185. Daëron, M. 1997. Fc receptor biology. *Annual Review of Immunology* 15: 203-234.
186. Ravetch, J. V., and F. Nimmerjahn. 2013. Fc receptors and their role in immune regulation and inflammation. In *Fundamental Immunology*, 7th ed. W. E. Paul, ed. Lippincott Williams and Wilkins, Philadelphia. 583-600.
187. Paetz, A., M. Sack, T. Thepen, M. K. Tur, D. Bruell, R. Finnern, R. Fischer, and S. Barth. 2005. Recombinant soluble human Fcγ receptor I with picomolar affinity for immunoglobulin G. *Biochemical and Biophysical Research Communications* 338: 1811-1817.
188. Allen, J. M., and B. Seed. 1989. Isolation and expression of functional high-affinity Fc receptor complementary DNAs. *Science* 243: 378-381.
189. Kato, K., W. H. Fridman, Y. Arata, and C. Sautès-Fridman. 2000. A conformational change in the Fc precludes the binding of two Fcγ receptor molecules to one IgG. *Immunology Today* 21: 310-312.
190. Sondermann, P., R. Huber, V. Oosthuizen, and U. Jacob. 2000. The 3.2-Å crystal structure of the human IgG1 Fc fragment-FcγRIII complex. *Nature* 406: 267-273.
191. Kiefer, F., J. Brumell, N. Al-Alawi, S. Latour, A. Cheng, A. Veillette, S. Grinstein, and T. Pawson. 1998. The Syk protein tyrosine kinase is essential for Fcγ receptor signaling in macrophages and neutrophils. *Molecular and Cellular Biology* 18: 4209-4220.
192. Yeung, T., B. Ozdamar, P. Paroutis, and S. Grinstein. 2006. Lipid metabolism and dynamics during phagocytosis. *Current Opinion in Cell Biology* 18: 429-437.
193. Katsumata, O., M. Hara-Yokoyama, C. Sautès-Fridman, Y. Nagatsuka, T. Katada, Y. Hirabayashi, K. Shimizu, J. Fujita-Yoshigaki, H. Sugiya, and S. Furuyama. 2001. Association of FcγRII with low-density detergent-resistant membranes is important for cross-linking-dependent initiation of the tyrosine phosphorylation pathway and superoxide generation. *The Journal of Immunology* 167: 5814-5823.
194. Tian, W., X. J. Li, N. D. Stull, W. Ming, C. I. Suh, S. A. Bissonnette, M. B. Yaffe, S. Grinstein, S. J. Atkinson, and M. C. Dinauer. 2008. FcγR-stimulated activation of the NADPH oxidase: phosphoinositide-binding protein $p40^{phox}$ regulates NADPH oxidase activity after enzyme assembly on the phagosome. *Blood* 112: 3867-3877.
195. Anderson, K. E., T. A. Chessa, K. Davidson, R. B. Henderson, S. Walker, T. Tolmachova, K. Grys, O. Rausch, M. C. Seabra, V. L. Tybulewicz, L. R. Stephens,

and P. T. Hawkins. 2010. PtdIns3P and Rac direct the assembly of the NADPH oxidase on a novel, pre-phagosomal compartment during FcR-mediated phagocytosis in primary mouse neutrophils. *Blood* 116: 4978-4989.

196. Ono, M., S. Bolland, P. Tempst, and J. V. Ravetch. 1996. Role of the inositol phosphatase SHIP in negative regulation of the immune system by the receptor FcγRIIB. *Nature* 383: 263-266.
197. Koncz, G., and J. Gergely. 1996. Human type II Fcγ receptors inhibit B cell activation by interacting with the $p21^{ras}$-dependent pathway. *Journal of Biological Chemistry* 271: 30499-30504.
198. Pearse, R. N., T. Kawabe, S. Bolland, R. Guinamard, T. Kurosaki, and J. V. Ravetch. 1999. SHIP recruitment attenuates FcγRIIB-induced B cell apoptosis. *Immunity* 10: 753-760.
199. Nimmerjahn, F., and J. V. Ravetch. 2005. Divergent immunoglobulin G subclass activity through selective Fc receptor binding. *Science* 310: 1510-1512.
200. Woof, J. M. 2005. Tipping the scales toward more effective antibodies. *Science* 310: 1442-1443.
201. Wilson, T. J., A. Fuchs, and M. Colonna. 2012. Cutting edge: human FcRL4 and FcRL5 are receptors for IgA and IgG. *Journal of Immunology* 188: 4741-4745.
202. McIntosh, R. S., J. Shi, R. M. Jennings, J. C. Chappel, T. F. de Koning-Ward, T. Smith, J. Green, M. van Egmond, J. H. W. Leusen, M. Lazarou, J. van de Winkel, T. S. Jones, B. S. Crabb, A. A. Holder, and R. J. Pleass. 2007. The importance of human FcγRI in mediating protection to malaria. *PLoS Pathogens* 3: e72.
203. Clatworthy, M. R., L. Willcocks, B. Urban, J. Langhorne, T. N. Williams, N. Peshu, N. A. Watkins, R. A. Floto, and K. G. C. Smith. 2007. Systemic lupus erythematosus-associated defects in the inhibitory receptor FcγRIIb reduce susceptibility to malaria. *Proceedings of the National Academy of Sciences* 104: 7169-7174.
204. Shi, J., R. McIntosh, J. Adame-Gallegos, P. Dehal, M. van Egmond, J. van de Winkel, S. Draper, E. Forbes, P. Corran, A. Holder, J. M. Woof, and R. J. Pleass. 2011. The generation and evaluation of recombinant human IgA specific for *Plasmodium falciparum* merozoite surface protein 1-19 ($PfMSP1_{19}$). *BMC biotechnology* 11: 77-94.
205. Shi, Y. P., B. L. Nahlen, S. Kariuki, K. B. Urdahl, P. D. McElroy, J. M. Roberts, and A. A. Lal. 2001. Fcγ receptor IIa (CD32) polymorphism is associated with protection of infants against high-density *Plasmodium falciparum* infection. VII. Asembo Bay Cohort Project. *Journal of Infectious Diseases* 184: 107-111.
206. Schuldt, K., C. Esser, J. Evans, J. May, C. Timmann, C. Ehmen, W. Loag, D. Ansong, A. Ziegler, T. Agbenyega, C. G. Meyer, and R. D. Horstmann. 2009. FCGR2A functional genetic variant associated with susceptibility to severe malarial anemia in Ghanaian children. *Journal of Medical Genetics* 47: 471-475.
207. Nasr, A., N. C. Iriemenam, M. Troye-Blomberg, H. A. Giha, H. A. Balogun, O. F. Osman, S. M. Montgomery, G. ElGhazali, and K. Berzins. 2007. Fc gamma receptor IIa (CD32) polymorphism and antibody responses to asexual blood-stage antigens of *Plasmodium falciparum* malaria in Sudanese patients. *Scandinavian Journal of Immunology* 66: 87-96.
208. Cooke, G. S., C. Aucan, A. J. Walley, S. Segal, B. M. Greenwood, D. P. Kwiatkowski, and A. V. Hill. 2003. Association of Fcγ receptor Ila (CD32) polymorphism with severe malaria in West Africa. *American Journal of Tropical Medicine and Hygiene* 69: 565-568.
209. Ouma, C., G. Davenport, S. Garcia, P. Kempaiah, A. Chaudhary, T. Were, S. Anyona, E. Raballah, S. Konah, J. Hittner, J. Vulule, J. Ong'echa, and D. Perkins. 2011.

Functional haplotypes of Fc gamma (Fcγ) receptor (FcγRIIA and FcγRIIIB) predict risk to repeated episodes of severe malarial anemia and mortality in Kenyan children. *Human Genetics*: 1-11.

210. Ouma, C., C. C. Keller, D. A. Opondo, T. Were, R. O. Otieno, M. F. Otieno, A. S. Orago, J. M. Ong'Echa, J. M. Vulule, R. E. Ferrell, and D. J. Perkins. 2006. Association of Fcγ receptor IIA (CD32) polymorphism with malarial anemia and high-density parasitemia in infants and young children. *American Journal of Tropical Medicine and Hygiene* 74: 573-577.
211. Omi, K., J. Ohashi, J. Patarapotikul, H. Hananantachai, I. Naka, S. Looareesuwan, and K. Tokunaga. 2002. Fcγ receptor IIA and IIIB polymorphisms are associated with susceptibility to cerebral malaria. *Parasitology International* 51: 361-366.
212. Jenner, E. 1798. *An inquiry into the causes and effects of the variolae vaccinae, a disease discovered in some of the western counties of England, particularly Gloucestershire, and known by the name of the cow pox*. Printed for the author, by Sampson Low, London.
213. Strassburg, M. A. 1982. The global eradication of smallpox. *American Journal of Infection Control* 10: 53-59.
214. World Organisation for Animal Health. 2011. Declaration of global eradication of rinderpest and implementation of follow-up measures to maintain world freedom from rinderpest In *World Assembly of Delegates of the OIE*, 79th ed. World Organisation for Animal Health, Paris. 1-4.
215. U.S. Food and Drug Administration. 2014. Complete list of vaccines licensed for immunization and distribution in the US. Available at: http://www.fda.gov/BiologicsBloodVaccines/Vaccines/ApprovedProducts/UCM093833.
216. Seder, R. A., L.-J. Chang, M. E. Enama, K. L. Zephir, U. N. Sarwar, I. J. Gordon, L. A. Holman, E. R. James, P. F. Billingsley, A. Gunasekera, A. Richman, S. Chakravarty, A. Manoj, S. Velmurugan, M. Li, A. J. Ruben, T. Li, A. G. Eappen, R. E. Stafford, S. H. Plummer, C. S. Hendel, L. Novik, P. J. M. Costner, F. H. Mendoza, J. G. Saunders, M. C. Nason, J. H. Richardson, J. Murphy, S. A. Davidson, T. L. Richie, M. Sedegah, A. Sutamihardja, G. A. Fahle, K. E. Lyke, M. B. Laurens, M. Roederer, K. Tewari, J. E. Epstein, B. K. L. Sim, J. E. Ledgerwood, B. S. Graham, S. L. Hoffman, and t. V. S. Team. 2013. Protection against malaria by intravenous immunization with a nonreplicating sporozoite vaccine. *Science* 341: 1359-1365.
217. McAleer, W. J., E. B. Buynak, R. Z. Maigetter, D. E. Wampler, W. J. Miller, and M. R. Hilleman. 1984. Human hepatitis B vaccine from recombinant yeast. *Nature* 307: 178-180.
218. Asante, K. P., S. Abdulla, S. Agnandji, J. Lyimo, J. Vekemans, S. Soulanoudjingar, R. Owusu, M. Shomari, A. Leach, E. Jongert, N. Salim, J. F. Fernandes, D. Dosoo, M. Chikawe, S. Issifou, K. Osei-Kwakye, M. Lievens, M. Paricek, T. Moller, S. Apanga, G. Mwangoka, M. C. Dubois, T. Madi, E. Kwara, R. Minja, A. B. Hounkpatin, O. Boahen, K. Kayan, G. Adjei, D. Chandramohan, T. Carter, P. Vansadia, M. Sillman, B. Savarese, C. Loucq, D. Lapierre, B. Greenwood, J. Cohen, P. Kremsner, S. Owusu-Agyei, M. Tanner, and B. Lell. 2011. Safety and efficacy of the RTS,S/AS01E candidate malaria vaccine given with expanded-programme-on-immunisation vaccines: 19 month follow-up of a randomised, open-label, phase 2 trial. *Lancet Infectious Diseases* 11: 741-749.
219. The RTSS Clinical Trails Partnership. 2012. A phase 3 trial of RTS,S/AS01 malaria vaccine in African infants. *New England Journal of Medicine* 367: 2284-2295.

220. Sheehy, S. H., C. J. A. Duncan, S. C. Elias, K. A. Collins, K. J. Ewer, A. J. Spencer, A. R. Williams, F. D. Halstead, S. E. Moretz, K. Miura, C. Epp, M. D. J. Dicks, I. D. Poulton, A. M. Lawrie, E. Berrie, S. Moyle, C. A. Long, S. Colloca, R. Cortese, S. C. Gilbert, A. Nicosia, A. V. S. Hill, and S. J. Draper. 2011. Phase Ia clinical evaluation of the *Plasmodium falciparum* blood-stage antigen MSP1 in ChAd63 and MVA vaccine vectors. *Molecular Therapy* 19: 2269-2276.
221. Tatsis, N., and H. C. J. Ertl. 2004. Adenoviruses as vaccine vectors. *Molecular Therapy* 10: 616-629.
222. Nwanegbo, E., E. Vardas, W. Gao, H. Whittle, H. Sun, D. Rowe, P. D. Robbins, and A. Gambotto. 2004. Prevalence of neutralizing antibodies to adenoviral serotypes 5 and 35 in the adult populations of The Gambia, South Africa, and the United States. *Clinical and Diagnostic Laboratory Immunology* 11: 351-357.
223. Catanzaro, Andrew T., Richard A. Koup, M. Roederer, Robert T. Bailer, Mary E. Enama, Z. Moodie, L. Gu, Julie E. Martin, L. Novik, Bimal K. Chakrabarti, Bryan T. Butman, Jason G. D. Gall, C. R. King, Charla A. Andrews, R. Sheets, Phillip L. Gomez, John R. Mascola, Gary J. Nabel, and V. R. C. S. Team. 2006. Phase 1 safety and immunogenicity evaluation of a multiclade HIV-1 candidate vaccine delivered by a replication-defective recombinant adenovirus vector. *Journal of Infectious Diseases* 194: 1638-1649.
224. O'Hara, G. A., C. J. A. Duncan, K. J. Ewer, K. A. Collins, S. C. Elias, F. D. Halstead, A. L. Goodman, N. J. Edwards, A. Reyes-Sandoval, P. Bird, R. Rowland, S. H. Sheehy, I. D. Poulton, C. Hutchings, S. Todryk, L. Andrews, A. Folgori, E. Berrie, S. Moyle, A. Nicosia, S. Colloca, R. Cortese, L. Siani, A. M. Lawrie, S. C. Gilbert, and A. V. S. Hill. 2012. Clinical assessment of a recombinant simian adenovirus ChAd63: a potent new vaccine vector. *Journal of Infectious Diseases* 205: 772-781.
225. Drexler, I., C. Staib, and G. Sutter. 2004. Modified vaccinia virus Ankara as antigen delivery system: how can we best use its potential? *Current Opinion in Biotechnology* 15: 506-512.
226. Draper, S. J., A. L. Goodman, S. Biswas, E. K. Forbes, A. C. Moore, S. C. Gilbert, and A. V. S. Hill. 2009. Recombinant viral vaccines expressing merozoite surface protein-1 induce antibody- and T cell-mediated multistage protection against malaria. *Cell Host & Microbe* 5: 95-105.
227. Reyes-Sandoval, A., T. Berthoud, N. Alder, L. Siani, S. C. Gilbert, A. Nicosia, S. Colloca, R. Cortese, and A. V. S. Hill. 2010. Prime-boost immunization with adenoviral and modified vaccinia virus Ankara vectors enhances the durability and polyfunctionality of protective malaria $CD8^+$ T-cell responses. *Infection and Immunity* 78: 145-153.
228. Goodman, A. L., A. M. Blagborough, S. Biswas, Y. Wu, A. V. Hill, R. E. Sinden, and S. J. Draper. 2011. A viral vectored prime-boost immunization regime targeting the malaria Pfs25 antigen induces transmission-blocking activity. *PLoS ONE* 6: e29428.
229. Hill, A. V., A. Reyes-Sandoval, G. O'Hara, K. Ewer, A. Lawrie, A. Goodman, A. Nicosia, A. Folgori, S. Colloca, R. Cortese, S. C. Gilbert, and S. J. Draper. 2010. Prime-boost vectored malaria vaccines: progress and prospects. *Human Vaccines & Immunotherapeutics* 6: 78-83.
230. McConkey, S. J., W. H. H. Reece, V. S. Moorthy, D. Webster, S. Dunachie, G. Butcher, J. M. Vuola, T. J. Blanchard, P. Gothard, K. Watkins, C. M. Hannan, S. Everaere, K. Brown, K. E. Kester, J. Cummings, J. Williams, D. G. Heppner, A. Pathan, K. Flanagan, N. Arulanantham, M. T. M. Roberts, M. Roy, G. L. Smith, J. Schneider, T. Peto, R. E. Sinden, S. C. Gilbert, and A. V. S. Hill. 2003. Enhanced T-

cell immunogenicity of plasmid DNA vaccines boosted by recombinant modified vaccinia virus Ankara in humans. *Nature Medicine* 9: 729-735.

231. Goodman, A. L., C. Epp, D. Moss, A. A. Holder, J. M. Wilson, G. P. Gao, C. A. Long, E. J. Remarque, A. W. Thomas, V. Ammendola, S. Colloca, M. D. J. Dicks, S. Biswas, D. Seibel, L. M. van Duivenvoorde, S. C. Gilbert, A. V. S. Hill, and S. J. Draper. 2010. New candidate vaccines against blood-stage *Plasmodium falciparum* malaria: prime-boost immunization regimens incorporating human and simian adenoviral vectors and poxviral vectors expressing an optimized antigen based on merozoite surface protein 1. *Infection and immunity* 78: 4601-4612.
232. Draper, S. J., A. C. Moore, A. L. Goodman, C. A. Long, A. A. Holder, S. C. Gilbert, F. Hill, and A. V. S. Hill. 2008. Effective induction of high-titer antibodies by viral vector vaccines. *Nature Medicine* 14: 819-821.
233. Capone, S., A. Reyes-Sandoval, M. Naddeo, L. Siani, V. Ammendola, C. S. Rollier, A. Nicosia, S. Colloca, R. Cortese, A. Folgori, and A. V. Hill. 2010. Immune responses against a liver-stage malaria antigen induced by simian adenoviral vector AdCh63 and MVA prime-boost immunisation in non-human primates. *Vaccine* 29: 256-265.
234. Bruña-Romero, O., G. González-Aseguinolaza, J. C. R. Hafalla, M. Tsuji, and R. S. Nussenzweig. 2001. Complete, long-lasting protection against malaria of mice primed and boosted with two distinct viral vectors expressing the same plasmodial antigen. *Proceedings of the National Academy of Sciences* 98: 11491-11496.
235. Douglas, A. D., S. C. de Cassan, M. D. J. Dicks, S. C. Gilbert, A. V. S. Hill, and S. J. Draper. 2010. Tailoring subunit vaccine immunogenicity: Maximizing antibody and T cell responses by using combinations of adenovirus, poxvirus and protein-adjuvant vaccines against *Plasmodium falciparum* MSP1. *Vaccine* 28: 7167-7178.
236. Draper, S. J., S. Biswas, A. J. Spencer, E. J. Remarque, S. Capone, M. Naddeo, M. D. J. Dicks, B. W. Faber, S. C. de Cassan, A. Folgori, A. Nicosia, S. C. Gilbert, and A. V. S. Hill. 2010. Enhancing blood-stage malaria subunit vaccine immunogenicity in Rhesus macaques by combining adenovirus, poxvirus, and protein-in-adjuvant vaccines. *The Journal of Immunology* 185: 7583-7595.
237. Stewart, V. A., S. M. McGrath, P. M. Dubois, M. G. Pau, P. Mettens, J. Shott, M. Cobb, J. R. Burge, D. Larson, L. A. Ware, M. A. Demoitie, G. J. Weverling, B. Bayat, J. H. Custers, M. C. Dubois, J. Cohen, J. Goudsmit, and D. G. Heppner, Jr. 2007. Priming with an adenovirus 35-circumsporozoite protein (CS) vaccine followed by RTS,S/AS01B boosting significantly improves immunogenicity to *Plasmodium falciparum* CS compared to that with either malaria vaccine alone. *Infection and Immunity* 75: 2283-2290.
238. Duffy, P. E., T. Sahu, A. Akue, N. Milman, and C. Anderson. 2012. Pre-erythrocytic malaria vaccines: identifying the targets. *Expert Review of Vaccines* 11: 1261-1280.
239. Goodman, A. L., and S. J. Draper. 2010. Blood-stage malaria vaccines - recent progress and future challenges. *Annals of Tropical Medicine and Parasitology* 104: 189-211.
240. Thera, M. A., O. K. Doumbo, D. Coulibaly, M. B. Laurens, A. Ouattara, A. K. Kone, A. B. Guindo, K. Traore, I. Traore, B. Kouriba, D. A. Diallo, I. Diarra, M. Daou, A. Dolo, Y. Tolo, M. S. Sissoko, A. Niangaly, M. Sissoko, S. Takala-Harrison, K. E. Lyke, Y. Wu, W. C. Blackwelder, O. Godeaux, J. Vekemans, M. C. Dubois, W. R. Ballou, J. Cohen, D. Thompson, T. Dube, L. Soisson, C. L. Diggs, B. House, D. E. Lanar, S. Dutta, D. G. Heppner, Jr., and C. V. Plowe. 2011. A field trial to assess a blood-stage malaria vaccine. *New England Journal of Medicine* 365: 1004-1013.

241. Genton, B., I. Betuela, I. Felger, F. Al-Yaman, R. F. Anders, A. Saul, L. Rare, M. Baisor, K. Lorry, G. V. Brown, D. Pye, D. O. Irving, T. A. Smith, H.-P. Beck, and M. P. Alpers. 2002. A recombinant blood-stage malaria vaccine reduces *Plasmodium falciparum* density and exerts selective pressure on parasite populations in a phase 1-2b trial in Papua New Guinea. *Journal of Infectious Diseases* 185: 820-827.
242. Graves, P., and H. Gelband. 2006. Vaccines for preventing malaria (SPf66). *Cochrane Database Systematic Review* 19: CD005966.
243. Sirima, S. B., S. Cousens, and P. Druilhe. 2011. Protection against malaria by MSP3 candidate vaccine. *New England Journal of Medicine* 365: 1062-1064.
244. Williams, A. R., A. D. Douglas, K. Miura, J. J. Illingworth, P. Choudhary, L. M. Murungi, J. M. Furze, A. Diouf, O. Miotto, C. Crosnier, G. J. Wright, D. P. Kwiatkowski, R. M. Fairhurst, C. A. Long, and S. J. Draper. 2012. Enhancing blockade of *Plasmodium falciparum* erythrocyte invasion: assessing combinations of antibodies against PfRH5 and other merozoite antigens. *PLoS Pathogens* 8: e1002991.
245. Miura, K., H. Zhou, A. Diouf, S. E. Moretz, M. P. Fay, L. H. Miller, L. B. Martin, M. A. Pierce, R. D. Ellis, G. E. D. Mullen, and C. A. Long. 2009. Anti-apical-membrane-antigen-1 antibody is more effective than anti-42-kilodalton-merozoite-surface-protein-1 antibody in inhibiting *Plasmodium falciparum* growth, as determined by the *in vitro* growth inhibition assay. *Clinical and Vaccine Immunology* 16: 963-968.
246. Bergmann-Leitner, E. S., E. H. Duncan, G. E. Mullen, J. R. Burge, F. Khan, C. A. Long, E. Angov, and J. A. Lyon. 2006. Critical evaluation of different methods for measuring the functional activity of antibodies against malaria blood stage antigens. *American Journal of Tropical Medicine and Hygiene* 75: 437-442.
247. Crompton, P. D., K. Miura, B. Traore, K. Kayentao, A. Ongoiba, G. Weiss, S. Doumbo, D. Doumtabe, Y. Kone, C.-Y. Huang, O. K. Doumbo, L. H. Miller, C. A. Long, and S. K. Pierce. 2010. *In vitro* growth-inhibitory activity and malaria risk in a cohort study in Mali. *Infection and Immunity* 78: 737-745.
248. Spring, M. D., J. F. Cummings, C. F. Ockenhouse, S. Dutta, R. Reidler, E. Angov, E. Bergmann-Leitner, V. A. Stewart, S. Bittner, L. Juompan, M. G. Kortepeter, R. Nielsen, U. Krzych, E. Tierney, L. A. Ware, M. Dowler, C. C. Hermsen, R. W. Sauerwein, S. J. de Vlas, O. Ofori-Anyinam, D. E. Lanar, J. L. Williams, K. E. Kester, K. Tucker, M. Shi, E. Malkin, C. Long, C. L. Diggs, L. Soisson, M. C. Dubois, W. R. Ballou, J. Cohen, and D. G. Heppner, Jr. 2009. Phase 1/2a study of the malaria vaccine candidate apical membrane antigen-1 (AMA-1) administered in adjuvant system AS01B or AS02A. *PLoS ONE* 4: e5254.
249. Khusmith, S., and P. Druilhe. 1983. Cooperation between antibodies and monocytes that inhibit *in vitro* proliferation of *Plasmodium falciparum*. *Infection and Immunity* 41: 219-223.
250. Lunel, F., and P. Druilhe. 1989. Effector cells involved in nonspecific and antibody-dependent mechanisms directed against *Plasmodium falciparum* blood stages *in vitro*. *Infection and Immunity* 57: 2043-2049.
251. Bouharoun-Tayoun, H., C. Oeuvray, F. Lunel, and P. Druilhe. 1995. Mechanisms underlying the monocyte-mediated antibody-dependent killing of *Plasmodium falciparum* asexual blood stages. *The Journal of Experimental Medicine* 182: 409-418.
252. Jafarshad, A., M. H. Dziegiel, R. Lundquist, L. K. Nielsen, S. Singh, and P. L. Druilhe. 2007. A novel antibody-dependent cellular cytotoxicity mechanism involved in defense against malaria requires costimulation of monocytes FcγRII and FcγRIII. *The Journal of Immunology* 178: 3099-3106.

253. Oeuvray, C., H. Bouharoun-Tayoun, H. Gras-Masse, E. Bottius, T. Kaidoh, M. Aikawa, M. Filgueira, A. Tartar, and P. Druilhe. 1994. Merozoite surface protein-3: a malaria protein inducing antibodies that promote *Plasmodium falciparum* killing by cooperation with blood monocytes. *Blood* 84: 1594-1602.
254. Theisen, M., S. Soe, S. G. Jessing, L. M. Okkels, S. Danielsen, C. Oeuvray, P. Druilhe, and S. Jepsen. 2000. Identification of a major B-cell epitope of the *Plasmodium falciparum* glutamate-rich protein (GLURP), targeted by human antibodies mediating parasite killing. *Vaccine* 19: 204-212.
255. Soe, S., S. Singh, D. Camus, T. Horii, and P. Druilhe. 2002. *Plasmodium falciparum* serine repeat protein, a new target of monocyte-dependent antibody-mediated parasite killing. *Infection and Immunity* 70: 7182-7184.
256. Druilhe, P., F. Spertini, D. Soesoe, G. Corradin, P. Mejia, S. Singh, R. Audran, A. Bouzidi, C. Oeuvray, and C. Roussilhon. 2005. A malaria vaccine that elicits in humans antibodies able to kill *Plasmodium falciparum*. *PLoS Medicine* 2: e344.
257. Seidel, U. J. E., P. Schlegel, and P. Lang. 2013. Natural killer cell mediated antibody-dependent cellular cytotoxicity in tumor immunotherapy with therapeutic antibodies. *Frontiers in Immunology* 4: 76.
258. Tippett, E., L. A. Fernandes, S. J. Rogerson, and A. Jaworowski. 2007. A novel flow cytometric phagocytosis assay of malaria-infected erythrocytes. *Journal of Immunological Methods* 325: 42-50.
259. Hill, D. L., E. M. Eriksson, A. B. Carmagnac, D. W. Wilson, A. F. Cowman, D. S. Hansen, and L. Schofield. 2012. Efficient measurement of opsonising antibodies to *Plasmodium falciparum* merozoites. *PLoS ONE* 7: e51692.
260. Osier, F. H., G. Feng, M. J. Boyle, C. Langer, J. Zhou, J. S. Richards, F. J. McCallum, L. Reiling, A. Jaworowski, R. F. Anders, K. Marsh, and J. G. Beeson. 2014. Opsonic phagocytosis of *Plasmodium falciparum* merozoites: mechanism in human immunity and a correlate of protection against malaria. *BMC Medicine* 12: 108.
261. Chan, C. L., L. Rénia, and K. S. W. Tan. 2012. A simplified, sensitive phagocytic assay for malaria cultures facilitated by flow cytometry of differentially-stained cell populations. *PLoS ONE* 7: e38523.
262. Kumaratilake, L. M., and A. Ferrante. 2000. Opsonization and phagocytosis of *Plasmodium falciparum* merozoites measured by flow cytometry. *Clinical and Diagnostic Laboratory Immunology* 7: 9-13.
263. Kapelski, S., T. Klockenbring, R. Fischer, S. Barth, and R. Fendel. 2014. Assessment of the neutrophilic antibody-dependent respiratory burst (ADRB) response to *Plasmodium falciparum*. *Journal of Leukocyte Biology* epub.
264. Moon, R. W., J. Hall, F. Rangkuti, Y. S. Ho, N. Almond, G. H. Mitchell, A. Pain, A. A. Holder, and M. J. Blackman. 2013. Adaptation of the genetically tractable malaria pathogen *Plasmodium knowlesi* to continuous culture in human erythrocytes. *Proceedings of the National Academy of Sciences* 110: 531-536.
265. Shakri, A. R., M. M. A. Rizvi, and C. E. Chitnis. 2012. Development of quantitative receptor-ligand binding assay for use as a tool to estimate immune responses against *Plasmodium vivax* duffy binding protein region II. *Journal of Immunoassay and Immunochemistry* 33: 403-413.
266. Moorthy, V. S., R. D. Newman, and J. M. Okwo-Bele. 2013. Malaria vaccine technology roadmap. *Lancet* 382: 1700-1701.
267. Takai, T., M. Ono, M. Hikida, H. Ohmori, and J. V. Ravetch. 1996. Augmented humoral and anaphylactic responses in FcγRII-deficient mice. *Nature* 379: 346-349.
268. Quan, J., and J. Tian. 2009. Circular polymerase extension cloning of complex gene libraries and pathways. *PLoS ONE* 4: e6441.

269. Quan, J., and J. Tian. 2011. Circular polymerase extension cloning for high-throughput cloning of complex and combinatorial DNA libraries. *Nature Protocols* 6: 242-251.
270. Ogun, S. A., L. Dumon-Seignovert, J. B. Marchand, A. A. Holder, and F. Hill. 2008. The oligomerization domain of C4-binding protein (C4bp) acts as an adjuvant, and the fusion protein comprised of the 19-kilodalton merozoite surface protein 1 fused with the murine C4bp domain protects mice against malaria. *Infection and immunity* 76: 3817-3823.
271. Takai, T., M. Li, D. Sylvestre, R. Clynes, and J. V. Ravetch. 1994. FcR γ chain deletion results in pleiotrophic effector cell defects. *Cell* 76: 519-529.
272. Forbes, E. K., S. C. de Cassan, D. Llewellyn, S. Biswas, A. L. Goodman, M. G. Cottingham, C. A. Long, R. J. Pleass, A. V. S. Hill, F. Hill, and S. J. Draper. 2012. T cell responses induced by adenoviral vectored vaccines can be adjuvanted by fusion of antigen to the oligomerization domain of C4b-binding protein. *PLoS ONE* 7: e44943.
273. Goodman, A. L., E. K. Forbes, A. R. Williams, A. D. Douglas, S. C. de Cassan, K. Bauza, S. Biswas, M. D. Dicks, D. Llewellyn, A. C. Moore, C. J. Janse, B. M. Franke-Fayard, S. C. Gilbert, A. V. Hill, R. J. Pleass, and S. J. Draper. 2013. The utility of *Plasmodium berghei* as a rodent model for anti-merozoite malaria vaccine assessment. *Scientific Reports* 3: 1-13.
274. Marsh, K., and S. Kinyanjui. 2006. Immune effector mechanisms in malaria. *Parasite Immunology* 28: 51-60.
275. Daley, J. M., A. A. Thomay, M. D. Connolly, J. S. Reichner, and J. E. Albina. 2008. Use of Ly6G-specific monoclonal antibody to deplete neutrophils in mice. *Journal of Leukocyte Biology* 83: 64-70.
276. Carr, K. D., A. N. Sieve, M. Indramohan, T. J. Break, S. Lee, and R. E. Berg. 2011. Specific depletion reveals a novel role for neutrophil-mediated protection in the liver during *Listeria monocytogenes* infection. *European Journal of Immunology* 41: 2666-2676.
277. Adame-Gallegos, J. R., J. Shi, R. S. McIntosh, and R. J. Pleass. 2012. The generation and evaluation of two panels of epitope-matched mouse IgG1, IgG2a, IgG2b and IgG3 antibodies specific for *Plasmodium falciparum* and *Plasmodium yoelii* merozoite surface protein 1-19 ($MSP1_{19}$). *Experimental Parasitology* 130: 384-393.
278. Miura, K., A. C. Orcutt, O. V. Muratova, L. H. Miller, A. Saul, and C. A. Long. 2008. Development and characterization of a standardized ELISA including a reference serum on each plate to detect antibodies induced by experimental malaria vaccines. *Vaccine* 26: 193-200.
279. de Cassan, S. C., E. K. Forbes, A. D. Douglas, A. Milicic, B. Singh, P. Gupta, V. S. Chauhan, C. E. Chitnis, S. C. Gilbert, A. V. S. Hill, and S. J. Draper. 2011. The requirement for potent adjuvants to enhance the immunogenicity and protective efficacy of protein vaccines can be overcome by prior immunization with a recombinant adenovirus. *The Journal of Immunology* 187: 2602-2616.
280. Choe, H., M. J. Moore, C. M. Owens, P. L. Wright, N. Vasilieva, W. Li, A. P. Singh, R. Shakri, C. E. Chitnis, and M. Farzan. 2005. Sulphated tyrosines mediate association of chemokines and *Plasmodium vivax* Duffy binding protein with the Duffy antigen/receptor for chemokines (DARC). *Molecular Microbiology* 55: 1413-1422.
281. Lambros, C., and J. P. Vanderberg. 1979. Synchronization of *Plasmodium falciparum* erythrocytic stages in culture. *The Journal of Parasitology* 65: 418-420.

282. Rosenthal, P. J., K. Kim, J. H. McKerrow, and J. H. Leech. 1987. Identification of three stage-specific proteinases of *Plasmodium falciparum*. *The Journal of Experimental Medicine* 166: 816-821.
283. Salmon, B. L., A. Oksman, and D. E. Goldberg. 2001. Malaria parasite exit from the host erythrocyte: A two-step process requiring extraerythrocytic proteolysis. *Proceedings of the National Academy of Sciences* 98: 271-276.
284. Koch, G. G. 1983. Intraclass Correlation Coefficient. In *Encyclopedia of Statistics*. S. Kotz, and N. L. Johnson, eds. Wiley, New York.
285. Chevan, A., and M. Sutherland. 1991. Hierarchical partitioning. *The American Statistician* 45: 90-96.
286. Canty, A., and B. Ripley. 2008. boot: Bootstrap R (S-Plus) Functions. R package version 1.2-34.
287. Efron, B., and R. Tibshirani. 1993. *An introduction to the bootstrap*. CRC press, New York.
288. Bouharoun-Tayoun, H., and P. Druilhe. 1992. *Plasmodium falciparum* malaria: evidence for an isotype imbalance which may be responsible for delayed acquisition of protective immunity. *Infection and Immunity* 60: 1473-1481.
289. Pleass, R. J., S. A. Ogun, D. H. McGuinness, J. G. van de Winkel, A. A. Holder, and J. M. Woof. 2003. Novel antimalarial antibodies highlight the importance of the antibody Fc region in mediating protection. *Blood* 102: 4424-4430.
290. Greve, B., L. G. Lehman, B. Lell, D. Luckner, R. Schmidt-Ott, and P. G. Kremsner. 1999. High oxygen radical production is associated with fast parasite clearance in children with *Plasmodium falciparum* malaria. *Journal of Infectious Diseases* 179: 1584-1586.
291. Pleass, R. J., J. I. Dunlop, C. M. Anderson, and J. M. Woof. 1999. Identification of residues in the CH2/CH3 domain interface of IgA essential for interaction with the human Fcα receptor (FcαR) CD89. *Journal of Biological Chemistry* 274: 23508-23514.
292. Sanchez-Mejorada, G., and C. Rosales. 1998. Signal transduction by immunoglobulin Fc receptors. *Journal of Leukocyte Biology* 63: 521-533.
293. Pribluda, V. S., C. Pribluda, and H. Metzger. 1994. Transphosphorylation as the mechanism by which the high-affinity receptor for IgE is phosphorylated upon aggregation. *Proceedings of the National Academy of Sciences* 91: 11246-11250.
294. Pleass, R. J. 2009. Fc-receptors and immunity to malaria: from models to vaccines. *Parasite Immunology* 31: 529-538.
295. Pleass, R. J., and J. M. Woof. 2001. Fc receptors and immunity to parasites. *Trends in Parasitology* 17: 545-551.
296. Hulett, M. D., and P. M. Hogarth. 1994. Molecular basis of Fc receptor function. *Advances in Immunology* 57: 1-127.
297. Hirunpetcharat, C., J. H. Tian, D. C. Kaslow, N. van Rooijen, S. Kumar, J. A. Berzofsky, L. H. Miller, and M. F. Good. 1997. Complete protective immunity induced in mice by immunization with the 19-kilodalton carboxyl-terminal fragment of the merozoite surface protein-1 ($MSP1_{19}$) of *Plasmodium yoelii* expressed in *Saccharomyces cerevisiae*: correlation of protection with antigen-specific antibody titer, but not with effector $CD4^+$ T cells. *The Journal of Immunology* 159: 3400-3411.
298. Pleass, R. J., M. L. Lang, M. A. Kerr, and J. M. Woof. 2007. IgA is a more potent inducer of NADPH oxidase activation and degranulation in blood eosinophils than IgE. *Molecular Immunology* 44: 1401-1408.
299. Tan, P. S., A. L. Gavin, N. Barnes, D. W. Sears, D. Vremec, K. Shortman, S. Amigorena, P. L. Mottram, and P. M. Hogarth. 2003. Unique monoclonal antibodies

define expression of FcγRI on macrophages and mast cell lines and demonstrate heterogeneity among subcutaneous and other dendritic cells. *The Journal of Immunology* 170: 2549-2556.

300. Ioan-Facsinay, A., S. J. de Kimpe, S. M. M. Hellwig, P. L. van Lent, F. M. A. Hofhuis, H. H. van Ojik, C. Sedlik, S. A. da Silveira, J. Gerber, Y. F. de Jong, R. Roozendaal, L. A. Aarden, W. B. van den Berg, T. Saito, D. Mosser, S. Amigorena, S. Izui, G. J. B. van Ommen, M. van Vugt, J. G. J. van de Winkel, and J. S. Verbeek. 2002. FcγRI (CD64) contributes substantially to severity of arthritis, hypersensitivity responses, and protection from bacterial infection. *Immunity* 16: 391-402.
301. Selvaraj, P., N. Fifadara, S. Nagarajan, A. Cimino, and G. Wang. 2004. Functional regulation of human neutrophil Fc γ receptors. *Immunologic Research* 29: 219-229.
302. Clynes, R., J. S. Maizes, R. Guinamard, M. Ono, T. Takai, and J. V. Ravetch. 1999. Modulation of immune complex–induced inflammation *in vivo* by the coordinate expression of activation and inhibitory Fc receptors. *The Journal of Experimental Medicine* 189: 179-186.
303. Tebo, A. E., P. G. Kremsner, and A. J. F. Luty. 2001. *Plasmodium falciparum*: A major role for IgG3 in antibody-dependent monocyte-mediated cellular inhibition of parasite growth *in vitro*. *Experimental Parasitology* 98: 20-28.
304. Waki, S., S. Uehara, K. Kanbe, H. Nariuch, and M. Suzuki. 1995. Interferon-gamma and the induction of protective lgG2a antibodies in non-lethal *Plasmodium berghei* infections of mice. *Parasite Immunology* 17: 503-508.
305. White, W. I., C. Evans, and D. W. Taylor. 1991. Antimalarial antibodies of the immunoglobulin G2a isotype modulate parasitemias in mice infected with *Plasmodium yoelii*. *Infection and immunity* 59: 3547-3554.
306. Hirunpetcharat, C., J. Wipasa, S. Sakkhachornphop, T. Nitkumhan, Y. Z. Zheng, S. Pichyangkul, A. M. Krieg, D. S. Walsh, D. G. Heppner, and M. F. Good. 2003. CpG oligodeoxynucleotide enhances immunity against blood-stage malaria infection in mice parenterally immunized with a yeast-expressed 19 kDa carboxyl-terminal fragment of *Plasmodium yoelii* merozoite surface protein-1 ($MSP1_{19}$) formulated in oil-based Montanides. *Vaccine* 21: 2923-2932.
307. Majarian, W. R., T. M. Daly, W. P. Weidanz, and C. A. Long. 1984. Passive immunization against murine malaria with an IgG3 monoclonal antibody. *The Journal of Immunology* 132: 3131-3137.
308. Hazenbos, W. L. W., I. A. F. M. Heijnen, D. Meyer, F. M. A. Hofhuis, C. Renardel de Lavalette, R. E. Schmidt, P. J. A. Capel, J. G. J. van de Winkel, J. E. Gessner, T. K. van den Berg, and J. S. Verbeek. 1998. Murine IgG1 complexes trigger immune effector functions predominantly via FcγRIII (CD16). *The Journal of Immunology* 161: 3026-3032.
309. Arnold, R., F. Werner, B. Humbert, H. Werchau, and W. König. 1994. Effect of respiratory syncytial virus-antibody complexes on cytokine (IL-8, IL-6, TNF-α) release and respiratory burst in human granulocytes. *Immunology* 82: 184-191.
310. Truong, M. J., V. Gruart, J. P. Kusnierz, J. P. Papin, S. Loiseau, A. Capron, and M. Capron. 1993. Human neutrophils express immunoglobulin E (IgE)-binding proteins (Mac-2/εBP) of the S-type lectin family: role in IgE-dependent activation. *The Journal of Experimental Medicine* 177: 243-248.
311. Mackenzie, S. J., and M. Kerr. 1995. IgM monoclonal antibodies recognizing FcαR but not FcγRIII trigger a respiratory burst in neutrophils although both trigger an increase in intracellular calcium levels and degranulation. *Biochemical Journal* 306: 519-523.

312. Lundquist, R., L. K. Nielsen, A. Jafarshad, D. SoeSoe, L. H. Christensen, P. Druilhe, and M. H. Dziegiel. 2006. Human recombinant antibodies against *Plasmodium falciparum* merozoite surface protein 3 cloned from peripheral blood leukocytes of individuals with immunity to malaria demonstrate antiparasitic properties. *Infection and Immunity* 74: 3222-3231.
313. Galamo, C. D., A. Jafarshad, C. Blanc, and P. Druilhe. 2009. Anti–MSP1 block 2 antibodies are effective at parasite killing in an allele-specific manner by monocyte-mediated antibody-dependent cellular inhibition. *Journal of Infectious Diseases* 199: 1151-1154.
314. Koussis, K., C. Withers-Martinez, S. Yeoh, M. Child, F. Hackett, E. Knuepfer, L. Juliano, U. Woehlbier, H. Bujard, and M. J. Blackman. 2009. A multifunctional serine protease primes the malaria parasite for red blood cell invasion. *The EMBO Journal* 28: 725-735.
315. Blackman, M. J., H. G. Heidrich, S. Donachie, J. S. McBride, and A. A. Holder. 1990. A single fragment of a malaria merozoite surface protein remains on the parasite during red cell invasion and is the target of invasion-inhibiting antibodies. *The Journal of Experimental Medicine* 172: 379-382.
316. The malERA Consultative Group on Vaccines. 2011. A Research Agenda for Malaria Eradication: Vaccines. *PLoS Medicine* 8: e1000398.
317. Langhorne, J., F. M. Ndungu, A.-M. Sponaas, and K. Marsh. 2008. Immunity to malaria: more questions than answers. *Nature Immunology* 9: 725-732.
318. Duncan, C. J. A., S. H. Sheehy, K. J. Ewer, A. D. Douglas, K. A. Collins, F. D. Halstead, S. C. Elias, P. J. Lillie, K. Rausch, J. Aebig, K. Miura, N. J. Edwards, I. D. Poulton, A. Hunt-Cooke, D. W. Porter, F. M. Thompson, R. Rowland, S. J. Draper, S. C. Gilbert, M. P. Fay, C. A. Long, D. Zhu, Y. Wu, L. B. Martin, C. F. Anderson, A. M. Lawrie, A. V. S. Hill, and R. D. Ellis. 2011. Impact on malaria parasite multiplication rates in infected volunteers of the protein-in-adjuvant vaccine AMA1-C1/Alhydrogel+CPG 7909. *PLoS ONE* 6: e22271.
319. Turrini, F., H. Ginsburg, F. Bussolino, G. P. Pescarmona, M. V. Serra, and P. Arese. 1992. Phagocytosis of *Plasmodium falciparum*-infected human red blood cells by human monocytes: involvement of immune and nonimmune determinants and dependence on parasite developmental stage. *Blood* 80: 801-808.
320. Jepsen, M. P. G., P. S. Jogdand, S. K. Singh, M. Esen, M. Christiansen, S. Issifou, A. B. Hounkpatin, U. Ateba-Ngoa, P. G. Kremsner, M. H. Dziegiel, S. Olesen-Larsen, S. Jepsen, B. Mordmüller, and M. Theisen. 2013. The malaria vaccine candidate GMZ2 elicits functional antibodies in individuals from malaria endemic and non-endemic areas. *Journal of Infectious Diseases* 208: 479-488.
321. Kapelski, S., T. Klockenbring, R. Fischer, S. Barth, and R. Fendel. 2014. Assessment of the neutrophilic antibody-dependent respiratory burst (ADRB) response to *Plasmodium falciparum*. *Journal of Leukocyte Biology* 96: 1-12.
322. Sun, T., and C. Chakrabarti. 1985. Schizonts, merozoites, and phagocytosis in *falciparum* malaria. *Annals of Clinical & Laboratory Science* 15: 465-469.
323. Llewellyn, D., S. C. de Cassan, A. R. Williams, A. D. Douglas, E. K. Forbes, J. R. Adame-Gallegos, J. Shi, R. J. Pleass, and S. J. Draper. 2014. Assessment of antibody-dependent respiratory burst activity from mouse neutrophils on *Plasmodium yoelii* malaria challenge outcome. *Journal of Leukocyte Biology* 95: 369-382.
324. Clark, I. A., and N. H. Hunt. 1983. Evidence for reactive oxygen intermediates causing hemolysis and parasite death in malaria. *Infection and Immunity* 39: 1-6.
325. Murray, H. 1981. Susceptibility of leishmania to oxygen intermediates and killing by normal macrophages. *The Journal of Experimental Medicine* 153: 1302-1315.

326. Murray, H. W., and Z. A. Cohn. 1979. Macrophage oxygen-dependent antimicrobial activity. I. Susceptibility of *Toxoplasma gondii* to oxygen intermediates. *The Journal of Experimental Medicine* 150: 938-949.
327. Friedman, M. J. 1979. Oxidant damage mediates variant red cell resistance to malaria. *Nature* 280: 245-247.
328. Sanni, L. A., S. Fu, R. T. Dean, G. Bloomfield, R. Stocker, G. Chaudhri, M. C. Dinauer, and N. H. Hunt. 1999. Are reactive oxygen species involved in the pathogenesis of murine cerebral malaria? *Journal of Infectious Diseases* 179: 217-222.
329. Camous, L., L. Roumenina, S. Bigot, S. Brachemi, V. Frémeaux-Bacchi, P. Lesavre, and L. Halbwachs-Mecarelli. 2011. Complement alternative pathway acts as a positive feedback amplification of neutrophil activation. *Blood* 117: 1340-1349.
330. Morgan, B. P. 1989. Complement membrane attack on nucleated cells: resistance, recovery and non lethal effects. *Biochemical Journal* 264: 1-14.
331. Voice, J. K., and P. J. Lachmann. 1997. Neutrophil Fcγ and complement receptors involved in binding soluble IgG immune complexes and in specific granule release induced by soluble IgG immune complexes. *European Journal of Immunology* 27: 2514-2523.
332. International Conference on Harmonization of Technical Requirements for Registration of Pharmaceuticals for Human Use (ICH). 2005. Validation of analytical procedures: text and methodology Q2(R1). ICH Official web site http://www.ich.org.
333. Pan, L., R. Kreisle, and Y. Shi. 1998. Detection of Fcγ receptors on human endothelial cells stimulated with cytokines tumour necrosis factor-alpha (TNF-a) and interferon-gamma (IFN-g). *Clinical and Experimental Immunology* 112: 533-538.
334. Polhemus, M. E., A. J. Magill, J. F. Cummings, K. E. Kester, C. F. Ockenhouse, D. E. Lanar, S. Dutta, A. Barbosa, L. Soisson, C. L. Diggs, S. A. Robinson, J. D. Haynes, V. A. Stewart, L. A. Ware, C. Brando, U. Krzych, R. A. Bowden, J. D. Cohen, M.-C. Dubois, O. Ofori-Anyinam, E. De-Kock, W. R. Ballou, and D. G. Heppner Jr. 2007. Phase I dose escalation safety and immunogenicity trial of *Plasmodium falciparum* apical membrane protein (AMA-1) FMP2.1, adjuvanted with AS02A, in malaria-naïve adults at the Walter Reed Army Institute of Research. *Vaccine* 25: 4203-4212.
335. Aoki, S., J. Li, S. Itagaki, B. A. Okech, T. G. Egwang, H. Matsuoka, N. M. Q. Palacpac, T. Mitamura, and T. Horii. 2002. Serine repeat antigen (SERA5) is predominantly expressed among the SERA multigene family of *Plasmodium falciparum*, and the acquired antibody titers correlate with serum inhibition of the parasite growth. *Journal of Biological Chemistry* 277: 47533-47540.
336. Zeituni, A. E., K. Miura, M. Diakite, S. Doumbia, S. E. Moretz, A. Diouf, G. Tullo, T. M. Lopera-Mesa, C. D. Bess, N. K. Mita-Mendoza, J. M. Anderson, R. M. Fairhurst, and C. A. Long. 2013. Effects of age, hemoglobin type and parasite strain on IgG recognition of *Plasmodium falciparum*–infected erythrocytes in Malian children. *PLoS ONE* 8: e76734.
337. Dent, A. E., E. S. Bergmann-Leitner, D. W. Wilson, D. J. Tisch, R. Kimmel, J. Vulule, P. O. Sumba, J. G. Beeson, E. Angov, A. M. Moormann, and J. W. Kazura. 2008. Antibody-mediated growth inhibition of *Plasmodium falciparum*: relationship to age and protection from parasitemia in Kenyan children and adults. *PLoS ONE* 3: e3557.
338. Corran, P. H., R. A. O'Donnell, J. Todd, C. Uthaipibull, A. A. Holder, B. S. Crabb, and E. M. Riley. 2004. The fine specificity, but not the invasion inhibitory activity, of 19-kilodalton merozoite surface protein 1-specific antibodies is associated with

resistance to malarial parasitemia in a cross-sectional survey in The Gambia. *Infection & Immunity* 72: 6185-6189.

339. Murhandarwati, E. E., L. Wang, C. G. Black, D. H. Nhan, T. L. Richie, and R. L. Coppel. 2009. Inhibitory antibodies specific for the 19-kilodalton fragment of merozoite surface protein 1 do not correlate with delayed appearance of infection with *Plasmodium falciparum* in semi-immune individuals in Vietnam. *Infection & Immunity* 77: 4510-4517.
340. Marsh, K., L. Otoo, R. J. Hayes, D. C. Carson, and B. M. Greenwood. 1989. Antibodies to blood stage antigens of *Plasmodium falciparum* in rural Gambians and their relation to protection against infection. *Transactions of the Royal Society of Tropical Medicine and Hygiene* 83: 293-303.
341. Ricke, C. H., T. Staalsoe, K. Koram, B. D. Akanmori, E. M. Riley, T. G. Theander, and L. Hviid. 2000. Plasma antibodies from malaria-exposed pregnant women recognize variant surface antigens on *Plasmodium falciparum*-infected erythrocytes in a parity-dependent manner and block parasite adhesion to chondroitin sulfate A. *The Journal of Immunology* 165: 3309-3316.
342. Giha, H. A., T. Staalsoe, D. Dodoo, I. M. Elhassan, C. Roper, G. M. Satti, D. E. Arnot, T. G. Theander, and L. Hviid. 1999. Nine-year longitudinal study of antibodies to variant antigens on the surface of *Plasmodium falciparum*-infected erythrocytes. *Infection & Immunity* 67: 4092-4098.
343. Ofori, M. F., D. Dodoo, T. Staalsoe, J. A. L. Kurtzhals, K. Koram, T. G. Theander, B. D. Akanmori, and L. Hviid. 2002. Malaria-induced acquisition of antibodies to *Plasmodium falciparum* variant surface antigens. *Infection and Immunity* 70: 2982-2988.
344. Staalsoe, T., C. E. Shulman, J. N. Bulmer, K. Kawuondo, K. Marsh, and L. Hviid. 2004. Variant surface antigen-specific IgG and protection against clinical consequences of pregnancy-associated *Plasmodium falciparum* malaria. *The Lancet* 363: 283-289.
345. Osier, F. H. A., G. Fegan, S. D. Polley, L. Murungi, F. Verra, K. K. A. Tetteh, B. Lowe, T. Mwangi, P. C. Bull, A. W. Thomas, D. R. Cavanagh, J. S. McBride, D. E. Lanar, M. J. Mackinnon, D. J. Conway, and K. Marsh. 2008. Breadth and magnitude of antibody responses to multiple *Plasmodium falciparum* merozoite antigens are associated with protection from clinical malaria. *Infection and Immunity* 76: 2240-2248.
346. Dodoo, D., M. Theisen, J. A. L. Kurtzhals, B. D. Akanmori, K. A. Koram, S. Jepsen, F. K. Nkrumah, T. G. Theander, and L. Hviid. 2000. Naturally acquired antibodies to the glutamate-rich protein are associated with protection against *Plasmodium falciparum* malaria. *Journal of Infectious Diseases* 181: 1202-1205.
347. Branch, O. H., A. J. Oloo, B. L. Nahlen, D. Kaslow, and A. A. Lal. 2000. Anti-merozoite surface protein-1 19-kDa IgG in mother-infant pairs naturally exposed to *Plasmodium falciparum*: subclass analysis with age, exposure to asexual parasitemia, and protection against malaria. V. The Asembo Bay cohort project. *Journal of Infectious Diseases* 181: 1746-1752.
348. Miura, K., M. Diakite, A. Diouf, S. Doumbia, D. Konate, A. S. Keita, S. E. Moretz, G. Tullo, H. Zhou, T. M. Lopera-Mesa, J. M. Anderson, R. M. Fairhurst, and C. A. Long. 2013. Relationship between malaria incidence and IgG levels to *Plasmodium falciparum* merozoite antigens in Malian children: impact of hemoglobins S and C. *PLoS ONE* 8: e60182.
349. Malkin, E. M., D. J. Diemert, J. H. McArthur, J. R. Perreault, A. P. Miles, B. K. Giersing, G. E. Mullen, A. Orcutt, O. Muratova, and M. Awkal. 2005. Phase 1 clinical

trial of apical membrane antigen 1: an asexual blood-stage vaccine for *Plasmodium falciparum* malaria. *Infection and immunity* 73: 3677-3685.
350. Gupta, S., R. W. Snow, C. A. Donnelly, K. Marsh, and C. Newbold. 1999. Immunity to non-cerebral severe malaria is acquired after one or two infections. *Nature Medicine* 5: 340-343.
351. O'Meara, W. P., T. W. Mwangi, T. N. Williams, F. E. McKenzie, R. W. Snow, and K. Marsh. 2008. Relationship between exposure, clinical malaria, and age in an area of changing transmission intensity. *The American Journal of Tropical Medicine and Hygiene* 79: 185-191.
352. Price, R. N., E. Tjitra, C. A. Guerra, S. Yeung, N. J. White, and N. M. Anstey. 2007. Vivax malaria: neglected and not benign. *The American Journal of Tropical Medicine and Hygiene* 77: 79-87.
353. Baird, J. K. 2013. Evidence and implications of mortality associated with acute *Plasmodium vivax* malaria. *Clinical Microbiology Reviews* 26: 36-57.
354. Horuk, R., C. E. Chitnis, W. C. Darbonne, T. J. Colby, A. Rybicki, T. J. Hadley, and L. H. Miller. 1993. A receptor for the malarial parasite *Plasmodium vivax*: the erythrocyte chemokine receptor. *Science* 261: 1182-1184.
355. Menard, D., E. R. Chan, C. Benedet, A. Ratsimbasoa, S. Kim, P. Chim, C. Do, B. Witkowski, R. Durand, M. Thellier, C. Severini, E. Legrand, L. Musset, B. Y. M. Nour, O. Mercereau-Puijalon, D. Serre, and P. A. Zimmerman. 2013. Whole genome sequencing of field isolates reveals a common duplication of the Duffy binding protein gene in Malagasy *Plasmodium vivax* strains. *PLoS Neglected Tropical Diseases* 7: e2489.
356. Adams, J. H., D. E. Hudson, M. Torii, G. E. Ward, T. E. Wellems, M. Aikawa, and L. H. Miller. 1990. The Duffy receptor family of *Plasmodium knowlesi* is located within the micronemes of invasive malaria merozoites. *Cell* 63: 141-153.
357. Chitnis, C. E., and L. H. Miller. 1994. Identification of the erythrocyte binding domains of *Plasmodium vivax* and *Plasmodium knowlesi* proteins involved in erythrocyte invasion. *The Journal of Experimental Medicine* 180: 497-506.
358. Adams, J. H., B. K. Sim, S. A. Dolan, X. Fang, D. C. Kaslow, and L. H. Miller. 1992. A family of erythrocyte binding proteins of malaria parasites. *Proceedings of the National Academy of Sciences* 89: 7085-7089.
359. Batchelor, J. D., J. A. Zahm, and N. H. Tolia. 2011. Dimerization of *Plasmodium vivax* DBP is induced upon receptor binding and drives recognition of DARC. *Nature Structural & Molecular Biology* 18: 908-914.
360. King, C. L., J. H. Adams, J. Xianli, B. T. Grimberg, A. M. McHenry, L. J. Greenberg, A. Siddiqui, R. E. Howes, M. da Silva-Nunes, M. U. Ferreira, and P. A. Zimmerman. 2011. Fy^a/Fy^b antigen polymorphism in human erythrocyte Duffy antigen affects susceptibility to *Plasmodium vivax* malaria. *Proceedings of the National Academy of Sciences* 108: 20113-20118.
361. Beeson, J. G., and B. S. Crabb. 2007. Towards a vaccine against *Plasmodium vivax* malaria. *PLoS Medicine* 4: e350.
362. Singh, A. P., S. K. Puri, and C. E. Chitnis. 2002. Antibodies raised against receptor-binding domain of *Plasmodium knowlesi* Duffy binding protein inhibit erythrocyte invasion. *Molecular and Biochemical Parasitology* 121: 21-31.
363. Bushell, K. M., C. Söllner, B. Schuster-Boeckler, A. Bateman, and G. J. Wright. 2008. Large-scale screening for novel low-affinity extracellular protein interactions. *Genome Research* 18: 622-630.

364. Maier, T., N. Drapal, M. Thanbichler, and A. Böck. 1998. Strep-tag II affinity purification: an approach to study intermediates of metalloenzyme biosynthesis. *Analytical Biochemistry* 259: 68-73.
365. Bushkin, G. G., D. M. Ratner, J. Cui, S. Banerjee, M. T. Duraisingh, C. V. Jennings, J. D. Dvorin, M.-J. Gubbels, S. D. Robertson, M. Steffen, B. R. O'Keefe, P. W. Robbins, and J. Samuelson. 2010. Suggestive evidence for Darwinian selection against asparagine-linked glycans of *Plasmodium falciparum* and *Toxoplasma gondii*. *Eukaryotic Cell* 9: 228-241.
366. Chitnis, C. E., A. Chaudhuri, R. Horuk, A. O. Pogo, and L. H. Miller. 1996. The domain on the Duffy blood group antigen for binding *Plasmodium vivax* and *P. knowlesi* malarial parasites to erythrocytes. *The Journal of Experimental Medicine* 184: 1531-1536.
367. Singh, S., K. Pandey, R. Chattopadhayay, S. S. Yazdani, A. Lynn, A. Bharadwaj, A. Ranjan, and C. Chitnis. 2001. Biochemical, biophysical, and functional characterization of bacterially expressed and refolded receptor binding domain of *Plasmodium vivax* Duffy-binding protein. *Journal of Biological Chemistry* 276: 17111-17116.
368. Yazdani, S., A. Shakri, P. Pattnaik, M. M. Rizvi, and C. Chitnis. 2006. Improvement in yield and purity of a recombinant malaria vaccine candidate based on the receptor-binding domain of *Plasmodium vivax* Duffy binding protein by codon optimization. *Biotechnol Lett* 28: 1109-1114.
369. Sampath, S., C. Carrico, J. Janes, S. Gurumoorthy, C. Gibson, M. Melcher, C. E. Chitnis, R. Wang, W. R. Schief, and J. D. Smith. 2013. Glycan masking of *Plasmodium vivax* Duffy binding protein for probing protein binding function and vaccine development. *PLoS Pathogens* 9: e1003420.
370. Sellhorn, G., Z. Caldwell, C. Mineart, and L. Stamatatos. 2009. Improving the expression of recombinant soluble HIV Envelope glycoproteins using pseudo-stable transient transfection. *Vaccine* 28: 430-436.
371. Kincaid, R., E. Angov, and J. Lyon. 2004. Protein expression by codon harmonization and translational attenuation. In *Google Patents*. Veritas.
372. Ophorst, O. J. A. E., K. Radošević, J. M. Klap, J. Sijtsma, G. Gillissen, R. Mintardjo, M. J. M. van Ooij, L. Holterman, A. Companjen, J. Goudsmit, and M. J. E. Havenga. 2007. Increased immunogenicity of recombinant Ad35-based malaria vaccine through formulation with aluminium phosphate adjuvant. *Vaccine* 25: 6501-6510.
373. Tissot, A. C., R. Renhofa, N. Schmitz, I. Cielens, E. Meijerink, V. Ose, G. T. Jennings, P. Saudan, P. Pumpens, and M. F. Bachmann. 2010. Versatile virus-like particle carrier for epitope based vaccines. *PLoS One* 5: e9809.
374. Correia, B. E., J. T. Bates, R. J. Loomis, G. Baneyx, C. Carrico, J. G. Jardine, P. Rupert, C. Correnti, O. Kalyuzhniy, V. Vittal, M. J. Connell, E. Stevens, A. Schroeter, M. Chen, S. MacPherson, A. M. Serra, Y. Adachi, M. A. Holmes, Y. Li, R. E. Klevit, B. S. Graham, R. T. Wyatt, D. Baker, R. K. Strong, J. E. Crowe, P. R. Johnson, and W. R. Schief. 2014. Proof of principle for epitope-focused vaccine design. *Nature* 507: 201-206.
375. Azoitei, M. L., B. E. Correia, Y. E. Ban, C. Carrico, O. Kalyuzhniy, L. Chen, A. Schroeter, P. S. Huang, J. S. McLellan, P. D. Kwong, D. Baker, R. K. Strong, and W. R. Schief. 2011. Computation-guided backbone grafting of a discontinuous motif onto a protein scaffold. *Science* 334: 373-376.
376. Ofek, G., F. J. Guenaga, W. R. Schief, J. Skinner, D. Baker, R. Wyatt, and P. D. Kwong. 2010. Elicitation of structure-specific antibodies by epitope scaffolds. *Proc Natl Acad Sci U S A* 107: 17880-17887.

377. King, C. L., P. Michon, A. R. Shakri, A. Marcotty, D. Stanisic, P. A. Zimmerman, J. L. Cole-Tobian, I. Mueller, and C. E. Chitnis. 2008. Naturally acquired Duffy-binding protein-specific binding inhibitory antibodies confer protection from blood-stage *Plasmodium vivax* infection. *Proceedings of the National Academy of Sciences* 105: 8363-8368.
378. Miller, L. H., M. F. Good, and D. C. Kaslow. 1997. The need for assays predictive of protection in development of malaria bloodstage vaccines. *Parasitology Today* 13: 46-47.
379. Mehlin, C., E. Boni, F. S. Buckner, L. Engel, T. Feist, M. H. Gelb, L. Haji, D. Kim, C. Liu, N. Mueller, P. J. Myler, J. T. Reddy, J. N. Sampson, E. Subramanian, W. C. Van Voorhis, E. Worthey, F. Zucker, and W. G. J. Hol. 2006. Heterologous expression of proteins from *Plasmodium falciparum*: results from 1000 genes. *Molecular and Biochemical Parasitology* 148: 144-160.
380. Kemp, D. J., R. L. Coppel, A. F. Cowman, R. B. Saint, G. V. Brown, and R. F. Anders. 1983. Expression of *Plasmodium falciparum* blood-stage antigens in *Escherichia coli*: detection with antibodies from immune humans. *Proceedings of the National Academy of Sciences of the United States of America* 80: 3787-3791.
381. Zenonos, Z. A., J. C. Rayner, and G. J. Wright. 2014. Towards a comprehensive *Plasmodium falciparum* merozoite cell surface and secreted recombinant protein library. *Malaria Journal* 13: 93.
382. Crosnier, C., L. Y. Bustamante, S. J. Bartholdson, A. K. Bei, M. Theron, M. Uchikawa, S. Mboup, O. Ndir, D. P. Kwiatkowski, M. T. Duraisingh, J. C. Rayner, and G. J. Wright. 2011. Basigin is a receptor essential for erythrocyte invasion by *Plasmodium falciparum*. *Nature* 480: 534-537.
383. de Jongh, W. A., S. Salgueiro, and C. Dyring. 2013. The use of *Drosophila* S2 cells in R&D and bioprocessing. *Pharmaceutical Bioprocessing* 1: 197-213.
384. Wright, K. E., K. A. Hjerrild, J. Bartlett, A. D. Douglas, J. Jin, R. E. Brown, J. J. Illingworth, R. Ashfield, S. B. Clemmensen, W. A. de Jongh, S. J. Draper, and M. K. Higgins. 2014. Structure of malaria invasion protein RH5 with erythrocyte basigin and blocking antibodies. *Nature* epub.
385. Mestas, J., and C. C. W. Hughes. 2004. Of mice and not men: differences between mouse and human immunology. *The Journal of Immunology* 172: 2731-2738.
386. Trevani, A. S., A. Chorny, G. Salamone, M. Vermeulen, R. Gamberale, J. Schettini, S. Raiden, and J. Geffner. 2003. Bacterial DNA activates human neutrophils by a CpG-independent pathway. *European Journal of Immunology* 33: 3164-3174.
387. Lund, J., A. Sato, S. Akira, R. Medzhitov, and A. Iwasaki. 2003. Toll-like receptor 9-mediated recognition of Herpes simplex virus-2 by plasmacytoid dendritic cells. *Journal of Experimental Medicine* 198: 513-520.
388. Doeing, D. C., J. L. Borowicz, and E. T. Crockett. 2003. Gender dimorphism in differential peripheral blood leukocyte counts in mice using cardiac, tail, foot, and saphenous vein puncture methods. *BMC Clinical Pathology* 3: 3.
389. Douglas, A. D., A. R. Williams, E. Knuepfer, J. J. Illingworth, J. M. Furze, C. Crosnier, P. Choudhary, L. Y. Bustamante, S. E. Zakutansky, D. K. Awuah, D. G. W. Alanine, M. Theron, A. Worth, R. Shimkets, J. C. Rayner, A. A. Holder, G. J. Wright, and S. J. Draper. 2014. Neutralization of *Plasmodium falciparum* merozoites by antibodies against PfRH5. *The Journal of Immunology* 192: 245-258.
390. Biswas, S., M. D. J. Dicks, C. A. Long, E. J. Remarque, L. Siani, S. Colloca, M. G. Cottingham, A. A. Holder, S. C. Gilbert, A. V. S. Hill, and S. J. Draper. 2011. Transgene optimization, immunogenicity and *in vitro* efficacy of viral vectored

vaccines expressing two alleles of *Plasmodium falciparum* AMA1. *PLoS ONE* 6: e20977.

391. Wrammert, J., K. Smith, J. Miller, W. A. Langley, K. Kokko, C. Larsen, N. Y. Zheng, I. Mays, L. Garman, C. Helms, J. James, G. M. Air, J. D. Capra, R. Ahmed, and P. C. Wilson. 2008. Rapid cloning of high-affinity human monoclonal antibodies against influenza virus. *Nature* 453: 667-671.
392. Batchelor, J. D., J. A. Zahm, and N. H. Tolia. 2011. Dimerization of Plasmodium vivax DBP is induced upon receptor binding and drives recognition of DARC. *Nat Struct Mol Biol* 18: 908-914.
393. Danner, R., S. N. Chaudhari, J. Rosenberger, J. Surls, T. L. Richie, T.-D. Brumeanu, and S. Casares. 2011. Expression of HLA class II molecules in humanized NOD.Rag1KO.IL2RgcKO mice is critical for development and function of human T and B cells. *PLoS ONE* 6: e19826.
394. Singh, A. P., H. Ozwara, C. H. Kocken, S. K. Puri, A. W. Thomas, and C. E. Chitnis. 2005. Targeted deletion of Plasmodium knowlesi Duffy binding protein confirms its role in junction formation during invasion. *Mol Microbiol* 55: 1925-1934.

APPENDIX

APPENDIX 1

1.1 J136

2.1 Version Number 2.2

3.1 Recombinant protein expression + purification in E. Coli

This protocol uses GMO. All users MUST be registered with the University Occupational Health Service as set out in the University's health and safety regulations. Health surveillance is a legal requirement under COSHH.

If you are not currently registered with the Occupational Health Service for work with GMO, or need to check your registration, please contact the ORCRB NDM Personnel team.

4.1 Other documents

See also J117, J118, J119 re protein production in insect cells

5.1 Definitions

None

6.1 Objective

Production of recombinant protein in E coli, with either GST or N terminal His tag.

7.1 Procedure

The construct of interest should be cloned into the following plasmid for purification with a GST tag:

pGEX2T: glutathione-S-transferase tag
For purification on glutathione affinity column (Novagen GST-bind kit).

OVERVIEW

Day 1 = Set up 100ml overnight cultures

Day 2 = Scale-up from 100ml cultures → 500ml cultures (~1hr)
Induction of protein expression with IPTG (~2hrs)
Centrifugation of cultures to pellet cells

Freeze pellets overnight

Day3 = Protein extraction and purification.

Day 3 can take MANY hours with Novagen GST bind kit.
Book centrifuge in advance for 1-2hr slots on the afternoon of day2 and morning of day3.

1.1.1. CULTURE AND INDUCTION OF EXPRESSION

REAGENTS (per protein)

Terrific broth (Sigma T0918) - 1 litre
Ampicillin 1ml of 50mg/ml = 1000x stock
Chloramphenicol (if required) 1ml of 1000x stock
- make up in MeOH to15mg/mL (i.e. to a 20mg vial add 1.33mL MeOH) and store at -20^{o}C

IPTG (Sigma I5502-1g) 240ul of 250mg/ml stock (dissolve 1g IPTG in 50% ethanol in water)

500ml centrifuge flasks (2 per litre of culture)

ADVANCE PREPARATION
Check the antibiotic resistance pattern of the plasmid (see s drive: reagents info. Plasmids)

Terrific broth preparation: make up 47.6g in 1L with 8mL glycerol and autoclave. Allow sufficient volume for evaporation

Easiest to mix antibiotics into the broth once autoclaved then can be used at all steps without further addition of antibiotics.

IPTG preparation: mix 1g in 4mL 50% ethanol to make a 250mg/mL (=1M) stock which can be stored at -20)

DAY 1
Add 1.5µl frozen glycerol bacteria stock to 100ml TB/antibiotics**.**
Incubate in 37ºC shaker overnight.

DAY 2
Make up to 500ml with fresh medium and antibiotics **&** incubate as before for 1h.

Add IPTG at final concentration 60µg/mL (120µl per flask of 250mg/ml stock) and incubate the cultures for a further 2h. This is to induce protein expression. If desired, samples of culture before and after induction can be taken to run on a gel to monitor efficacy of induction.

If using GST-bind kit, weigh empty centrifuge flasks (500ml flasks).

Harvest cells by centrifugation (JLA 10.5 6,000rpm 15min) and re-weigh to calculate pellet weights. Discard the supernatant (leave in microsol for 10 mins before disposable in sink).

Store at -20ºC overnight. It may be possible to store pellet for longer at -80.

1.1.2. GST PURIFICATION

Example yields from 1 litre of culture:

	Novagen
PfMSP1-19 QKNG	2ml of 8mg/ml (second elution fraction)
PfRH2	4ml of 1.5mg/ml (1^{st} +2^{nd} elution fractions)

DAY 3
REAGENTS + MATERIALS
Novagen GST·Bind Purification Kit includes the following, which can also be separately ordered
BugBuster (70794-3)
GST bind column beads
Bind/wash buffer
GST elution buffer
Benzonase

Ultracentrifuge tubes to hold ~30ml eg Beckman 326823 (2 per litre of culture)

METHOD

1. Thaw the pellets.

2. Lyse bacteria with BugBuster and Benzonase endonuclease.
   5ml BugBuster per g of pellet (usually 4-8g so need 20-40ml BugBuster) plus 25U Benzonase per 1ml BugBuster used (using the benzonase which comes with the kit this is 1ul per ml, using Sigma benzonase you will need to do a calculation).
   Vortex vigorously for 10-20 mins until fully dissolved.
   Ensure the 500ml centrifuge tubes are balanced (weight the tubes and top up with bugbuster if necessary).

3. Transfer to corning 50mL falcons (unless BugBuster/pellet mix is >1/2 centrifuge tube volume). Centrifuge at 15,000G for 25 min at 4ºC (JA12).

4. Transfer the supernatant to new 50mL Falcon tubes. Spin in the JA12 rotor at 6,000 xg, 4°C, for at least 1h 15mins (spin for 2h if possible).

   Supernatant can be stored for a few hours at 4°C but should be brought back to room temp (with a room temp water bath) before use.

5. During final spin, set up the columns + begin to wash them (should take ~30min). The GST-bind resin is only 50% slurry so use twice the volume you require for the columns. E.g. for a 2.5ml column volume load the column with 5ml of slurry. The column slurry binds 5-8mg/ml so a 2.5ml column can bind up to 20mg of protein. To load the column, gently mix the resin and transfer 5ml into the column gently using a pipette. Allow the slurry to settle which will be about half way down the column. *Take great care to avoid presence of air bubbles underneath the resin- they*

will slow down the column dramatically. A pipette can be used to pack down the resin and extract air. The storage buffer should begin to drip through.
Make a 1x solution of the GST bind/wash buffer- you will need 15 column volumes in total. Use the 10x wash solution from the kit and dilute with dH_20.
Once the level of storage buffer (20% ethanol) drops below the top of the column bed, wash the resin with 5 volumes (e.g.12.5ml) of GST Bind/wash buffer.

Once the Bind/Wash is running, the bugs can be prepared, all the time keeping the column topped up with Bind/Wash.

6. Load the clarified extract onto the prepared GST-affinity chromatography columns. Sterile filtering s/n at this stage will prevent large debris blocking the column.

7. Wash again with 10 column volumes (25ml) of GST bind/wash buffer.

8. Prepare 10ml of 1x glutathione elution buffer.
   10 x buffer is made up with 1g reduced glutathione and 32.5mL 10 x glutathione reconstitution buffer. Can be stored at -20 but should be freeze-thawed a maximum of 5 times.
   Fresh 1 x buffer should be made up immediately before use with dH_20.

9. Elute proteins using the 1 x glutathione elution buffer (3x column volumes = 7.5mL) and collect the eluted fractions into labelled tubes in 1-2ml fractions.

NOTE – if storing proteins at -20ºC and reading later on the nanodrop, keep an aliquot of 1x elution buffer for use as a blank / reference.

10. Measure concentration with a nanodrop and only keep the tubes with high protein concentrations (eg >1mg/ml). Store at 4ºC or freeze.

11. Packed columns can be stored in 20% ethanol at 4 degrees for re-use with the same protein.

APPENDIX 2

1. Jenner Laboratory Protocol Number: J238

2. Version Number: 2.0

3. Production of recombinant proteins in transiently transfected suspension 293 cells

This protocol uses GMOs. All users MUST be registered with the University Occupational Health Service as set out in the University's health and safety regulations. Health surveillance is a legal requirement under COSHH.
If you are not currently registered with the Occupational Health Service for work with GMOs, or need to check your registration, please contact the ORCRB NDM Personnel team.

4. Other Documents

MSDS refer to MSDS for the relevant safety information on the individual reagents

See S:\PROTOCOLS\Protein expression\Transient 293:

- "Transient 293 protocols Bushell Durocher and CSHL.docx"
  - Summary of transient 293 production protocols from the following sources
    -Gavin Wright's publications from the Sanger Centre
    -Yves Durocher's publications from Canadian NRC
    -Cold Spring Harbour Laboratory protocols, 2008
- "Invitrogen Freestyle 293 system manual.pdf"

5. Definitions

***293F cells*-** 293 cells available from Invitrogen which are adapted to suspension growth in serum-free Freestyle medium
***293T cells*-** 293 cells expressing SV40 large T antigen. This allows for episomal replication of transfected plasmids containing the SV40 origin of replication. This allows for amplification of transfected plasmids and extended temporal expression of the desired gene products. Adherent 293T cells originally obtained by Sandy Douglas

from Strubi/ OPPF, and were adapted to suspension culture in serum-free medium by Sandy. Can be grown in the presence of G418, but not necessary as the SV40 large T antigen gene is integrated into the genome along with the neomycin resistance cassette.

293E cells- 293 cells expressing EBV EBNA1 antigen. This allows for episomal replication of transfected plasmids containing the EBNA1 origin of replication. Adherent 293T cells originally obtained by Sandy Douglas from Strubi/ OPPF, and were adapted to suspension culture in serum-free medium by Sandy. As for 293Ts, it is not clear whether G418 selection is required during stock culture maintenance.

PEI- Polyethyleneimine.

6. Objective

Expression of soluble secreted recombinant proteins by transfection of suspension 293 cells.
Associated methods (eg Western blotting to detect protein, ELISA to quantify protein, NiNTA or Streptactin purification of protein) may be discussed here, but detailed methods are elsewhere

7. Reagents

Invitrogen Freestyle 293 expression medium or Invitrogen Expi293 expression medium (cat # 2082258)

G418 antibiotic solution at 50 mg/mL for cell culture (optional, for use with 293E cells, add to medium at 1:1000 ratio)

Foetal calf serum

Trypan blue

25KDa linear PEI from Alfa Aesar at 1 mg/mL in dH_2O. This needs to be prepared overnight in the molecular biology lab. Add an appropriate volume of ddH_2O to the PEI. PEI is insoluble at room temperature and so must be mixed at high temperature. Use the heated mixer on the molecular biology side, set the heater to 90^oC. Loosen the lid to allow steam to escape and **clearly label the bottle and heater** so people are aware it is hot. Use an appropriate sized magnetic stirring rod. Initially the mixture will be cloudy but eventually it will become transparent. After at least 12 hours, the mixture can be put through a 0.22 um filter to remove insoluble clumps of PEI. Take an aliquot and check the pH, which should be pH 8.0. Aliquot and store at room temperature – **low temperatures will cause the PEI to come out of solution.**

Cells: 293F, 293T and 293E cells are banked in the ORCRB 40K LN2 tank, tower D6, box 7, at various stages of suspension and serum-free adaptation. It is critical that the records of remaining vials in the LN2 freezer spreadsheet are accurately maintained. *Do not take vials from the LN2 without updating the spreadsheet and consulting Joe Illingworth: S:\Reagent Storage Info\LN2, cells and serum storage\ORCRB LN2 Storage\40K ORCRB tank*

Useful Plasmids:

-pTT BirA #2938 – secreted biotin ligase for biotinylating proteins with a biotin acceptor peptide
-nonsecreted eGFP #1733 – useful for measuring transfection efficiency

Equipment

Class II BioSafety Cabinet	Scanlaf	Mars
CO_2 incubator	RS Biotech	Galaxy R
37°C water bath	Grant	SUB6
Microscope	Leica	DMIL
Disposable haemocytometer	Immune Systems, cat# BVS100	

Trypan blue stain
V well plate (no need to be sterile)
Erlenmeyer culture flasks (vented or unvented are both fine, e.g. Corning 430421)
15 ml sterile tubes
5, 10 and 25 ml sterile pipettes
Sterile transfer pipette

8. Method

OVERVIEW – All performed in sterile hood

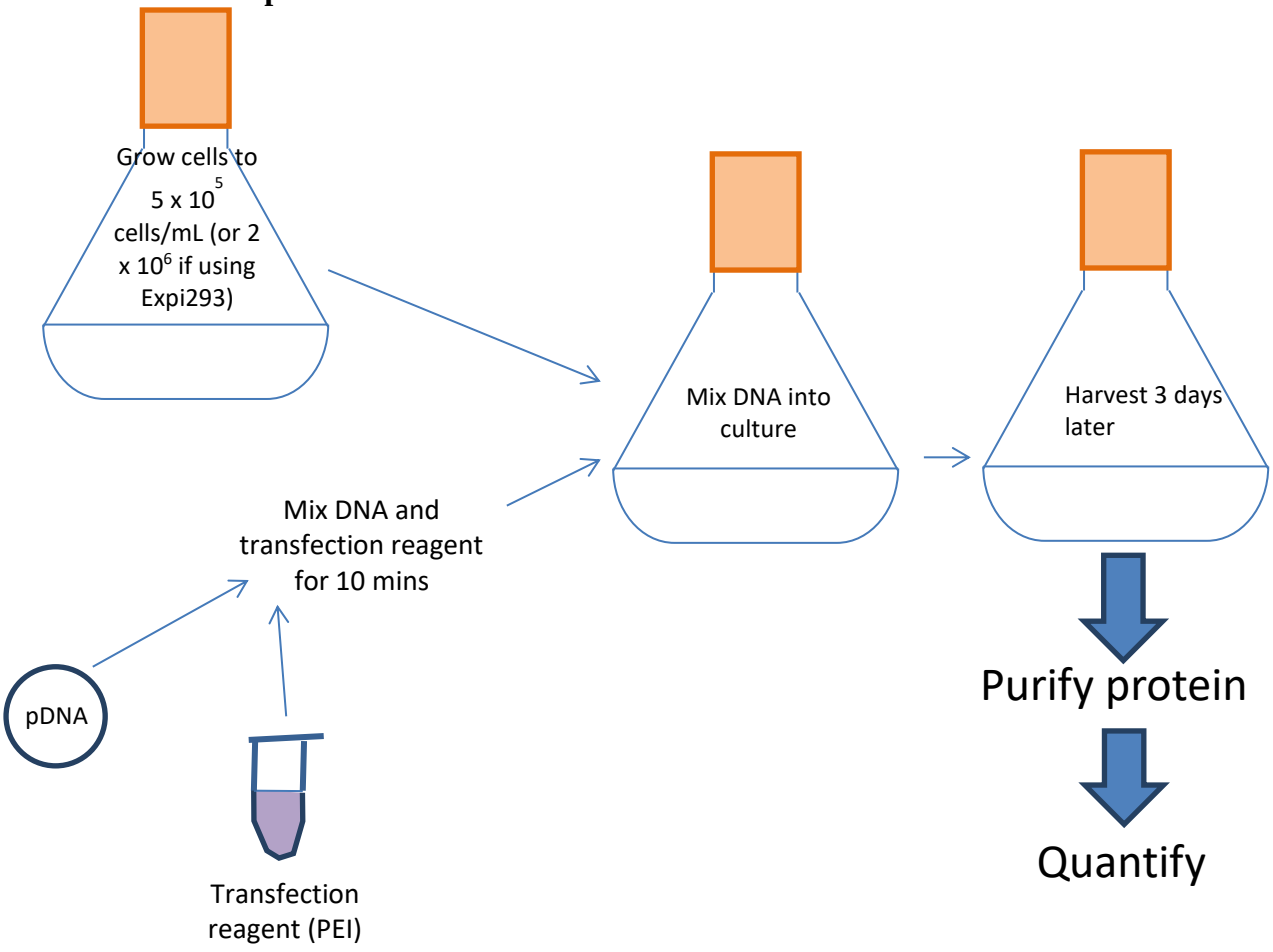

Central to the success of this procedure is the health of the cell culture. This can be fairly easily assessed microscopically: healthy cells tend to double approx every 20 hours and grow either as a single-cell suspension or small clumps of 2, 3 or 4 cells. If more than 20% of cells in a culture are in clumps of 5 or more cells, this is a sign of poor culture health and will likely result in low transfection efficiency.

8.1 Thawing and Establishing Cells

8.1.1 Store frozen cells in liquid nitrogen until ready to use. To thaw and establish cells:

8.1.2 Remove the cryovial of cells from the liquid nitrogen and thaw quickly in a 37°C water bath.

8.1.3 Just before the cells are completely thawed, decontaminate the outside of the vial with 70% ethanol. Triturate and transfer the entire contents of the cryovial into a 125 ml polycarbonate, disposable, sterile Erlenmeyer shaker flask containing 30 ml of pre-warmed FreeStyle™ 293 Expression Medium.Incubate cells in a 37°C incubator containing a humidified atmosphere of 8% CO_2 in air on an orbital shaker platform rotating at 125 rpm. Loosen the cap of the flask a quarter turn and tape into position to allow oxygenation/aeration.

8.1.4 Once the culture has reached greater than 1 x 10_6 viable cells/ml (typically 3 to 5 days), transfer the cell suspension aseptically into a centrifuge tube and vortex for 10 seconds.

8.1.5 Determine viable and total cell counts (see protocol on page 4).

Important Note: Subculture cells for a minimum of 6 days (e.g. thaw on Friday for use the following Thursday) before use in transfection experiments to allow opportunity for recovery from thawing. To subculture cells, see section 8.3.

8.2 Counting cell density

8.2.1 Prepare a sterile 2 mL stripette and pipetteboy, open up and wipe down a class II safety cabinet.

8.2.2 Take the culture flask from the incubator.

8.2.3 Take a small (<100 uL) sample from the flask using the 2 mL stripette and put into a single well of a v-well plate.

8.2.4 Return the flask to the incubator.

8.2.5 Add 20 uL of Trypan blue to a well in the V-well plate adjacent to where the cell culture was deposited.

8.2.6 Take 20 uL of the cell culture and mix with the 20 uL of trypan blue by pipetting up and down.

8.2.7 Put 20 uL of 50:50 mixed trypan blue:cell culture into a disposable cell counting chamber.

8.2.8 Count all of the cells found in one of the large blocks of 4x4 smaller squares.

8.2.9 To obtain the cells/mL value, take the number of cells counted in the 4x4 square box, and multiply by $2x10^4$.

8.3. Subculturing cells

Splitting should be done on a Monday and a Friday. For routine maintenance, cells should be seeded into a new flask each time they are split. Seed cells at a density such that they will not reach a density of $>5x10^5$ cells/mL (or $4x10^6$ cells/mL if using Expi293) before they are next

split (except before transfections). Don't split the culture so low that after one week the cell density will still be $<5x10^5$ (this is because Freestyle293 medium is light-sensitive and so should be replenished after not more than one week). It is crucial that the culture is kept at 37°C and experiences as few temperature perturbations as possible – otherwise the cells will clump. This can cause them slow down their growth-rate and become refractory to transfection.

8.3.1 Obtain a cell count (see 8.1).

8.3.2 For routine maintenance, split the cells so that they achieve a density of not more than $5x10^5$ cells/mL (or $2x10^6$ cells/mL is using Expi293) by the next splitting date. On a Friday, this means splitting the culture to ~$3.2x10^4$ cells/mL (or ≈$5x10^6$ cells/mL if using Expi293), if they'll next be looked at on Monday (assuming divisions every approx 20h). On Monday, split the culture to ~$1.6x10^4$ cells/mL (or $1.5x10^5$ cells/mL if using Expi293) .

8.3.3 At least half an hour before splitting the cells, decide on how large a culture you want to set up. As a rule of thumb, try to avoid filling a cell culture flask more than one-third of its stated volume (e.g. for a 125 mL flask, ~40mL is the max volume).

8.3.4 Take a new flask and fill it with an appropriate volume of Freestyle 293 medium (or Expi293), and add G418 at a 1:1000 if culturing 293E cells.

8.3.5 Place in the shaking incubator for 30 minutes to allow equilibration to 37 degrees.

8.3.6 At the time of seeding, the fresh medium should be the same temperature as the cell culture will be split from. If it's perceptibly cooler, it is not warm enough and you should delay the splitting.

8.3.7 Once the medium is up to temperature, turn on and wipe down a microbiological safety cabinet.

8.3.8 Take the two flasks (one containing medium, one containing culture) to the hood, and seed an appropriate volume of culture into the fresh medium.

8.3.9 Return the newly inoculated culture to the incubator immediately.

8.4 Transfecting cells

This procedure needs to be planned in advance as it can take a while to grow up a culture of suitable size. The smallest transfection volume that should be performed in flasks is 30mL. Transfection in sterile 96 deep-well tissue culture plates has been described but never performed at the Jenner Institute. This protocol assumes that the transfection *per se* will be performed on a Friday, but it could easily be shifted (e.g. make Friday day 1).

DNA guidelines

Every transfected DNA mix should contain 5% by mass of plasmid #1733. This plasmid expresses GFP and is useful for estimating transfection efficiency. To obtain sufficient DNA, at least a Maxiprep's worth of DNA is necessary, and occasionally a megaprep may be required. EndoFree prepped DNA is not essential to achieve good transfection efficiency, but it will improve cell health and can be considered as part of troubleshooting. J

On Monday (day 1)

8.4.1 On Monday, whilst performing the routine culture splitting, seed a culture that will reach $1x10^6$ cells/mL (or $4x10^6$ cells/mL if using Expi293) on Thursday. Seeding the new culture at $1.2x10^5$ cells/mL (or $0.5x10^6$cells/mL is using Expi293) should achieve this. The culture seeded on Monday should be at least 25% of volume of the planned transfection culture.

On Thursday (day 4)

8.4.2 On Thursday, approx 24hrs before the transfection, get another cell count of the culture seeded on Monday. Calculate the dilution factor needed to seed a new culture at $2.5x10^5$ cells/mL ($1x10^6$ cells/mL is using Expi293).

8.4.3 Calculate the volume of medium required to start the transfection culture. E.g. if the stock is at $1x10^6$ cells/mL, and the total planned transfection culture volume is 500 mL, prepare 375 mL of medium.

8.4.4 If using Freestyle293, prepare the transfection medium by taking Freestyle 293 medium, adding G418 solution if using 293E cells at 1:1000 and adding FCS to 1% of the final culture volume (e.g. if the final culture volume will be 500 mL, take 375 mL medium, and add 375 uL G418 solution and 5 mL FCS). If using Expi293, no addition of FCS is necessary, simply add G-418 at 1:1000.

8.4.5 Place the flask containing the medium into the incubator and allow to equilibrate to 37 degrees for at least 30 minutes, preferably an hour. This is crucial as the culture will not have time to recover from any temperature perturbations before the transfections.

8.4.6 Once the medium is up to temperature, seed it with the culture at $2.5x10^5$ cells/mL (or $1x10^6$ cells/mL if using Expi293).

8.4.7 Place the culture in the incubator. It should not be removed again until the transfection.

On Friday (day 5) – stagger this process if more than one culture is being transfected

8.4.8 For every 100 mL of culture to be transfection, warm up 4 mL of Freestyle 293 medium to **room temperature**. **Do not add 1% FCS as this can interfere with the interaction of PEI and DNA.**

8.4.9 For every 100 mL of culture to be transfected, add 66 ug of DNA to the room temperature Freestyle 293 medium (or 100ug of DNA per 100mL of culture if using Expi293). Vortex vigorously for 5 seconds. The DNA mixture should contain plasmid of interest and 5% by mass #1733. If the protein is to be biotinylated and contains a biotin acceptor peptide, also include 5% by mass plasmid #2938.

8.4.10 For every 100 mL of culture to be transfected at 100 uL of PEI to the room temperature medium/DNA mix (if using Expi293, use 200uL of PEI per 100mL of culture). Vortex vigorously for 5 seconds, and leave at room temperature for 10 minutes to allow PEI/DNA complexes to form.

8.4.11 After 10 minutes, remove the transfection culture from the incubator.

8.4.12 Add the DNA/PEI/medium mixture **dropwise** to the culture, whilst swirling. **Immediately** return the culture to the incubator.

Next Monday (day 7)

8.4.13 Turn on the fluorescence laser attached to the microscope in the cell-line tissue culture room.

8.4.14 Perform a standard cell count as in 8.2. Cell density will by now be $>1x10^6$ ($>5x10^6$ if using Expi293) and the will likely be some cell clumping. This is normal at this density, especially as PEI is toxic. Importantly, cell viability should still be >95%.

8.4.15 Dim the lights in the room, turn the stage illuminator all the way down to nothing and switch to the blue filter. If the transfection has been successful, green circles representing GFP-transfected cells will be visible.

8.4.16 Calculate the ratio of GFP+ve vs GFP-ve cells to determine the transfection efficiency. Typically 40% of cells will be GFP+ve. Less than 30% indicates a less successful transfection. >80% GFP+ve cells is a bumper transfection.

Next Tuesday or Wednesday (day 8)

8.4.17 When cell viability falls below 80% the culture should be harvested. Spin at 750g for 10 minutes to pellet the cells and decant off the supernatant (cell pellet can be discarded, or stored to test for protein retention in the cells).

8.4.18 If intending to store for more than a few hours, add a protease inhibitor cocktail and refrigerate. If intending to store for more than a few days, freeze at -20 degrees.

9. Freezing Cells

Introduction

You may freeze FreeStyle™ 293-F cells directly in FreeStyle™ 293 Expression Medium. When freezing the FreeStyle™ 293-F cell line, we recommend the following:

- Freeze cells at a density of 5-8 x 10^6 viable cells/ml.
- Use a freezing medium composed of 90% fresh FreeStyle™ 293 Expression Medium and 10% DMSO.

Guidelines to prepare freezing medium and to freeze cells are provided in this section.

Preparing Freezing Medium

Prepare freezing medium immediately before use.

1. In a sterile, conical centrifuge tube, mix together the following reagents for every 1 ml of freezing medium needed:
    - FreeStyle™ 293 Expression Medium 0.9 ml
    - DMSO 0.1 ml
2. Filter-sterilize the freezing medium and place the tube on ice until use.

Discard any remaining freezing medium after use.

Freezing Cells

Before starting, label cryovials and prepare freezing medium. Keep the freezing medium on ice.

1. Grow the desired quantity of FreeStyle™ 293-F cells in shaker flasks, harvesting when the cell density reaches 0.5 to 1 x 10^6 viable cells/ml. Transfer cells to a sterile, conical centrifuge tube.
2. Determine the viable and total cell counts (see protocol on page 4) and calculate the volume of freezing medium required to yield a final cell density of 5-8 x 10^6 viable cells/ml.
3. Centrifuge cells at 100 x g for 5 minutes at room temperature and carefully aspirate the medium.
4. Resuspend the cells in the pre-determined volume of chilled freezing medium.
5. Place cryovials in a microcentrifuge rack and aliquot 1 ml of the cell suspension into each cryovial.

6. Freeze cells in an automated or manual, controlled-rate freezing apparatus following standard procedures. For ideal cryopreservation, the freezing rate should be a decrease of 1°C per minute.
7. Transfer frozen vials to liquid nitrogen for long-term storage.

Note: You may check the viability and recovery of frozen cells 24 hours after storing cryovials in liquid nitrogen by following the procedure outlined in **Thawing and Establishing Cells**

Scaling Up Transfections

Can be performed with linear increases of each ingredient. Largest transfection volume attempted here is 500 mL.

APPENDIX 3

1.0 Jenner Laboratory Protocol Number: J314

2.0 Version Number v1.0

3.0 Culture and transfection of Expres2ion Biotech S2 cells

4.0 Other documents:

5.0 Definitions:

6.0 Objective

7.0 Reagents/Equipment

- Media: Ex-cell 420 Insect serum free medium from SAFC Biosciences, with glutamine, cat no. 14420C.
    - Always add pen-strep to the media, even while producing.
- FBS: GibcoBRL, mycoplasma and virus-screened. Heat inactivated. Origin: Australian. Cat no. 10100-147.
    - Use 10% when first thaw cells, to keep them happy. They are much happier in FBS. However, want to remove FBS when transfect or when producing cells.
    - When opening a new bottle of FBS, first thaw it in the fridge. Then aliquot into 40 ml aliquots in Falcon tubes and re-freeze all but one. Keep the current stock in the fridge.
- Zeocin: selection for pExpress2.1 vector. Used at 1500 µg/ml (or 2000 µg/ml if necessary). Life Technologies is the only vendor. Stable for 1 month at 4°C.
    - Zeocin binds to DNA, and is more toxic than G418 which binds to ribosomes.
    - Rh5 is in the pExpress2.1 (zeocin) vector.
- Pen strep: Biological Industries. 10,000 U/ml penicillin, 10 mg/ml streptomycin. Use 10 ml in 1 L media (add when open a fresh bottle of media).
- G418: selection for pExpress2.2 vector. Rh5 is not currently in this vector.
- Transfection reagent: proprietary lipofectamine-based reagent. Sold by Expres2ions, in a 1x or a 5x concentration. Stable for years at 4°C. (Kathryn has 1 ml of 5x transfection reagent.)
- DMSO: Sigma HybriMax, cell-culture tested, D2650.
- T25 and T75: close lids all the way; they have enough air. Don't use vented lids, as

too much evaporates. Do not have a filter.
- Corning flasks: use vented lids. There is a filter in flasks. They are not baffled.
- Filter tips: only use filter tips

8.0 Method

I. **General cell handling:**

- Transfect in T25s, transfer to T75s, grow in increasing sizes of flasks (125, 175, up to 1 L). Optimal volumes for each of these containers is given in the chart below. When transferring cells from T-flask to shake flask no trypsin is required, merely tap T-flask smartly on the bench top to loosen the cells and transfer by pipetting.

Flask	Optimal Vol.	Min Vol.	Max Vol.	Optimal rpm
RK125	25	20	30	115
RK250	50	30	60	115
RK500	100	60	150	115
RK1000	200	150	300	115
RK2000	400	300	550.00	130

- Shake smaller flasks at 115 rpm, and RK2000 (2 L) flasks at 130 rpm. These values are given in the above table as well. Don't shake faster than 150 rpm, as the flasks will fall off!

- Keep all cultures at 25°C. Can also keep at 23°C or 27°C (or even above 30°C to stress the cells; the promoter is part actin and part heat shock promoter, which is stress induced).

- Split cells every Monday and Friday. In general, the Friday (3-day) split is by dilution, whereas the Monday split (4-day) is by centrifugation and resuspension in completely fresh media. (If you centrifuge and change the medium 100% then you can let them grow for 4 days (Mon-Fri) but when you dilute them, they are rarely left to grow for more than 3 days (Friday to Monday). The only exception is in cells undergoing selection, which have 1-3 ml removed and replaced, as complete media change would kill them. The cells have no complete media changes before freezing (cells don't like it; can if you absolutely have to...). If cells are going into production, the Monday split by centrifugation is into minus FBS media in a fresh flask.

- Selection is with zeocin or G418 (see below). You want to select but not too strongly, as you don't want to select cells that are just good survivors and not good producers. As it is you end up with a polyclonal population, some of which produce better than others.

- Looking at cells under the microscope:
    - The cells are approximately 9-10 um diameter (approximately half the diameter of Sf9 cells, which have a diameter about 18 um).
    - Happy cells will be of a similar size, and round.
    - Unhappy cells will be thinner, and will stick to the bottom of the flask. We

looked at unhappy cells which were transfected 2 days ago, with selection added yesterday. After 2 days, half of the cells of the GFP control are green.
    - They change size (bigger and smaller) after transfection. They do get a bit bigger probably while they are producing protein.

- The cells are tested for mycoplasma and spiroplasma by sending to different companies. The cell stocks we have will have been mycoplasma and spiroplasma tested.

II – reagents section- moved above

III. **Cell counting**:

1. Mix cells with 0.4% trypan blue (working solution in PBS) 1:1; e.g. 20 µl cells + 20 µl 0.4% trypan blue. For higher concentrations of cells, mix 20 µl trypan blue + 15 µl 1xPBS + 5 µl cells.
2. Multiply the number of cells in one large square by 10^4 to give the number of cells in 1 ml. Make sure to account for the trypan blue dilution.

IV. **Cell splitting**

1. If happy, the cells double approximately every 24 hours, though can grow considerably slower.
2. Split on Fridays and Mondays, giving a 3-day and a 4-day split. Generally, change media on Monday, and dilute on Friday.
3. Make sure media is at room temperature before splitting so as not to shock the cells.
4. Normally cells have grown to about 30 million cells/ml by the day of splitting.
5. When cells are growing in FBS, split to 5 million cells/ml. Without FBS, split to 8 million cells/ml. In T-flasks the cells are split to 2 million cells/ml (presumably because they don't get aerated).
6. To dilute, the cell count must be high enough. 80% fresh media is required. Always change the media after 4 days.
7. On Mondays, can sometimes split and return to the same flask. When you can see a ring of dead cells around the base of the flask, it's time to change. Likewise, if you are removing FBS, use a new flask.

V. **Stable transfection**:

- Overview of process:

1. The cells need to have been split with a complete change of medium (SFM/PenStrep/FBS) the day before transfection. (Keep FBS in until the day of transfection.)
2. Typically split Monday, transfect Tuesday, add selection on Wednesday. Check on Friday to see if extra medium is required.
3. Transfect in T25 at 2 million cells/ml, in 5 ml.
4. Also transfect GFP-containing plasmid, to assess transfection efficiency in a fluorescent microscope.
5. Select for 3 weeks in zeocin (pExpress2.1) or G418 (pExpress2.2). Normal concentration of zeocin is 1500 µg/ml (recently 2000 µg/ml). Always select in the presence of FBS to keep the cells happy. If it's necessary to select in minus FBS media use a lower concentration of zeocin eg. 500-700ug/ml.
6. During selection, change media on Mondays and Fridays as usual, or several times a

week if cells look unhappy. To change media, just remove 1-3 ml (usually 2 ml) and add the same volume of media containing zeocin back. (Keep cultures in about 6 ml.)

7. Perform a kill curve meanwhile. Want untransfected cells to die (and be completely dead after 3 weeks). Recently, they have found that untransfected cells survive 3 weeks in 1500 μg/ml zeocin so they have been using 2000 μg/ml zeocin in the latest batches of cells (since Christmas).
    a. Note: the untransfected cells Kathryn has in the freezer are the old cells, and hence 1500 μg/ml should be sufficient.
8. After 3 weeks, transfer to a T75 to begin expansion of the cells.

- Reagents required:
    - Serum free media (+Pen-strep)
    - 100% FBS
    - Transfection reagent: 1x or 5x
    - DNA: 12.5 μg per transfection. Use maxiprep or even midiprep, endotoxin-free. Minimum concentration required is about 200 ng/μl, ideal is 1ug/ml. They perform maxipreps in the molecular biology lab, then heat inactivate the DNA for 5 minutes at 95°C. In addition to constructs, also transfect the GFP control plasmid (Kathryn has the plasmid).
    - Cells: 5 ml at 2 million cells/ml
    - T25 flask- **plug seal** cap
    - 15- and 50-ml Falcons
    - Filter tips

- Detailed protocol:

1. The S2 cells for transfection are thawed every 2-3 months. They are passaged every Monday and Friday, and discarded after 2-3 months or if they look unhealthy.
2. The day before the transfection (usually Monday), split the cells by centrifugation and resuspension in 100% fresh media containing FBS. [Centrifuging the cells rather than diluting them the day before transfection is useful as it stresses the cells a bit—they will be centrifuged two days in a row—which increases the efficiency of tranfection; furthermore, if you simply diluted them, there would be differing amounts of cell debris which would cause variations among transfections.]
3. 20-30 minutes before beginning transfection, get the serum-free media and transfection reagent out of the fridge to come to room temperature. (If opening a new bottle of media, add 10 ml Pen/strep).
4. Allow 2 million cells/ml in 5 ml for each transfection.
5. Aliquot the volume of cells required into a 50-ml Falcon.
6. Centrifuge 1500 rpm for 3 minutes (5 minutes if lots of cells) at 25°C.
7. During centrifugation, get a fresh T25 and label. Also retrieve a 15-ml Falcon tube for mixing.
8. After the centrifugation, pour or pipette off the supernatant (be careful; the cells are not very heavily pelleted and will start sliding if pouring).
9. Resuspend the cells to 2 million cells/ml in media with Pen/Strep but without FBS. Resuspend very gently, careful not to introduce any bubbles. Do as little pipetting up and down as necessary.
10. Pipette 5 ml of cells into the 15-ml mixing tube for each transfection—invert cells first to re-mix, as they settle quickly. Also pipette slightly more than 5 ml (approx. 5.3-5.4 ml) to account for the extra media which gets stuck in the pipette.
11. Add transfection reagent to cells, either 250 μl of 1x transfection reagent, or 50 μl of 5

x transfection reagent. Pipette onto the side of the Falcon tube, and let it run down the side of the tube. Tip/invert the tube 1-2 times. (If performing more than one transfection, can add transfection reagent to all tubes of cells—then for each in turn, add DNA and pour into T25.)

12. Add 12.5 μg DNA to the tube. Add the DNA to the side of the tube and allow to slide down the side. Invert the tube a few times (gently).
13. Pour the mixture into the labeled T25. Close the lid all of the way—it has enough air.
14. Place T25 flasks in the incubator (without shaking) for 2-4 hours. After this time, add 0.75 ml of 100% FBS (all the above steps done in SFM), bringing the total volume to 6 ml. This is 12.5% FBS, rather than 10%, but it works fine.
15. Return the T25s to the incubator and leave overnight.
16. Don't select until 24 hours after transfection (they need 24 hours to recover). Add selection (1500 μg/ml zeocin, or more recently 2000 μg/ml), straight to the cells.
17. Check the cells under the microscope the day after transfection:
    a. Even cells with no transfected DNA, just transfection reagent, are looking unhealthy; uneven surfaces, cracked (dying), different shapes.
    b. Can calculate transfection efficiency using GFP transfection and a fluorescence microscope. Dilute the cells and count in the microscope. Can be anywhere from 30-80% efficiency, commonly 50% efficiency. As long as the GFP transfection was performed at the same time as the other transfections, it is a good indicator of the transfection efficiencies for all transfected constructs.
18. Leave for 3 weeks in zeocin- and FBS-containing media, changing media 2-3 times a week by dilution (to keep conditioned media in flask).
19. To change media (as usual, on Mondays and Fridays, or every 3-5 days), whack the T25 once on the desk, flat. Count the cells (the cells are hard to count in zeocin, so they count by "eye"). Then pipette up and down and remove 2-3 ml of media, and return 2-3 ml fresh media containing zeocin and FBS. Usually 2 ml.
    a. Always select with FBS. If select without FBS, only use 500-700 μg/ml zeocin instead of 1500-2000 μg/ml. (Usually, have FBS+zeocin or neither; only exceptions are just after thawing, or when growing untransfected S2 cells—only have FBS.)
20. Wait until 90% viable, approximately 3 weeks. Also perform a kill curve, to be assured that no untransfected cells are alive at the end of 3 weeks. After three weeks, the cells in the GFP control transfection should fluoresce 100%.
21. After three weeks, split the culture into 1) a RK125 flask with continued selection for freezing (keep selecting until you freeze them); and 2) a RK125 flask for production/growth, with removed FBS and selection.

VI. **Transient transfection**:

- Transients of many constructs--take samples for a Western after 4 days. Then you can choose the best expressor to make stable cell line.
- Do without FBS. More cells and DNA needed.
- Need 5x transfection reagent.
- Do each transient transfection in 10 ml volume, in a 50 ml Falcon.
- Need 50 ml Falcon holder in the incubator, so that the Falcons can be shaken faster than 150 rpm—at 200 rpm, at a 45° angle.

VII. **Cell freezing/thawing**:

Freezing:

- Expres2ions generally freeze three 1-ml vials of each protein to begin with. When one is thawed, an additional 10 vials are made.
- There is no difference in expression after thawing.
- 250 million cells in 1 ml per vial. When thawed (in 24 ml), they will be at a density of maximally 10 million cells/ml (in practice more like 5-8 million cells/ml, since about half of the cells die in the freezing process).

Protocol:

- Always freeze cells after 3 days since last split (usually freeze on Mondays, after Friday split), as they will be in log phase then.
- Three days before freezing, change the media of the cells (media/PenStrep/FBS/zeocin) by dilution only. Do not spin down and resuspend in completely fresh media containing FBS/zeocin (as they get unhappy; keep them in conditioned media, without exposure to the centrifuge). The cells will thus be in zeocin when they are frozen.
- Before freezing, pre-chill a Stratacooler in the fridge.
- Prepare freezing media in a 50-ml Falcon tube.

Freezing media: 40% media (containing PenStrep)
50% FBS
10% DMSO (Sigma)

- In practice, usually add a little more DMSO, and a little less medium (in case some DMSO gets stuck in the pipette). E.g. in 10 ml: 5 ml FBS, 1.1 ml DMSO, 3.9 media.
- Place freezing media in the fridge to chill.
- Put 1.8-ml freezing vials into the -20°C freezer.
- Count the S2 cells. For the first freezing of a new construct, will make 3 vials with 250 million cells in each (later, will make 10 vials). Prepare a Falcon tube containing 250 million cells multiplied by the number of vials to freeze. Thus, if freezing three vials, put 750 million cells into the Falcon tube.
- Centrifuge the cells for 3 minutes, 1500 rpm (300xg), at 4°C. (The temperature should be 4°C if there are lots of cells to freeze—keep them cold.) The DMSO is toxic to the cells, but helps to keep them alive during freezing; thus the longer they're alive at room temperature before freezing the more difficult it is for them to recover. Holding them on ice slows their metabolism and reduces the toxic effects of DMSO.
- Get the step freezer box ready in the hood.
- Pour the media off of the cells, careful not to pour the cells off as they weren't spun down very hard.
- Add 1 ml freezing medium per vial to be made. In practice, actually add less by about 0.5-1 ml, to account for the volume of the cells. Thus, if making 10 vials, add 9-9.5 ml freezing media. Add the media very gently, but quickly as they now have DMSO in them. Be especially careful not to introduce bubbles. Pipette up and down as little as possible; a few small lumps are OK.
- Take up the entire volume of cells and aliquot 1 ml into each vial, careful to not introduce bubbles.
- Quickly close the vials, place them in the step freezer and then run them to the -80°C freezer.

- Leave in the -80C freezer for 48 hours. Then keep in liquid nitrogen for years. (They are also fine for 1-2 months at -80°C).

Thawing:

- Typically thaw cells on Monday, allowing them to be monitored all week, and split as normal on Friday.
- Before thawing, allow media/pen strep/FBS to come to room temperature (or ideally 25°C).
- Prepare a fresh RK125 flask with 23 ml of pre-warmed media containing PenStrep and 10% FBS. To this, the 1 ml of cells will be added. (Final volume 24 ml; could also have a final volume of 25 ml, but it's better to aim for a bit higher density after thawing. If they were known to be especially unhappy when frozen could add to 20mls media/FBS.)
    - Once thawed, they will hopefully be at around 5-8 million cells/ml (they were at 250 million/ml in 1 ml, resuspended in 24 ml; but approximately half of them are dead). Usually about 60% viability.
- Thaw the cell line using hands, VERY gently rolling them together. Don't let the cells get too warm, and don't invert the tube. Alternatively, could place in 25^{o}C water bath.
- When, by gently tilting the vial, you can see the liquid moving, then it's fine to continue (small ice blocks are OK, as they will soon thaw; don't want big ice blocks).
- In the hood, on the slowest (long) pipette setting, pipette up 1 ml cells, without introducing any bubbles. Leave the last little bit.
- Tilt the flask, put the pipette tip all the way into the media, and slowly release the 1 ml of cells. For the last few bubbles in the pipette, raise the pipette tip out of the media, and release the bubbles onto the side of the flask, 1 cm above the media.
- Pipette up 1 ml of media and return it to the vial to remove cells which were settled onto the bottom of the vial. Again, avoid bubbles. Pipette this 1 ml into the media as before.
- Don't even swirl the cells. Leave them for 5 minutes in the hood to acclimatize, and then place them gently into the incubator.
- Leave for a week, monitoring the viability and cell count every day.
- The timing of first splitting will depend on how the cells behave. There are major variations in freeze vials, with some easy to thaw and quick to recover, and others hard to thaw and slow to recover. It depends on how good the freezing was. In general:
    - If the viability continues to increase after day 2, then the cells can probably be left until Friday (4 days) before splitting by centrifugation and changing the media 100%.
    - If the viability drops after 2 days, then change the media 100% after two days, not four. In this case, spin the cells at a lower speed (1300 rpm) and a shorter time (2 min), to be as gentle as possible while removing as many dead cells and as much debris as possible.
- Typical profile of (fast-recovering) newly thawed cells:
    - Day 1 (thaw): 6million cells/ml, 60% viability
    - Day 2: 6 million cells/ml; 70%
    - Day 3: 8 million cells/ml; 90%
    - Day 4: Split back to 8 million cells/ml

- For the first splitting, spin cells down and resuspend in completely fresh SFM/PenStrep/FBS. Split to 8 million/ml. This will remove residual DMSO, and also dead cells.
- For the next few splits, return cells to 8 million cells/ml by dilution.
- If the cells are to be kept in FBS, start splitting to 7 million cells/ml, then 6 million cells/ml, then 5 million cells/ml.
- If the cells are to be taken out of FBS, count the cells, then split to 8 million cells/ml in media lacking FBS.
- After 3 months, discard the cells and thaw a new vial.

VIII. **Production from shake flasks**

- Batch run: can make 500 ml in Shaker flasks. Harvest after 3-4 days (can use a Western to ascertain the best day to harvest; it is usually 4 days, unless it looks bad after 3 days…)
- A cell line, once thawed, can be used for 2-3 months of production. Any wild-type cells left after selection will grow in number over time, leading to loss of productivity over time. After 3 months, thaw a new vial.
- It takes about 2 weeks to get the cells growing after thawing.
- Always split cells back to 8 million/ml when setting up a production run.
- To harvest, spin the cells hard (maximum of the centrifuge) and then filter with a 0.22 um filter. Their filters contain PES membrane (Corning), which has low protein binding.
- If the cells are going to be reused, then only spin at 1500 rpm as normal, and then resuspend in fresh media at the desired concentration. The supernatant from the spin can then be centrifuged at full speed.

APPENDIX 4

1.0 Jenner Laboratory Protocol Number: J119

2.0 Version Number: 3.1

3.0 Title: Detection of epitope-tagged proteins by western blotting.

4.0 Other Documents

MSDS	refer to MSDS for the relevant safety information on the individual reagents: \\Imsnw3_jenner_server\jenner\hill_group\Safety\COSHH assessments\Manufacturers material safety data sheets
C036	Protein gel electrophoresis

5.0 Definitions

PPE	Personal protective equipment
DNA	Deoxyribonucleic acid
SDS	sodium dodecyl sulphate
PAGE	Poly-acrylamide gel electrophoresis
BCIP/NBT	5-Bromo-4-Chloro-3'-Indolyphosphate p-Toluidine Salt / Nitro-Blue Tetrazolium Chloride
ECL	chemiluminescence

6.0 Objective

To test for protein expression by SDS-PAGE followed by western blotting. The primary antibody may target an epitope tag engineered into the protein sequence. This protocol describes the detection by primary antibody, signal amplification by secondary antibody and then visualisation by either BCIP/NBT (colourimetric) reagent or ECL (chemiluminescence).

7.0 Reagents

Anti-penta-His monoclonal antibody	Qiagen	34660
Sheep Anti-mouse-HRP	Amersham	NA931V
Donkey anti-mouse-AP	Jackson labs	715-055-150

Colorplus Prestained Protein Ladder, Broad Range (10-230 kDa)	NEB	P7711S
10% SDS	Gibco	15553-035
Elix H_2O		
1 x PBS (in Elix water) pre-chilled	Oxoid	
Tween 20	Sigma	P2287
Laemmli sample buffer	Made in-house	
β-mercaptoethanol	Sigma	M3148
Methanol	Sigma	34860
Precast minigels	Pierce	
Nitrocellulose/Filter Paper Sandwiches, 0.45 μm, 7 x 8.5 cm, 50 pack	Bio-Rad	162-0215
2 ml screw caps tubes	App Woods	AZ037
Microcentrifuge	Hettich	
Hot Block	Techne	
Miniprotean 3 cell kit	Biorad	
Power pack argo	Anachen	
BCIP/NBT	Sigma	B5655
Ponceau S Staining Solution	Sigma	P7170
Digital camera		
10% sodium azide solution		

Reducing Laemmli buffer

	For 20 ml:
125 mM Tris-HCl pH6.3	2.5 ml
20% v/v glycerol	4 ml
4% w/v SDS	0.8 g
20 mg/ml Brilliant Blue	400 mg
10% v/v β–mercaptoethanol	2 ml
Make up to 20 ml with 18Ωohm water	

Filter (0.45 μm) to remove any Brilliant Blue crystals.
(for non-reducing buffer, omit the β-mercaptoethanol).

Anti-penta-His antibody
Dilute lyophilised antibody with 500 μl dH_2O (0.2 mg/ml)
Store in 25 μl aliquots at -20°C
Working concentration = 1:1000 in 3% BSA in PBS.
For long-term storage add sodium azide to a final concentration o f 0.02% w/v

Tris-HEPES-SDS Running Buffer (10X)

Tris Base (MW = 121)	121 g
HEPES (free acid MW = 238)	238 g
SDS (MW = 288)	10 g
Add ultrapure water to 1 L	

• Before use dilute 10-fold with water. The pH of the 1X buffer should be ~8.0; do not adjust pH.

• Final composition of the 1X buffer is 100 mM Tris, 100 mM HEPES, 1% (~3 mM) SDS, pH 8.0.

Transfer Buffer (1L)

Tris base	6 g
Glycine	30 g
Methanol	200 ml
Elix H_2O	up to 1 litre

Blocking buffer (50 ml)

BSA	1.5g
PBS	up to 50ml

Washing buffer (1 L)

Tween 20	1 ml
PBS	up to 1 L

8.0 Equipment

Electrophoresis tank
Genie blotter or BioRad Trans-Blot Turbo
Power pack for electrophoresis tank
Large polystyrene box to contain blotting equipment and ice
Pipettes and tips
Orbital shaking platform

9.0 Method

9.1 Sample preparation

Harvest supernatant from S2 cells 3 days after induction of expression and transfer to a suitable container.
Pellet cells (1000 rpm, 5 min, RT)
Transfer supernatant to fresh tube
Add 4x reducing laemmli buffer to samples.
Heat to 95°C for 5 min.
Allow to cool.
Store at -20°C until ready to run gel.

For each gel, either use 10 µl of positope and heat this in the same manner as the samples, or use a previously qualified protein sample.

9.2 Running SDS-PAGE

a) Fill the electrophoresis tank up to the relevant fill line with Tris-HEPES-SDS running buffer.
b) Place the Pierce pre-cast gel/s in the gel holder, using a blanking plate if only one gel is being run.
c) Fill the central reservoir with 1 x Tris-HEPES-SDS running buffer.
d) Use a p200 pipette to rinse the wells with running buffer.
e) Load samples and molecular weight markers.

f) Close tank.
g) Run at 70 V until the samples have entered the gel, then increase the voltage to 100 V. Run time should be approximately 45 min.

9.3 Transfer method (BioRad Trans-Blot Turbo System)

a) Use pre-soaked Nitrocellulose transfer packs as described in the User Manual. Copy stored here: S:\PROTOCOLS\Protein expression\Trans-Blot Turbo System manuals (Read before use!)
b) Assemble transfer pack with SDS gel as described. Load into cassette. NOTE: Midi transfer packs can run 2 mini gels side by side and are more cost effective than running 2 mini transfer packs. Ensure no buffer is leaking.
c) Load cassette(s) into Trans-Blot Turbo unit. Switch on and select appropriate running programme (15 or 30 minute standard transfer is suitable for most gels. Only use 7 minute turbo programme if using BioRad TGX pre cast gels)
d) When run is finished, carefully disassemble cassette and transfer pack (NOTE: if running a fast programme, this can get quite hot). Remove membrane (use forceps) to a clean tip box lid for the next stage.
e) Without exception, carefully clean the cassette and electrode surfaces with distilled water. Dry thoroughly before re-assembling. Check the cassette contacts and visually inspect the electrode contacts within Turbo Blot unit for any buffer residue build up. If noted, clean as described in manual and Notification letter (S:\PROTOCOLS\Protein expression\Trans-Blot Turbo System manuals).

9.4 Blocking and antibodies

f) Wash the membrane twice for 10 min each in PBS.
g) Block the membrane for 1hr at R/T in 3% BSA/PBS, on the shaking platform.
h) Wash membrane 2 x 10 min in PBS-T.
i) Wash membrane for 10 min in PBS.
j) Incubate in 20 ml 1° antibody for 1 hour RT (anti-His Ab 1:1000 in blocking buffer).
k) Wash 2 x 10 min in PBS-T.
l) Wash 1 x 10 min in PBS.

Incubate with secondary antibody solution for 1 hour at RT. (Donkey anti-mouse-AP, diluted 1:3000 in blocking buffer - 6.7 µl in 20 ml)

m) Wash 4 x 10 min with PBS-T.

9.5 Development

a. Dilute 1 SIGMAFAST BCIP/NBT tablet in 10 ml water (vortex to dissolve)
b. Lay the nitrocellulose blot on some Saran wrap and pipette the BCIP/NBT solution carefully on top, ensuring it is fully covered.
c. Develop for 5 – 10 min.
d. Rinse with water.
e. Photograph or scan.
f. Dry and store away from light.

APPENDIX 5

Appendix 5-1: ADRB activity in cohort prior to the 2009 transmission season

Sample	Log_{10} RLU_p	Sample	Log_{10} RLU_p	Sample	Log_{10} RLU_p	Sample	Log_{10} RLU_p	Sample	Log_{10} RLU_p	Sample	Log_{10} RLU_p	Sample	Log_{10} RLU_p
KN0003	-0.89	KN0333	-0.91	KN0490	-0.86	KN0631	-1.28	KN0835	-1.31	KN0982	-1.31	KN1162	-0.86
KN0008	-0.76	KN0335	-1.20	KN0495	-1.04	KN0639	-0.43	KN0859	-1.12	KN0983	-1.42	KN1163	-1.10
KN0015	-0.44	KN0337	-0.95	KN0504	-1.17	KN0640	-0.58	KN0864	-0.99	KN0992	-0.69	KN1169	-0.99
KN0018	-0.95	KN0340	-1.26	KN0506	-0.97	KN0644	-0.57	KN0865	-1.27	KN0993	-1.30	KN1172	-0.93
KN0020	-1.03	KN0342	-1.13	KN0509	-0.77	KN0648	-0.94	KN0866	-0.59	KN0995	-0.96	KN1173	-0.92
KN0025	-0.97	KN0344	-1.28	KN0510	-0.58	KN0649	-0.39	KN0869	-1.13	KN1002	-0.89	KN1176	-0.75
KN0028	-1.17	KN0348	-1.15	KN0512	-1.35	KN0653	-0.53	KN0878	-0.55	KN1004	-1.08	KN1183	-1.01
KN0034	-1.12	KN0351	-0.96	KN0516	-0.94	KN0654	-0.91	KN0879	-1.15	KN1005	-1.00	KN1189	-0.72
KN0035	-1.16	KN0358	-1.02	KN0517	-1.33	KN0658	-1.33	KN0884	-0.88	KN1008	-1.38	KN1190	-0.79
KN0046	-1.20	KN0359	-1.28	KN0520	-1.18	KN0659	-1.45	KN0887	-1.08	KN1009	-1.35	KN1191	-0.50
KN0048	-1.26	KN0361	-1.29	KN0522	-0.96	KN0662	-1.22	KN0894	-1.06	KN1022	-1.04	KN1192	-0.85
KN0050	-1.12	KN0373	-1.03	KN0524	-1.29	KN0664	-0.68	KN0900	-1.34	KN1026	-1.05	KN1195	-0.47
KN0068	-1.41	KN0385	-0.76	KN0529	-1.15	KN0683	-0.79	KN0901	-1.38	KN1029	-1.02	KN1197	-1.03
KN0069	-0.81	KN0386	-0.64	KN0533	-1.38	KN0687	-0.70	KN0903	-0.93	KN1031	-0.98	KN1204	-0.85
KN0073	-0.74	KN0391	-0.95	KN0534	-0.96	KN0703	-0.94	KN0924	-1.27	KN1032	-0.57	KN1205	-0.97
KN0084	-1.23	KN0392	-1.22	KN0538	-1.08	KN0705	-1.08	KN0925	-0.64	KN1034	-0.98	KN1215	-0.47
KN0086	-1.12	KN0395	-1.40	KN0539	-1.18	KN0708	-0.88	KN0926	-1.15	KN1047	-1.13	KN1229	-1.17
KN0095	-0.93	KN0403	-1.41	KN0549	-1.25	KN0726	-1.07	KN0929	-0.91	KN1048	-0.92	KN1237	-0.68
KN0127	-1.22	KN0410	-1.17	KN0554	-1.44	KN0735	-1.25	KN0930	-0.86	KN1051	-0.48	KN1238	-0.47
KN0134	-0.90	KN0414	-0.46	KN0556	-1.11	KN0739	-0.55	KN0931	-0.80	KN1059	-1.02	KN1256	-1.12
KN0305	-1.31	KN0416	-1.11	KN0580	-1.33	KN0758	-1.37	KN0938	-0.04	KN1060	-0.84		
KN0306	-1.23	KN0420	-0.68	KN0582	-1.42	KN0759	-1.24	KN0939	-1.04	KN1084	-1.10		
KN0307	-1.03	KN0426	-1.31	KN0585	-1.41	KN0760	-0.88	KN0946	-1.05	KN1087	-0.92		
KN0308	-1.26	KN0428	-0.89	KN0588	-0.81	KN0761	-1.02	KN0947	-1.05	KN1088	-0.97		
KN0309	-1.40	KN0435	-1.19	KN0589	-1.15	KN0767	-1.19	KN0953	-0.98	KN1098	-0.96		
KN0310	-1.25	KN0440	-1.19	KN0595	-1.14	KN0776	-1.21	KN0954	-0.60	KN1105	-1.07		
KN0312	-1.14	KN0444	-0.71	KN0602	-1.33	KN0778	-1.16	KN0958	-1.06	KN1106	-0.89		
KN0313	-0.77	KN0446	-1.16	KN0605	-0.92	KN0785	-1.16	KN0961	-0.80	KN1108	-0.99		
KN0314	-1.22	KN0449	-1.27	KN0609	-1.24	KN0786	-1.41	KN0963	-0.97	KN1109	-0.91		
KN0317	-1.03	KN0450	-1.07	KN0613	-0.92	KN0788	-0.81	KN0964	-1.34	KN1112	-0.93		
KN0322	-0.81	KN0483	-1.10	KN0614	-0.09	KN0789	-0.83	KN0971	-0.58	KN1116	-0.87		
KN0323	-0.88	KN0484	-1.21	KN0619	-0.46	KN0793	-0.47	KN0973	-1.22	KN1123	-0.63		
KN0324	-1.03	KN0485	-0.95	KN0621	-0.98	KN0803	-0.99	KN0976	-0.21	KN1129	-0.97		
KN0330	-1.02	KN0487	-0.77	KN0626	-1.08	KN0804	-1.48	KN0978	-1.26	KN1133	-0.97		
KN0332	-1.19	KN0489	-1.05	KN0628	-0.56	KN0830	-1.38	KN0979	-1.39	KN1147	-1.06		

Appendix 5-2: ADRB activity in cohort prior to the 2011 transmission season

Sample	Log_{10} RLU_p	Sample	Log_{10} RLU_p	Sample	Log_{10} RLU_p	Sample	Log_{10} RLU_p	Sample	Log_{10} RLU_p	Sample	Log_{10} RLU_p	Sample	Log_{10} RLU_p
KN0001	-1.21	KN0323	-1.15	KN0450	-1.23	KN0628	-0.70	KN0844	-1.41	KN0992	-0.86	KN1183	-0.87
KN0003	-1.12	KN0324	-1.25	KN0483	-1.06	KN0631	-1.45	KN0859	-1.07	KN0993	-1.49	KN1189	-0.46
KN0007	-0.61	KN0330	-1.07	KN0484	-1.14	KN0639	-0.99	KN0864	-0.89	KN0995	-0.95	KN1191	-0.46
KN0008	-0.66	KN0332	-1.16	KN0485	-0.59	KN0640	-1.30	KN0865	-1.14	KN0997	-1.38	KN1192	-1.00
KN0015	-0.42	KN0333	-0.61	KN0487	-0.93	KN0644	-1.04	KN0866	-1.22	KN1002	-0.55	KN1195	-0.27
KN0018	-0.75	KN0334	-1.33	KN0495	-0.94	KN0648	-1.33	KN0869	-1.23	KN1004	-1.09	KN1197	-0.67
KN0028	-1.00	KN0335	-1.29	KN0504	-1.15	KN0649	-0.10	KN0878	-0.56	KN1009	-1.00	KN1204	-0.94
KN0034	-0.93	KN0337	-0.47	KN0506	-1.07	KN0653	-0.23	KN0879	-1.26	KN1019	-0.90	KN1205	-0.88
KN0035	-1.05	KN0339	-1.28	KN0509	-0.78	KN0654	-1.19	KN0884	-1.26	KN1022	-0.84	KN1256	-0.89
KN0042	-0.80	KN0340	-1.28	KN0510	-0.55	KN0658	-1.39	KN0887	-1.14	KN1026	-1.43		
KN0046	-1.07	KN0342	-0.98	KN0516	-0.83	KN0659	-1.43	KN0894	-1.20	KN1029	-1.37		
KN0047	-1.17	KN0348	-1.12	KN0517	-1.20	KN0660	-1.47	KN0901	-1.27	KN1031	-1.32		
KN0048	-1.32	KN0349	-1.37	KN0520	-0.97	KN0662	-1.36	KN0903	-0.93	KN1032	-1.17		
KN0050	-1.18	KN0351	-1.16	KN0522	-1.11	KN0664	-1.12	KN0924	-1.23	KN1046	-0.35		
KN0068	-1.32	KN0358	-1.19	KN0524	-1.33	KN0683	-0.55	KN0925	-1.22	KN1051	-0.61		
KN0073	-0.62	KN0359	-1.24	KN0528	-1.27	KN0703	-1.13	KN0926	-0.76	KN1059	-1.03		
KN0084	-1.21	KN0361	-1.10	KN0529	-0.76	KN0724	-1.46	KN0928	-1.37	KN1060	-0.75		
KN0086	-1.08	KN0373	-1.12	KN0533	-1.25	KN0726	-1.20	KN0929	-1.13	KN1061	-0.87		
KN0088	-1.39	KN0386	-0.56	KN0534	-1.07	KN0735	-1.37	KN0930	-0.68	KN1084	-1.05		
KN0095	-1.11	KN0391	-0.88	KN0538	-0.71	KN0736	-1.18	KN0931	-0.65	KN1087	-0.96		
KN0127	-1.16	KN0392	-1.26	KN0539	-1.21	KN0739	-0.89	KN0938	0.11	KN1105	-1.01		
KN0187	-1.25	KN0393	-1.36	KN0549	-1.15	KN0758	-0.86	KN0939	-0.72	KN1106	-0.94		
KN0219	-0.84	KN0395	-1.26	KN0554	-1.20	KN0759	-0.93	KN0946	-1.27	KN1108	-1.03		
KN0232	-0.79	KN0398	-1.25	KN0556	-1.08	KN0760	-0.90	KN0947	-1.27	KN1109	-0.54		
KN0305	-1.21	KN0410	-1.11	KN0580	-1.46	KN0761	-1.08	KN0953	-1.13	KN1112	-1.00		
KN0306	-1.04	KN0414	-0.52	KN0582	-0.85	KN0776	-1.41	KN0954	-1.24	KN1116	-0.62		
KN0307	-1.22	KN0416	-1.21	KN0585	-1.37	KN0778	-1.30	KN0958	-1.34	KN1123	-0.46		
KN0308	-0.86	KN0420	-0.59	KN0589	-1.03	KN0785	-1.14	KN0961	-0.30	KN1129	-0.80		
KN0309	-1.31	KN0426	-1.05	KN0595	-1.29	KN0788	-0.97	KN0964	-1.34	KN1133	-0.93		
KN0310	-0.96	KN0428	-1.04	KN0602	-0.95	KN0789	-0.86	KN0971	-0.56	KN1147	-0.88		
KN0312	-1.29	KN0435	-1.09	KN0605	-1.03	KN0793	-0.99	KN0973	-1.26	KN1162	-1.02		
KN0313	-0.97	KN0440	-1.05	KN0609	-0.97	KN0802	-1.49	KN0976	-0.87	KN1163	-0.98		
KN0314	-1.00	KN0444	-0.73	KN0613	-0.76	KN0830	-1.33	KN0978	-1.23	KN1172	-0.73		
KN0317	-1.02	KN0446	-1.23	KN0621	-1.11	KN0835	-1.48	KN0979	-1.12	KN1173	-0.35		
KN0322	-1.00	KN0449	-1.21	KN0626	-0.95	KN0841	-1.52	KN0983	-0.99	KN1176	-0.47		

Appendix 5-3: ADRB analysis groups

Samples tested for ADRB activity and the analysis groups they were included (1, 2 or 3) in for Chapter 5. Analysis group 1 = samples with ADRB data for both 2009 and 2011. Analysis group 2 = 2009 samples with ADRB, ELISA and GIA data. Analysis group 3 = 2009 samples with ADRB, ELISA and SRA data.

Sample	Analysis			Sample	Analysis			Sample	Analysis			Sample	Analysis		
KN0001				KN0313	1	2		KN0001				KN0313	1	2	
KN0003	1	2	3	KN0314	1	2		KN0003	1	2	3	KN0314	1	2	
KN0007				KN0317	1	2		KN0007				KN0317	1	2	
KN0008	1	2	3	KN0322	1	2	3	KN0008	1	2	3	KN0322	1	2	3
KN0015	1	2	3	KN0323	1	2	3	KN0015	1	2	3	KN0323	1	2	3
KN0018	1	2	3	KN0324	1			KN0018	1	2	3	KN0324	1		
KN0020		2		KN0330	1	2	3	KN0020		2		KN0330	1	2	3
KN0025		2		KN0332	1			KN0025		2		KN0332	1		
KN0028	1	2	3	KN0333	1	2	3	KN0028	1	2	3	KN0333	1	2	3
KN0034	1	2		KN0334				KN0034	1	2		KN0334			
KN0035	1	2	3	KN0335	1	2	3	KN0035	1	2	3	KN0335	1	2	3
KN0042				KN0337	1	2	3	KN0042				KN0337	1	2	3
KN0046	1	2	3	KN0339				KN0046	1	2	3	KN0339			
KN0047				KN0340	1	2	3	KN0047				KN0340	1	2	3
KN0048	1	2	3	KN0342	1	2	3	KN0048	1	2	3	KN0342	1	2	3
KN0050	1	2	3	KN0344		2	3	KN0050	1	2	3	KN0344		2	3
KN0068	1	2	3	KN0348	1	2	3	KN0068	1	2	3	KN0348	1	2	3
KN0069		2		KN0349				KN0069		2		KN0349			
KN0073	1	2	3	KN0351	1	2	3	KN0073	1	2	3	KN0351	1	2	3
KN0084	1	2	3	KN0358	1			KN0084	1	2	3	KN0358	1		
KN0086	1	2	3	KN0359	1	2	3	KN0086	1	2	3	KN0359	1	2	3
KN0088				KN0361	1	2	3	KN0088				KN0361	1	2	3
KN0095	1	2	3	KN0373	1	2	3	KN0095	1	2	3	KN0373	1	2	3
KN0127	1	2		KN0385		2	3	KN0127	1	2		KN0385		2	3
KN0134				KN0386	1	2	3	KN0134				KN0386	1	2	3
KN0187				KN0391	1	2	3	KN0187				KN0391	1	2	3
KN0219				KN0392	1	2	3	KN0219				KN0392	1	2	3
KN0232				KN0393				KN0232				KN0393			
KN0305	1	2	3	KN0395	1	2	3	KN0305	1	2	3	KN0395	1	2	3
KN0306	1	2	3	KN0398				KN0306	1	2	3	KN0398			
KN0307	1	2	3	KN0403		2	3	KN0307	1	2	3	KN0403		2	3
KN0308	1	2	3	KN0410	1	2	3	KN0308	1	2	3	KN0410	1	2	3
KN0309	1	2	3	KN0414	1	2	3	KN0309	1	2	3	KN0414	1	2	3
KN0310	1	2	3	KN0416	1	2	3	KN0310	1	2	3	KN0416	1	2	3
KN0312	1	2	3	KN0420	1	2		KN0312	1	2	3	KN0420	1	2	

Appendix 5-3: cont.

Sample	Analysis			Sample	Analysis			Sample	Analysis			Sample	Analysis		
KN0736				KN0925	1	2	3	KN0736				KN0925	1	2	3
KN0739	1	2		KN0926	1	2	3	KN0739	1	2		KN0926	1	2	3
KN0758	1	2		KN0928				KN0758	1	2		KN0928			
KN0759	1	2	3	KN0929	1			KN0759	1	2	3	KN0929	1		
KN0760	1	2	3	KN0930	1	2	3	KN0760	1	2	3	KN0930	1	2	3
KN0761	1	2	3	KN0931	1	2		KN0761	1	2	3	KN0931	1	2	
KN0767				KN0938	1	2		KN0767				KN0938	1	2	
KN0776	1	2	3	KN0939	1	2		KN0776	1	2	3	KN0939	1	2	
KN0778	1	2	3	KN0946	1	2	3	KN0778	1	2	3	KN0946	1	2	3
KN0785	1	2	3	KN0947	1			KN0785	1	2	3	KN0947	1		
KN0786		2	3	KN0953	1	2	3	KN0786		2	3	KN0953	1	2	3
KN0788	1	2	3	KN0954	1	2	3	KN0788	1	2	3	KN0954	1	2	3
KN0789	1	2	3	KN0958	1	2	3	KN0789	1	2	3	KN0958	1	2	3
KN0793	1	2		KN0961	1	2	3	KN0793	1	2		KN0961	1	2	3
KN0802				KN0963		2	3	KN0802				KN0963		2	3
KN0803		2	3	KN0964	1	2	3	KN0803		2	3	KN0964	1	2	3
KN0804		2		KN0971	1	2		KN0804		2		KN0971	1	2	
KN0830	1	2	3	KN0973	1	2	3	KN0830	1	2	3	KN0973	1	2	3
KN0835	1	2	3	KN0976	1	2	3	KN0835	1	2	3	KN0976	1	2	3
KN0841				KN0978	1	2	3	KN0841				KN0978	1	2	3
KN0844				KN0979	1	2	3	KN0844				KN0979	1	2	3
KN0859	1	2		KN0982		2	3	KN0859	1	2		KN0982		2	3
KN0864	1	2	3	KN0983	1	2		KN0864	1	2	3	KN0983	1	2	
KN0865	1	2	3	KN0992	1	2		KN0865	1	2	3	KN0992	1	2	
KN0866	1	2	3	KN0993	1	2	3	KN0866	1	2	3	KN0993	1	2	3
KN0869	1	2		KN0995	1	2		KN0869	1	2		KN0995	1	2	
KN0878	1	2	3	KN0997				KN0878	1	2	3	KN0997			
KN0879	1			KN1002	1	2	3	KN0879	1			KN1002	1	2	3
KN0884	1	2	3	KN1004	1	2	3	KN0884	1	2	3	KN1004	1	2	3
KN0887	1	2		KN1005		2	3	KN0887	1	2		KN1005		2	3
KN0894	1	2	3	KN1008				KN0894	1	2	3	KN1008			
KN0900		2		KN1009	1	2	3	KN0900		2		KN1009	1	2	3
KN0901	1	2		KN1019				KN0901	1	2		KN1019			
KN0903	1	2	3	KN1022	1	2	3	KN0903	1	2	3	KN1022	1	2	3
KN0924	1	2	3	KN1026	1	2	3	KN0924	1	2	3	KN1026	1	2	3

APPENDIX 6

Plasmid maps for protein constructs made in Chapter 6. Orange: tPA leader sequence, dark green: DARC, light green: 6His, Blue: DBP_RII, light blue: DBP_FL, purple: BAP, pink: CD4 tag, black: Strep tag, yellow: IMX313, light pink: PK tag, mustard: C-tag.

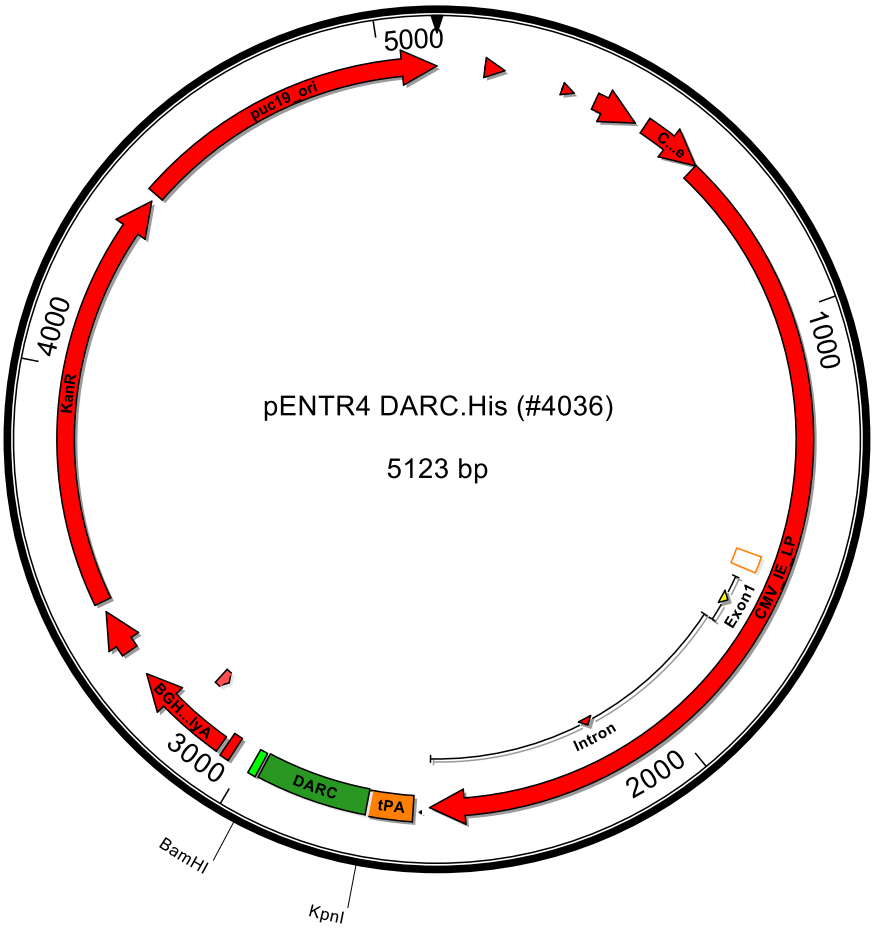

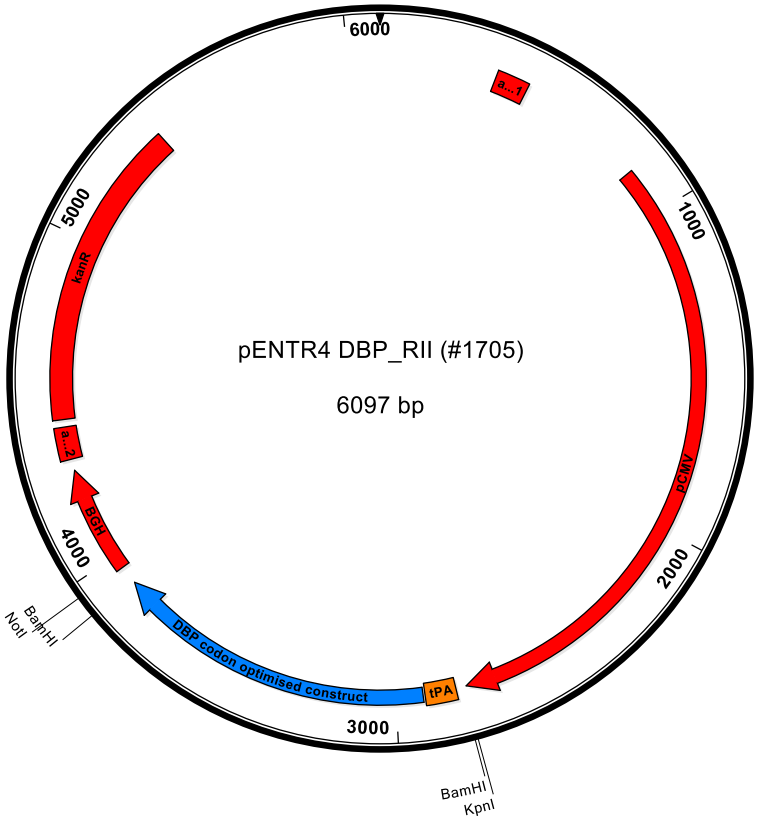
pENTR4 DBP_RII (#1705)
6097 bp
6000
1000
2000
3000
4000
5000
a...1
pCMV
tPA
DBP codon optimised construct
a...2
BGH
KanR
BamHI
NotI
BamHI
KpnI

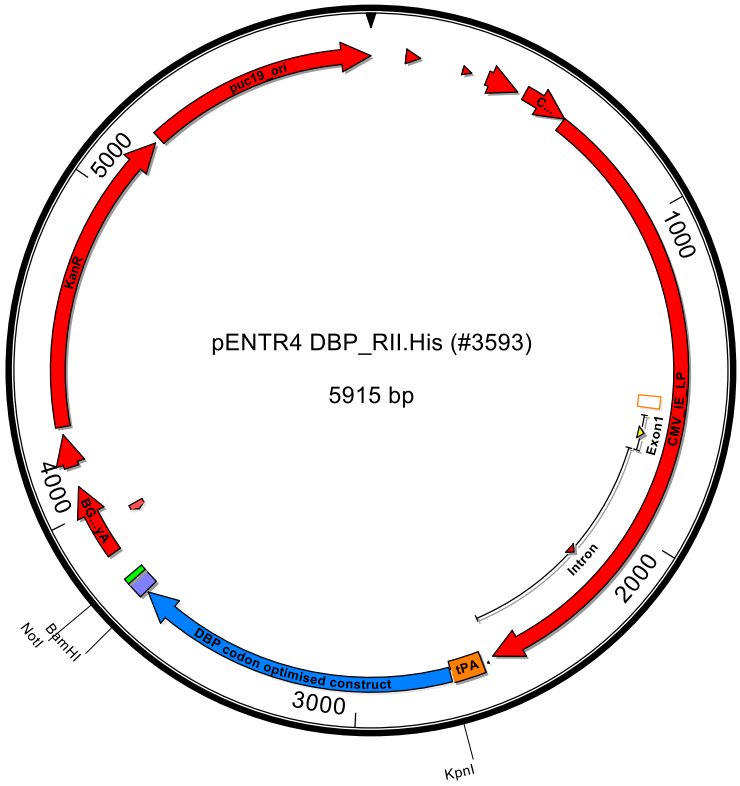
pENTR4 DBP_RII.His (#3593)
5915 bp
5000
1000
2000
3000
4000
puc19_ori
C...
CMV_IE_I_P
Exon1
Intron
tPA
DBP codon optimised construct
BG_pA
KanR
NotI
BamHI
KpnI

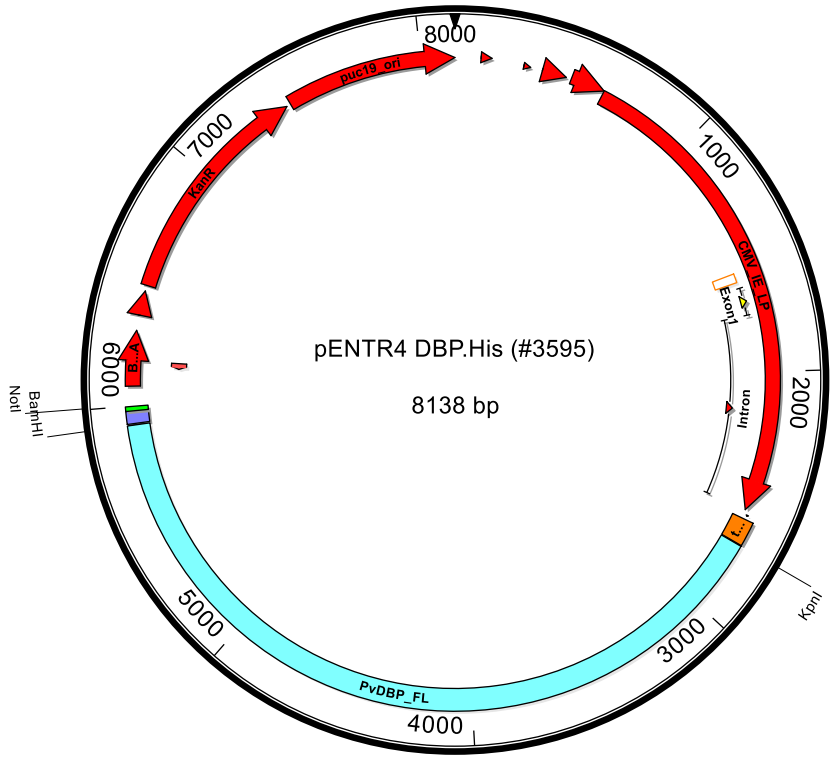
pENTR4 DBP.His (#3595)
8138 bp
8000
1000
2000
3000
4000
5000
6000
7000
puc19_ori
KanR
CMV IE LP
Exon1
Intron
PvDBP_FL
BamHI
NotI
KpnI

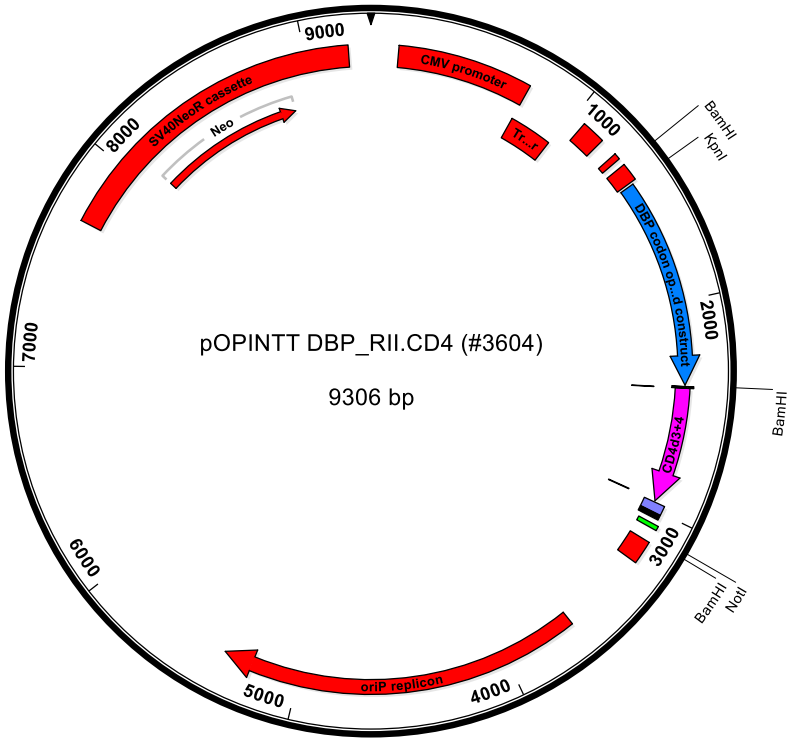
pOPINTT DBP_RII.CD4 (#3604)
9306 bp
9000
1000
2000
3000
4000
5000
6000
7000
8000
CMV promoter
SV40NeoR cassette
Neo
DBP codon op...d construct
CD4d3+4
oriP replicon
BamHI
KpnI
BamHI
NotI

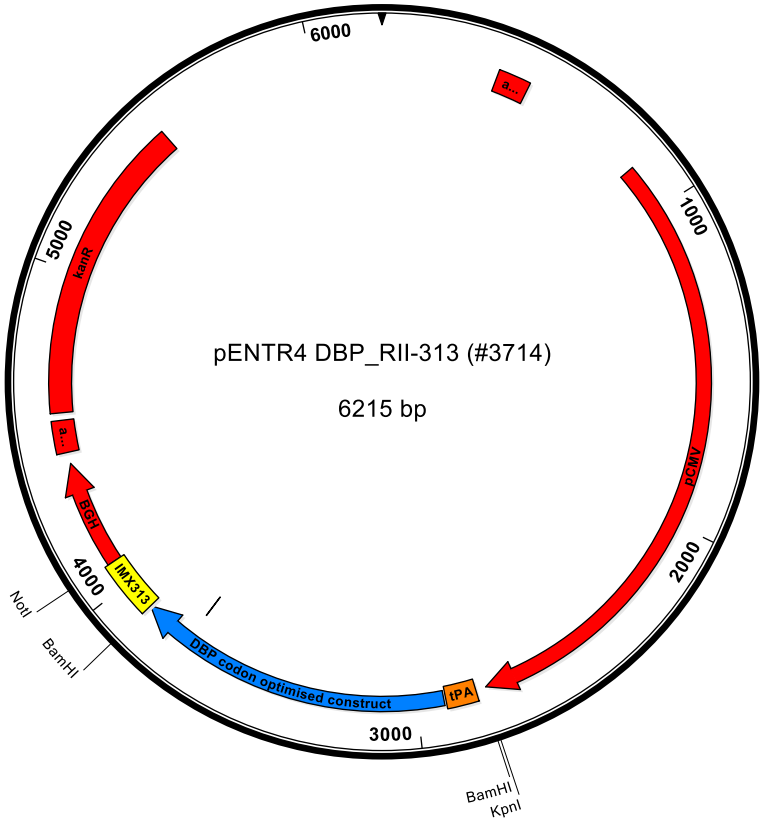
pENTR4 DBP_RII-313 (#3714)
6215 bp
6000
1000
2000
3000
4000
5000
a...
KanR
a...
BGH
IMX313
DBP codon optimised construct
tPA
pCMV
NotI
BamHI
BamHI
KpnI

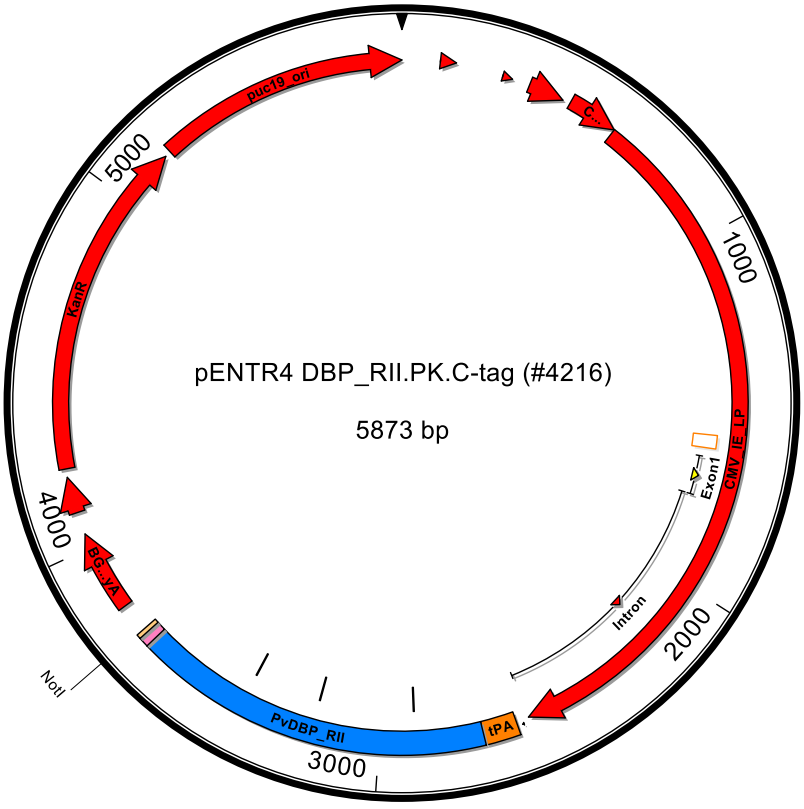
pENTR4 DBP_RII.PK.C-tag (#4216)
5873 bp
5000
1000
2000
3000
4000
puc19_ori
KanR
C...
CMV_IE_LP
Exon1
Intron
BG...yA
PvDBP_RII
tPA
NotI

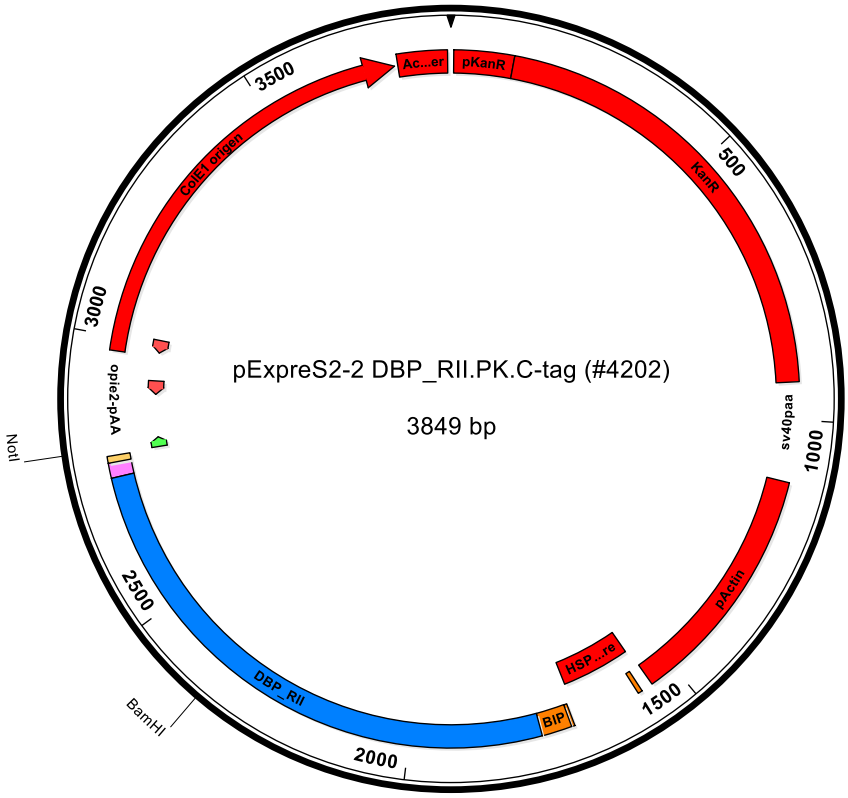
pExpreS2-2 DBP_RII.PK.C-tag (#4202)
3849 bp
Ac...er
pKanR
KanR
sv40paa
pActin
HSP...re
BIP
DBP_RII
opie2-pAA
CoIE1 origen
NotI
BamHI
500
1000
1500
2000
2500
3000
3500